**UNIVERSITY OF SOUTHAMPTON**

FACULTY OF MEDICINE

ACADEMIC UNIT OF CLINICAL AND EXPERIMENTAL SCIENCE

Volume 1 of 1

# Investigating host regulatory pathways that limit immunopathology in tuberculosis

by

**Patience Tenkoramaa Brace**

Thesis for the degree of Doctor of Philosophy

June_2017

**UNIVERSITY OF SOUTHAMPTON**

# ABSTRACT

FACULTY OF MEDICINE

Academic Unit of Clinical and Experimental Science

Thesis for the degree of Doctor of Philosophy

## INVESTIGATING HOST REGULATORY PATHWAYS THAT LIMIT IMMUNOPATHOLOGY IN TUBERCULOSIS

PATIENCE TENKORAMAA BRACE

Pulmonary Tuberculosis (TB) is characterized by cavitation following lung extracellular matrix (ECM) destruction. The architectural framework of the lung is usually protected from degradation that is driven by proteases. Matrix metalloproteinases (MMPs), especially the collagenase MMP-1, can cleave types I, II and III fibrillar collagens of the lung ECM at neutral pH, and there is a significant increase of MMP-1 concentrations in TB. Although the pathways driving inflammation in TB are well understood, relatively little is known about host regulatory mechanisms that suppress pathology. I investigate the PI3K/AKT/mTORC-1 axis and Mnk1/2 signalling pathway and demonstrate their negative regulatory role that limits tissue destruction. *M.tb* up-regulates the gene expression and secretion of MMP-1 in human monocyte derived macrophages (MDMs) and THP-1 cells. LY294002, a pan-PI3K inhibitor and IC87114, a PI3Kδ selective inhibitor significantly further increased MMP-1 secretion and gene expression in infected MDMs. Pharmacological inhibition of AKT and mTORC-1 similarly increased MMP-1.

The MAP kinase-interacting kinases, Mnk1 and Mnk2, are downstream effectors of Erk and p38, which are also downstream of the Ras to MAPK pathway. Mnk1/2 is known to mainly promote mRNA translation by phosphorylating the initiation factor, eIF4E to drive the formation

ofeukaryotic initiation complex, eIF4F. This results in 5'-cap-dependent mRNA translation. Chemical blockade of Mnk1 also surprisingly augmented MMP-1 secretion compared to the levels driven by *M.tb* infection. Conversely, disrupting interaction between eIF4E and the scaffolding protein eIF4G attenuated MMP-1 secretion. This suggests that the effect of Mnk1/2 inhibitors on MMP-1 production is not via interference with formation of the eukaryotic initiation complex, eIF4F. *M.tb* suppressed PI3Kδ mRNA and protein expression in MDMs, and also suppressed MKNK1 expression, which encoded Mnk1. This suppression was associated with increased accumulation of miRNAs that target the 3' UTR of these genes. Taken together, *M.tb* induces MMP-1 secretion in primary macrophages and that the PI3K/AKT/mTORC-1 axis and signalling via Mnk1 limit the excessive production of such tissue damaging proteases. Inhibitors that target components of these intracellular signalling are entering clinical trials for cancer and diabetes therapies, but conversely they may accentuate tissue damage in inflammatory conditions such as tuberculosis.

# LAY STATEMENT

Tuberculosis (TB) is an infection which kills 1.5 million people each year and lung TB patients are the most infectious. TB patients develop air filled cavities within their lungs, where bacteria are able to replicate massively. Upon development of a cough, infection spreads to healthy people. The body's response to TB infection is the accumulation of immune cells called a granuloma. This leads to a lung destruction, which must involve actions of protein damaging enzymes known as proteases, in particular Matrix metalloproteinases (MMPs). Although much is known about mechanisms increasing enzymes and causing disease progression, little is known about the host protective regulatory mechanisms in TB. I investigate these immune systems, and show specific pathways that protect lungs from excessive enzymes. I have identified that in order to be successful; the bacteria disrupt the normal immune cell activity. This leads to excessive lung destruction and cavity formation, thereby promoting spread of TB.

# CONTENTS

ABSTRACT ..... i

LAY STATEMENT ..... iii

List of tables ..... v

List of figures ..... vii

DECLARATION OF AUTHORSHIP ..... xi

Acknowledgements ..... xiii

Definitions and Abbreviations ..... xv

CHAPTER 1: INTRODUCTION ..... 1

1.1 Tuberculosis epidemiology ..... 1
1.2 Tuberculosis situation in London ..... 2
1.3 Tuberculosis in other regions of the word ..... 3
1.4 Limiting disease transmission is crucial to combatting TB ..... 3
1.5 Tuberculosis life cycle ..... 4
1.6 Initiation of TB infection ..... 5
1.7 Host and pathogen immune response ..... 5
1.8 Granuloma Formation: Hallmark of Tuberculosis ..... 6
1.9 Lung cavitation in tuberculosis ..... 9
1.9.1 Lung cavities exacerbate TB immunopathology ..... 9
1.9.2 The current paradigm of cavity formation ..... 11
1.9.3 Cavity formation has been linked to tissue caseation ..... 12
1.10 Protease activities mediate matrix destruction ..... 13
1.11 Matrix metalloproteinases (MMPs) ..... 15
1.11.1 Structure and function of MMPs ..... 15
1.11.2 Pathogenic role of MMPs in non-pulmonary diseases ..... 18
1.11.3 Pathogenic role of MMPs in pulmonary diseases ..... 20
1.11.4 Regulation of MMPs ..... 22
1.12 Intracellular signalling pathways ..... 23
1.12.1 PI3K proteins and their signalling ..... 24
1.12.2 Overview of the PI3K pathway ..... 33
1.13 The TOR proteins, mTOR complexes and their functions ..... 38
1.13.1 mTORC-1 promotes ribosomal biogenesis and translation ..... 39
1.14 MAP-Kinase-interacting kinase (Mnk) signalling ..... 42

1.14.1 Mnk1 drives cap-dependent eukaryotic translation initiation ..... 43
1.15 Regulatory role of PI3K/AKT/mTORC-1 signalling in disease..... 47
1.16 *M.tb* engages TLRs to activate PI3K signalling..... 49
1.17 *M.tb* suppresses host regulatory signalling mechanisms..... 50
1.18 Micro RNAs ..... 52
1.18.1 Micro RNA biogenesis ..... 53
1.19 Hypothesis ..... 56
1.20 Experimental plan ..... 56
2. CHAPTER 2: MATERIALS AND METHODS..... 57
2.1 List of equipment ..... 57
2.2 List of reagents ..... 58
2.3 Cell culture ..... 63
2.3.1 THP-1 cells ..... 63
2.3.2 Isolation of PBMC ..... 64
2.3.3 Adherence purification of monocytes ..... 64
2.4 *M.tb* culture ..... 65
2.5 Pharmacological treatment and *M.tb* infection ..... 66
2.6 Enzyme-linked Immunosorbent Assay (ELISA) ..... 66
2.7 Luminex Assay ..... 67
2.7.1 Principle of Luminex assay ..... 68
2.7.2 Cytokine 30-plex panel: Samples and standard preparation ... 73
2.7.3 MMP multiplex: Samples and standard preparation ..... 73
2.7.4 Running the multiplex assay ..... 73
2.8 Lactic Dehydrogenase (LDH) Cytotoxicity detection assay ..... 74
2.9 Antibody staining for flow cytometry ..... 75
2.10 Total Protein extraction ..... 76
2.11 BCA Assay ..... 77
2.12 Western Blotting ..... 77
2.13 Total RNA extraction ..... 79
2.13.1 Phase separation ..... 79
2.13.2 RNA Precipitation ..... 80
2.13.3 RNA wash and re-suspension ..... 80
2.14 Reverse transcription and quantitative PCR (RT-qPCR) ..... 80
2.14.1 Reverse transcription (mRNA) ..... 80
2.14.2 Micro-reverse transcription (micro-RT) ..... 82
2.14.3 Quantitative PCR (qPCR) ..... 85
2.15 Transfection of Anti-miRs into macrophages ..... 86
2.16 Validation of reference genes (geNormTM Kit) ..... 86
2.17 4-TU labelling of macrophages ..... 87

2.17.1 Biotinylation of 4-TU labelled RNA ..... 87
2.17.2 Precipitation of biotinylated 4-TU-labelled RNA ..... 90
2.17.3 Purification of biotinylated 4-TU labelled RNA (Pull down) ..... 90
2.17.4 Elution and precipitation of bound, 4-TU labelled RNA ..... 91
2.17.5 Superscript III Reverse Transcription ..... 93
2.18 Immunohistochemistry ..... 93
2.19 Statistical analysis ..... 95
3. CHAPTER 3: RESULTS PART I ..... 97
3.1 Overview ..... 97
3.2 Methods ..... 97
3.3 Chapter Hypothesis ..... 97
3.4 Aims ..... 98
3.5 M-CSF-induced Monocyte Derived Macrophages (MDMs) ..... 98
3.5.1 MDMs express known macrophage markers ..... 99
3.5.2 Kinetics of the ability of MDMs to phagocytose *M.tb* ..... 101
3.6 Optimisation Experiments ..... 102
3.6.1 Kinetics of MMP-1 secretion by MDMs ..... 102
3.6.2 MMP-1 secretion profile in THP-1 cell ..... 103
3.7 PI3K signalling negatively regulates MMP-1 in TB ..... 104
3.7.1 PI3K inhibitors augment *M.tb* -driven MMP-1 in MDMs ..... 105
3.8 LY294002 represses AKT phosphorylation ..... 107
3.9 PI3Kδ mediates MMP-1 regulation in MDMs ..... 108
3.10 Targeting PI3K in THP-1 cells suppresses MMP-1 ..... 110
3.11 MMP-1 regulation by PI3K inhibitors is AKT-dependent ..... 111
3.12 mTOR signalling negatively regulates MMP-1 in macrophages. 112
3.13 Modulation of MMP-1 by PTEN inhibitors ..... 113
3.14 Chemical inhibitors were non-toxic to macrophages ..... 116
3.15 PI3K and mTORC-1 inhibitors modulate MMPs in MDMs ..... 116
3.16 Pathway inhibition modulates *M.tb* -driven cytokines ..... 120
3.17 PI3K and mTORC-1 inhibition augments Th1-type cytokines .. 120
3.17.1 PI3K and mTORC-1 inhibition augments Th2-type cytokines .. 123
3.17.2 PI3K and mTORC-1 inhibition modulate chemokines ..... 125
3.17.3 PI3K and mTORC-1 inhibition augment growth factors ..... 128
3.17.4 PI3K and mTORC-1 inhibition augment a range of cytokines .. 130
3.17.5 Summary . ..... 133
3.18 Discussion of results chapter I ..... 136
4. CHAPTER 4: RESULTS PART II ..... 147
4.1 Overview ..... 147

4.2 Methods....147
4.3 Chapter Hypothesis....147
4.4 Aims....148
4.5 Mnk1 inhibitors drive MMP-1 in *M.tb* infected macrophages ...149
4.6 Modulation of MMP-1 by Mnk1 inhibitors is not via the eIF4F..150
4.7 The negative regulatory to MMP-1 is not via p90RSK....155
4.8 PI3K and Mnk pathways crosstalk in the negative regulation ...156
4.9 Mnk regulation of MMPs is relatively specific....157
4.10 Mnk1 inhibition suppresses *M.tb* -driven cytokine levels....157
*4.11* Mnk1 inhibition suppresses pro-inflammatory cytokine....159
4.9 Mnk inhibition suppresses Th2-type cytokine....160
4.12 Mnk1 inhibition differentially modulate chemokine....161
4.13 Mnk1 inhibition suppresses production of growth factors....163
4.14 Mnk1 inhibition exerted no significant change in cytokines...164
4.15 Summary....166
4.16 Discussion of results chapter II....167
5. CHAPTER 5: RESULTS PART III....174
5.1 Overview....174
5.2 Methods....174
5.3 Chapter hypothesis....175
5.4 Aim....175
5.5 *M.tb* suppresses PI3Kδ mRNA in infected macrophages....176
5.6 *M.tb* represses PI3Kδ protein in infected macrophages....178
5.7 *M.tb* represses PI3Kδ expression in TB lung tissues....179
5.8 *M.tb* post transcriptionally represses PI3Kδ via micro RNAs ....190
5.9 *M.tb* induces upregulation of micro RNAs....197
5.10 Discussion of results chapter III....203
6. CHAPTER 6: GENERAL DISCUSSION AND FUTURE WORK....208
6.1 CONCLUDING REMARKS....216
6.2 FUTURE WORK....217
7. APPENDICES....221
7.1 Appendix 1: Materials and buffer recipes....223
7.2 Appendix 2: Culture of *M.tb* (H37RV)....227
7.3 Appendix 3: Manufacturer's protocols used....231
7.4 Appendix 4: Software used....232
8. LIST OF REFERENCES....235

# List of tables

Table 1: Gel casting protocol for Western Blotting. ..... 79

Table 2: Reaction recipe for reverse transcription ..... 81

Table 3: Conditions for reverse transcription thermal cycle. ..... 82

Table 4: Sequences details of stem loop and mature miRNAs for microRNAs' reverse transcription. ..... 84

Table 5: Reaction recipe for micro RNA reverse Transcription. ..... 84

Table 6: Conditions for micro RT thermal cycle. ..... 85

Table 7: Typical Master Mix recipes for qPCR ..... 85

Table 8: Amplification conditions using Taqman universal master mix. ..... 86

Table 9: Simplified schematic of 4-TU labelling. ..... 89

Table 10: Simplified schematic of 4-TU labelling and RNA pull down. ..... 92

Table 11a: Alignment and sequence information (miRs) ..... 193

# List of figures

Figure 1: Tuberculosis; a lethal infectious disease. ..... 1

Figure 2: Transmission cycle of Mycobacterium tuberculosis (*M.tb*). ..... 4

Figure 3: A schematic representation of tuberculosis granuloma. ..... 8

Figure 4: Lung cavities are several centimetres across. ..... 10

Figure 5: Structural features of mammalian MMPs. ..... 17

Figure 6: Principle of cell signalling. ..... 24

Figure 7: Structural features of the different classes of PI3Ks. ..... 27

Figure 8: Structural features of the classes II and III PI3Ks..... 29

Figure 9: Phosphoinositide 3-kinase (PI3K) Signalling..... 30

Figure 10: PI3Ks catalyse phosphorylation reactions in cells. ..... 31

Figure 12: Structural features of TOR protein and mTOR complexes. ..... 40

Figure 13: PI3K to mTORC-1 and Erk signal convergence. ..... 45

Figure 14: PI3K to mTORC-1 and Erk signal convergence. ..... 46

Figure 15: Schematic representation of microRNA biogenesis in humans..... 54

Figure 16: Microscopic images of purified monocytes. ..... 65

Figure 17: Schematic of the 100 unique xMAP microspheres. ..... 69

Figure 18: Steps involved in Luminex immunoassay. ..... 70

Figure 19: Measurement of analytes within the Luminex analyser..... 72

Figure 20: MDMs express receptors found on macrophages in vivo. ..... 101

Figure 21: Kinetics of MDMs ability to phagocytose *M.tb* . ..... 102

Figure 22: Optimisation Experiments..... 103

Figure 23: Optimisation Experiments. (THP-1 cells)..... 104

Figure 24: Simplified schematic of the PI3K pathway ..... 105

Figure 25: PI3K inhibitors augment *M.tb* -driven MMP-1..... 105

Figure 26: NVP-BAG956 also augments *M.tb* -driven MMP-1..... 106

Figure 27: Modulation of AKT phosphorylation by PI3K & PTEN inhibitors.... 107

Figure 28: Modulation of MMP-1 by α, β, γ and δ PI3K isoforms. ..... 109

Figure 29: PI3K inhibition profile in THP-1 cells..... 111

Figure 30: AKT inhibition drives MMP-1 secretion ..... 112

Figure 31: Rapamycin augments *M.tb* -driven MMP-1..... 113

Figure 32: Modulation of *M.tb* -driven MMP-1 by PTEN inhibitor..... 115

Figure 33: Cell viability after treatment with chemical inhibitors. ..... 117

Figure 34: LY294002 globally modulates multiple MMPs..... 118

Figure 35: Rapamycin similarly modulates multiple MMPs globally..... 119

Figure 36: PI3K inhibition drives inflammatory cytokine..... 121

Figure 37: mTORC-1 inhibition drives inflammatory cytokine. ..... 122

Figure 38: PI3K inhibition induce low levels of IL-4, IL-10 and IL-13 ..... 123

Figure 39: mTORC-1 inhibition induce low levels of IL-4, IL-10 and IL-13 .. 124

Figure 40: LY294002 differentially modulates a wide range of chemokines.. 126

Figure 41: Rapamycin differentially modulates a wide range of chemokines. 127

Figure 42: LY294002 augments a wide range of growth factors..... 128

Figure 43: mTOC1 inhibition augments a range of growth factors ..... 129

Figure 44: PI3K inhibition augments a wide range of cytokines cytokines. ... 131

Figure 45: mTOC1 inhibition augments various other cytokines..... 132

Figure 46: PI3K inhibition globally modulates a wide range of pro-inflammatory signalling molecule secretion. ..... 134

Figure 47: mTORC-1 inhibition globally modulates a wide range of pro-inflammatory signalling molecule secretion.. ..... 135

Figure 48: Mnk1 inhibitor enhances *M.tb* -driven MMP-1. MDMs were pre-treated with Mnk1 inhibitor for two hours prior to *M.tb* infection. ..... 149

Figure 49: Interfering with the interaction between eIF4E and eIF4G suppresses MMP-1.....151

Figure 50: Various Mnk1 inhibitors suppress *M.tb* -driven MMP-1 in macrophages. .....153

Figure 51: Mnk inhibitors suppress eIF4E phosphorylation.. ..... 154

Figure 52: p90RSK signalling does not mediate MMP-1 regulation. ..... 155

Figure 53: The PI3K and Mnk pathways converge at the level of eIF4E phosphorylation.. ..... 156

Figure 54: Mnk1 inhibition globally modulates multiple MMPs in MDMs. ..... 158

Figure 55: Mnk1 inhibition suppresses cytokine production in macrophages. 159

Figure 56:Mnk1 inhibition suppresses cytokine production in macrophages.160

Figure 57: Mnk1 inhibition modulates a wide range of chemokines.....162

Figure 58: Mnk1 inhibition suppressed *M.tb*-driven growth factor..... 163

Figure 59: Mnk1 inhibition had no effect on a wide range of cytokines..... 164

Figure 60: Mnk1 inhibition modulate multiple MMPs but suppresses a wide range of pro-inflammatory signalling molecule secretion..... 166

Figure 61: *M.tb* suppresses PI3Kδ mRNA..... 177

Figure 62: *M.tb* -induced suppression of PI3Kδ protein. ..... 178

Figure 63: Anti-PI3Kδ antibodies show immune reactivity on positive control tissue. .....180

Figure 64: Anti-CD68 antibodies show immune reactivity on positive control tissue.....181

Figure 65:Macrophages express both CD68 and PI3Kδ in normal lunga.....183

Figure 66: *M.tb* suppresses PI3Kδ expression in TBgranulomas.....184

Figure 67: *M.tb* suppresses PI3Kδ expression in giant cells. ..... 185

Figure 68: Whole TB lung sections show wide spread CD68, but little or no PI3Kδ expression..... 188

Figure 69: Negative control confirms specificity of antibodies..... 189

Figure 70: M.tb reduces mRNA stability of PIK3CD, MKNK1 and MLST8..... 191

Figure 71: Diagram of the micro RNAs studied and their mRNA targets..... 192

Figure 72: *M.tb* infection upregulated multiple microRNAs..... 198

Figure 73: Anti-miRs reverse *M.tb* effect on PIK3CD and MMP-1genes..... 200

Figure 74: Anti-miRs modulate PIK3CD, MKNK1, MLST8 MMP-1 genes..... 201

Figure 75: Anti-miRs drive PIK3CD, MKNK1 and MLST8 gene expression.... 202

Figure 76: Proposed model..... 216

# DECLARATION OF AUTHORSHIP

I, Patience Tenkoramaa Brace, declare that the thesis entitled and the work presented in the thesis is both my own, and have been generated by me as the result of my own original research.

**Thesis Title**

INVESTIGATING HOST REGULATORY PATHWAYS THAT LIMIT IMMUNOPATHOLOGY IN TUBERCULOSIS;

I confirm that:

This work was done wholly or mainly while in candidature for a research degree at this University;

Where any part of this thesis has previously been submitted for a degree or any other qualification at this University or any other institution, this has been clearly stated;

Where I have consulted the published work of others, this is always clearly attributed;

Where I have quoted from the work of others, the source is always given. With the exception of such quotations, this thesis is entirely my own work;

I have acknowledged all main sources of help;

Where the thesis is based on work done by myself jointly with others, I have made clear exactly what was done by others and what I have contributed myself.

Parts of the data from this work have been published in PLOS Pathogens before submission of the final Thesis (Brace et al., 2017).

Signed: ……..

Date……

# Acknowledgements

I can do all things through Christ who strengthens me (Philippians 4:13). I write this section with great humility, giving thanks to God for His grace, protection and provision for my family, whilst seeing me through my PhD programme.

Next I wish to express my deepest appreciation to you Professor P. T. Elkington, firstly for believing in me and taking a chance on me. I deem myself extremely blessed to have had you as my supervisor. You have not only taken time to teach me great science, you went out of your way to ensure I succeeded in life, even that beyond my PhD years. You have taught me valuable and transferable skills that define the scientist I am today. You genuinely cared about my family, making sure that my husband and daughter were not adversely affected by my rather 'mad' mother, wife and student life style. You never gave up on me when life got tougher than I could ever imagine, but rather supported me through the rocky times. I would not have made it this far without your incredible support Paul. In my eyes, you are officially the world's greatest PhD supervisor and I'm honoured to have been your student. Thank you.

Thank you Dr Liku Tezera (my boss). As a fresh BSc graduate with such minimal laboratory experience, I am not ashamed to admit that my mind was pretty much in a state of *Tabula rasa* prior to your training. Not only did you exercise great patience with me, you treated me as though I was your sister and encouraged me all the way. Again, it has been a privilege to learn under your guidance and directions. Thank you.

My next thanks go to the rest of 'Team TB'. Most especially to Dr Magdalena K. Bielecka (my bosstress), Diana Garay and Dr Michaela Reichmann, I am truly grateful to you for your friendship and all your technical and emotional support. You guys really cared about me and I would never forget that. Thank you.

I thank you all at level E for making the department such a wonderful environment to work. You saw a potential in me Prof Tilman Sanchez-

Elsner, and you have ensured this was developed to the fullest. I owe this achievement to you, Thank you. Dr Jane Collins, I will never forget your support, especially your pastoral advice that kept me going, even now. What can I say to you Regina, Berenice and Theresa; I'm lucky to call you my friends. Thank you for all your support and encouragements.

To Dr. Matthew Bellamy, words cannot express my profound gratitude for your friendship, continues support, encouragement and chats. You thought me that hard work pays, and this truth has got me this far. Thanks Matt, I will forever cherish our friendship. Thank you my absolutely 'Best Friends Forever' Jess, Marisa, Sharifa and Fabrina (Germany). It didn't matter how long we hadn't heard from one another, you girls loved me. You have been extremely patient with my hectic life style and you never gave up on me. You are true friends indeed and I thank you for being there for me every step of the way.

I wish to thank all my friends, many of whom have now become family. There are too many of you to do you justice. Many of you have supported me financially; others became baby sitters, and yet more were very committed to ensure I kept smiling through it all. Thank you to Ruth and Ian Chidle for being parents to me. You have loved my family and accepted us into yours. God bless you for everything. Thanks to my absolutely beautiful friends Nike and Folabi, Hadiza and Ola, Naana and girls, Theodora and Abraham, Kenechi and family, Honour and Dan, Chika and Emeka, Kelsie and John Ackland, Sandy Matthews, maa Felicity and daa Richard, John and Nana Iyamu (Australia), Korkor Dora Ohene-Gyan (Ghana). Thank you all for your prayer support and for being such a blessing to my family.

I wish to thank my mother-in-law Georgina, her husband Norbert and my auntie Bernice Frey (all in Germany); my mum Elizabeth Ocansey, Brothers Clement and Daniel and to my sisters Gertrude and Kate (all in Ghana), and my cousin Aretha and her husband Robert Jiagge for your love and prayer support. Thanks to Manfred and Afia Ampim (+ girls), and Afua

and Ebenezer Arhin (affectionately known as *uncle Bo by* Jenelle). We love you all loads.

Now to the lovely Rachel Walters, Caroline Richens, Charnelle Dearing, Caroline Lomas, Kerrie Gaughan, Ciaran Abbey (all of whom are mums of kids in Jenelle's class, Appleton C of E primary school). Although I have only recently met you beautiful ladies, I cannot even contemplate how I would have managed to complete the last huddles of this work without your true selfless and outpour of love towards myself and Jenelle. All of you have cared for Jenelle as though she was your own, and asked for absolutely nothing in return. You are amazing ladies! My faith in humanity has been restored as a result of your kind gesture. Thanks a million.

Finally to my gorgeous husband Jerome, you deserve a medal for your incredible support. You became mum and dad to our precious and adorable Jenelle, and encouraged me to keep on moving forward. In your own unique way, you instilled in me a 'can do' attitude, even when all hope was gone. I'm a very lucky woman to have you baby. To you and Jenelle, I dedicate this PhD Thesis. Thank you.

# Definitions and Abbreviations

| | |
|---|---|
| TB | Tuberculosis |
| ECM | Extracellular matrix |
| FKHR-L1 | Forkhead-related transcription factor-1 |
| COPD | Chronic Obstructive Pulmonary Diseases |
| XDR | Extensively-drug resistance |
| GPCRs | G-protein-coupled receptors |
| GEFs | Guanosine nucleotide exchanging factors |
| GAPs | Guanosine triphosphatase (GTPase)-activating proteins |
| AKT | Mammalian homologue of retroviral transforming protein v-AKT |
| mTORC | Mammalian target of rapamycin complex |
| Mnk1 | MAP kinase-interacting kinases-1 |
| MMPs | Matrix metalloproteinases |
| MAP | Mitogen activated protein |
| MDMs | Monocyte Derived Macrophages |
| PPR | Pattern Recognition Receptor |
| PTEN | phosphatase and tensin homologue |
| PI3K | Phosphatidylinositol-3 Kinase |
| PtdIns | Phosphatidylinositols |
| PDK-1 | Phosphoinositol-dependent kinase-1 |
| PtdIns(4,5)$P_2$ | PtdIns-4,5-bisphosphate |
| RTK | Receptor tyrosine kinases |
| TIMPs | Tissue inhibitors of metalloproteinases |
| TIMPs | Tissue inhibitors of metalloproteinases |
| TACE | TNF-alpha-converting enzyme |
| TLRs | Toll-like receptors |
| TGF | Transforming growth factors |
| WHO | World Health Organization |
| 4-TU | 4-Thio Uradine |

# CHAPTER 1: INTRODUCTION

## 1.1 Tuberculosis epidemiology

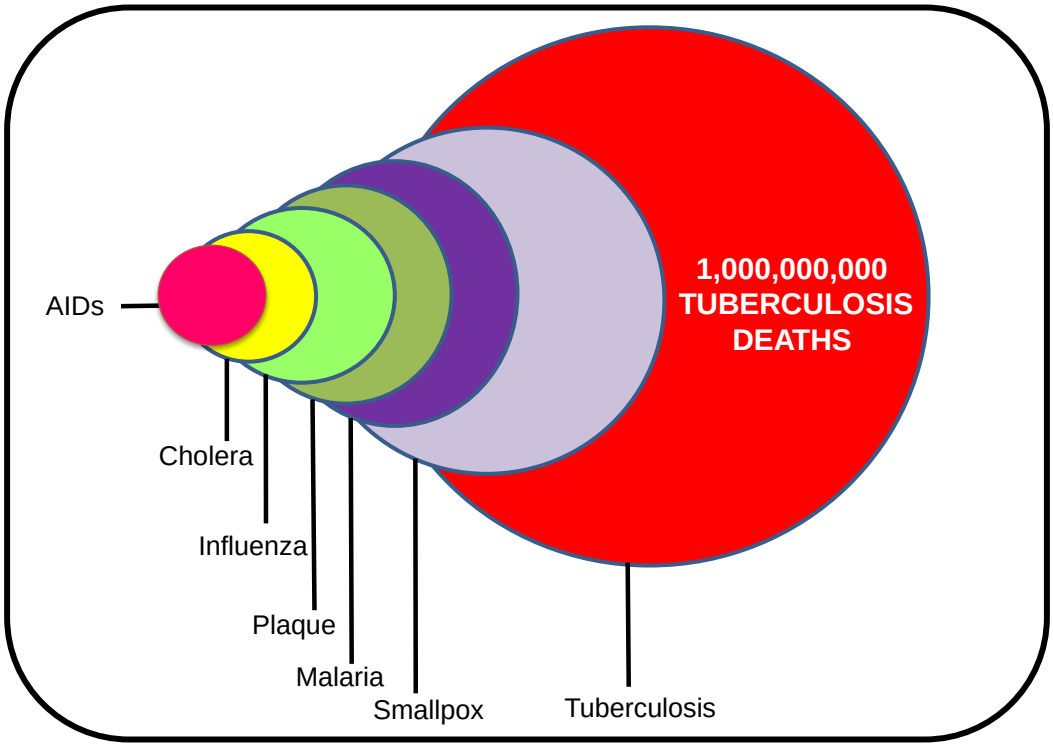


**Figure 1: Tuberculosis; a lethal infectious disease.** This is a simplified schematic illustrating the estimated proportion of global deaths caused by each of the diseases shown since their emergence. With over 1 billion people killed since its emergence TB has killed more people worldwide than any other infectious disease. Although Acquired Immune Deficiency Syndrome (AIDs) appears to have killed the least number of people according to this diagram, it is currently the second most lethal infectious disease, having just been surpassed again by Tuberculosis. (Created by P T Brace, by modification from Tom Paulson, Nature Outlook, 2013)

Tuberculosis (TB), caused by Mycobacterium tuberculosis (*M.tb* ), is the most lethal global communicable disease and predominantly affects the lung. Since its emergence, TB has killed over a billion people worldwide (Figure 1) (Paulson, 2013). One third of the world's population harbour *M.tb* (Dye, 2010, Russell, 2007) of which 9 million people were estimated to developed TB and 1.5 million people died from the disease in 2014 (World Health Organization's (WHO) report, 2015). The majority of TB deaths occur in poor countries, with 60% in Asia and 24% in Africa. Over 2.2 million people are estimated to have TB in India alone. In sub-Saharan Africa, the majority of TB deaths occur amongst people living with HIV. Although most of the so called 'highest TB burden countries' are poor, there is no region in any part of the world that is completely free of TB (WHO, 2015).

## 1.2 Tuberculosis situation in London

London saw a rise in TB incidence between 1999 and 2009 when TB cases increased by almost 50% (Paulson, 2013). Although the city has not yet been able to completely class TB as a bygone disease, strategies to prevent it from becoming a disease of the future continues to pose formidable challenges to London health services and Public Health England. According to a report published by the health committee of London assembly, London accounts for 40% of all TB cases in England, with 9% of this figure being drug resistant TB (Onkar Sahota, 2015).

The economic burden of the disease is increasingly becoming a national concern. London health services are estimated to spend over £30 million on TB cases each year (Onkar Sahota, 2015). With an average of 7 individuals presenting with TB symptoms each day, and a third of London boroughs included in the 'High Incidence' of TB category in the world, the city has recently been described as the TB capital of Western Europe (Onkar Sahota, 2015). The issue of TB cases rising in London should receive considerable and critical attention, as recent evidence shows

significant failures and insufficiencies in efforts by London health services to contain disease transmission (Onkar Sahota, 2015).

## 1.3 Tuberculosis in other regions of the word

The global TB incidences are on the increase. To highlight a few examples of TB cases in certain regions of the world, the Americas reported 260,000 TB incidences with 21,000 deaths in 2014. These figures were higher in Europe with 380,000 and 45,000 deaths. There were 660,000 TB incidences in the Eastern Mediterranean and estimated 1.7 million in Western Pacific with 130,000 and 480,000 deaths respectively (WHO, 2015). The past four decades have seen intense strategic efforts by WHO to combat TB. However, the rapid rate of emergence of Multi-drug resistance (MDR) and Extensively-drug resistance (XDR) TB, as well as co-infection with HIV, have highlighted the continued challenge of TB globally (Dye, 2010, Corbett et al., 2003).

## 1.4 Limiting disease transmission is crucial to combatting tuberculosis

One key issue is that several of the WHO strategies to eradicate TB have been aimed at limiting the rate of disease progression in patients, and to ultimately cure the disease. Efforts to manage the rate of TB transmission have not received such widespread attention. There is a recent emergence of totally drug resistant TB (TDR-TB) strains which are insensitive to all of the most effective TB treatment regimens (Velayati, 2009, Velayati, 2013). Similar drug resistant strains were identified in TB patients in Italy and India (Migliori GB and DM., 2007, Udwadia ZF, 2012), and in South Africa (Klopper et al., 2013). TB continues to pose a threat to public health, even after decades of WHO intervention. It is therefore critical for new strategies to focus on limiting the spread of TB; as well as the development of novel approaches to enhance host mechanisms that limit disease pathogenesis.

## 1.5 Tuberculosis life cycle

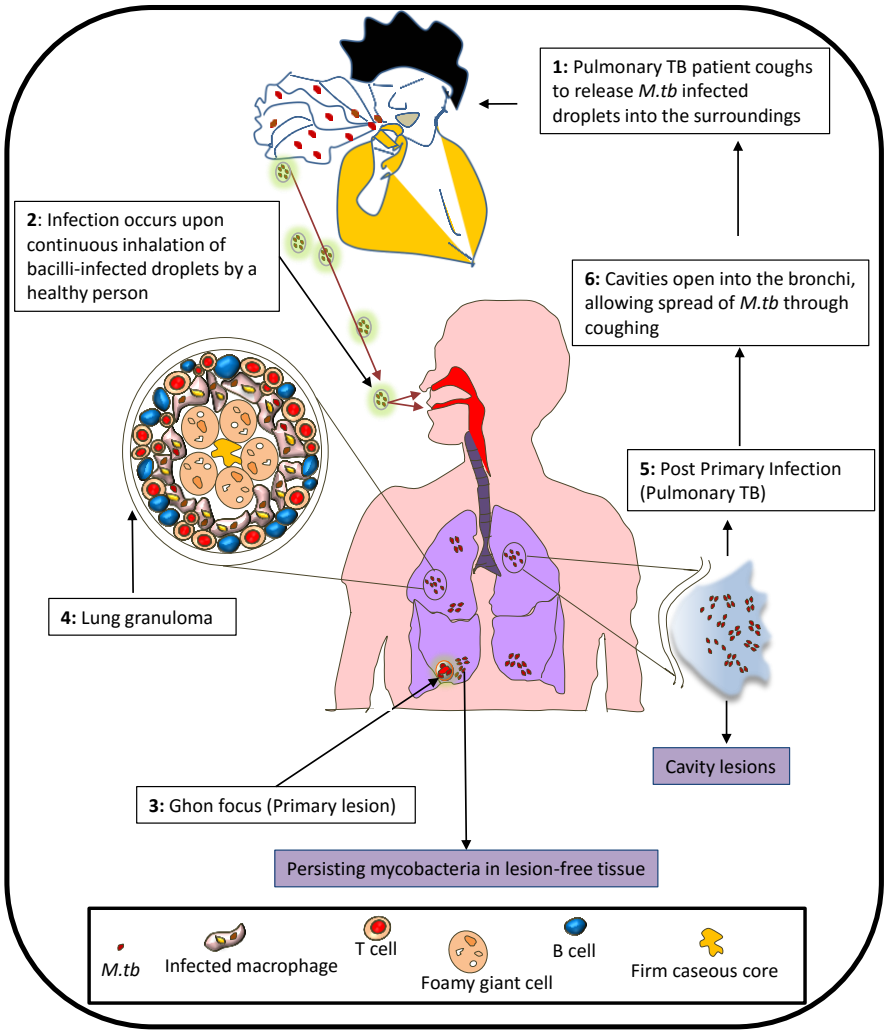


**Figure 2: Transmission cycle of Mycobacterium tuberculosis (*M.tb*).** Pulmonary TB patients release *M.tb* -containing droplets through coughing. Upon inhalation by healthy hosts, the bacilli are captured by alveolar macrophages within the lower parts of the lung to form a Ghon focus. The initial immune response to TB is typified by formation of granulomas to maintain and contain the pathogen. Some patients go on to develop active disease (primary infection) immediately following established *M.tb* infection. 90–95% of infected individuals remains asymptomatic (Latent TB), and may never develop TB. Over time, the remaining 5–10% may develop active TB (reactivation), which occurs at the lung apex. Crucially, *M.tb* drives lung tissue degradation which is critical for cavitation. (Created by P T Brace through adaptation from Anne O'Garra et al, Annu Rev. Immuno. 2013; and P. Elkington et al, Sci Transl. Med. 2011).

## 1.6 Initiation of TB infection

TB infection begins with inhalation of aerosol containing *M.tb*, typically coughed by a person with active Pulmonary TB (Figure 2). Approximately six weeks following inhalation of the bacilli, some patients progress to develop primary infection immediately. Primary infection may result in the dissemination of *M.tb* to other organs such as the brain to cause miliary infection, including TB meningitis. Although miliary TB can be fatal, patients are not infectious and therefore are not a threat to public health. Approximately 90-95% of infected individuals harbour the bacilli in a latent form, remaining asymptomatic and may never develop TB in their life time (O'Garra et al., 2013). The mechanisms that explain latent TB progresses to fully blown active disease are not well understood. At some point of the infection however, *M.tb* may become reactivated in the remaining 5-10% to develop active TB, which can be fatal if left untreated (O'Garra et al., 2013).

Upon inhalation, the infected droplets are initially deposited at the lower zones of the lung which are known to be well-ventilated (Elkington et al., 2011c). Here, what is known as a Ghon focus is formed which characterises the beginning of host immune response to TB (Figure 2). A key aspect of the initial host immune response to curtail TB infection is the capture of *M.tb* by alveolar macrophages, some of which are activated by type I interferons produced locally by the macrophages and cells of the lung tissue. These locally activated macrophages initiate a killing mechanism in attempt to eradicate the ingested *M.tb* (Guirado, 2013).

## 1.7 Host and pathogen immune response

The bacilli have devised various ways of evading host immune response. Virulent *M.tb* successfully replicates and kill the infected, un-activated macrophages due to impaired phagosome maturation process (Guirado et al., 2013). As the infection persists, the adaptive immune response is activated following presentation of *M.tb* antigens by macrophages. T

lymphocytes are recruited to further activate macrophages to wall off the intracellular *M.tb* (Yoder, 2004, Dannenberg, 2009). Peripheral monocytes are subsequently recruited to capture *M.tb* released from dying macrophages. With such limited ability of macrophages to wall off the bacteria however, the whole replication of *M.tb* and killing of macrophages to liberate the bacilli into the surrounding tissue continues. As the immune response persists, production of key antibacterial cytokines and chemokines occur, as well as recruitment of various immunocytes to the site of infection, leading to the formation of granulomas (Figure 3) (Ehlers and Schaible, 2013). Although genetically inherited granulomas are present in conditions such as chronic granulomatous disease (CGD), granuloma development is not unique to TB infection. Other granulomatous disease includes sarcoidosis (development of granulomas in organs such as skin and lymph nodes), chronic foreign body reaction, Leishmaniasis (parasitic disease) and Crohn's disease (inflammation of the intestinal tract).

## 1.8 Granuloma Formation: Hallmark of Tuberculosis

Granuloma formation is the characteristic immune response which forms upon persistent *M.tb* infection, and has long been thought to constrain the bacilli, but rarely able to eradicate it (Russell, 2007, Corbett et al., 2003, Guirado, 2013). Cellular composition of typical granulomas comprise of *M.tb* infected macrophages at the central part of aggregated immune cells including neutrophils, epithelial cells, NK cells, fibroblasts and dendritic cells, all surrounded by a rim of B and T-lymphocytes (Guirado, 2013, Ehlers, 2013). Infiltration of B- and T- cells at the site of the developing granuloma further advance tissue remodelling and accelerate recruitment of uninfected monocytes to ''wall off'' *M.tb* , in attempt to limit bacterial growth and to curtail exacerbation of infection (Lugo-Villarino et al., 2012, Ehlers and Schaible, 2013).

The bulk of TB granulomas are comprised of a variety of macrophage populations which differentiate from mature macrophages at the site of infection (Lugo-Villarino et al., 2012). These include the development of high lipid content which enables macrophages to differentiate into foamy cells (Russel et al, 2009, (Lugo-Villarino et al., 2012); tightly interconnected cell membranes that confers an epithelial-like morphology of macrophages (Adams, 1975); or the fusion together of polarised macrophages to form multinucleated giant cells (Helming and Gordon, 2007, Lugo-Villarino et al., 2012). The presence of granulomas has long been believed to be a host-driven strategy to limit *M.tb* growth and its dissemination (Guirado, 2013). This host protective role of granulomas continues to predominate, albeit a consensus is emerging in recent years which propose with strong evidence that the granuloma may also serve as a fertile ground for *M.tb* proliferation and promotes bacilli pathogenesis (Ehlers and Schaible, 2013).

Granulomas undergo caseous necrosis; a term coined over a century ago to describe a phenomenon whereby the core of TB-associated granulomas undergo extensive cell death and consist of accumulated necrotic material (Guirado, 2013). The solid caseum further undergoes liquefaction, where the extracellular bacilli released from dying macrophages provide an ideal 'culture medium' for further replication of tubercle bacteria, contributing to disease progression (Dannenberg, 1976, Dannenberg, 2009). The exact mechanisms that trigger disease progression from latent to active TB are not fully characterised. Studies suggest that processes that lead to the immune system being compromised trigger reactivation of TB. Such processes include natural causes such as aging, chronic ill health evoked by life style factors including malnutrition, drug and alcohol abuse, smoking as well as HIV co-infection (Onkar Sahota, 2015).

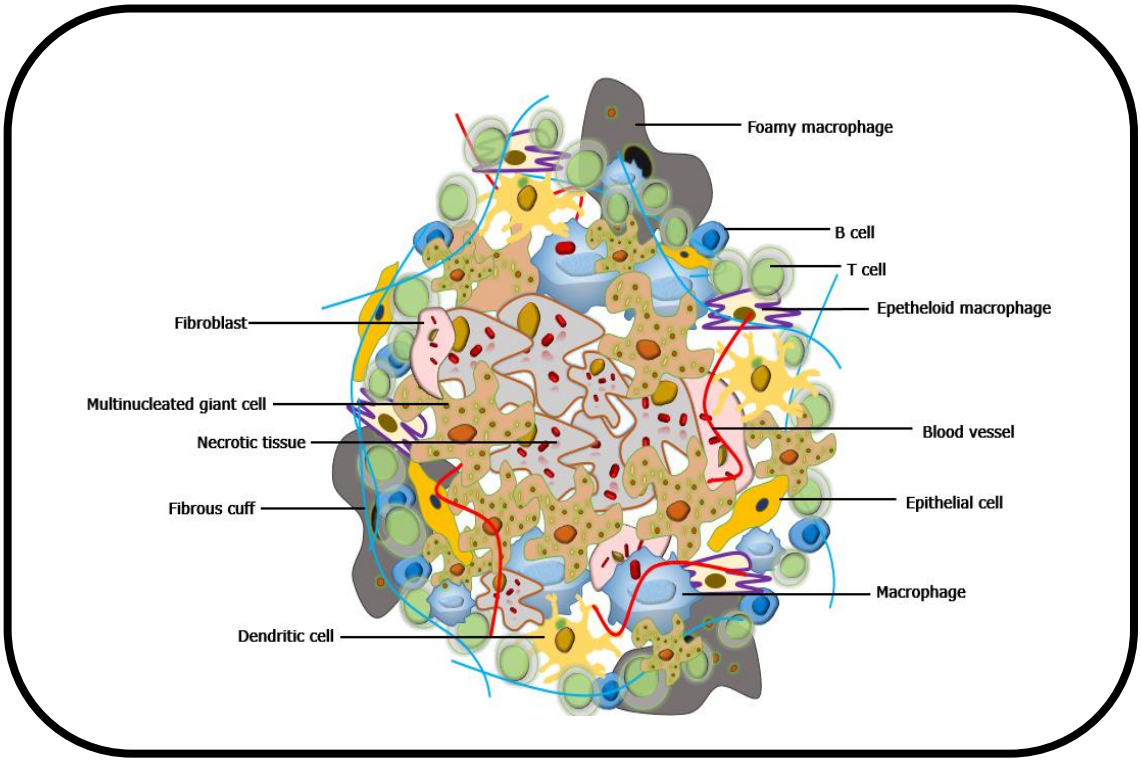


Figure 3: **A schematic representation of tuberculosis granuloma**. Once *M.tb* is captured by alveolar macrophages, the host immune response is triggered. This leads to infiltration of lymphocytes and recruitment of various immune cells to the site of infection. Macrophages further differentiate and develop into foamy macrophages, epitheloid macrophages and multinucleated giant cells. The presence of blood vessels and fibrous cuff contribute to the stability of the granuloma. As the disease progresses the centre of granulomas undergoes caseous necrosis and liquefaction. Granulomas are thought to contain *M.tb* , but have not been proven to eradicate it. Recent emerging evidence suggests that granulomas may also contribute to the success of the bacilli's life cycle (Created by P T Brace by adaptation from E Guirado and L.S Schlesinger, 2013).

As TB infection progresses, some patients develop lung cavitation which manifests in advanced stages of the disease. Here the fine, intricate network of alveoli and extracellular matrix of the lung is completely destroyed, causing extensive large air-filled lung cavity lesions (Elkington et al., 2011c). Lung cavities are clinically thought to be immunoprivileged sites, where not only *M.tb* , but various opportunistic mycobacteria including *M. xenopi* and *M. avium intracellular* are able to colonise and replicate exponentially even amongst individuals with normal immune

response (Yoder, 2004). Similarly, the environmental fungi, *Aspergillus* species which are known to drive disease mainly in patients whose immune systems are severely compromised, are able to successfully form a fungus ball within pre-existing cavities, suggesting immune-privileged nature of the cavity niche (Elkington et al., 2011c).

## 1.9 Lung cavitation in tuberculosis

Lung matrix destruction and cavitation are critical steps that mediate TB transmission (Yoder, 2004, Elkington et al., 2011b). *M.tb* is able to proliferate up to $10^9$ bacilli within cavities (Helke et al., 2006). However, the cellular and molecular mechanisms that lead to formation of such lesions remain yet to be fully understood. Although it has long been demonstrated that patients with smear-negative, culture positive TB are able to transmit disease (Behr, 1999), pulmonary TB patients with cavity lesions have much higher chance of spreading TB. In fact, patients who develop lung cavities are known to be the most infectious (Dye, 2010), and are said to be responsible for the global TB pandemic (Elkington et al., 2011c). The presence of cavities are thought to aid the passage of mycobacterium into the airways, thereby greatly contributing to aerosol transmission upon development of a cough by the patient (Yoder, 2004)

### 1.9.1 Lung cavities exacerbate TB immunopathology

In addition to being the most infectious, patients with cavitary TB are more difficult to treat (Telzak, 1997). Telzak and colleagues investigated the time causes for sputum smears to convert to culture, and demonstrated that smear-positivity from HIV-co-infected TB patients were rapidly converted in cultures following treatment. Conversely, patients with cavitary disease were deemed to be the group with major risk factor for longer time taken for continues observed smear positivity, suggesting slow response to treatment.

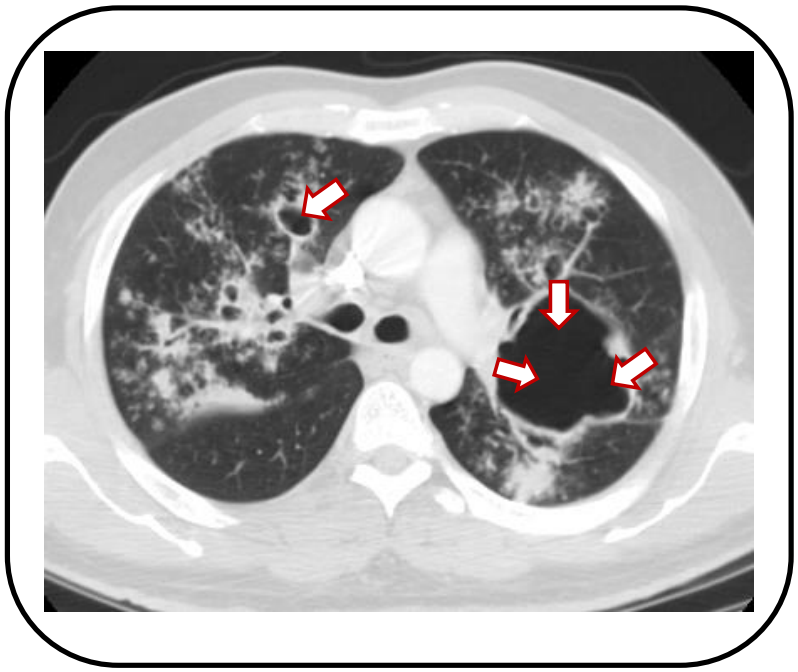

**Figure 4: Lung cavities are several centimetres across.** Given that some cavities (arrowed) are larger than 4cm across, the physical size of cavities present in TB patients suggests the involvement of protease activity (Taken from Paul Elkington *et al*, Sci Trans Med 2011).

Cavitary TB patients have high chance of disease recurrence after treatment (Benator et al., 2002). This clinical trial was to ascertain amongst HIV-negative TB patients the effectiveness of rifapentine/isoniazid combination regimen taken once a week, compared to the established rifampicin/isoniazid combination taken twice a week (Both as a continuation therapy after daily intake of either combination for the first two months of a standard six months regimen). In this study, patients with cavitary disease and patients who presented with initial smear-positivity were identified to be of major risk factors for disease relapse. In particular, 15.8% and 9.5% of cavitary TB patients had disease relapse compared to 3.6% and 2.6% in patients without cavitation in the rifapentine/isoniazid and rifampicin/isoniazid cohorts respectively (Benator et al., 2002).

Cavitary TB patients would be more susceptible to harbouring drug-resistant bacilli. Given the exponential rate at which *M.tb* is able to proliferate in cavities, there is a high probability of the emergence of spontaneous mutations that results in drug-resistant strains. As described above, *M.tb* is able to proliferate up to $10^9$ in cavities and the patient can sometimes continue to appear in good health. One bacterial develops resistant to ethambutol in a population of $10^4$, with resistance to rifampin occurring at 1 in $10^8$ bacterial load (David, 1970). A better understanding of the pathogenesis of cavity formation in TB could therefore lead to the design of therapies to suppress their development and progression, thereby limiting disease transmission.

### 1.9.2 The current paradigm of cavity formation

Lung cavity formation in TB has traditionally been thought to occur at the very last step in the sequence of events that mediate the process of infection to disease progression (Yoder, 2004). Although the mechanism is poorly characterised, pathogenesis of cavity formation has been typically attributed to the effect of various aspects of the host immune response to the bacilli at the site of infection. Cavitation has been linked to the consequences of granuloma caseation and liquefaction, with proposals that granuloma formation is a necessary initial step that leads to lung cavitation (Reviewed by Yoder and co; (Yoder, 2004). Given that cavities can be over 4cm long, it is unlikely that cell death alone is responsible for the development of such large lesions in the lung. This model therefore fails to explain the extent of ECM damage that results in cavities. The severity of the damage caused to lung ECM in cavity lesions suggest the involvement of some sort of enzymatic cleavage of the structural network of the lung (Elkington et al., 2011b).

### 1.9.3 Cavity formation has been mechanistically linked to tissue caseation

In support of claims that mediators of host cellular immunity are responsible for the evolution of cavities in TB, Tsao and colleagues demonstrated potential key roles played by inflammatory mediators such as tumour necrosis factor alpha (TNF-α) and interleukin (IL)-1β (Tsao et al., 2000) in cavity formation. The authors categorised pulmonary TB patients under three groups; patients who presented with cavity lesions that were equal to or greater than 4cm long were considered to have large lesions and were classed as group 1, with patients who had cavity lesions that were less than 4cm long deemed to have small cavities and classed group 2. A third group consisted of patients whose chest radiographs showed no signs of the presence of cavities.

Tsao and co examined the abundance of TNF-α and IL-1β, and compared it to levels of their naturally occurring inhibitors such as soluble TNF-receptors (sTNF-RI and sTNF-RII) for TNF- α binding, and IL-1 receptor antagonist (IL-1RA). IL-1RA competitively blocks the binding of IL-1α and IL-1β to types I/II IL-1 receptors. Samples analysed were broncho-alveolar lavage fluid (BALF) and serum of all groups of TB patients under study. The group demonstrated significant elevation of both TNF-α and IL-1β, with corresponding lower levels of sTNF-RI, sTNF-RII and IL-1RA respectively in BALF and serum samples harvested from patients from group 1, compared to groups 2 and 3. The results lead to the conclusion that TNF-α and IL-1β secreted by macrophages and other immune cells present in granulomas cause tissue necrosis which promotes pathogenesis of TB cavities (Tsao et al., 2000).

Given that both TNF-α and IL-1β are inflammatory mediators, the suggestion that they may contribute to tissue necrosis and cell death within granulomas is plausible. However, attributing the cause of cavity formation to actions of TNF-α and IL-1β alone does not only neglect activities of proteases, it also suggests that cavities solely emanate from

the so called erosion of granulomas following necrosis; a claim which does not explain the lung matrix destruction observed in cavity lesions. Similarly, other groups have linked IL-4 produced by CD4+ and CD8+ T cells in pulmonary TB patients to the development of cavities (van Crevel et al., 2000). As a TH-2 type cytokine, the authors proposed that perhaps IL-4 antagonises host protective responses against tissue necrosis, thereby driving the development of lung cavities. Again, tissue necrosis has been related to the genesis of cavitation, without accounting for the fundamental causes of lung destruction.

$CD4^+$-T cells have been suggested to play a critical role in lung cavitation (Wagner and Bishai, 2001). HIV-co-infected TB patients have low $CD4^+$-T cells, and do not develop cavitation. Even the most severe HIV patients who progress to fully active AIDs suffer rapidly progressive TB which tends to be fatal, and yet have very little chance of developing cavities. This observation suggests that normal levels of $CD4^+$-T cell response in TB patients who are not HIV-co-infected, would promote cavity formation (Wagner and Bishai, 2001). Although intriguing, yet again the model does not take into consideration the extensive lung extracellular matrix destruction involved in cavitation. It does not provide an explanation of how the tensile components of the lung is degraded, thus overlooking the potential role of protease activities.

## 1.10 Protease activities mediate matrix destruction

Destruction of the lung extracellular matrix is critical for lung cavitation and subsequent TB transmission (Elkington et al., 2011a, Rand et al., 2009, Elkington et al., 2011c). However, the exact mechanisms underlying the degradation of lung ECM have not been adequately explained. Cavities are large, air-filled spaces in the lung (Figure 4). The extent of lung ECM destruction observed in cavity lesions in TB must involve some form of protease activity. Using data from humans, mice, rats and rabbit models, Yoder and colleagues reviewed that although

inflammatory and anti-inflammatory mediators involved in host immune response against TB contributes towards cavity formation, tissue-damaging enzymes produced by macrophages and neutrophils must be the most important contributing factors to the pathogenic evolution of cavities in pulmonary TB patients (Yoder, 2004). Other groups have suggested that hydrolytic enzymes, such as proteinase (Cathepsin D), play key roles in cavity formation (Dannenberg, 2009, Dannenberg and Sugimoto, 1976).

There is no evidence to show that such hydrolytic enzymes are primarily responsible for the development of lung cavitation. Although the activities of tissue damaging enzymes were highly elevated in macrophages harvested from granulomatous lesions, moderate levels of the enzymes were recovered from tissues that were at the early stages of caseation and liquefaction, and were greatly diminished or completely absent in late caseating and fully liquefied tissues (Dannenberg, 2009, Weiss and Singer, 1953, Weiss and Boyar-Manstein, 1951, Weiss et al., 1954). These suggest that although hydrolytic enzymes present in completely formed granulomas may play a role during the early stages of caseation and liquefaction, evolution of cavitation in itself could be actively mediated by different type of protease activities. The evidence explaining the potential drivers of lung cavitation in TB suggests that caseation and cavitation may be independent processes. The high degree of lung ECM destruction confirms the involvement of protease activity, particularly those that can destroy the fibrillar collagen structure of the lung such as matrix metalloproteinases (MMPs) (Elkington and Friedland, 2006, Elkington et al., 2011b).

My group has previously reported that MMPs mediate the critical extracellular matrix destruction that result in cavitation in TB (Elkington et al., 2011c, Elkington et al., 2009, Elkington et al., 2005, Elkington et al., 2011b). *M.tb* increased the gene expression and secretion of MMPs-1,-3,-7 and MMP-10 in primary macrophages, with MMP-1 upregulation

being specific to virulent *M.tb* infection (Elkington et al., 2005). Elevated levels of MMP-1 and MMP-3 were detected in BALF and induced sputum taken from TB patients compared to patients with symptoms of other non-TB respiratory conditions (Elkington et al., 2011a). Taken together, it can be speculated that caseation and cavity formation are separate processes in TB pathogenesis, and that MMPs play central role in lung matrix degradation, an important initial step which precedes cavity formation.

## 1.11 Matrix metalloproteinases (MMPs)

Since their discovery in 1962 by Gross and Lapiere as enzymes that are responsible for fibrillar collagen degradation in the tadpole tail during metamorphosis (Gross, 1962), a further 25 related MMP enzymes have been identified.

### 1.11.1 Structure and function of MMPs

Structurally, all mammalian MMPs have a conserved pro-domain consisting of approximately 80 amino acids, and a catalytic domain consisting of 160-170 residues. The active site of MMPs contains a zinc ion and conserved methionine residues (Page-McCaw et al., 2007, Parks et al., 2004, Bode, 1993, Stocker, 1995) (Figure 5). The C-terminus of most MMPs (apart from MMP-7, MMP-23 and MMP-26) contain a hemopexin domain, which is linked to the catalytic domain by a proline-rich flexible hinge region. The hemopexin domain interacts with other proteins such as tissue inhibitors of metalloproteinases (TIMPs) (Parks et al., 2004), and is involved in the recognition of specific MMP substrates (Page-McCaw et al., 2007, Parks et al., 2004, Overall, 2002). The hemopexin domain also plays a regulatory role in activation, localisation and inactivation processes of MMPs.

A number of MMPs are membrane bound and therefore have either one or both transmembrane (TM) and cytoplasmic (Cs) domains. These

include MMPs-14,-15,-16,-24; MMPs-17 and 25 which have glycosylphosphatidyl- inositol (GPI)-anchoring signals, or a signal anchor (SA) at the N-terminal as seen on MMP-23. Other structural features such as the signal peptide (SP), furin-cleavage site (Fr), Cysteine array, the type-V-collagen-like domain (C5), fibronectin repeat (Fn) and the IgG-like domain are present on particular MMPs for specialised functions (not covered in this report)

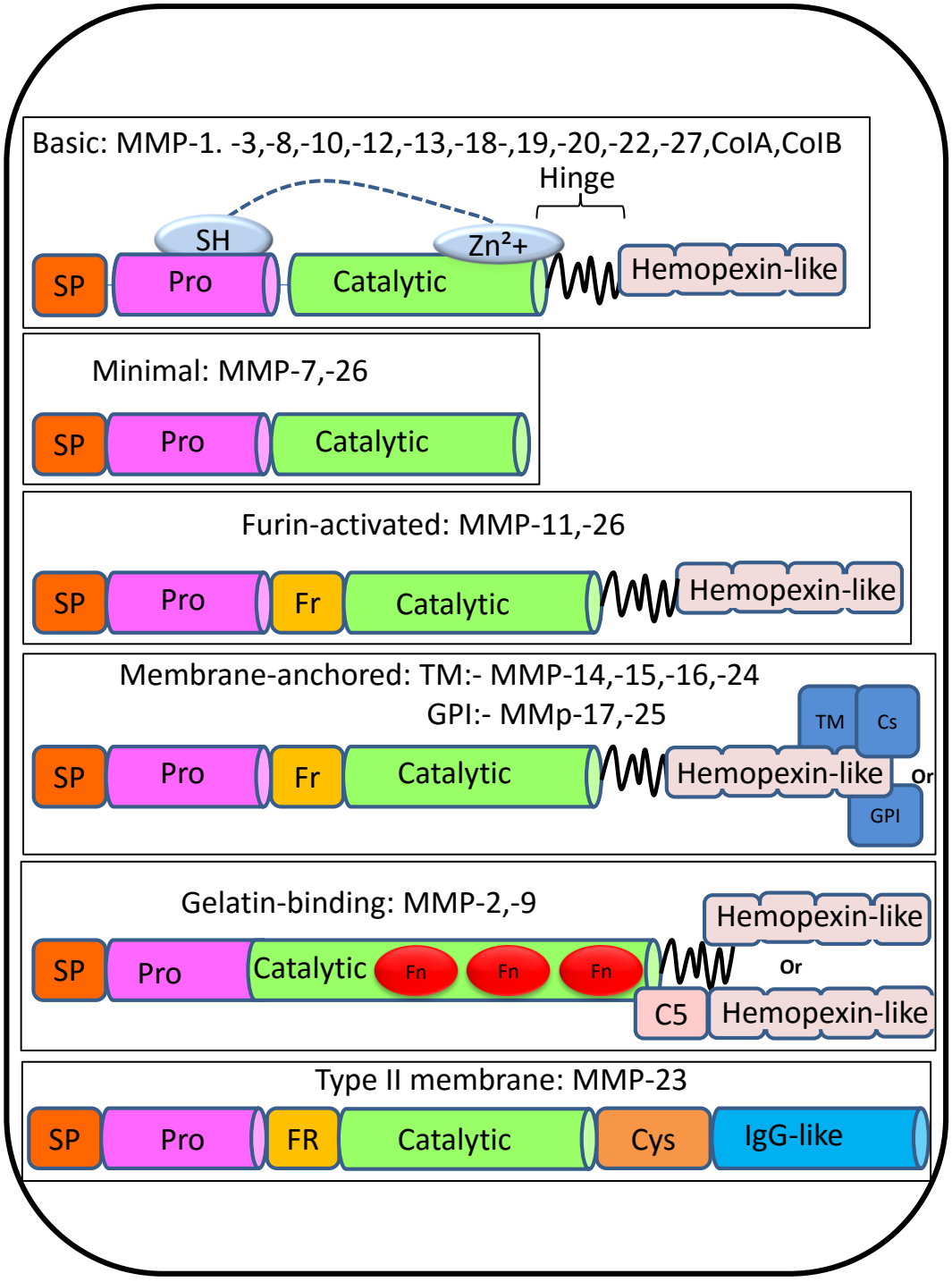


**Figure 5: Schematic representation of the structural features of mammalian MMPs.** The pro-domain contains a thiol group, and the catalytic domain contain zinc. Both domains have evolutionally conserved sequences which are common to all the MMPs shown. The most important structural features are addressed in details in text. (Created by P T Brace by adaptation from W. C Parks et al, 2004)

### 1.11.2 Pathogenic role of MMPs in non-pulmonary diseases

MMPs play critical roles in various diseases, where their up-regulation often correlated with disease severity (Zeng et al., 2006) (Shiozawa et al., 2000, Malemud, 2006, Mancini, 2006). As a result of their ability to turn over the ECM of bone and degrade articular cartilage, MMPs, especially the colagenases-1 and -3 (MMP-1 and MMP-13), have been reported to play active roles in osteoarthritis (Malemud, 2006, Mancini, 2006, Brinckerhoff and Matrisian, 2002). Cancer cells must destroy multiple structural barriers and various components of the ECM to ensure their spread into tissues that are distant from the site of the primary tumour mass. The gelatinases in particular have been shown to be prominent in metastatic cancers, with elevated levels of MMP-2 and MMP-9 correlating with degree of tissue tumour invasion (Mancini, 2006, Jasti S.Rao and Sawava, 1993, Vos et al., 2000). Degradation of the collagen network that forms protective fibrous cap around artheromas have been suggested to be attributed to the ECM destructive function of MMPs produced by macrophages in atherosclerosis and restenosis experimental models (Gasche et al., 2001). Subsequent exposure of the artheromas is the cause of cardiovascular disease.

Actions of MMPs have also been implicated in diseases of the central nervous system (CNS). V. Wee Yong et al extensively reviewed the evidence supporting reports that MMPs are involved in pathogenic neurological conditions. Interestingly, apart from their upregulation in neurological disorders, MMPs are either completely absent or significantly low level are detected in adult human CNS. (V. Wee Yong, 2001). Multiple sclerosis (MS) is an auto-immune disease characterised by axonal loss and demyelination. MMP-9 has been reported to be upregulated in the CNS of patients with MS (with enhanced levels detected in patients experiencing MS relapse than those in remission), but absent in the brains of normal individuals (V. Wee Yong, 2001). The authors explained that

multiple MMPs were induced, particularly MMP-9 and MMP-12 produced by perivascular and parenchymal microglia, CNS infiltrating lymphocytes and macrophages, as well as produced by intrinsic cells of the CNS degrade the ECM of basement membrane which forms a barrier around cerebral capillaries (M.K. Matyszak *, 1996). This results in a breakdown of the blood brain barrier (BBB) and subsequent penetration of cells into the CNS parenchyma where disruption of myelin can occur, contributing to MS pathogenesis (M.K. Matyszak, 1996). A growing body of evidence has linked MMPs to tissue destruction in stroke (Gary A. Rosenberg, 1996, Anne M. Romanic, 1997, Arthur W. Clarka, 1997, V. Wee Yong, 2001). In rat models of focal cerebral ischaemia, MMP-2 and MMP-9 were rapidly elevated (Gary A. Rosenberg, 1996, Anne M. Romanic, 1997). A few days following infarction, neutrophil-secreted MMP-9 was detected in humans, and this persisted up to one week (Arthur W. Clarka, 1997). In other stroke-affected patients, MMP-9 could be detected in their brains even months after their death (Arthur W. Clarka, 1997). Other groups have demonstrated pathogenic role of MMPs in bacterial meningitis (BM). MMP-8 and MMP-9 where significantly up-regulated in CSF of children suffering from BM, and their presence were associated with damage of BBB (Leppert et al., 2000).

There are several mechanisms through which elevated levels of MMPs in the CNS can be neurotoxic. MMP-1 and MMP-2 have both been shown to be toxic to spinal neurons *in vitro*. (Vos, 2000, V. Wee Yong, 2001). Attachment of cells to ECM substrate through integrin signalling is critical for cell survival. By degrading ECM in the CNS, MMPs (particularly MMP-1 and MMP-2) cause neuronal death by interfering with integrin signalling (Wee Yong, 2001). Tumour-necrosis factor (TNF)-α in the brain is toxic to oligodendrocytes. With mechanism similar to the naturally occurring TNF-alpha-converting enzyme (TACE), elevated MMP-7 and MT4-MMP have the capacity to efficiently mediate the conversion of the inactive 26kDa membrane-bound TNF-α to the fully active, pro-inflammatory and mature 17kDa TNF-α, thereby promoting neuro-inflammation (William R.

English, 2000, V. Wee Yong, 2001). In similar regards, MMPs produced in the CNS during pathological conditions can process inactive precursor molecules including transforming growth factors (TGF)-α, FAS LIGAND (FasL), and IL-6 into their active mature forms, enabling these molecules to modulate inflammation.

### 1.11.3 Pathogenic role of MMPs in pulmonary diseases

The architectural framework of the lung is usually protected from degradation that is caused by proteolytic activities (Elkington et al., 2011a, Davidson, 1990, Greenlee et al., 2007) and exposure to harsh conditions, including decades of smoking (Fletcher and Peto, 1977). The lung is composed of fibrillar collagen and matrix components such as laminin, fibronectin, vitronectin and proteoglycans. Even though several MMPs, particularly stromelysin-I,-II, collagenase-III, matrilysin and macrophage metalloelastase have non-specific substrates and can act on multiple components of the lung, collagenase-I,-II and -III are the only MMPs that can cleave types I, II and III fibrillar collagens and are the only proteases that can degrade the native fibrillar collagens of the lung ECM at neutral pH (Elkington et al., 2011c, Page-McCaw et al., 2007, Parks et al., 2004, Kessenbrock et al., 2010).

Recent years have seen the development of animal models of acute and chronic inflammatory lung diseases revealing a functional role of MMPs in the destruction of lung architecture as seen in human emphysema. Human MMP-1 transgenic mice developed extensive lung destruction which presented in the form of large air spaces in the lung, following enhanced MMP-1 activity (D'Armiento et al., 1992b). In a guinea pig model where lung destruction was induced by cigarette smoke, lung collagenase mRNA expression in macrophages, alveolar epithelial and interstitial cells was significantly upregulated, and this correlated with enhanced collagenase activity which was parallel with a reduction in lung collagen (Selman 1996). This pathological phenomenon was reversed

upon administration of a compound that targets a variety of MMPs (Selman 2003).

Several MMPs have been shown to mediate extensive lung destruction in Chronic Obstructive Pulmonary Diseases (COPD) (Finlay et al., 1997). Alveolar macrophages retrieved from COPD patients expressed elevated levels of MMP-1 mRNA, and elastin-degrading proteases compared to control macrophages from healthy individuals. This was associated with increased elastolytic and collagenolytic activities in BAL fluids from the same patients (Finlay GA, 1997).

MMP-1 has been demonstrated to drive lung ECM destruction in TB, a critical process for lung cavitation (Elkington et al., 2011a, Elkington et al., 2011c). Padmini Salgame reviewed evidence of involvement of MMP activities in the formation of granuloma and tissue destruction (Salgame, 2011). The author highlighted that epithelial-cells-secreted MMP-9 mediate recruitment of monocyte to the developing granuloma, and that upon granuloma caseation and necrosis, macrophage-secreted MMP-1 plays a bigger role in the breakdown of lung collagen, leading to tissue destruction(Salgame, 2011).

Mice do not express a functional MMP-1 in their lungs. *M.tb* infected mice may exhibit necrosis but do not cavitate, regardless of the degree of mycobacterium load they are subjected to (Elkington et al., 2011a, North and Jung, 2004, Young, 2009). Mice models over-expressing human MMP-1 were unable to form stable alveolar walls (Greenlee et al., 2007, D'Armiento et al., 1992b), reinforcing MMP-1 activity in degradation of vital structural components of the lung ECM. Expression of MMP-1 in macrophages and infection with a virulent clinical strain led to caseation (AL-Shammari 2015). These studies demonstrate that caseation and cavitation may indeed be separate processes. Further exploration of this field would yield a reward of increased understanding of mechanism of MMP activities during such pathogenic conditions. Particularly, identification of crucial host immune responses that functions to dampen

down MMP secretion in disease would pave a way for novel approaches to enhance such host regulatory responses in order to limit TB immunopathology.

### 1.11.4 Regulation of MMPs

As a result of their potent ability to cause disease when dysregulated, MMPs gene expression and synthesis are very tightly regulated at many different points (Parks et al., 2004, Mancini, 2006, Parks and Shapiro, 2001). MMPs are typically not expressed by resting cells, and they are secreted in their inactive zymogen form when upregulated. A cysteine residue within the pro-domain engages with the zinc ion in the catalytic site to catalytically inactivate the enzyme (Parks et al., 2004, Parks and Shapiro, 2001). Most MMPs are secreted by activated cells. Secretion is either positively or negatively regulated at both transcriptional, post-transcriptional and post-translational levels (Mancini, 2006). Further regulation occurs at their secretion, localisation and activation of pro-enzyme via a mechanism known as cysteine-switch. For activation, the pro-domain can undergo proteolysis or modification to disrupt its interaction with the zinc metal in the catalytic site (Parks et al., 2004, Malemud, 2006, Mancini, 2006, Parks and Shapiro, 2001, Van Wart and Birkedal-Hansen, 1990, Crawford and Matrisian, 1996, Overall et al., 1991, Shapiro et al., 1993a).

Once activated, MMPs can be inactivated by their naturally occurring inhibitors, the tissue inhibitors of metalloproteinases (TIMPs) and also by internalisation (Yang et al., 2001, Barmina et al., 1999). Oxidants that are secreted during inflammatory conditions may also provide additional control by either oxidation of the pro-domain to induce MMP activation, or modify critical residues to trigger a cysteine switch mechanism as described above (Parks and Shapiro, 2001).

In their review, Arturo Mancini *and co* listed several cytokines, chemokines, pathogens and inflammatory mediators that activate MMP

gene expression. Here the authors suggested the involvement of cellular mechanisms, including intracellular protein kinase signalling cascade that may be activated to either negatively or positively regulate MMP production in response to such stimuli (Mancini, 2006). However, these regulations by intracellular signalling pathways are inadequately unravelled in tuberculosis. Although the inflammatory pathways that mediate TB immunity have been explored, host mechanisms that limit pathology are incompletely characterised.

## 1.12 Intracellular signalling pathways

Intracellular signal transduction is initiated upon binding of extracellular ligands such as hormones, cytokines and growth factors to the extracellular portion of a membrane bound receptor including receptor tyrosine kinases (RTK) and G protein–coupled receptors (GPCRs) (Figure 6). This results in activation of kinases that target downstream cellular effectors, generating signalling cascades which culminates in DNA transcription and numerous cellular responses. The binding of pathogens to pattern recognition receptor (PPR) such as Toll-like receptors (TLRs) (explained in detail below) also trigger intracellular signalling which leads to the production of cytokines that mediate immune responses. The best studied intracellular signalling pathways include signalling through PPRs such as TLR signalling, which regulates inflammation; the insulin receptor signalling which regulates glucose uptake; the mitogen activated protein (MAP) kinase and the Phosphatidylinositol-3 Kinase (PI3K) pathways which control cell growth, proliferation and survival.

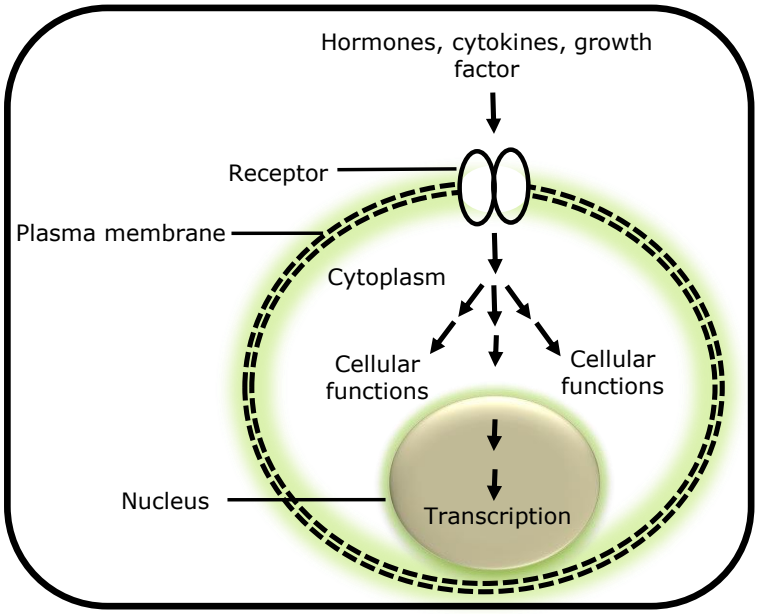


**Figure 6: Principle of cell signalling.** Cell signalling begins when external stimuli such as hormones, cytokines and growth factors bind to the extracellular portion of a membrane-bound receptor. This triggers a series of phosphorylation events at the cytoplasmic domain of the receptor, which interacts with distinct effector proteins in the context of specific phosphorylated amino acid sequences. This activates kinases that mediate the generation of second messages that promote signal transduction events, leading to cellular functions and the transcription of a plethora of genes that are critical for vital physiological functions of the cell (Created by P T Brace).

### 1.12.1 Phosphatidylinositol-3 kinase (PI3K) proteins and their signalling

Membrane inositol phospholipids, the phosphatidylinositols (PtdIns) and their phosphorylated products, the phosphoinositides, have been shown to possess a regulatory role in inflammation and several pathological conditions. PI3K signalling has been implicated in cardiovascular homeostasis, metabolic regulation, angiogenesis and immunity, as well as human diseases such as diabetes and cancer. At the cellular level, PI3K signalling is known to mediate multiple physiological functions such as membrane permeability and transport, cytoskeletal control and regulation

of nuclear events (Di Paolo and De Camilli, 2006, Thomas et al., 2005, Vanhaesebroeck et al., 2010)

Given the existence of eight known PI3K isoforms, exploration of the PI3K pathway is associated with a degree of complexity. PI3K isoforms have been categorised into three main classes (class I, class II and Class III), depending on their structural features and lipid substrate preferences (Figures 7 and 8) (Vanhaesebroeck et al., 2010). Although there is much to be understood about their interaction with upstream signals and their relative functional output, the basic framework of the class I PI3Ks and their signalling are better understood compared to classes II and III. Class I PI3Ks are further divided into class IA and Class IB. Structurally, the class IA PI3Ks consist of p85 type regulatory subunit of which there are five isoforms (p50α, p55α, p85α, p85β and p55γ) in a heterodimeric structure with a 110kDa catalytic subunit, of which there are three isoforms in mammals (p110α, p110β and p110δ) (Vanhaesebroeck et al., 2012, Cantley, 2002, Tzenaki and Papakonstanti, 2013). Whereas both p110α and p110β are expressed in all cells, the p110δ catalytic subunit is predominantly expressed in leukocytes and therefore thought to mediate various immune responses (Cantley, 2002, Tzenaki and Papakonstanti, 2013).

Class IB PI3Ks consist of p110γ catalytic subunit which does not bind a p85 regulatory subunit, but instead interacts with either p101 or P87 (also known as p84) regulatory subunits (Vanhaesebroeck et al., 2010, Di Paolo and De Camilli, 2006). Class IB PI3Ks are known to be activated through GPCRs by interaction between p110γ and the Gβγ subunit of GPCRs (Vanhaesebroeck et al., 2010). On the other hand, class IA PI3Ks are activated upon binding of specific amino acid sequences of phosphorylated tyrosine (pTyr) to Src homology2 (SH2) domains found on all p85 regulatory subunits. The interaction between pTyr and SH2 domains of p85 subunits trigger activation of p110 isoforms through disruption of the p85-mediated repression of class IA PI3Ks, thereby

regulating their recruitment to the plasma membrane where their lipid substrates are localised (Vanhaesebroeck et al., 2010, Cantley, 2002). However, it is becoming increasingly clear that not only class IB, but a number of class I PI3K subunits are probably activated via GPCRs (Vanhaesebroeck et al., 2010, Vanhaesebroeck et al., 2012). For example p110β and p110γ may be directly activated by GPCRs through the Gβγ protein subunit (Vanhaesebroeck et al., 2010). Given the presence of a Ras-binding domain in all p110 subunits, and the fact that both Tyr kinases and GPCRs can activate Ras, class I PI3Ks can therefore be indirectly activated through GPCRs-Ras interaction (Cantley, 2002, Di Paolo and De Camilli, 2006, Vanhaesebroeck et al., 2010).

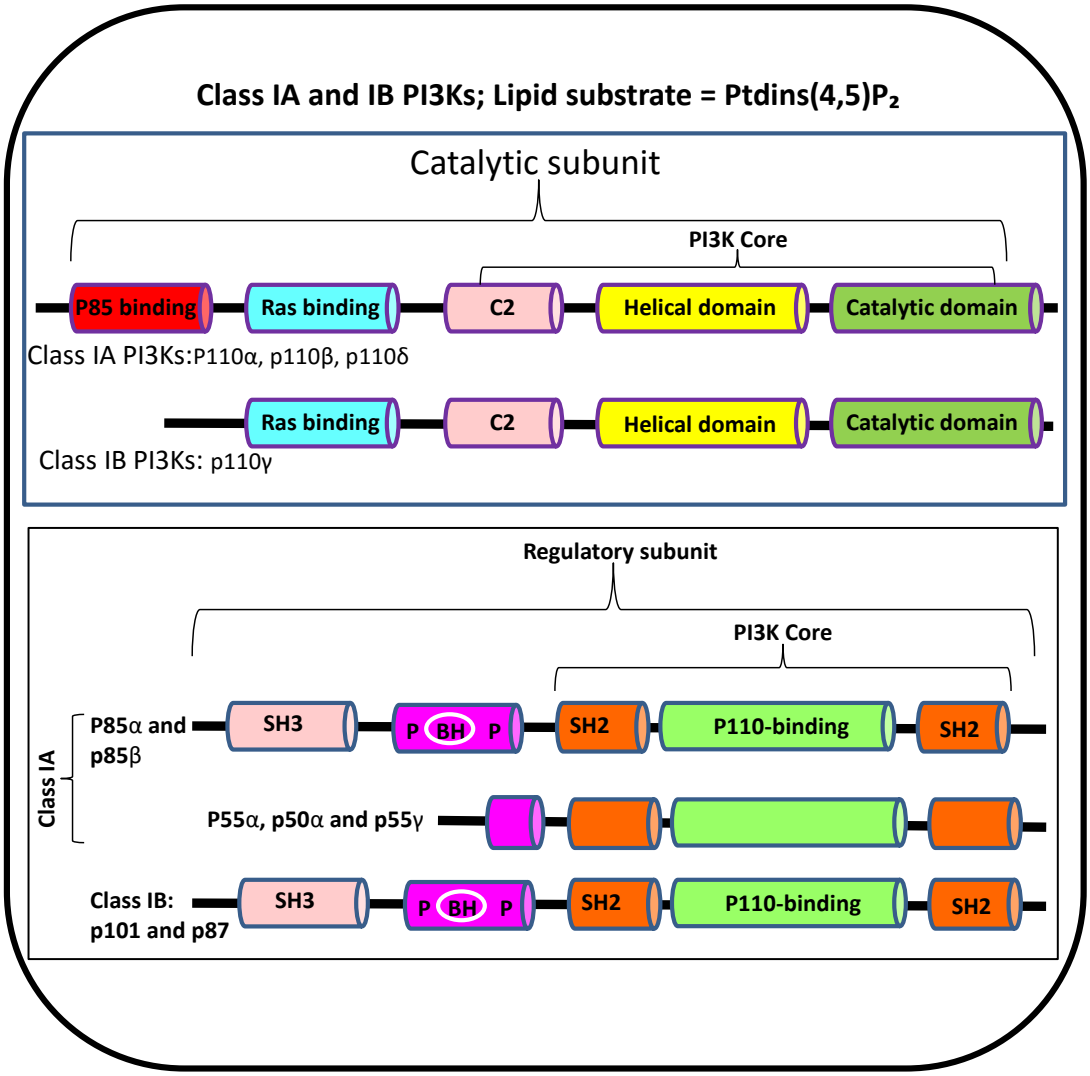


**Figure 7: Structural features of the different classes of PI3Ks.** Class IA PI3Ks come in three isoforms, p110α, p110β and p110δ. They are known to be activated by receptor tyrosine kinases via interaction with their regulatory p85 (or p50/p55) subunits. There is a growing body of evidence suggesting that this class of PI3K proteins may also be activated through GPCRs (See text). Class IB PI3Ks are activated by GPCRs and catalyse the reaction of $PI(3,4,5)P_3$ by p101 interaction. Activation of class I PI3Ks lead to generation of $PI(3,4,5)P_3$ from $PI(4,5)P_2$ . $PI(3,4,5)P_3$ mediate signalling cascade events that lead to cellular responses and the transcription of numerous genes that are critical for the general physiological functions of the cell (Created by P T Brace through adaptation from (Vanhaesebroeck et al., 2010).

Both the direct and indirect activation of p110γ (class IB PI3K) through Gβγ protein subunit or Ras activation respectively involves signal relay via p101 and p87 regulatory subunits (Vanhaesebroeck et al., 2010). Upon input from upstream signals, p101 and p87 differentially respond to generate specific PtdIns(3,4,5)$P_3$ molecules. Whereas the PtdIns(3,4,5)$P_3$ generated by p87-p110γ interaction is believed to mediate downstream intracellular signalling cascade, PtdIns(3,4,5)$P_3$ generated from p101-p110γ binding is endocytosed to motile microtubule-associated vesicles, with their physiological contribution yet to be understood (Kurig et al., 2009, Vanhaesebroeck et al., 2010). The role of class II and class III PI3Ks (Figure 8) in intracellular signalling is not well characterised. Three isoforms of class II PI3Ks (PI3K-C2α, PI3KC2β and PI3KC2γ) are known, but their relative contribution to signal transduction has not been investigated. VPS34 (Also referred to as PIK3C3) is the only known class III PI3K protein, and is thought to be involved in vacuolar protein sorting (Vanhaesebroeck et al., 2010).

Inositol phospholipids consist of an inositol ring and fatty acid chain (Figure 9). PI3K reversibly phosphorylates the 3-hydroxyl group on the inositol ring of either PtdIns, PtdIns-4-phosphate (PtdIns4P) or PtdIns-4,5-bisphosphate (PtdIns(4,5)$P_2$) (Figure 10) to generate seven distinct phosphoinosidites species with diverse roles in signal transduction (Di Paolo and De Camilli, 2006, Vanhaesebroeck et al., 2012, Cantley, 2002). By binding to specific lipid-binding domains (Pleckstrin (PH) homology, FYVE domains and Phox (PX) homology) on the effector proteins, the phosphoinositides mediate recruitment of multiple cytosolic effector proteins to the plasma membrane where their substrates are localised (Cantley, 2002, Di Paolo and De Camilli, 2006, Vanhaesebroeck et al., 2012). This leads to initiation of intracellular signal transduction events that results in regulation of cell proliferation, differentiation, growth, cell metabolism and migration as well as control of cell survival pathways and signalling molecules that mediate various downstream intracellular

events (Cantley, 2002, Di Paolo and De Camilli, 2006, Vanhaesebroeck et al., 2010).

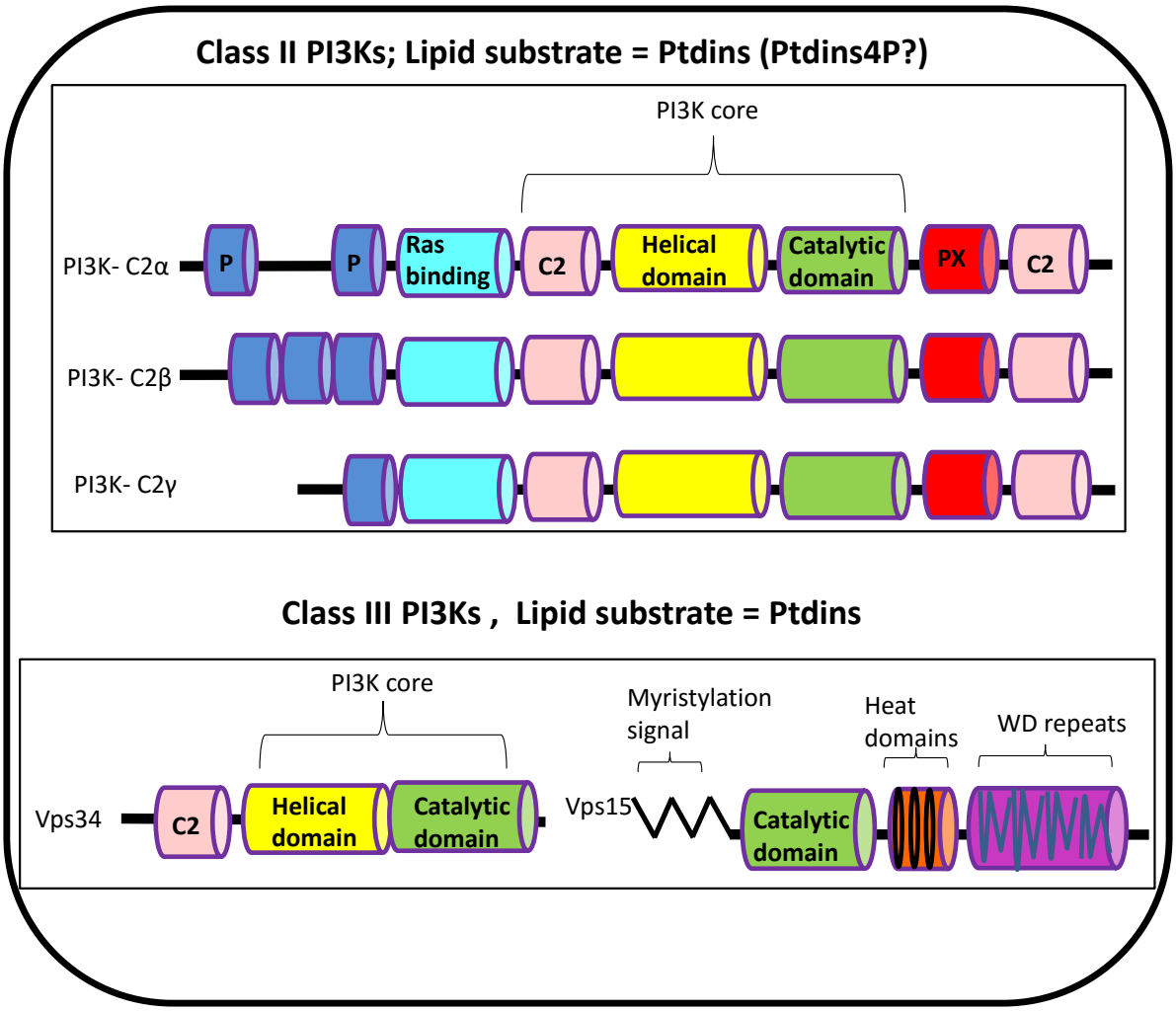


**Figure 8: Structural features of the classes II and III PI3Ks.**The role of class II and class III PI3Ks in intracellular signalling is not well characterised. Three isoforms of class II PI3Ks (PI3K-C2α, PI3KC2β and PI3KC2γ). VPS34 (Also referred to as PIK3C3) is the only known class III PI3K protein, and is thought to be involved in vacuolar protein sorting. Class II and III generate PI(3,5)$P_2$ and PI(3)P respectively. C2 = PKC homology domain 2 (Created by P T Brace through adaptation from (Vanhaesebroeck et al., 2010).

A variety of phosphatases are involved in mediating dephosphorylation reactions at distinct points of the metabolic pathway. The class II and class III PI3Ks mediate the interconversion of membrane inositols directly and indirectly to PI(3)P and PI(3,5)$P_2$ respectively. PI(3)P function as signal tags

within mammalian cell membranes. Here they play important role in phagolysosome maturation during an infection. It has been shown that *M.tb* secretes an acid phosphatase, SapM which antagonises the actions of the class II/III PI3Ks by hydrolysing PI(3)P to PtdIns (PI). By ensuring a PI(3)P-free environment, *M.tb* is able to replicate and survive in host cells for longer periods. Phospholipase C (PLC) catalyses the conversion of $PI(4,5)P_2$ to diacylglycerol (DAG) and $Ins(1,4,5)P_3$, which play critical roles in calcium signalling to elicit various intracellular biological responses. MTM=myotubularin; PTEN=phosphatase and tensin homologue; FAB1=PtdIns(3)P 5-kinase (Taken from Vanhaesebroeck *et al,* 2012).

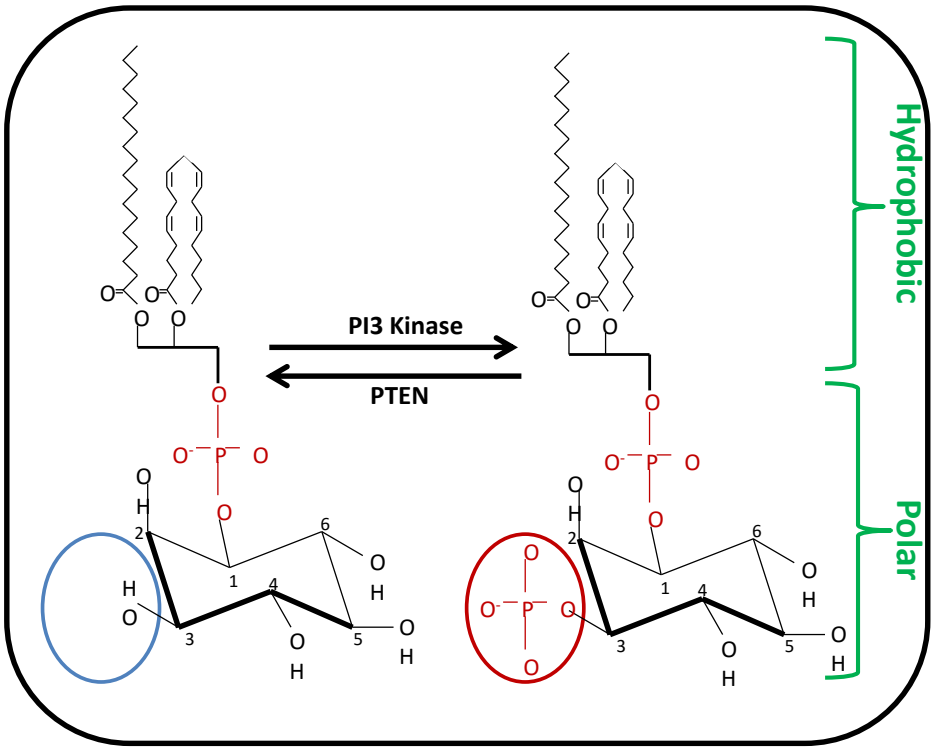


**Figure 9: Phosphoinositide 3-kinase (PI3K) Signalling.** PI3Ks catalyse the phosphorylation of the OH group at the D3-position of the inositol ring (circled blue), to generate lipid second messengers such as $PIP_3$. PTEN is a lipid phosphatase which antagonises the actions of PI3Ks (Created by P T Brace).

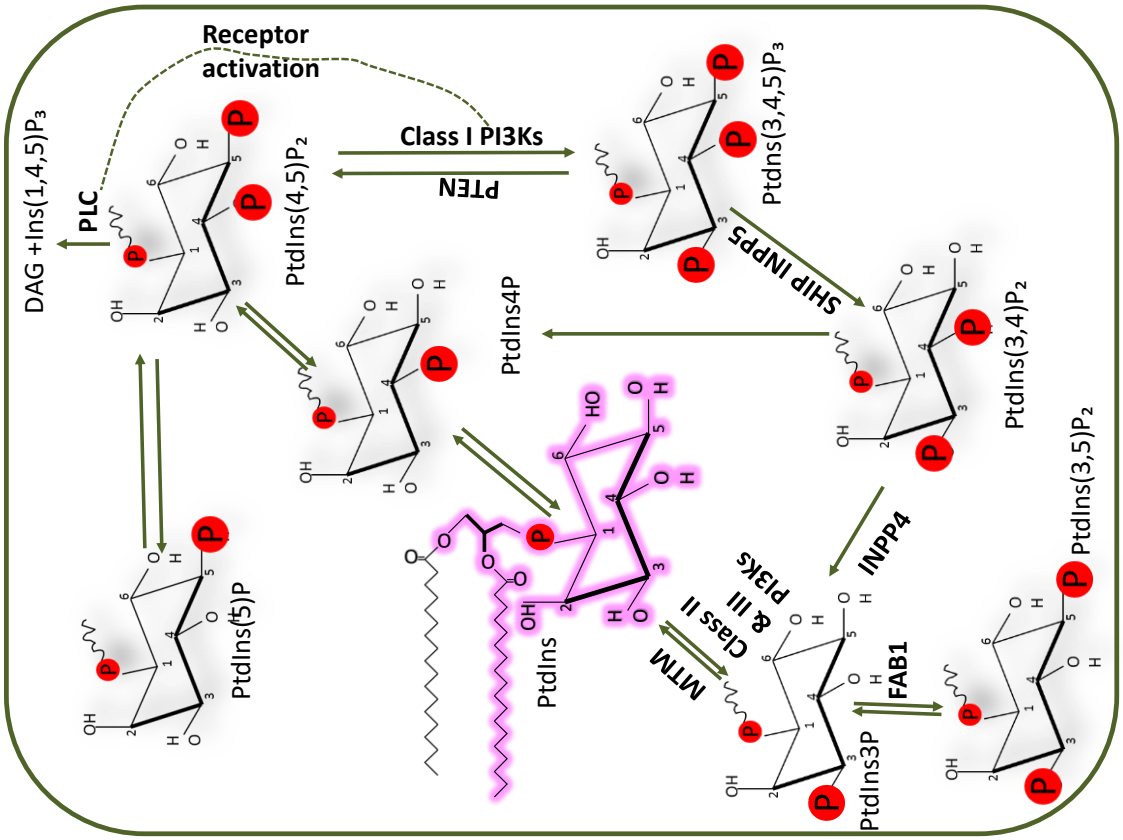


**Figure 10: PI3Ks catalyse reversible phosphorylation reactions in cells.** PI3Ks phosphorylate PtdIns in the above metabolic reaction pathways to generate a number of phosphainositide species. Once activated, the class I PI3Ks catalyse the conversion of $PI(4,5)P_2$ to $PI(3,4,5)P_3$. Dephosphorylation of $PI(3,4,5)P_3$ at the 5-position by SH2 domain-containing inositol 5'-phosphatase (SHIP) and/or inositol polyphosphate 5-phosphatase (INPP5) lead to the production of PI(3,4)P2. Both PI(3,4)P2 and $PI(3,4,5)P_3$ are signalling molecules that mediate various downstream intracellular events. A variety of phosphatases are involved in mediating dephosphorylation reactions at distinct points of the metabolic pathway. The class II and class III PI3Ks mediate the interconversion of membrane inositols directly and indirectly to PI(3)P and $PI(3,5)P_2$ respectively. PI(3)P function as signal tags within mammalian cell membranes. Here they play important role in phagolysosome maturation during an infection. It has been shown that *M.tb* secretes an acid phosphatase, SapM which antagonises the actions of the class II/III PI3Ks by hydrolysing PI(3)P to PtdIns (PI). By ensuring a PI(3)P-free environment, *M.tb* is able to replicate and survive in host cells for longer periods. Phospholipase C (PLC) catalyses the conversion of $PI(4,5)P_2$ to diacylglycerol (DAG) and $Ins(1,4,5)P_3$, which play critical roles in calcium signalling to elicit various intracellular biological responses.

MTM=myotubularin; PTEN=phosphatase and tensin homologue; FAB1=PtdIns(3)P 5-kinase (Taken from Vanhaesebroeck *et al,* 2012

### 1.12.2 Overview of the PI3K pathway

The PI3K pathway is a very complex and yet to be fully understood signalling cascade, consisting of many activators, inhibitors, effectors and second messengers. The pathway is initiated following activation of PI3K in response to cell stimulation by a number of extracellular stimuli including hormones and growth factors. These extracellular stimuli engage cell surface receptors including receptor tyrosine kinases (RTKs) and GPCRs to trigger intracellular signalling cascades such as the PI3K signal transduction (Di Paolo and De Camilli, 2006, Vanhaesebroeck et al., 2010, Cantley, 2002). In the case of signalling through RTKs such as the insulin growth factor-1 (IGF-1), the receptor monomers dimerise upon external growth factor binding, followed by autophosphorylation of specific tyrosine residues on the receptor (Di Paolo and De Camilli, 2006, Thomas et al., 2005, Vanhaesebroeck et al., 2012, Cantley, 2002, Tzenaki and Papakonstanti, 2013). Depending on the receptor, different proteins may bind to phosphorylated Tyrosine (pTyr) domains. For example the insulin receptor substrate-1 (IRS-1) binds to pTyr residues on the activated insulin growth factor-1 (IGF-1) receptor (Tzenaki and Papakonstanti, 2013, Vanhaesebroeck et al., 2010). Receptor bound IRS-1 serves as a binding and activation site for the PI3K protein via the regulatory subunit.

PI3K may also bind directly to specific pTyr residues on a phosphorylated receptor to be activated (Cantley, 2002, Vanhaesebroeck et al., 2012). Active PI3K migrates to the plasma membrane where it typically catalyses the phosphorylation of phosphatidylinositol-4,5-bisphosphate ($PI(4,5)P_2$ (also known as $PIP_2$) to generate phosphatidylinositol-3,4,5-trisphosphate ($PI(3,4,5)P_3$, also known as $PIP_3$) (Figure 9) (Di Paolo and De Camilli, 2006, Thomas et al., 2005, Vanhaesebroeck et al., 2012, Cantley, 2002, Tzenaki and Papakonstanti, 2013). As described above, by associating with the PH, FYVE and PX domains of distinct effector proteins, $PIP_3$ mediates the accumulation and activation of specific cytosolic proteins at the plasma membrane (Vanhaesebroeck et al., 2012, Vanhaesebroeck et al., 2010, Di Paolo and De Camilli, 2006, Cantley, 2002). For example $PI(3,4,5)P_3$ phosphorylates PH

domain containing effector proteins such as guanosine nucleotide exchanging factors (GEFs) and guanosine triphosphatase (GTPase)-activating proteins (GAPs). GAPs control the activities of small GTPases, thereby regulating cell locomotion (Cantley, 2002). Two of such cytosolic effector proteins that are of particular interest in PI3K signalling are the Serine/Threonine kinases phosphoinositol-dependent kinase-1 (PDK-1), and the mammalian homologue of retroviral transforming protein v-AKT, simply known as AKT (also as PKB). PI(3,4,5)$P_3$ phosphorylates PDK-1 and AKT to mediate their recruitment to the plasma membrane. In order for AKT to be fully activated, it requires phosphorylation by PDK-1 on Thr 308 and phosphorylation by the mammalian target of rapamycin complex 2 (mTORC2) on Ser 473 (described below) (Tzenaki and Papakonstanti, 2013, Cantley, 2002).

AKT is a proto-oncogene with a plethora of substrates and effectors including the tumour suppressor transcription factor, Forkhead-related transcription factor-1 (FKHR-L1) (also known as Forkhead box O-class (FOXO)), the apoptosis-inducing protein, Bcl-2-associated death promotor (BAD) protein, glycogen synthase kinase (GSK)-3α/β, the tumour suppressor, p27 and mTORC-1, which are all involved in regulation of biological responses (Figure 11). AKT phosphorylates most of its target proteins to inhibit their activity, or in some cases, mediate their activation (Di Paolo and De Camilli, 2006, Thomas et al., 2005, Vanhaesebroeck et al., 2012, Cantley, 2002, Tzenaki and Papakonstanti, 2013).

AKT prevents FOXO from inhibiting proliferation. FOXO contains binding site for the 14-3-3 family of proteins, but the two proteins do not interact in quiescent cells. Upon AKT phosphorylation and subsequent activation of FOXO, the 14-3-3 protein binding sites become available for formation FOXO-14-3-3 protein complexes, which are retained in the cytosol (Tzenaki and Papakonstanti, 2013, Huang and Tindall, 2011). AKT phosphorylation of FOXO therefore excludes it from the nucleus, promoting transcription of cyclin D1 to enable cell cycle entry, and suppressed transcription of the p27 CDK inhibitor (CK1) (Tzenaki and Papakonstanti, 2013). Once FOXO accumulates in

the cytoplasm, cell death is inhibited as transcription of FasL is suppressed (Tzenaki and Papakonstanti, 2013). Phosphorylated FOXO is also a substrate of the enzyme ubiquitine lipase, which transfers ubiquitine peptides onto the protein. Ubiquitinated FOXO is then destroyed by a complex of proteases in the proteosome, thereby promoting cell proliferation (Huang and Tindall, 2011). Similar to AKT interaction with FOXO, phosphorylation of BAD by AKT allows the 14-3-3 binding site on BAD to be made available for 14-3-3 protein interaction. This way BAD is not available to bind Bcl-2 and Bcl-x, thereby enabling the free Bcl-2 and Bcl-x to promote cell survival (Vanhaesebroeck et al., 2012, Cantley, 2002, Tzenaki and Papakonstanti, 2013).

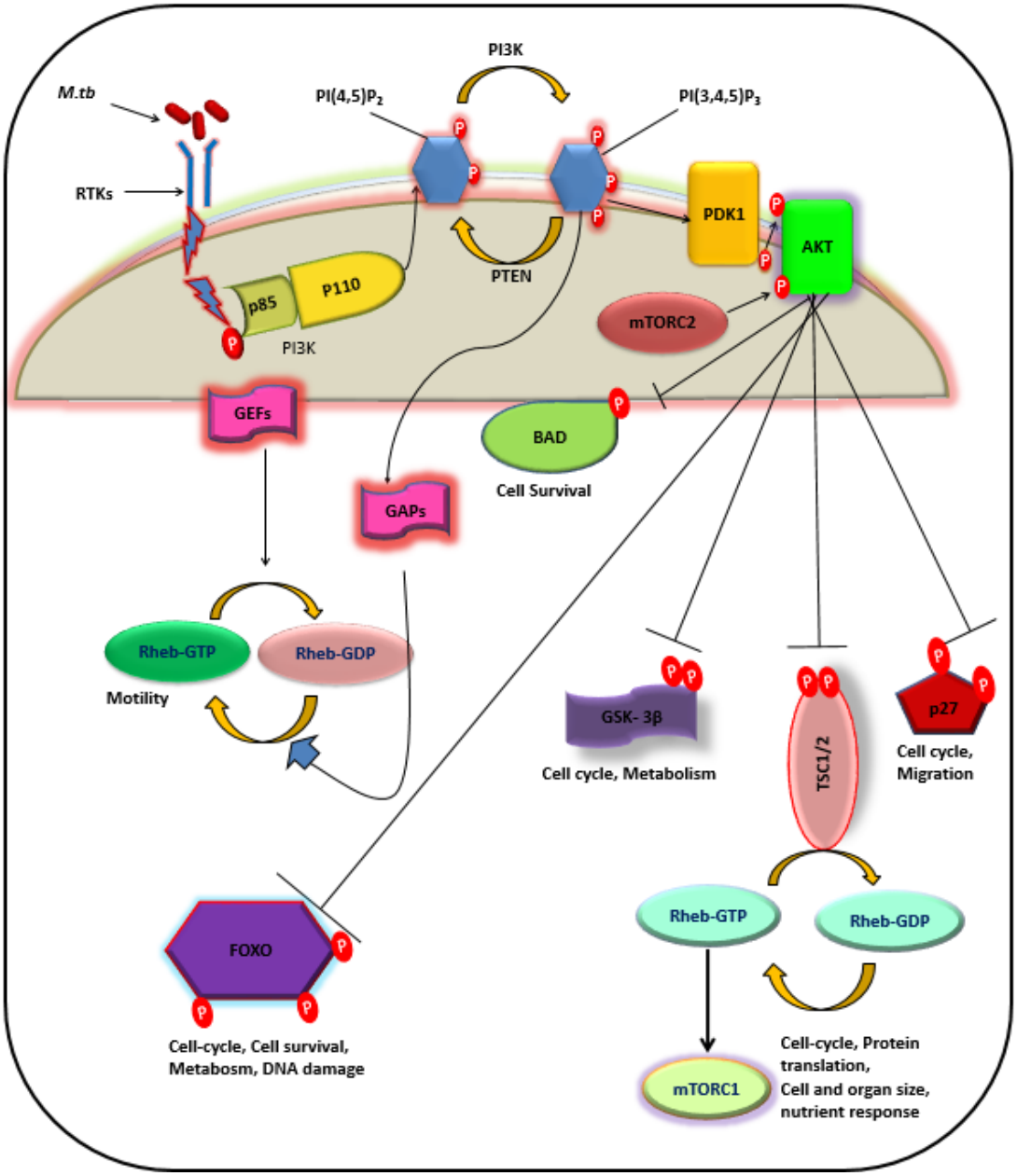


**Figure 11: A Highly simplified schematic representation of the role of class IA PI3Ks.**The class IA PI3Ks catalyse the generation of intracellular signalling molecules that mediate downstream events to bring about numerous biological responses. Each pathway has been discussed in the text above. In a completely different mechanism of activation, PI3Ks bind to active GTP-bound form of the small membrane bound GTPase, Ras leading to activation of the p38, Erk/Mek/MAP Kinase pathway (mechanism described below) (Created by P T Brace by adaptation from N. Tzenaki and E Papakonstanti 2013).

GSK-3β (and GSK-3α) are constitutively active in unstimulated resting cells, and they phosphorylate their downstream substrates including cyclin D, glycogen synthase and c-Myc to inhibit or promote degradation of their activity (Tzenaki and Papakonstanti, 2013, Cantley, 2002). By phosphorylating GSK-3, AKT mediates its dissociation from proteins that GSK-3 normally interacts with to inhibit, thereby resulting in activation of signalling pathways that are normally repressed by GSK-3β (and GSK-3α), such as glycogenesis and cell cycle entry (Cantley, 2002). AKT phosphorylates and suppresses the actions of the tumour suppressor p27 (as well as many other tumour suppressors not discussed in this report), thereby promoting cell proliferation (Di Paolo and De Camilli, 2006, Vanhaesebroeck et al., 2012, Cantley, 2002, Tzenaki and Papakonstanti, 2013).

Furthermore, through phosphorylation of tuberous sclerosis complex 1/2 (TSC1/2), AKT activates Ras homologue enriched in brain (Rheb) by preventing TSC1/2 from inactivating Rheb. Activated Rheb in turn activates mTORC-1, which interacts and activates the translation factor p70 ribosomal S6 kinase (also known as S6K) (Tzenaki and Papakonstanti, 2013, Cantley, 2002). As well as AKT, PDK-1 also phosphorylates p70 S6-kinase to activate it, allowing S6K to mediate ribosomal biogenesis and translation of specific mRNA transcripts (Cantley, 2002). Cytokine-independent survival kinase (CISK) is closely related to AKT, and has similar downstream signalling properties. Although the physiological functions of protein kinase-Cζ (PKCζ) in response to upstream signals are not fully elucidated, their signalling is thought to contribute to cellular response. PDK-1 therefore further phosphorylate both CISK and PKCζ to promote biological responses and cell survival (Cantley, 2002).

In order to terminate the actions of PI3K signalling, two main different phosphatases, the phosphatase and tensin homologue (PTEN) and the SH2 domain-containing inositol 5'-phosphatase (SHIP1/2) mediate dephosphorylation of the 3' and 5' position of $PI(3,4,5)P_3$ respectively (Di Paolo and De Camilli, 2006, Thomas et al., 2005, Vanhaesebroeck et al., 2012, Cantley, 2002, Tzenaki and Papakonstanti, 2013). This generates $PI(4,5)P_2$ in

the case of PTEN, and $PI(3,4)P_2$ following dephosphorylation by SHIP1/2. $PI(3,4)P_2$ is also an intracellular signalling molecule which mediate PI3K-dependent signalling events that are completely separate from that of $PI(3,4,5)P_3$. (Vanhaesebroeck et al., 2012, Cantley, 2002). Mutations in PTEN in particular leads to continues activation of the PI3K pathway, and this has been identified as the cause of many cancers. As described above, by activating AKT, PI3K signalling feeds into mTOR signalling which is also critical in regulating cell growth and survival. For this reason, the PI3K pathway is often referred to as the PI3K/AKT/mTOR axis of intracellular signalling.

## 1.13 The TOR proteins, mTOR complexes and their functions

Target of rapamycin (TOR) are protein kinases found in all eukaryotes. The human version is known as mammalian target of rapamycin (mTOR), and is very important in the control of a variety of cellular functions. Structurally, TOR proteins have different domains, with a kinase domain similar to that of PI3-kinases. Best known features of TOR proteins include Huntington elongation factor 1A-protein phosphatase 2A-A subunit-TOR (HEAT), FKBP12-rapamycin-binding (FRB), PI3-kinase-related kinase(PIKK), FATC (FAT, C terminal), RD (regulatory domain) and FAT (FRAP, ATM, TTRAP2) domains (Figure 12) (Choi et al., 1996, AlQurashi et al., 2013). FRB domain confers sensitivity to inhibition by rapamycin; Rapamycin binds together with FK506-binding protein, 12kDa (FKBP12) to the FRB domain on the mTOR protein to inhibit it (Laplante and Sabatini, 2012, Bhaskar and Hay, 2007, AlQurashi et al., 2013)

Two types of mTOR complexes exist; mTORC-1 and mTORC-2 (Figure 12B and C), with each complex having a distinct cellular functionality (Guertin and Sabatini, 2007, Hwang and Mendell, 2006, AlQurashi et al., 2013). Whereas mTORC-1 is rapamycin sensitive, mTORC-2 is not (AlQurashi et al., 2013). mTORC-1 contains mTOR, which interacts with the rapamycin sensitive target proteins GβL/mLST8 (G protein beta subunit-like/mammalian lethal with Sec 13 protein 8), RAPTOR (regulatory-associated protein of mTOR), DEPTOR, and

PRAS40 (Choi et al., 1996, AlQurashi et al., 2013). mTORC-2 comprises mTOR, which interacts with a set of different protein components. These are RICTOR, DEPTOR, PROTOR, SIN1 and GβL/mLST8. mTORC-1 and mTORC-2 also differ in their effector proteins (AlQurashi et al., 2013, Choi et al., 1996). The most studied substrate of mTORC-2 is AKT, which is downstream of the PI3K pathway (Guertin and Sabatini, 2007, Brown et al., 2011). mTORC-2 has been shown to regulate cell growth and survival by activating AKT to promote PI3K signalling (Bartel, 2004). Regulation of actin cytoskeleton by mTORC-2 via activation of PKCα has also been reported (Gregory et al., 2005). Unlike mTORC-2, more is known about the functions of mTORC-1. Signalling through mTORC-1 represses autophagy, regulates metabolism, and promotes ribosomal biosynthesis and mRNA translation to regulate cell growth and proliferation.

### 1.13.1 Active mTORC-1 promotes ribosomal biogenesis and eukaryotic translation initiation

The two most studied substrates of mTORC-1 are S6K1 and eukaryotic initiation factor- 4E (eIF4E)-binding protein (4E-BP) (Reviewed by (Mendoza et al., 2011), both of which play key roles in ribosomal biogenesis and mRNA translation (Mendoza et al., 2011). In resting cells, 4E-BP interacts through the YDRKFLM biding motif, and sequesters the $m^7$GTP-cap mRNA binding protein, eIF4E (Martelli et al., 2011). When bound to eIF4E, 4E-BP represses mRNA translation by preventing eIF4E from binding to eIF4G (described below) and the $m^7$GTP-cap structure of mRNA, thereby disrupting formation of a stable eukaryotic translation initiation complex, eIF4F (Martelli et al., 2011, Anne-Claude Gingras et al., 1999). This leads to the repression of 5'-cap-dependent translation of mRNA (Hay, 2010, Anne-Claude Gingras et al., 1999). Upon phosphorylation by active mTORC-1, 4E-BP is hyper-phosphorylated at multiple sites to cause its inactivation and detachment from eIF4E (Sonenberg, 2008, Bhaskar and Hay, 2007, Martelli et al., 2011),

permitting the docking of translation factors that form eukaryotic translation initiation complex (eIF4F) at the 5'-untranslated region (5'-UTR) of mRNA.

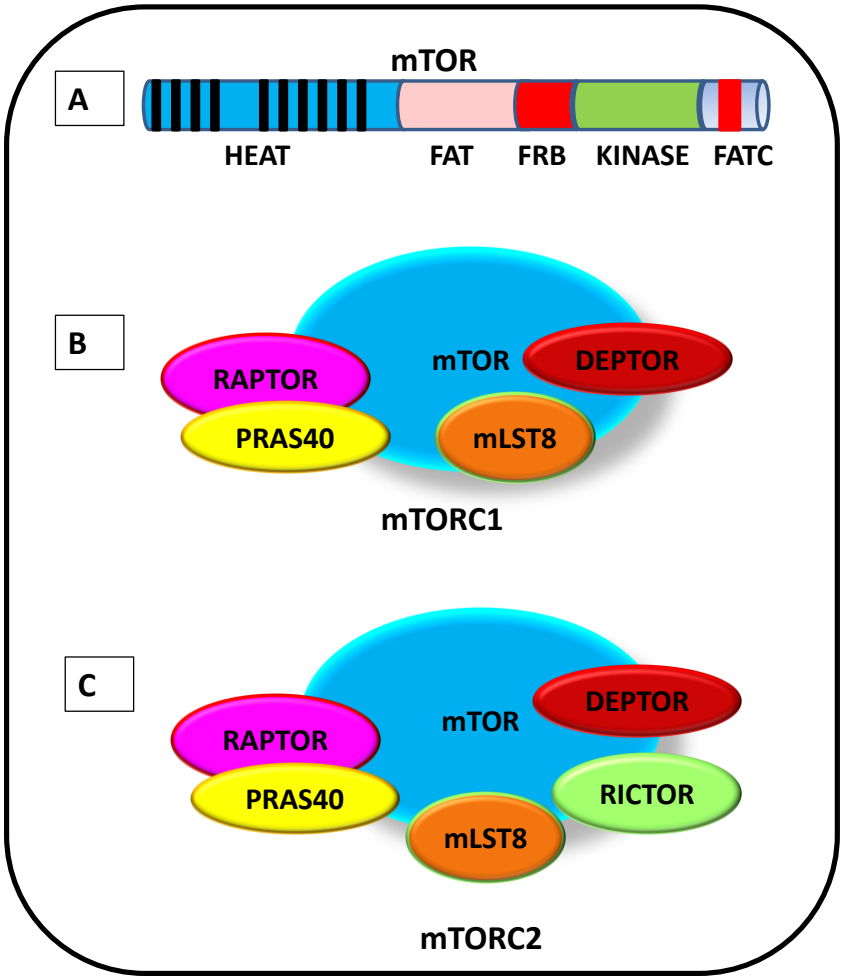


**Figure 11: Structural features of TOR protein and mTOR complexes. A:** Main features of mTOR protein. **B:** Schematic diagrams of mTORC-1 and **C:** mTORC2 protein complexes. (See text for detailed description of the features of mTORC-1 and mTORC2). mTORC-1 is the best studied complex of the two, and its activation drives ribosomal biogenesis and mRNA translation (Created by P T Brace through adaptation from (AlQurashi et al., 2013).

Eukaryotic protein synthesis requires the formation of a stable eIF4F. This begins by the assembly of a variety of translation initiation factors (eIF) including eIF4E (cap-binding protein), eIF4A (helicase) and eIF4G (scaffolding

protein), each of which has multiple isoforms in eukaryotes, and constitute the core units of eIF4F complex (Anne-Claude Gingras et al., 1999). Other accessory components crucial for cap-dependent translation include eIF4B (co-factor of eIF4A) and eIF3 (binds small 40S ribosomal complex) (Pyronnet et al., 1999, Hay, 2010, Furic et al., 2010, Raught and Gingras, 1999).

Each translation initiation factor contributes towards the formation of a stable eIF4F complex to enable the initiation of mRNA translation. Free eIF4E associates with the scaffolding protein eIF4G through the binding motif, YDREFLL (Wang et al., 2012). Coupling of eIF4E to eIF4G enables eIF4E to bind $m^7$GTP-cap on the 5'-UTR of the precursor mRNA which also contains poly-A tail, bound to Poly (A)-binding protein (PAB or PABP) at the 3'-UTR (Pyronnet et al., 1999, Scheper and Proud, 2002b, Martelli et al., 2011). The eIF4G-eIF4E- $m^7$GTP-cap-mRNA complex is said to form the rate limiting step in eukaryotic protein synthesis. The precursor mRNA contains secondary, inhibitory, hairpin structures that serve to prevent premature translation to occur. Binding of eIF4E to the $m^7$GTP-cap mRNA induces recruitment of eIF4A and its co-factor eIF4B to the complex, by eIF4A binding to eIF4G (Wang et al., 2012, Raught and Gingras, 1999). The helicases eIF4A and eIF4B mediate unwinding of the secondary structures on the mRNA, permitting the mRNA to be fully available for translation. By associating with the small 40S ribosome, eIF3 regulates the docking of 40S ribosomal subunit onto the eIF4F complex by positioning it in close proximity with the ribosomal exit site (Lee and Pelletier, 2011). By serving as a central adaptor module in the pre-initiation complex, eIF4G also interacts with the c-terminal region of PABP bound to the 3'-UTR end of the mRNA, thereby causing the classic circularised loop structure of translation complex. Following eIF4A helicase activity, the mRNA binding channel is said to be in an 'open' conformation for 40S ribosome to be able to begin mRNA scanning, delivery of transfer RNA (tRNA) and recognition of the start codon (AUG) (Lee and Pelletier, 2011). Recognition of the start codon marks the beginning of protein synthesis.

Another downstream target of mTORC-1 is S6K1. Unlike the inhibitory effect conferred on 4E-BP, mTORC-1 phosphorylates S6K1 to activate it. Phosphorylation of S6K1 occurs at two crucial sites; within the catalytic activation loop on Threonine 229 (T229), and within the hydrophobic motif on T389 residues (reviewed by Martin and Blenis, 2002, marina K Holz)(Saitoh et al., 2002, Pullen and Thomas, 1997). In quiescent cells, S6K1 interacts with eIF3 in a complex which keeps S6K1 inactivated. Once phosphorylated by mTORC-1 on T389, S6K1 dissociates from eIF3 (Anne-Claude Gingras et al., 1999). The phosphorylation of S6K1 by mTORC-1 stimulates PDK1 to phosphorylate S6K1 on T229 (Alessi et al., 1998; Frodin et al., 2002)(Pullen and Thomas, 1997), reinforcing its full activation. Activated S6K1 phosphorylates to activate component of the ribosome, S6 ribosomal protein (S6), which interacts with eIF3, and the translation factor eIF4B on Serine 422 (S422), thereby contributing to ribosomal biogenesis and mRNA translation (Peterson and Schreiber, 1998).

The MAP-Kinase-interacting kinases, Mnk1 and Mnk2 (described below) are another key regulator of mRNA translation. These kinases are activated by p38 and extracellular signal-regulated kinase (Erk) MAP-kinases, which are both downstream of the Ras to MAP kinase pathway (explained below) (Scheper and Proud, 2002a). Similar to mTORC-1, Mnk protein kinases regulate mRNA translation by phosphorylating to further activate eIF4E on Ser 209 (Furic et al., 2010, Ueda et al., 2010).

## 1.14 MAP-Kinase-interacting kinase (Mnk) signalling

The Mnks are downstream of p38 and Erk, which are important components of the MAP kinase pathway. This pathway is activated by mitogens, heat shock, osmotic stress, and pro-inflammatory cytokines (Hay, 2010). Activation of the MAP kinase pathway can also begin by activation of the membrane bound small GTPase, Ras. Similar to PI3K pathway activation, the binding of external stimuli such as extracellular growth factor (EGF) to the external part of

extracellular receptors such as the RTK and TLRs (discussed below) also trigger the initiation of Ras/Erk/MAP kinase pathway (Figure 13).

Following autophosphorylation and dimerization of the cytoplasmic domain of the membrane bound receptor as described above, growth factor receptor bound protein-2 (GRB2) interacts with phosphotyrosines on the RTK via its SH2 domain. This triggers recruitment of SOS (son of sevenless in Drosophila) to the membrane where it is in close proximity with GRB2 and Ras (Skolnik et al., 1993, Mendoza et al., 2011). Interaction between GRB2 and SOS causes SOS to be activated, which in turn binds to the inactive GDP bound Ras. SOS is a Ras guanosine triphosphate exchange factor (GEF), which catalysis exchange of GDP for GTP to activate Ras. Similar to AKT, active Ras has several effector proteins including Raf kinase (Figure 13) (Mendoza et al., 2011).

Activated Raf triggers a kinase cascade, beginning with the activation of MEK1/2, which in turn phosphorylates and activates Erk1/2, culminating in the activation of the transcription factors Jun and Fos. These are members of the activated proetein-1 (AP-1) transcription factors family. Activated Jun and Fos translocate to the nucleus, form a heterodimer and interact with the AP-1 motif of DNA. This results in initiation of various gene expressions to activate cell proliferation (Mendoza et al., 2011).

### 1.14.1 Active Mnk1 drives cap-dependent eukaryotic translation initiation

Once phosphorylated and activated by Erk and p38 Map kinases, Mnks feed into the mTORC-1 pathway by further activating eIF4E to promote mRNA translation (Figure 13) (Hay, 2010, Mendoza et al., 2011). As described above, mTORC-1 phosphorylates 4E-BP, causing it to dissociate from eIF4E, thereby liberating eIF4E to interact with eIF4G and bind 5'-cap structure portion of the mRNA to be translated. To maximise its activation, Mnk1 and Mnk2 post-translationally modify eIF4E by phosphorylating it on serine 209 (Scheper and Proud, 2002a, Hay, 2010). Instead of directly forming a stable binary complex with eIF4E, Mnk requires binding to eIF4G in order to phosphorylate eIF4E

(Pyronnet et al., 1999). Mnk1 interaction with eIF4G enables Mnk to be localised in close proximity to its substrate, eIF4E. For this reason, phosphorylation of eIF4E by Mnk is believed to take place after eIF4E and eIF4G interact together in a complex (Pyronnet et al., 1999, Hay, 2010). Although eIF4E has been the best known substrate of the Mnks, recent studies have identified other Mnk targets including PSF.p54$^{nrb}$(polypyrimidine tract–binding (PTB) protein associated splicing factor) and hnRNP A1 (Heterogeneous nuclear ribonucleoprotein A1) (Buxade et al., 2008) (Reviewed in discussion session). Although various coordinated events and complexes mediate protein synthesis, formation of stable eukaryotic translation initiation complex crucially require tight regulation by the PI3K/AKT/mTOR and Ras/Map kinase signalling pathway

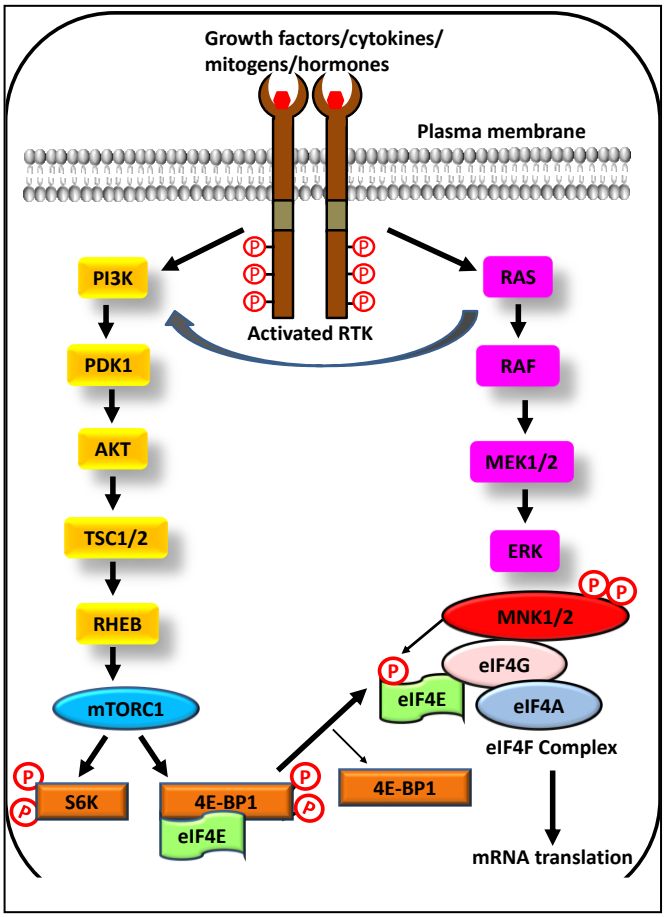


**Figure 12: PI3K to mTORC-1 and Erk signal convergence.** Active Ras phosphorylates Erk which in turn phosphorylates Mnks. Ras signalling also feed into the PI3K/AKT/mTORC-1 pathway. Mnk1 and Mnk2 are downstream effectors of Erk and p38 MAPKs. Following activation by Erk and/or p38, Mnk1/2 phosphorylates free eIF4E. Both mTORC-1 and the Mnks regulate cell proliferation by mediating the activity of eIF4E. (Created by P T Brace through adaptation from (Hay, 2010).

As a result of their ability to exert a positive feed-forward and negative feedback effects, the PI3K/AKT/mTOR and the Ras to MAP kinase signalling pathways can allosterically activate and inactivate each other. As shown in figure 14, in a completely different way of activation, GTP-bound Ras also feed into the PI3K pathway to enhance its activation during EGF binding to RTK (Mendoza et al., 2011). One of the most characterised mechanism by which *M.tb* is able to trigger intracellular signalling is by binding to and activating

the pattern recognition receptor (PRR), Toll-like receptors (TLRs). Signalling through TLRs feed into the signalling pathways discussed above.

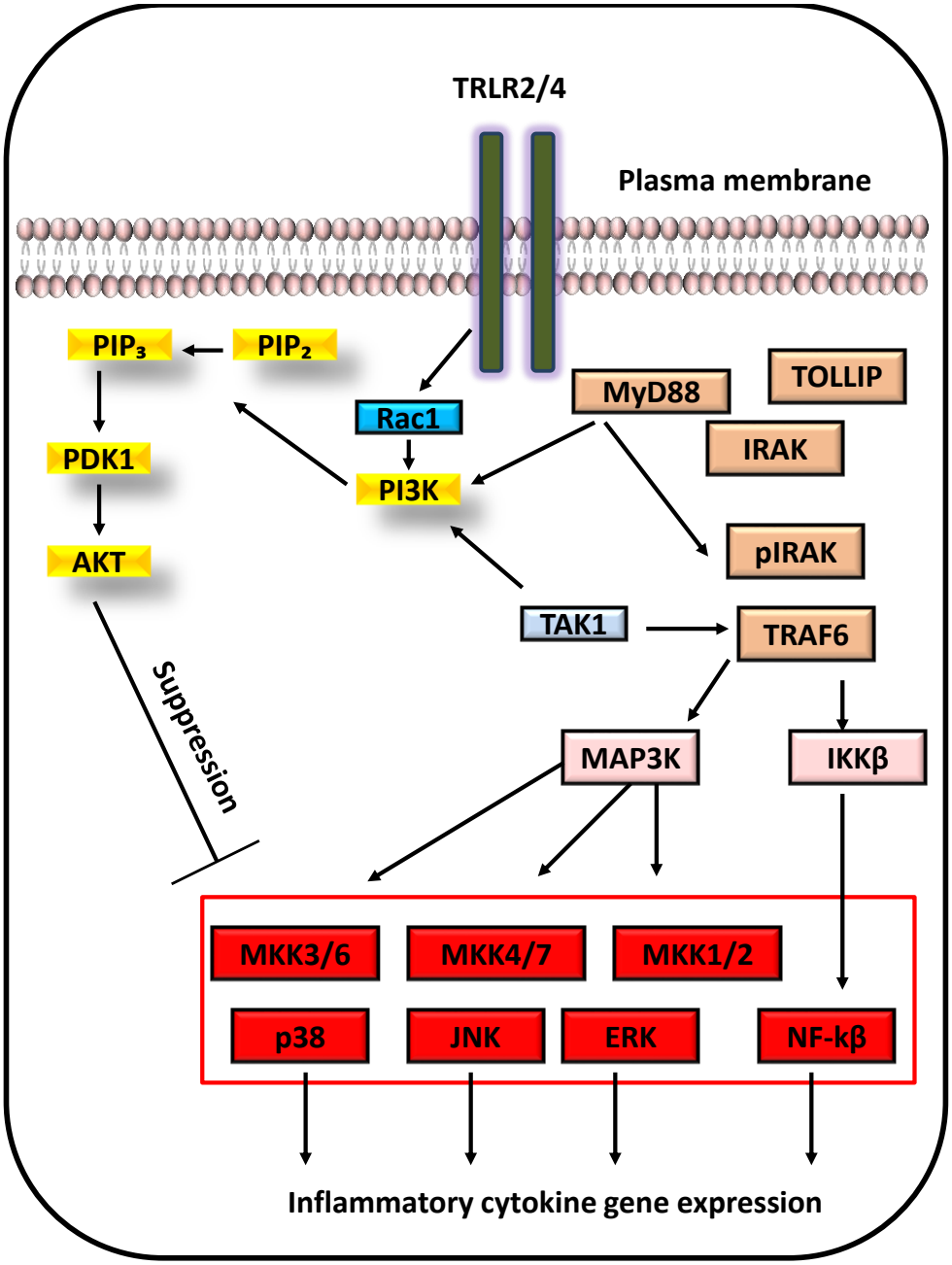


**Figure 13: PI3K to mTORC-1 and Erk signal convergence.** Pathogens bind to TLRs to trigger intracellular signalling. *M.tb* bind to TLRs to trigger PI3K signalling. MyD88 signalling also culminates in MAPK pathway activation to promote the expression of inflammatory cytokines (Created by P T Brace).

## 1.15 Regulatory role of PI3K/AKT/mTORC-1 signalling in disease.

Due to its role in cell cycle entry and cell survival, constitutive activation of the PI3K pathway leads to tumorigenesis. As a result, this pathway has been targeted in many cancers for therapeutic purposes. Recent developments in the field are however showing how this pathway may also play negative regulatory roles in immune disorders and pathological conditions. For example, in cell-mediated and humoral responses, the heterodimeric bioactive IL-12p70 has long been shown to play key roles in the development of TH1-type immunity (Trinchieri, 1994, Trinchieri, 1998, Gately, 1998). In a sharp contrast, excessive production of IL-12p70 in infection is not only deleterious to the development of anti-inflammatory Th2-type immune response, but also contributes to endotoxin shock (Trinchieri, 1994, Trinchieri, 1998, Fukao, 2002). By disrupting the p85α regulatory subunit of class 1A PI3Ks in mice, Fukao *et al* investigated evidence implicating the PI3K pathway as a negative regulator of IL-12p70 production in TLR signalling. In this study, the group demonstrated elevated IL-12 production in splenic DCs and BMDCs isolated from mutant compared to wild type mice. In line with this observation, the PI3K inhibitor, wortmannin also elicited pronounced IL-12p70 secretion (Fukao, 2002). Interestingly, IL-12p70 overproduction correlated with loss of anti-parasitic immunity due to sensitivity to intestinal parasite, strongyloides venezuelensisthis, and this was restored with TH-2 conditioned BMMCs but not with standard BMMCs. Data from this study indicates that the PI3K pathway negatively regulates IL-12 production in mice, and this ensures appropriate balance of Th1/Th2-type response to infection (Fukao et al., 2002).

Other groups have also reported similar negative regulatory roles played by the PI3K pathway to limit excessive production of a number of inflammatory mediators and transcription factors during infection (Vanhaesebroeck et al., 2001, Xia et al., 2004, Mukai et al., 2007, Tsukamoto et al., 2008). In support of reports that the modulation of inflammatory mediators produced by

macrophages that are stimulated with LPS is mediated by PI3K signalling, M. Martin and colleagues showed that the PI3K-AKT pathway differentially regulate IL-10 and IL-12 production both at the gene expression and protein secretion level in LPS-stimulated macrophages (Martin, 2003). The group firstly showed that LPS (isolated from P. gingivalis) mediated activation of PI3K pathway signals selectively through TLR2 but not TLR4 (Martin, 2003). Past studies had shown that PI3K is directly involved in TLR signalling which culminates in NF-kB transcriptional activity (Arbibe et al., 2000, Martin et al., 2003). This supports the notion that TLR signalling activates the PI3K pathway. To further extend this observation, the group showed that ERK1/2 activity, but not phosphorylation of p38 or JNK1/2 was negatively regulated by the PI3K inhibitors, wortmannin and LY294002. Previous studies had shown that IL-10 is positively regulated by ERK1/2 (Feng et al., 1999, Martin et al., 2003). Whereas IL-12 was shown to be negatively regulated by ERK1/2, it was positively regulated by p38 MAP kinase activity (Salmon et al., 2001, Feng et al., 1999, Yi et al., 2002). With the MEK1 inhibitor PD98059 mimicking the effects of PI3K inhibitors on IL-10 and IL-12 production in LPS-stimulated macrophages, the authors demonstrated that PI3K-mediated activation of ERK1/2 is responsible for the positive and negative regulation of IL-10 and IL-12 respectively, in response to Porphyromonas gingivalis-derived LPS stimulation of TLR2 (Martin, 2003).

The regulatory role of PI3K pathway has further been associated with clinical conditions linked with ischemic cardiovascular events such as thrombosis and atherosclerosis disease (Mukai, 2007). Mainly found in endothelial cells, tissue plasminogen activator (tPA or PLAT) is a serine protease critical for breaking down blood clots. Plasminogen activator inhibitor type-1 (PAI-1) antagonises tPA activity and thus inhibits the fibrinolytic system to promote the formation of intravascular thrombosis and atherosclerosis (Mukai et al., 2007, Huber et al., 2001). PAI-1 activity has been linked to development of vascular lesions and atherogenic processes (Sobel et al., 2003, Kohler and Grant, 2000, Huber et al., 2001), with pronounced overexpression of PAI-1 detected in diabetes, hypertension and dyslipidaemic patients, where their elevated levels correlates

with atherosclerotic disease severity (Schneiderman et al., 1992, Sobel et al., 2003, Kohler and Grant, 2000). Y. Mukai *et al.* have demonstrated PI3K negative regulation of PAI-1 expression in endothelial cells (ECs). In this study, PI3K inhibitors (wortmannin and LY294002) further enhanced insulin and TNF-α-induced PAI-1 production and activity in ECs (Mukai et al., 2007). The authors reported that MEK/ERK and the p38 MAP kinase pathway is responsible for TNF-α-induced PAI-1 expression in ECs, since both PD98059 (MEK/ERK inhibitor) and SB203580 (p38 MAP kinase inhibitor) specifically abrogated the TNF-α-induced PAI-1 expression in ECs (Mukai et al., 2007). Inhibition of PI3K prevented the statin, simvastatin, from blocking TNF-α-induced phosphorylation of ERK and p38 MAP kinase, as well as PAI-1 expression. This re-enforces the key role played by PI3K signalling in modulating PAI-1 expression and activity in ECs.

Bart Vanhaesebroeck's group has recently shown that by converting membrane $PI(4,5)P_2$ to $PI(3,4,5)P_3$ during LPS stimulation, the delta isoform of PI3K mediates a balance between pro and anti- inflammatory response (Aksoy et al., 2012). Here the authors demonstrated that $PI(4,5)P_2$ in the plasma membrane is essential for the TLR4 effector protein TIRAP binding, which is required for pro-inflammatory cytokine production. The actions of PI3Kδ (converting $PI(4,5)P_2$ to $PI(3,4,5)P_3$ therefore disrupts this interaction and most importantly shifts the TLR4 signalling from plasma membrane TIRAP-MYD88 dependent pro-inflammatory response to endosomal TRAM-TRIF-dependent anti-inflammatory phase (Aksoy et al., 2012).

## 1.16 *M.tb* engages TLRs to activate PI3K signalling

With mounting evidence indicating key regulatory roles played by PI3K pathway in a variety of infections and pathological conditions, it is important to ascertain molecular mechanisms by which *M.tb* infection triggers PI3K pathway activation. Although a number of pattern recognition receptors (PRRs) have been shown to mediate *M.tb*-driven induction of pro-inflammatory signalling, TLRs, particularly TLR2 signalling, is the most investigated (Jo et

al., 2007). Following an extensive review of this field, Jo E-K *et al* suggested that different types of TLRs may interact with distinct mycobacterial components or whole mycobacteria to drive host immunity that contributes to resistance to *M.tb* (Jo et al., 2007, Pathak et al., 2004). As discussed above, TLR signalling feeds into activation of the PI3K pathway. Indeed, *M.tb* has been shown to trigger PI3K pathway activation (Maiti et al., 2001), as well as engage with TLRs on macrophages to trigger activation of MAP kinase signalling (Yang et al., 2007, Pathak et al., 2004). In fact, *M.tb* can only induce phosphorylation of S6K and ERK1/2 by driving activation of PI3K signalling cascade (Yang et al., 2006a). In order to improve prevention and therapy, it is important to seek a deeper understanding of pathogen tactics that drive disease pathogenesis, as well as mechanisms underlying host immune system defence armoury such as the negative regulatory role played by the PI3K pathway.

## 1.17 *M.tb* suppresses host regulatory signalling mechanisms

The past few decades have seen a considerable amount of literature published on mechanisms by which *M.tb* successfully overcomes host immunity to drive disease progression. However, data about how the pathogen subverts critical host immune responses to successfully drive host tissue destruction in particular and subsequent cavitation (which is critical for transmission) is limited. MMP activity mediates lung matrix destruction in TB (Elkington et al., 2011b). *M.tb,* as well as components of its cell wall selectively upregulated MMP-1 and MMP-9 in human monocyte derived macrophages (Elkington et al., 2011a, Elkington et al., 2009, Chang et al., 1996). MMP-1 in particular has been shown to be the most highly up-regulated MMP in induced sputum and bronchoalveolar lavage (BAL) fluid from patients with pulmonary TB (Elkington et al., 2011a). Despite recent developments indicating key roles played by MMPs in lung tissue destruction, host mechanisms that limit cavitation, as well as the ability of *M.tb* to suppress such host responses to drive TB pathology, have not been investigated.

A review by Valerie Poirier and Y. Av-Gay highlighted the various mechanisms by which *M.tb* has evolved to evade host immunity by modulating several cellular events in host macrophages (Poirier and Av-Gay, 2012). Subscribing to the notion that cavity lesions emanate from caseous necrosis, researchers who have sought to address the question about host immune response against cavitation in TB have focused only on host immune mechanisms that targets pro-inflammatory factors that mediate granuloma caseation.

Based on a genome-wide search for *M.tb* genes that could potentially play a role in lung cavitation, genes that encode four phospholipase C, and those that regulate transcription were amongst the few suggested to be involved in tissue destruction when present in particular *M.tb* strains (Cooper et al., 2000). Other studies have shown that the 6kDa early secretory antigenic target 6 (ESAT-6) secreted via the RD1 pathogenicity region, mediate lung epithelial cell line necrosis (Kato-Maeda et al., 2001), whereas lipoarabinomannan (LAM) mediates induction of TNF and IL-1 (critical for necrosis) by macrophages (Fenhalls et al., 2002). For this reason, ESAT-6 and LAM have been suggested to play key roles in driving TB cavitation (Yoder, 2004), completely neglecting the importance of MMP activity in lung tissue destruction. Protein-tyrosine phosphatase A (PtpA) secreted by *M.tb* into culture media may interfere with host signalling pathways in order to establish successful survival and disease progression (Yoder, 2004). In a similar manner, *M.tb* may have ways of subverting important host signalling pathways that otherwise normally play a regulatory role to limit the production of tissue-destructive proteases such as MMP-1.

The only way that *M.tb* is able to completely evade host phagolysosome killing and survive for a long time in infection is to remove all PI3P protein from the phagolysosome membrane (Poirier and Av-Gay, 2012, Vergne et al., 2005, Malik et al., 2000). Secreted acid phosphatase M (SapM), a 28-kDa mycobacterial acid phosphatase secreted by *M.tb* (Saleh and Belisle, 2000) was shown to mediate dephosphorylation of PI3P within the membrane of phagosomes to PI, and this prevented the recruitment of proteins that play

important roles in membrane trafficking such as early endosome antigen-1 (EEA1). This thereby led to the blocking of phagosome maturation and late endosome fusion (Vergne et al., 2005).

Although these studies were focused on investigating how *M.tb* is able to survive in the hostile host environment of infected macrophages, they also suggest that the presence of phosphoinositides may be a threat to the success of *M.tb* in driving tissue damage, and that *M.tb* may have ways of suppressing the activities of such lipid signalling molecules. In this regard, it is possible that *M.tb* may have devised particular mechanisms to suppress signalling pathways that normally function to limit tissue destruction in TB. Given the negative regulatory role played by the PI3K pathway in disease, it is likely that this pathway also modulate tissue destruction in TB. Considering the global success of TB, *M.tb* may have evolved ways of subverting the PI3K pathway to successfully drive TB pathogenesis. One way by which *M.tb* could suppress the PI3K pathway is by inducing up-regulation of microRNAs that target various isoforms of PI3K proteins.

## 1.18 Micro RNAs

Micro RNAs (miRNAs) are genomic encoded, short non-coding RNA molecules of approximately 18-24 nucleotides. They mediate post transcriptional gene silencing by directly forming Watson-Crick base pairing with complementary sequences within the 3'-untranslated region (3'-UTR) of target mRNA molecules (Hwang, 2006). The role of micro RNAs has been implicated in a variety of homeostatic cellular processes involved in cell proliferation, differentiation and apoptosis, and they have been shown to play a critical role in development and progression of various diseases such as HIV, cancer, certain neurodegenerative, genetic disease and infectious diseases including tuberculosis (Hwang, 2006).

The idea of micro RNAs was initially described in *C. elegans* in the early 1990s by Ambros, Ruvkun *et al* (Lee *et al,* 1993). There have since been about 1000 micro RNA genes that encode over 3000 miRNAs discovered in viruses, plants

and animals, with about 300 identified to exist within the human genome (Bentwich, 2005, Bartel 2004). Functionally, the biological activities of micro RNAs can be likened to RNA interference (siRNA). SiRNA is the experimental or therapeutic procedure to knock down expression of particular genes to inhibit the over expression of certain proteins in particular cells. This helps to study the role of such proteins in particular metabolic pathways or cellular physiological processes. Similarly, but not identically, micro RNAs are endogenous molecules and carry out physiological post transcriptional processes by which genes can be negatively regulated (Hwang, 2006, Gregory, 2005). Both RNA interference and micro RNA activities require the same molecular machinery such as Dicer, Drosha and its co-factor molecules, an RNA induced silencing complex (RISC) (Gregory, 2005).

### 1.18.1 Micro RNA biogenesis

Although micro RNA genes only encode RNA and not proteins, their transcription processing and regulations is in a similar manner to protein coding genes. Their transcription is predominantly mediated by RNA polymerase II, to generate a large primary miRNA transcript termed pri-miRNA (Figure 15). This pri-miRNA may consist of different miRNA molecules of 60 to 80 nucleotides each, which folds up to generate hairpin loop structures, characteristic of miRNAs (Hwang, 2006, Gregory, 2005, Griffiths-Jones, 2008). The first specific process that distinguishes the micro RNA pathway from transcription expression of protein coding genes is the processing of pri-miRNA by a microprocessor enzyme complex, involving the class III ribonuclease protein, Drosha and its co-factor, DGCR8 (Griffiths-Jones, 2008).

Drosha ribonuclease processing of pri-miRNA takes place in the nucleus to form the precursor miRNA (pre-miRNA) molecule, with 2 bases overhung at the 3'-end (Griffiths-Jones, 2008, Hwang, 2006).

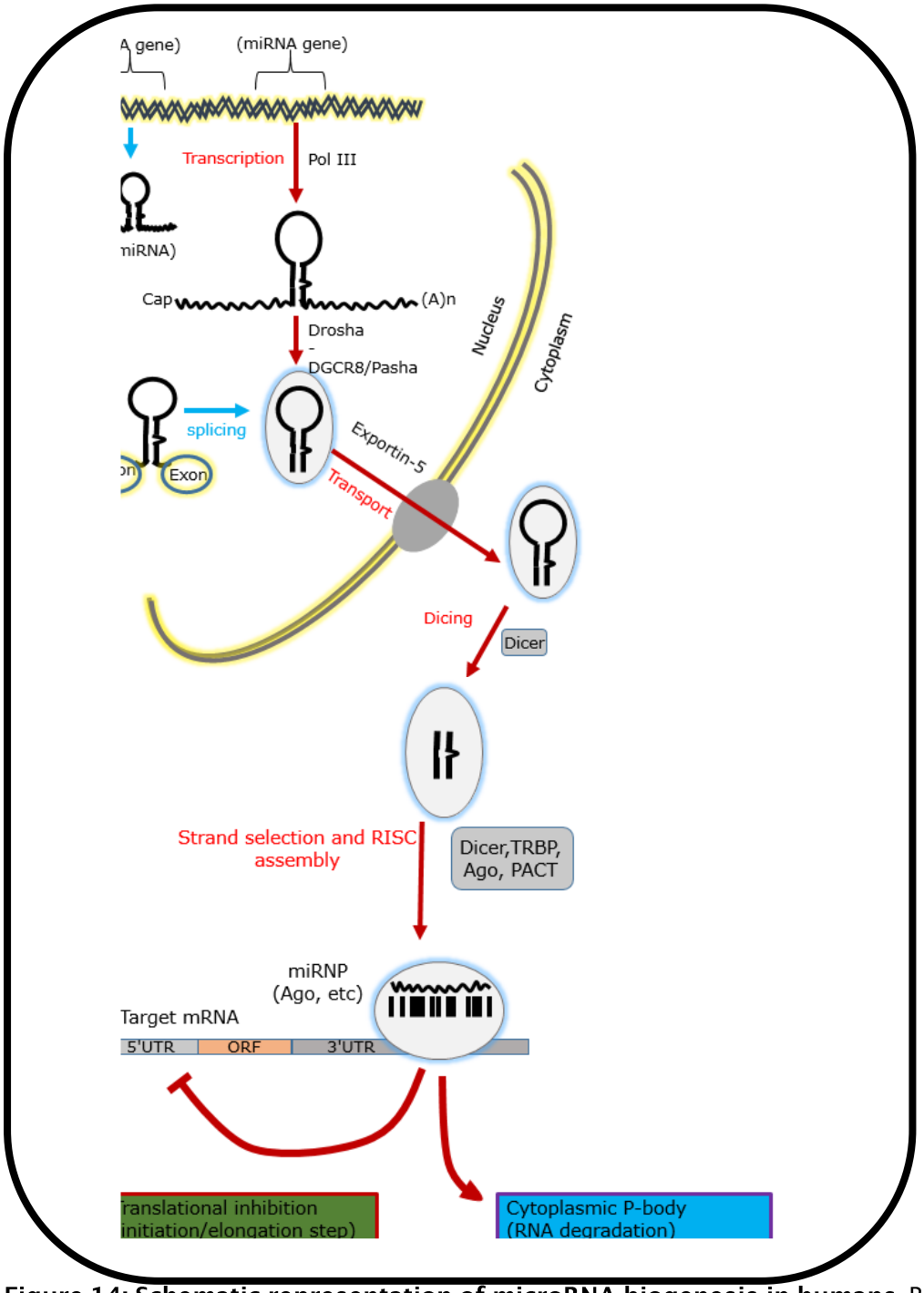


**Figure 14: Schematic representation of microRNA biogenesis in humans.** RNA polymerase II first transcribes the micro RNA gene to pri-RNA molecules. These are then sequentially processed by Drosha in the nucleus and Dicer in the cytoplasm (See text for details) (Created by P T Brace).

Next, the pre-miRNA molecule is transported across the nuclear membrane into the cytosol by exporting 5, a Ran-GTP-dependent nuclear export factor

(Yi et al., 2003). In the cytosol, pre-miRNA becomes a substrate for another ribonuclease enzyme type III called Dicer, which cleaves double stranded RNA molecules. Thus Dicer cleaves the hairpin loop structure of the pre-miRNA to generate a double stranded RNA species of about 18 -24 bases, with some mismatches in the base pairing (Hwang, 2006, Griffiths-Jones, 2008). Dicer recognises and cleaves size specific fragments.

Crystallographic studies have revealed that Dicer has specific domains such as Paz and connector helix, which are involved in cleaving the pre-miRNA transcript. There is about 18-24 nucleotide space between the Paz domain which binds the double stranded end, and the RNAase domains which cleave the loop from the precursor molecule, to generate approximately 18-22, double stranded (ds) nucleotide endogenous miRNA (Hwang, 2006). The ds miRNA molecule is then picked up by RISC, whose assembly involves another family of proteins called the Argonaute proteins. RISC selects one of the strands of the double stranded miRNA, termed the mature strand. Mature micro RNAs bind to their target mRNA to either degrade it or repress translation.

The other strand, termed passenger strand, is then degraded either by a possible duplex unwinding mechanism (Gregory, 2005) or it may just be cleaved by argonaute proteins. The mechanism by which RISC selects the mature strand as well as how the two strands are separated is still not fully elucidated. RISC, carrying one of the mature miRNA strands, binds to its target miRNA and forms a base pairing between the miRNA strand and the 3'-untranslated region(3'-UTR) of the target mRNA molecule which encodes a particular protein. This can either lead to degradation of the mRNA transcript by argonaute cleavage, if there is perfect Watson-Crick base pair match between the miRNA and the mRNA (common in plants); Or imperfect complementarity between the miRNA and mRNA leads to translational inhibition via possible sequestration of the mRNA transcript into P bodies, which exclude ribosomes (He and Hannon, 2004). It has however been shown that mismatched complementary miRNAs can also diminish the levels of target

mRNA molecules in the cytosol (He and Hannon, 2004). Both mechanisms result in repression of gene expression (Bartel 2004).

## 1.19 Hypothesis

I hypothesise that the PI3K/AKT/mTORC-1 pathway negatively regulates MMP-1 production in macrophages, and that *M.tb* subverts this pathway to achieve a tissue destructive phenotype in tuberculosis.

## 1.20 Experimental plan

- Study *M.tb* up-regulation of MMP-1 in THP-1 cells and primary human macrophages.
- Analyse effect of PI3K inhibition on *M.tb* -driven MMP-1 production
- Dissect the role of pathways downstream of PI3K in MMP-1 production
- Investigate suppression of PI3Kδ by *M.tb*

# 2. CHAPTER 2: MATERIALS AND METHODS

## 2.1 List of equipment

7900HT Fast Real-Time PCR System (#4329001, Applied Biosystems™, USA)

AllegraTM 6R centrifuge (Beckman CoulterTM)

BD FACS Aria™ and BD FACS Calibur™ Cytometers (BD Biosciences, UK)

BD Accuri C6 Flow Cytometer (BD Biosciences, UK).

Bench Top Centrifuges (Biofuge, Pico Heraeus)

DNA Engine TETRAD™2 Peltier Thermal Cycler (#TA001175, ESco Tech. Inc., USA)

Gel Electrophoresis system (VWR)

Luminex machine (Bio-Rad Laboratories Ltd.)

NanoDrop® ND-1000 Spectrophotomètre (NanoDrop Technologies Inc, DE, USA)

Thermo Scientific Heraeus Fresco 17 Centrifuge ( Fisher Scientific Ltd., #CFH-203-010K)

VersaDoc™ Imaging system (Bio-Rad Laboratories Ltd.)

Xcell *SureLock*® Mini-Cell and Xcell II TM Blot Module (#E10002, invitrogen)

## 2.2 List of reagents

0.2μm Durapore filters (Millipore)

0.5% Trypsin-EDTA solution 10X (Insight Biotechnology Ltd., #Sc-363354)

2-component DAB pack (BioGenex, #HK542-XAK)

4EG1-1 (eIF4E/eIF4G interacting inhibitor) (Merck Chemicals Ltd., #324519-5MG)

7H9 medium (BD Bioscience)

96-well microplate-maxiSorp (Fisher Scientific UK #10394751).

AKT Antibody (New England Biolabs, #9272S)

All Taqman qPCR Primers (Life Technologies Ltd.)

Ampicillin sodium salt, powder (Sigma-Aldrich Company Ltd., #A0166-5G)

Anti-eIF4E CT Antibody, rabbit monoclonal (MerckMillpore, #04-347)

Anti-miRTM miRNA inhibitors-has-miR-135a

Anti-miRTM miRNA inhibitors-has-miR-27a

Anti-miRTM miRNA inhibitors-has-miR-30a

Anti-mouse for β-actin (Sigma-Aldrich Company Ltd., #A9044)

Anti-phospho eIF4E (Ser209) Antibody (MerckMillpore, #07-823)

Anti-PIK3CD (LifeSpan BioScience,Inc #LS-C338531/63835)

AS-605240 (PI3K gamma inhibitor) (Insight Biotechnology Ltd., #sc-221272)

Biotinylated rabbit anti mouse (Dako, #E0413)

Blotting Filter Papers (Life Technologies Ltd., #LC2010)

BLUeye Prestained Protein Ladder (Geneflow Ltd., #S60024-P)

Bovin Serum Albumin (BSA) (Fisher Scientific UK Ltd., #BPE9705/100)

Dimethyl sulfoxide (DMSO) (Sigma-Aldrich Company Ltd., # D4540-100ML)

Elite vectastain ABC kit (Vector laboratories # PK-6100)

Empty Gel Cassette Combs, mini, 1.5 mm (Life Technologies Ltd., #NC3510)

Empty Gel Cassettes, mini, 1.5mm (Life Technologies Ltd., #NC2015)

EZ-Link biotin-HPDP (Pierce, Thermo Fisher Scientific UK Ltd)

Falcon tubes (Greiner Bio-One Ltd, #227261)

Ficoll-plaque™ premium (Fisher Scientific UK Ltd., #11570734)

Fluorokine MAP profiling kit (R&D systems)

Foetal Calf Serum (FCS) (Life Technologies Ltd., #FB-1001/500)

Goat anti-rabbit IgG-HRP (Santa Cruz Biotechnology, Inc., #sc-2004)

Goat anti-rabbit IgG-PE (Insight Biotechnology Ltd., #sc-3739)

Hanks balance salt solution (HBSS) (Life Technologies Ltd., #14170-138)

hsa-miR-125b (Life Technologies Ltd)

hsa-miR-135a (Life Technologies Ltd)

hsa-miR-199 (Life Technologies Ltd)

hsa-miR-203 (Life Technologies Ltd)

hsa-miR-22 (Life Technologies Ltd)

hsa-miR-221 (Life Technologies Ltd)

hsa-miR-27a (Life Technologies Ltd)

hsa-miR-30a (Life Technologies Ltd)

hsa-miR-7 (Human) (Life Technologies Ltd)

Human geNorm Kit (6 gene probe based kit) (Primerdesign Ltd., # GE-PP-HU-6)

Human M-CSF Recombinant Protein (eBioscience Ltd., #14-8789-80)

Human RNU44 (Life Technologies Ltd., #4427975)

Human Total MMP-1 DuoSet (R&D Systems Europe, Ltd., # DY901)

Invitrolon™ PVDF/Filter Paper Sandwich (Life Technologies Ltd., #LC2005)

LDH Cytotoxicity detection kit (Roche, #11644793001)

L-Lactic Dehydrogenase solution (L3916 Sigma, 1000 units/mL)

Luminata Forte Western HRP substrate (Fisher Scientific UK Ltd., #MDR-120-030C)

LY 294002 (Millipore:Calbiochem, #440202-5MG)

Macrophage Serum Free Medium (M-SFM) (Life Technologies Ltd., #12065074)

Magnetic Porous Glass (MPG) streptavidin beads (Pure Biotech LLC, #MSTR0502)

Methanol (Fisher Scientific UK Ltd., #M/3950/17)

MicroAmp® Optical 384-Well Reaction Plate (Life Technologies Ltd., #4309849)

MicroAmp® Optical Adhesive Film (Life Technologies Ltd., #4311971)

MK-2206 Dihydrochloride (AKT inhibitor) (Insight Biotechnology Ltd., #sc-364537)

Mouse anti β-actin (Sigma-Aldrich Company Ltd., #A1978)

Multi-well tissue culture plates (Greiner Bio-One Ltd)

Normal rabbit IgG-PE (Insight Biotechnology Ltd., #sc-3871)

Novex® HRP Chromogenic Substrate (TMB) (Life Technologies Ltd., #WP20004)

NP40 lysis buffer (Life Technologies Ltd., #FNN0021)

Nunclon 132mm x 88mm flat bottom 6 round well (Fisher, #10119831)

NuPAGE® LDS Sample Buffer (4X) (Life Technologies Ltd., #NP0008)

NuPAGE® MOPS SDS Running Buffer (20X) (Life Technologies Ltd., # NP0001)

NuPAGE® Novex 4-12% Bis-Tris Gel 1.0 mm (Life Technologies Ltd., #NP0323BOX)

NuPAGE® Transfer Buffer (20X) (Life Technologies Ltd., #NP00061)

Oligo (dt)12-18 primer (Invitrogen #18418-012)

Paraformaldehyde (Santa Cruz, USA)

PBS Powder for 5L of 10X (Insight Biotechnology Ltd., #Sc-24947)

Phosphatase inhibitor (Fisher Scientific UK Ltd., #BPE9718-1)

Phosphatase inhibitor cocktail III (Fisher Scientific UK Ltd., #12841650)

Phosphate Buffered 10X Solution (Fisher Scientific UK Ltd., #10204733)

Phospho-AKT (Ser473) (D9E) XP® Rabbit mAb (New England Biolabs, #4060S)

PI 3-K/PDK-1 Inhibitor, NVP-BAG956 (Merck Chemicals Ltd., #528121-5MG)

PI 3-Kdelta Inhibitor, IC87114 (Millipore: Calbiochem, #528118-5MG)

PI 3-kinase p110δ (H-219) (Santa Cruz Biotechnology, #sc-7176)

PI 3-Kα Inhibitor VIII (MerckMillpore, #528116-5MG)

PI 3-Kβ Inhibitor VI, TGX-221 (MerckMillpore, #528113-1MG)

PI3K total Oligo clonal Antibody (Life Technologies Ltd., #710400)

PMSF (Sigma-Aldrich Company Ltd., #P7626-250MG)

Precast Bis-Tris Gel, 1.0mm (Life Technologies Ltd, #NP0323BOX)

Precision Plus Protein™ Dual Colour Standards (Bio-Rad Labs Ltd., #161-0374)

Protease inhibitor (Sigma-Aldrich Company Ltd., #P-2714)

Protein assay kit, BCA Thermo Scientific Pierce (Life Technologies Ltd., #10741395)

PTEN inhibitor, bpV (phen) (Santa Cruz Biotechnology, Inc., # sc-221378)

PVDF (Life Technologies Ltd**,** #LC2005)

Rabbit Polyclonal anti PI3Kδ (Santa Cruz Biotechnology, #SC-7176)

Rapamycin (MerckMillpore, #553210-100UG)

rDNase DNA-free™ Kit (Ambion by life technologies, # AM1906)

ReBlot Plus Mild Antibody Stripping Solution (Merck Millipore, #2502)

Reference gene selection kit (geNorm™ kit) (Primerdesign Ltd, # GE-PP-HU-6).

RNAse free water (Fisher Scientific UK Ltd, # BPE561-1),

RNaseOUT (Invitrogen #10777-019)

RNaseZap RNase decontamination solution (Life Technologies Ltd., #AM9780)

RPMI-1640b AQmedia™ (Sigma-Aldrich Company Ltd., #R7509-6X500ML )

SeeBlue® Plus2 Pre-Stained Standard (Novex®) (Life Technologies Ltd., #LC5925)

Spectra Multicolour Broad range protein ladder (Fisher Scientific UK Ltd., #11874544)

sulfoxide (DMSO) (Sigma-Aldrich Company Ltd., # 67-68-5),

SuperScript™ III Reverse Transcriptase (Invitrogen, # 18080-044),

T75 tissue culture flasks (Greiner Bio-One Ltd., # 658175).

TMB liquid substrate system for ELISA (Sigma Aldrich #T0440-1L)

TRI-Reagent® Solution (Sigma-Aldrich Company Ltd., #T9424-25ML)

Tween 80 (Fisher Scientific UK Ltd., #BPE338-500)

TWEEN® 20 (Sigma-Aldrich Company Ltd., # P1379-250ML)

UltraPure™ N, N'- Methylenebisacrylamide (Life Technologies Ltd., #15516-024)

UltraPure™ Acrylamide (Life Technologies Ltd., #15512-023)

UltraPure™ Glycogen (Life Technologies Ltd., #10814010)

UltraPure™ TEMED (Life Technologies Ltd., #15524-010)

Versene (Life Technologies Ltd., #15040-066)

Water RNA grade sterile (Fisher Scientific UK Ltd., #BPE561-1)

## 2.3 Cell culture

Macrophages play crucial roles in *M.tb* infection. Following inhalation of the bacilli, alveolar macrophages provides the initial immune response by engulfing the bacteria. Peripheral blood monocytes are continuesly recruited to the developing granulomas in attempt to wall off *M.tb* . At the site of infection, macrophages become polarised and differentiate into various inflammatory phenotypes. For this reason, this project has used macrophage-like cell lines (e.g. THP-1 cells) and human-monocyte derived macrophages (MDMs) for its investigation.

### 2.3.1 THP-1 cells

THP-1 cells (and monocyte-derived macrophages (MDMs) were cultured in RPMI-1640 (Sigma-Aldrich Company Ltd., # R7509-6X500ML) supplemented with 5% L. glutamine (Sigma-Aldrich Company Ltd., # G7513-100ML), 5% ampicillin (Sigma-Aldrich Company Ltd., # A0166-5G) and 10% foetal bovine serum (Life Technologies Ltd., # FB-1001/500), and incubated at 37°C in humidified air, with 5% $CO_2$. This culture media will hereafter be referred to as

'complete media'. THP-1 cells were sub-cultured every two to three days and maintained between 1x105 and 5x105 cell per ml in a total media culture volume of 10ml or 20ml in T75 tissue culture flasks (Greiner Bio-One Ltd., # 658175). THP-1 cells were differentiated into macrophage-like cells in 1ml 4µg/ml of D3 25-Hydroxyvitamin D (Vitamin D) for 24 hours. This was followed by chemical inhibitor treatment for two hours and then UV-killed *M.tb* infection. Supernatant samples were harvested 72 hours post-infection and stored at -20oC for future MMPs analysis by ELISA or Luminex assay.

### 2.3.2 Isolation of PBMC

Peripheral blood mononuclear cells (PBMCs) were isolated from fresh blood by density centrifugation. Fresh blood was mixed in equal volume of warm Hanks balance salt solution (HBSS) (Life Technologies Ltd # 14170-138) and mixed well in T75 tissue culture flasks (Greiner Bio-One Ltd., # 658175). In experiments where leukocyte cones were used, the leukocyte-rich concentrated blood was transferred into T75 tissue culture flasks, topped up to 140ml with room temperature (RT) HBSS (with no calcium or magnesium supplements). Blood:HBSS mixture (35ml) was then carefully layered onto 15ml of ficoll plaque premium (Fisher Scientific UK Ltd # 10379484) in 50ml falcon tubes (Greiner Bio-One Ltd, # 227261). This was centrifuged at 480G (1500rpm) for 20 minutes with brake off. The cell layer was carefully removed and washed in HBSS by centrifugation for 8 minutes each time at 310G, with brake on. Cells were washed four more times before monocytes were counted.

### 2.3.3 Adherence purification of monocytes

In order to count monocytes, 20µl of PBMCs was used on haemocytometer counting chamber and incubated for 5 minutes at 37°C. Monocytes appear as grey adherent cells, with lymphocytes having a smaller and denser bright morphology. Cells were counted and seeded at 2.5 x $10^5$ monocytes per cm2 of various sizes of multi-well tissue culture plate (Greiner Bio-One Ltd) and tissue culture dish Nunclon 132mm x 88mm flat bottom 6 round well (Fisher,

#10119831). Cells were incubated in RPMI-1640 supplemented with 1% human serum, 5% glutamine and 5% ampicillin for 1 hour at 37oC to allow monocytes to adhere to the plate. Lymphocytes were carefully washed firstly using the medium that is already on the cells, washed for a further two more times using warm HBSS. Whenever 6-well tissue culture plates were used, 2ml of complete media (RPMI + L Glu + AMP + 10% FCS) supplemented with 100ng/ml of macrophage serum-free medium (M-SFM) (Life Technologies Ltd., #12065074) was added to monocytes and cultured for 5-7 days to differentiate to macrophages. Figure 16 is a microscopic image showing the morphological differences between human monocytes (Figure 16A) and monocyte-derived macrophages (MDMs) (Figure 16B).

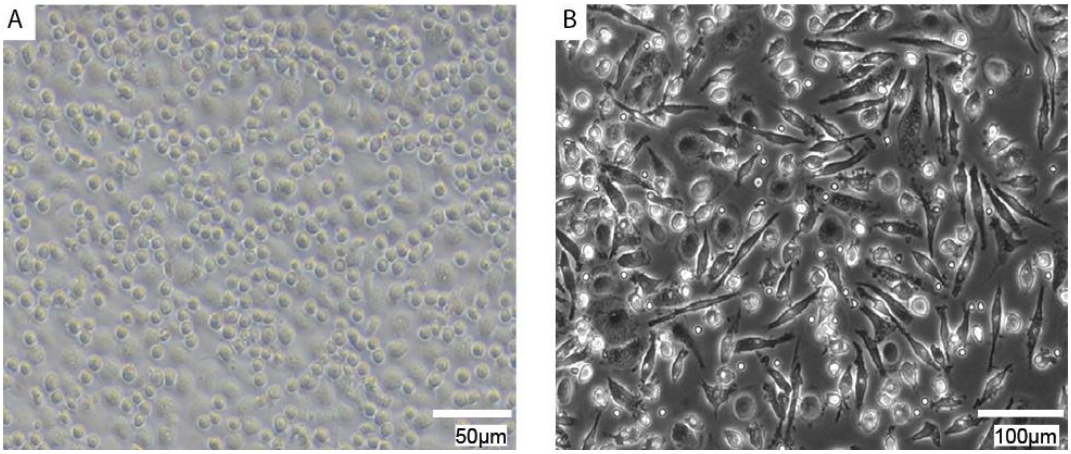


**Figure 15: Microscopic images of purified monocytes (A) and differentiated macrophages (B).** PBMCs were incubated in complete media supplemented with 5% human serum at 37°C for 1-2 hours. After washing off lymphocytes and cells that were in suspension, the adhered monocytes were incubated in 100ng/ml M-CSF for up to 5 days to differentiate to macrophages. Macrophage image shown was taken on day 5 following M-CSF incubation.

## 2.4 *M.tb* culture

*M.tb* was cultured in a total of 2ml Middlebrook 7H9 medium (BD Bioscience) which was prepared according to manufacturer's instructions with 10% ADC enrichment medium (BD Bioscience), 0.2% glycerol (Life Technologies Ltd) and 0.02% Tween 80 (Fisher Scientific UK Ltd., #BPE338-500), at 37oC with continues agitation. Upon reaching optical density (O.D) of between 0.8 and

1.0, *M.tb* was sub-cultured by diluting with 7H9 to five different optical densities ranging from 0.2 to 0.6. Cells were always infected with live (or UV killed) *M.tb* with OD at 0.6, which represents 1x108CFU/ml.

## 2.5 Pharmacological treatment and *M.tb* infection

The media containing M-CSF was changed on day four and cells allowed to rest in complete media for 1 day. On the day of *M.tb* infection, the cell culture media was removed and replaced with 300µl (in 48 well tissue culture plates) of M-SFM for control cells, or M-SFM solutions containing the appropriate chemical compounds that inhibit intracellular protein of interest for two hours. For compound that were originally re-constituted in Dimethyl Sulfoxide (DMSO) (Sigma-Aldrich Company Ltd., #67-68-5), stock solutions were diluted to achieve 0.1% DMSO content. Final working concentrations were therefore diluted in M-SFM supplemented with 0.1% DMSO. Again, this was followed by either UV-killed or live *M.tb* infection at multiplicity of infection (MOI) of 1 which assumes that one bacterium infects one macrophage. Supernatant samples were harvested 72 hours post-infection. Supernatant samples harvested from cells which were infected with viable *M.tb* were sterile-filtered using 0.2µm Durapore filters (Millipore) before they were taken out of containment laboratory into category 2 laboratory where they were stored in -20°C.

## 2.6 Enzyme-linked Immunosorbent Assay (ELISA)

Secreted MMP-1 levels were ascertained and analysed by Enzyme-linked Immunosorbent Assay (ELISA) assay according to manufacturer's protocol (R & D Duo set, # DY901). All reagents including recombinant MMP-1 (standard) and antibodies were supplied inside the kit by the manufacturer. Reagent diluent and antibody dilutions were prepared on the day of the experiment (Appendix 1). 100µl of 2.0µg/ml of capture antibodies were coated at room temperature (RT) overnight in 96-well microplate-maxiSorp (Fisher Scientific UK #10394751).

Each well was aspirated, followed by three washes using 300µl wash buffer (Appendix 1). Non-specific binding sites were blocked for 1 hour at RT using 300µl of reagent diluent. 100µl of samples and standard were loaded in the appropriate wells. Reagent diluent was always used as blank to subtract background optical density (OD). Plates were then tightly covered with adhesive strip and incubated for 2 hours at RT. The aspiration and washing steps were repeated as above, and 100µl of 100ng/ml of detection antibody added to each well. Again this was covered and incubated for 2 hours at RT.

After aspiration and washing, 100µl of streptavidin-HRP was added at a working dilution of 1:200 and incubated at RT for 20mins, aspirated and washed as above. 100µl of substrate solution (3,3′,5,5′-Tetramethylbenzidine (TMB) liquid substrate system for ELISA; Sigma Aldrich #T0440-1L) was then added per well and incubated at RT and in the dark for up to 30mins, checking for colour development at 10mins intervals. Reaction was stopped by adding 50µl of 2M H2SO4 per well. A microplate reader was used to measure the OD of each well at 450nm wavelength, with reference wavelength of 540nm. Levels of MMPs measured were further analysed and plotted on bar chart using GraphPad Prism 5.2. Adobe Illustrator CS6 and Adobe Photoshop CS6 were used to create consistency in all final figures.

## 2.7 Luminex Assay

The luminex platform (Bio-Rad Ltd) was used for the analysis of multiple MMPs (as well as human 30-plex panel of cytokines and chemokines (Invitrogen), in cell culture supernatants. The manufacturer's instructions were followed as detailed in the Fluorokine MAP profiling kit (R&D systems). All reagents, standards and calibrator diluents were provided by the manufacturer in a kit. Samples were diluted either 1:2.5 or 1:5 and analysed on the Luminex machine. Actual concentrations as calculated from the standard curve were used to analyse the data using GraphPad Prism 5.2.

### 2.7.1 Principle of Luminex assay

The Luminex system is based on Luminex's xMAP® technology, and is frequently used to decipher disease-specific biomarker patterns. Luminex combines the principle of traditional biochemistry, flow cytometry and the use of fluorescent microspheres into a multi-analyte profiling technology which is simple and flexible to obtain highly sensitive and accurate results. The two unique components of the luminex system are the xMAP microspheres and the luminex analyser machine. The system uses 100 distinct fluorescently encoded polystyrene microspheres, each of which is 5.6 microns, and internally impregnated with a mixture of red and infrared fluorophores of known ratios (Figure 17). This gives each bead set a unique spectra signature which allows their identification by the xMAP detection system. The steps in figure 18 outline the core processes involved in the principle of Luminex assay.

The microspheres are covalently linked to reagents (e.g. antibodies) that are specific for particular bioassay (Figure 18). This way, up to 100 different analytes can be captured for analysis from a heterogeneous sample. Target-specific analytes bind to the capture antibodies, and this is detected by the use of biotinylated detector antibodies and fluorescent protein, R-Phycoerythrin which is conjugated to streptavidin (streptavidin PE). By interacting with the biotin on the detector antibodies, the streptavidin PE serves to allow the formation of a four-member, solid phase sandwich. Analyte-specific bead sets are identified and the level of analyte present quantified in the fluidic system, by monitoring the unique spectra signature of each bead set and the intensity of PE associated with it

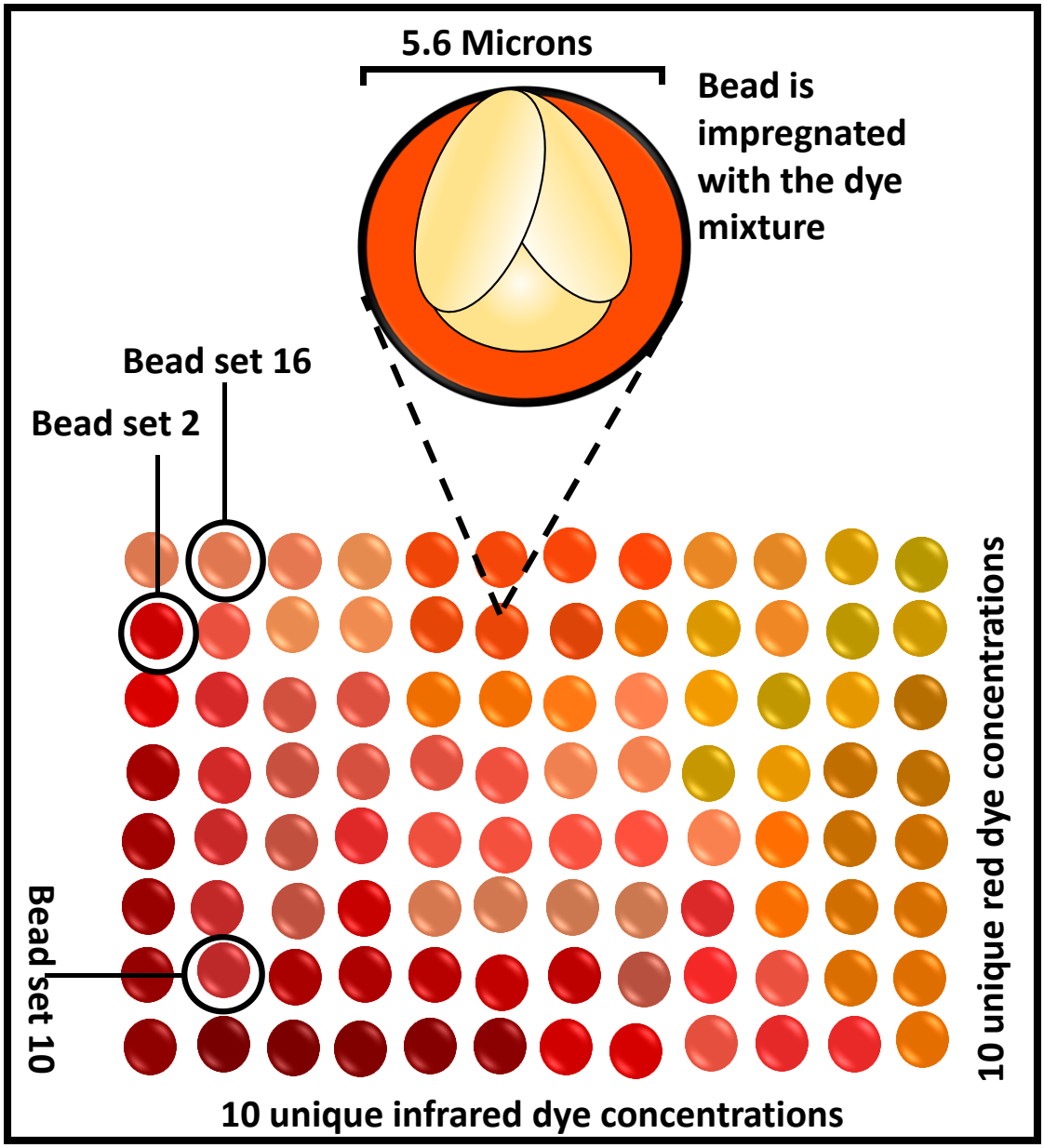


**Figure 16: Schematic of the 100 unique xMAP microspheres.** Luminex system uses 5.6 micron polystyrene-based magnetic microspheres. Red and infrared fluorophores of differing intensities are used to internally dye each bead. To enable differentiation of one bead from the other, each bead is given a unique number, or bead region (Further details are described in the text above).

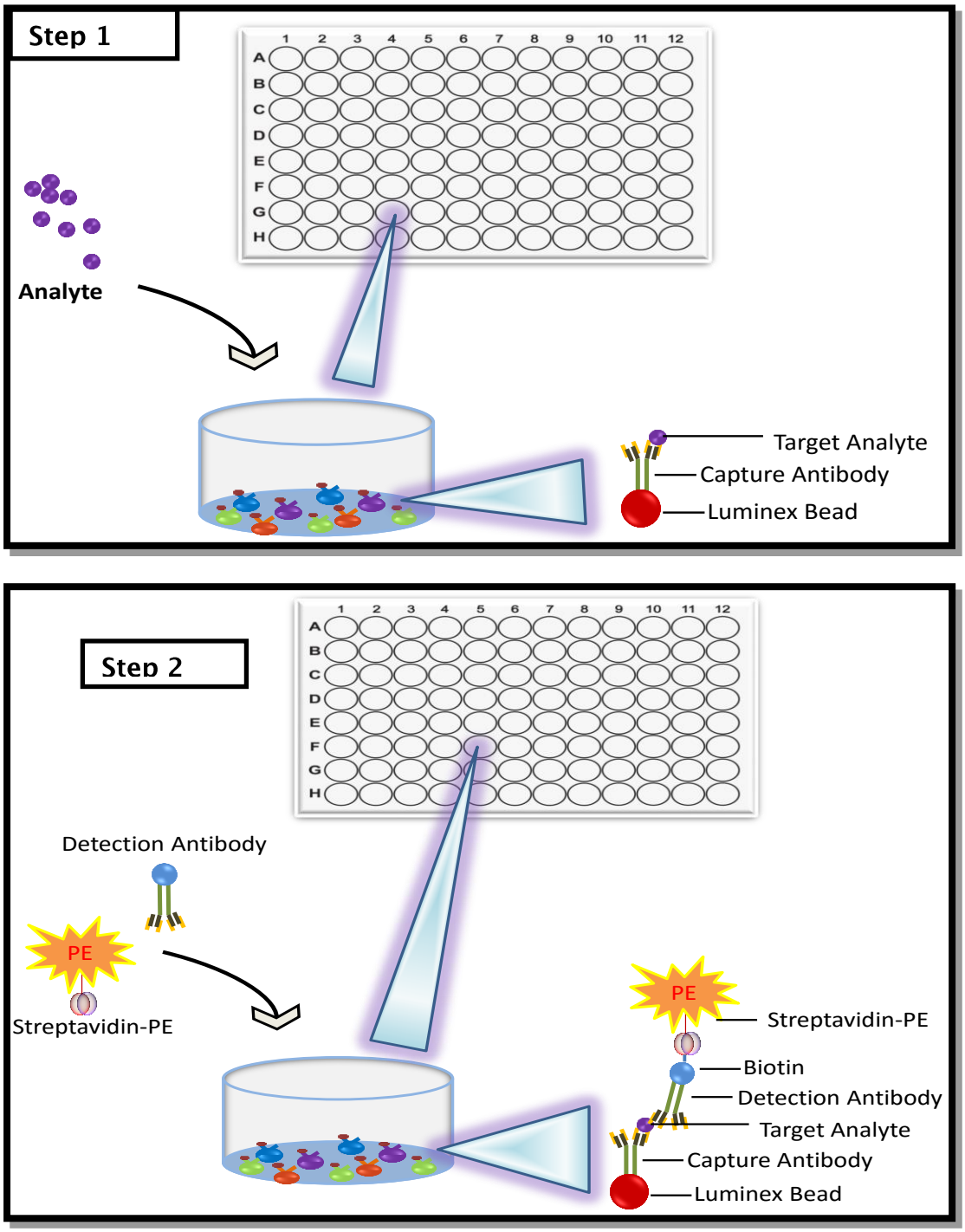


**Figure 17: Steps involved in Luminex immunoassay.** Unlike the assay format for conventional ELISA where the ELISA capture antibody is attached to the microplate well, the multiplex capture antibody is attached to a microsphere bead sets. Capture antibodies are conjugated to streptavidin-PE. (See text for more details). (Created by P T Brace).

The flow cytometry-based aspect of the luminex technology occurs within the luminex analyser. The machine combines the principle of fluidics, lasers, 4 different detectors and real-time digital signal processing to differentiate the bead sets. It does so by aligning the beads in a single file as they enter a flow cell via sheath fluid (Figure 19 A). This way a dual laser system is used to interrogate each bead set as it enters the flow cell, enabling their subsequent classification and quantification (Figure 19B). A red 635nm laser determines the colour of the beads by exciting the impregnated dyes, whilst a green 532nm laser excites the reporter dye, PE to allow quantification of specific analytes.

The detector system receives and distinguishes the fluorescent signals produced by the excitation of the different dyes by both lasers. Each detector measures specific signal emanating from the microspheres. The data is integrated and processed in real time by the digital signal processing system.

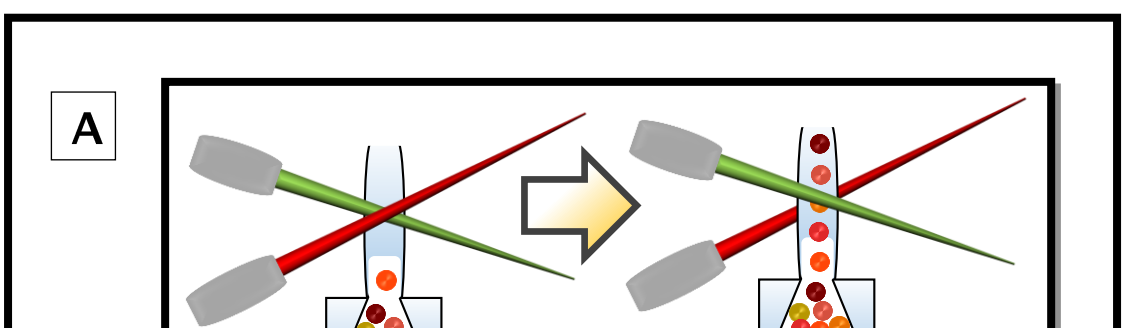

**Figure 18: Measurement of analytes within the Luminex analyser.** Both A and B depict how the Luminex analyser measures analytes. Beads are read in single-file as they enter a stream of flow cells (A) by dual lasers for classification and quantification of each analyte using the Bio-Plex Array Reader (B).

### 2.7.2 Human Cytokine 30-plex panel: Samples and standard preparation

Human 14-plex and 16-plex standards were separately reconstituted in a mixture of 50% assay diluent and 50% tissue culture medium for 15 minutes in advance to allow for sufficient rehydration of the standards. 500µl from each standard were combined to a final total volume of 1ml. Standard curve was generated by using calibrator diluent to prepare 8 different tubes of 1:3 serial dilutions which were gently mixed by pipetting up and down 5 to 10 times. Samples were diluted at required ratios in tissue culture medium. Capture antibody beads were vortexed and centrifuged for 30 seconds after which 833µl of 1X antibody beads was diluted in 1.67ml of wash solution.

### 2.7.3 MMP multiplex: Samples and standard preparation

Standard was reconstituted 15 minutes in advance in 0.95 ml of calibrator diluent. A standard curve was generated from preparing 1:3 serial dilutions (S1 to S8), starting from the reconstituted standard as S1. The chosen vials of microparticles, each for the capture of specified MMP were centrifuged at 1000g for 30 seconds before being vortexed for another 30 seconds. Samples were diluted 1:5 in calibrator diluent. 17µl of each of the microparticles was combined in the same mixing bottle containing 5.2ml of microparticle diluent. Wash buffer was prepared by diluting 20ml of wash buffer concentrate in 480ml of deionised water.

### 2.7.4 Running the multiplex assay

In case of the human cytokine 30-plex panel, a 96-well filter plate was pre-wet with 200µl (100µl in the case of MMP multiplex) of wash buffer by vacuum manifold aspiration. 25µl of the diluted bead solution was added to each well followed by 200µl of working wash solution, and the beads were allowed to soak for 30 seconds. The working wash solution was aspirated using a vacuum manifold, and this washing step repeated two more times. After ensuring that the bottom of the filter plate was blotted with clean paper towel to remove any

residual liquid, 50µl of incubation buffer was added to each well. 100µl of diluted standards and samples were added to the appropriate wells.

In the case of MMP multiplex, 50µl of microparticles were added to each well, followed by 50µl of standards and 50µl of samples in designated wells. In either the 30-plex or MMP multiplex panel, the filter plate was sealed with foil adhesive cover, shaken at full speed of 1000rpm for the first 30 seconds, then at 500rpm for 2 hours. For the human cytokine 30-plex panel, biotinylated secondary antibody was prepared by diluting 333µl of antibody concentrate in 10.2ml of detector antibody diluent. Secondary antibody for the MMP multiplex was first centrifuged at 1000g for 30 seconds and vortexed before 17µl of biotinylated secondary antibody for each MMP was combined in 5.2ml of the same biotin antibody diluent.

Following the two hour incubation, the liquid is aspirated by vacuum manifold and filter plate washed three times. 100µl of biotinylated secondary antibody was added per well of 30-plex panel (50µl in for MMP panel) and plate incubated on orbital shaker at high speed for 30 seconds, then at 500rpm for 1 hour at room temperature.

After 3 washes by vacuuming fluid, diluted streptavidin-PE, prepared by mixing 0.333µl of 10X concentrate Streptavidin-PE in 10.2ml streptavidin-PE diluent (in the case of MMP panel, 55µl streptavidin-PE in 5.5ml of wash buffer) was added and plate incubated on orbital shaker for 30 minutes. After three washes by vacuum aspiration, 100µl of working wash solution was added per well of 30-plex panel plate, with 80µl of wash buffer in the case of MMP panel. The plate was shaken for 2-3 minutes at full speed and inserted into the XY platform of Luminex 200™ for sample analysis.

## 2.8 Lactic Dehydrogenase (LDH) Cytotoxicity detection assay

An LDH assay was used to determine whether or not the chemical compounds being used were safe or toxic to the cells. Damaged or dying cells release LDH

into cell culture media. Measurement of the activity of this LDH released, in a non-radioactive colorimetric assay, is suitable for quantification of cell death and cell lysis. Catalyst (Diaphorase/NAD+ mixture), Dye solution (Iodotetrazolium chloride and sodium lactate), Lysis solution (0.1% Trizol) and Stop solution were provided in the LDH Cytotoxicity detection kit (Roche, #11644793001). 25U/ml of LDH L-Lactic Dehydrogenase solution (L3916 Sigma, 1000 units/mL) was diluted in culture media and used as a starting concentration for 8 standards of 1:3 serial dilutions for the generation of standard curve. Working reagents were prepared according to the manufacturer's protocol as follows: Distilled water (1ml) was added to the catalyst and mixed well, after which 250µl of reconstituted catalyst was diluted in 11.25ml of dye solution to make up the reaction mixture.

Supernatant sample harvested from cells were kept at 4°C for up to one week until day of LDH measurement. Equal number of cells were lysed in lysis reagent and used as high or LDH positive control, with supernatant from untreated samples as 'Low' control and culture medium used for background. 100µl of standards were loaded in duplicates along the first two columns, followed by 100µl per well of samples and all controls. 100µl of freshly prepared reaction mixture was added to each well and plate incubated at room temperature for 30 minutes in the dark. 50µl of stop solution was added to each well to halt the reaction, and absorbance was measured using a microplate reader with 490-492nm filter (reference wavelength more than 600nm). Absolute quantity of LDH was determined by 5P Logistic curve using GraphPad prism.

## 2.9 Antibody staining for flow cytometry

Macrophages were washed two times with PBS after which cells were detached in versene (Life Technologies Ltd., #15040-066) at 37°C for 10 minutes by scraping into 50ml falcon tubes. Cells were topped up to 50ml with PBS and centrifuged at 1500rpm in Allegra™ 6R centrifuge (Beckman Coulter™) for 10mins at 4°C. To inhibit non-specific binding of the secondary antibody, cells

were incubated in FACs blocking buffer (X1 PBS + 1%BSA + 0.1% $NaN_3$ + 10% human AB serum) on ice and in the dark for 30mins. Both *M.tb* infected and uninfected cells were split into appropriately labelled FACs tubes to enable separate staining of HLADR and other macrophage surface markers, PE-isotype control and tubes labelled for 'unstained' samples. FACs tubes were centrifuged for 10mins at 4°C, 1500rpm, followed by incubation with the appropriately diluted conjugated antibody. Cells were washed two times in FACs wash buffer (X1 PBS + 1%BSA + 0.1% $NaN_3$) by 10mins centrifugation, after which cells were incubated on ice for 2 hours in 2% paraformaldehyde (Santa Cruz, USA) to fix the cells and kill any viable *M.tb* . Cells were run using BD Accuri C6 Flow Cytometer and data analysed with BD CFlow software (BD Biosciences, UK).

## 2.10 Total Protein extraction

NP40 lysis buffer (Life Technologies Ltd., #FNN0021) was used to lyse cells according to manufacturer's protocol. Tissue culture plates containing cells were kept on ice pads to prevent protease activity and consequent protein degradation. Cells were quickly scraped and collected into 1.5ml Eppendorf tubes and washed with cold X1 PBS (supplemented with 0.1mM $Na_3VO_4$ and 0.01% $NaN_3$) by spinning for 5mins at 4°C, 120G in a bench top centrifuge.

100µl of ice cold NP40 lysis buffer supplemented with protease inhibitor (1µl of the 1ml protease inhibitor (Sigma-Aldrich Company Ltd., #P-2714) stock solution per 100µl of NP40lysis buffer) and 1ml of PMSF (Sigma-Aldrich Company Ltd., #P7626-250MG) was added to cell pellets from each 6-well plate. For complete cell lysis, the tubes were incubated on ice for 30mins and vortexed at 10mins intervals. Lysates were spun at 420G at 4°C for 10-20mins, and supernatant containing extracted protein transferred into fresh tubes. Again, in order to ensure that the cell lysate was free of viable *M.tb* , samples were sterile filtered using 0.2µm Durapore filters (Millipore) before being taken out of containment laboratory into category II laboratory where they were stored in -80°C for future use.

## 2.11 BCA Assay

In order to allow equal loading of sample for gel electrophoresis, colorimetric detection and quantitation of total protein was ascertained using bicinchonic acid (BCA) assay (Thermo Fisher Scientific, Pierce, # 23225). All reagents and stock solutions were supplied by the manufacturer of the BCA kit. To generate the standard curve, 2mg/ml of stock BSA standard was used to prepare 8 serial dilutions (S1 to S8 at 1:1, 1:2, 1:4, up to 1:64 dilutions and a zero) in nuclease free water, with 2mg/ml as the highest and 0.0625mg/ml lowest concentrations. Working Reagent was prepared in 50ml falcon tubes by adding 50 parts reagent A: 1 part reagent B. Samples were diluted 1:4 and 10µl of both standards and diluted protein samples were added to a clear 96-well plate in duplicate columns. 100µl working reagent was added to each well and plate shaken gently to mix. The plate was covered in aluminium foil, incubated at 37°C for 30mins and then absorbance was measured on the Glomax plate reader at 570nm. A standard curve was produced from the standards and the equation of the curve and the absorbance values of each sample were used to determine the sample protein concentration in µg/µl (mg/ml).

## 2.12 Western Blotting

Based on the calculations from BCA assay , 25µg to 50µg of cell lysate samples were mixed with NuPage LDS sample buffer (Life Technologies Ltd , #NP0008), and used to perform western blot according to the manufacturer's instruction (Invitrogen NuPage system). Protein concentrations were sometimes very high in the lysate samples, in which case less volume (15-25µl) of samples were required to load for electrophoresis. In such situations, precast Bis-Tris Gel, 1.0mm (Life Technologies Ltd, #NP0323BOX) were used. In some other situations however, sample volume between 25µl and 40µl were required, and gels were made in the laboratory. Table 1 shows the recipes of how both separating and stacking gels were casted.

MOPs SDS running buffer was diluted as recommended by the manufacturer and used to run the samples for 1 hour at 200V on constant to separate each protein. Protein bands were then transferred at 30V for 1 hour onto PVDF (Life Technologies Ltd, #LC2005) membrane for antibody staining. The membrane was incubated in a blocking buffer with 4% BSA (Fisher Scientific UK Ltd., #BPE9705/100) in 1X PBS, at room temperature with agitation for 1 hour. Based on knowledge of the molecular weight of the protein of interest, membranes were cut into two in some cases, to enable separate incubation with the primary antibodies of the loading control (β-actin), and that of the protein of interest. Primary antibodies specific to the protein of interest, and mouse anti β-actin (Sigma-Aldrich Company Ltd., #A1978, 1:5000) were diluted in blocking buffer (4% BSA in X1 PBS). Primary antibodies were incubated with the membranes at 4°C overnight with agitation.

After three times of 5mins washes in wash buffer (1X PBS + 4% bovine serum albumin (BSA) + 0.1% Tween 20 (Sigma-Aldrich Company Ltd., #P1379-250ML) with agitation, secondary antibodies were diluted in the same blocking buffer and incubated for 1 hour at RT with agitation. Luminata forte western-HRP substrate (Fisher Scientific UK Ltd., #MDR-120-030C) was used for 3-6 minutes to develop the blot, whilst chemiluminescence was detected using VersaDoc™ imaging system (Bio-Rad laboratories Ltd.). For proteins with molecular weight close to the house-keeping genes, membranes were stripped using 1X ReBlot Plus Mild Antibody Stripping Solution (Merck Millipore, #2502) to remove all bound antibodies before the second protein was probed accordingly.

| Separating Gel (10 % gel) | | 4% Stacking Gel (12.5.ml) | |
|---|---|---|---|
| **solution** | Amount | Solution | Amount |
| **30% Acrylamide/BIS** | 6.3mL | **30% Acrylamide/BIS** | 1.5mL |
| **Separating Gel Buffer (Tris-HCl, pH 8.8)** | 9.5mL | **Stacking Gel Buffer (Tris-HCl, pH 6.8)** | 5mL |
| **10% SDS** | 250µL | **10% SDS** | 125µL |
| **Water** | 3.mL | **Water** | 3.5µL |
| **TEMED (add late)** | 10µL | **TEMED (add late)** | 10µL |
| **Catalyst (add last)** | 63µL | **Catalyst (add last)** | 50µL |

**Table 1: Gel casting protocol for Western Blotting.**

## 2.13 Total RNA extraction

**Both THP-1 cells and MDMs were treated with TRI-reagent (Sigma-Aldrich #T9424-25ML) at 100µl per 1x10$^6$ cells. Cells were vortexed and either used on the day or immediately placed in -80$^o$C for future use.**

### 2.13.1 Phase separation

**On the day of RNA extraction, chloroform (20% of volume of TRI-reagent used) was added to each sample and vortexed for 30 seconds. Samples were allowed to stand at RT for 5-10 minutes and then centrifuged at 4$^o$C, at 1000rpm in a bench top microcentrifuge for 30 minutes. This**

results in a double layered suspension aqueous upper phase (with a volume of approximately half the volume of Tri- reagent used) and organic phase. The upper phase containing the RNA was carefully collected into newly labelled RNAse-free tubes, whilst the lower phase which mainly contains DNA, lipids and proteins were discarded.

### 2.13.2 RNA Precipitation

Glycogen is a carrier protein which enables easy visualisation of precipitated RNA. In order to precipitate the cellular RNA, Isopropanol (50% of the volume of upper phase collected) and 5-10µg of glycogen was added to the collected RNA. The samples were vortexed for 30 seconds and left at RT for 5-10 minutes before being placed in -80°C for 20-60minutes to enable RNA precipitation. RNA was then pelleted by centrifugation at 4°C at 13000rpm for 60 minutes.

### 2.13.3 RNA wash and re-suspension

RNA pellets were carefully washed by centrifugation each time at 4°C at 1000rpm for 5 minutes in firstly 500µl of 100% and then, 75% ice-cold ethanol, without disrupting the pellets. Ethanol was carefully and completely removed and RNA was allowed to air-dry. 30-50µl of RNAse-free water (Fisher Scientific, #BPE561-1) was used to re-suspend the RNA and mixed by pipetting up and down several times. RNA was quantified using NanoDrop spectrophotometer (ND1000 NanoDrop Technologies Ltd.) and stored at -80°C.

## 2.14 Reverse transcription and quantitative PCR (RT-qPCR)

### 2.14.1 Reverse transcription (mRNA)

The extracted RNA was retro-transcribed to complementary DNA (cDNA) according to the manufacturer's instruction as recommended by the High Capacity cDNA Reverse Transcription kit (Life Technologies Ltd,

**#4374966). 100ng/µl of RNA was diluted in RNAse free water (Fisher Scientific UK Ltd, # BPE561-1), and random hexamer (Life Technologies Ltd., #N8080127) was used to obtain the cDNA. Typical reaction master mix recipe and corresponding thermal cycle conditions have been shown in table 2 and 3 respectively.**

| Reagent | Volume used per reaction(µl) |
|---|---|
| **Water (RNase -free)** | Varied |
| **Buffer** | 1 |
| **dNTP** | 0.4 |
| **Enzyme** | 0.5 |
| **RNAase Inhibitor** | 0.5 |
| **Random hexamer** | 3.4 |
| **Random hexamer** | 3.4 |

Table 2: Reaction recipe for reverse transcription

| Thermal Cycle Conditions for mRNA Reverse Transcription | | |
|---|---|---|
| **Step** | Temperature (°C) | Duration (mins) |
| **Step 1** | 25 | 10 |
| **Step 2** | 37 | 120 |
| **Step 3** | 85 | 5 |
| **Step 4** | 15 | Holding time |

Table 3: Conditions for reverse transcription thermal cycle.

### 2.14.2 Micro-reverse transcription (micro-RT)

In order to quantify expression of the micro RNAs of interest, cellular RNA was converted to cDNA as above. In the case of Micro-RT however, 10ng/µl of RNA concentration (diluted using RNase-free water) and stem-loop primers that are specific for each of the micro RNA of interest were used. Tables 4 and 5 show details of stem-loop/mature micro RNA sequences and typical master mix recipes respectively, used for the micro RT and table 5 shows the thermal cycle conditions.

| MicroRNA | Stem-Loop Sequence | Mature miRNA sequence |
|---|---|---|
| **hsa-miR-27a-5p** | CUGAGGAGCAGGGCUUAGCUGCUUGUGAGCAGGGUCCACACCAAGUCGUGUUCACAGUGGCUAAGUUCCGCCCCCCAG | AGGGCUUAGCUGCUUGUGAGCA |
| **hsa-miR-30a** | GCGACUGUAAACAUCCUCGACUGGAAGCUGUGAAGCCACAGAUGGGCUUUCAGUCGGAUGUUUGCAGCUGC | UGUAAACAUCCUCGACUGGAAG |
| **hsa-miR-221-3p** | UGAACAUCCAGGUCUGGGGCAUGAACCUGGCAUACAAUGUAGAUUUCUGUGUUCGUUAGGCAACAGCUACAUUG | AGCUACAUUGUC |
| | UCUGCUGGGUUUCAGGCUACCUGGAAACAUGUUCUC | UGCUGGGUUUC |
| **hsa-mir-7-1** | UUGGAUGUUGGCCUAGUUCUGUGUGGAAGACUAGUGAUUUUGUUGUUUUUAGAUAACUAAAUCGACAACAAAU | UGGAAGACUAGUGA |
| | CACAGUCUGCCAUAUGGCACAGGCCAUGCCUCUACAG | UUUUGUUGU |
| **hsa-mir-455** | UCCCUGGCGUGAGGGUAUGUGCCUCCAUGCAGUCCAUGGGCAUAUACACUUGCCUCAAGGCCUAUGUCAUC | GCAGUCCAUGGGCAUAUACAC |
| **hsa-mir-135a-1** | AGGCCUCGCUGUUCUCUAUGGCUUUUUAUUCCUAUGUGAUUCUACUGCUCACUCAUAUAGGGAUUGGAGCCGUGGCGCACGGCGGGGACA | UAUGGCUUUUUAUUCCUAUGUGA |

| | | |
|---|---|---|
| **hsa-mir-22** | GGCUGAGCCGCAGUAGUUCUUCAGUGGCAAGCU UUAUGUCCUGACCCAGCUAAAGCUGCCAGUUGA AGAACUGUUGCCCUCUGCC | AAGCUGCC AGUUGAAG AACUGU |

**Table 4: Sequences details of stem loop and mature miRNAs for microRNAs' reverse transcription.**

| **Reagent** | **Volume used per reaction(µl)** |
|---|---|
| **Water (RNase -free)** | 4.081 |
| **Buffer** | 0.750 |
| **dNTP** | 0.075 |
| **Enzyme** | 0.500 |
| **RNAase Inhibitor** | 0.094 |
| **Primer (microRNA specific)** | **1.500** |

**Table 5: Reaction recipe for micro RNA reverse Transcription.**

| **Thermal Cycle Conditions for mRNA Reverse Transcription** | | |
|---|---|---|
| **Step** | Temperature (°C) | Duration (mins) |
| **Step 1** | 16 | 30 |
| **Step 2** | 42 | 30 |

| | | |
|---|---|---|
| **Step 3** | 85 | 5 |
| **Step 4** | 15 | Holding time |

**Table 6: Conditions for micro RT thermal cycle.**

### 2.14.3 Quantitative PCR (qPCR)

The cDNAs obtained were then used for microRNA and gene expression quantification assays by qPCR following manufacturer's instruction (Applied Biosystems™, USA). Taqman® Universal master mix and primers specific for the gene of study and GAPDH, as well as primers specific for micro RNAs and RNU44 were used for the typical reaction (Table 7 for master mix recipe and table 8 for qPCR thermal cycle conditions). Each RT-qPCR experiment was performed in duplicate and results were analysed using SDS version 2.3 sequence detection systems (Applied Biosystems™, USA). The comparative $C_T$ method was employed to analyse all qPCR data in this project.

| **Reagent** | **Gene expression assay** | **MicroRNA Assay** |
|---|---|---|
| Taqman Universal MM | 2.5 | 5 |
| RNAse free water | 1.25 | 3.8 |
| Primers (Specific/Random Hexamer) | 0.25 | 0.5 |
| Reference gene | GAPDH | RNU44 |

**Table 7: Typical Master Mix recipes for qPCR.**

| **Number of Cycles** | **Step** | **Temperature (°C)** | **Duration** |
|---|---|---|---|

| | | | |
|---|---|---|---|
| 40 | Denaturation and activation of enzyme | 95 | 10mins |
| | Denaturation | 95 | 15 sec |
| | Annealing/Extension /Hold | 60 | 1min |

**Table 8: Amplification conditions using Taqman universal master mix.**

## 2.15 Transfection of Anti-miRs into macrophages

Macrophages were transfected by directly adding 2ml of 50nM, 100nM or 150nM of specific anti-micro RNAs (anti-miRs) (Life Technologies LTD) which were reconstituted in M-SFM and incubated for 24 hours to repress the activity of their respective target micro RNAs. In experiments where the effect of multiple anti-miRs were investigated in comparison to that of individual anti-miRs, the final concentration of the multiple anti-miRs were used to standardise the final concentrations of the individual anti miRs. Following anti-miR transfection, macrophages were infected with *M.tb* for 48-72 hours, treated with TRI Reagent® and stored in -80°C for future total RNA isolation as described above.

## 2.16 Validation of reference genes (geNormTM Kit)

In order to ensure accurate densitometric analysis of gene expression, it was important to normalise the expression of the gene of interest against a stable internal control gene (house-keeping or reference gene). Reference genes must be stably expressed, and not regulated in both treated and untreated samples. Our model could potentially alter the expression of commonly used constitutively expressed genes. For this reason, reference gene selection kit (geNorm™ kit) (Primerdesign) was used to validate the ideal reference gene for this study.

The human geNorm Kit; 6 gene probe based contains primer/probe mix for six different genes (Genes: UBC, B2M, RPL13A, SDHA, TOP1, ATP5B). GAPDH, β-actin and r18s were included in the experiment to bring the total genes to 9. Each lyophilised primers and probe mix was re-suspended in 220µl of RNAse free water according to the manufacturer's protocol (Primerdesign Ltd, #GE-PP-HU-6). These were used to perform RT-qPCR as explained above. Taqman universal master mix was used for the qPCR recipe.

The data collected from the qPCR experiment was analysed using qBase software (Biogazelle, www.boigazelle.com). It would have been useful to evaluate additional candidate reference targets. As this was not done, geometric mean of the three most stable reference targets (B2M, UBC and TOP1) was used in most qPCR experiments. The use of multiple (non-optimal in this case) reference targets allows a more accurate normalization compared to the use of a single non-validated reference target.

## 2.17 4-TU labelling of macrophages

Macrophages were first infected with *M.tb* as described above for two hours, after which the extracellular bacilli were washed. 100µM of 4-Thio uridine was added directly to the cells in M-SFM for at least 24 hours. Cells were lysed in Tri-reagent and total RNA was extracted and quantified as described above. Figures 9-10 outline the underlying principle of 4-TU labelling and pull-down assay for the purification of newly synthesised mRNA.

### 2.17.1 Biotinylation of 4-TU labelled RNA

1mg/ml of EZ-Link biotin-HPDP (Pierce, Thermo Fisher Scientific UK Ltd) solution was prepared in Dimethylformamide (DMF). 1µl of 1mg/ml of EZ-Link biotin-HPDP solution was used per µg of total 4-TU labelled RNA. Master mix was prepared from 1M Tris (pH 7.4) and 0.5M EDTA to a final concentration of 10mM Tris and 1mM EDTA, using RNase free water to top up to a final reaction volume which is five times the original RNA volume. The mixture was incubated at room temperature for two hours in the dark.

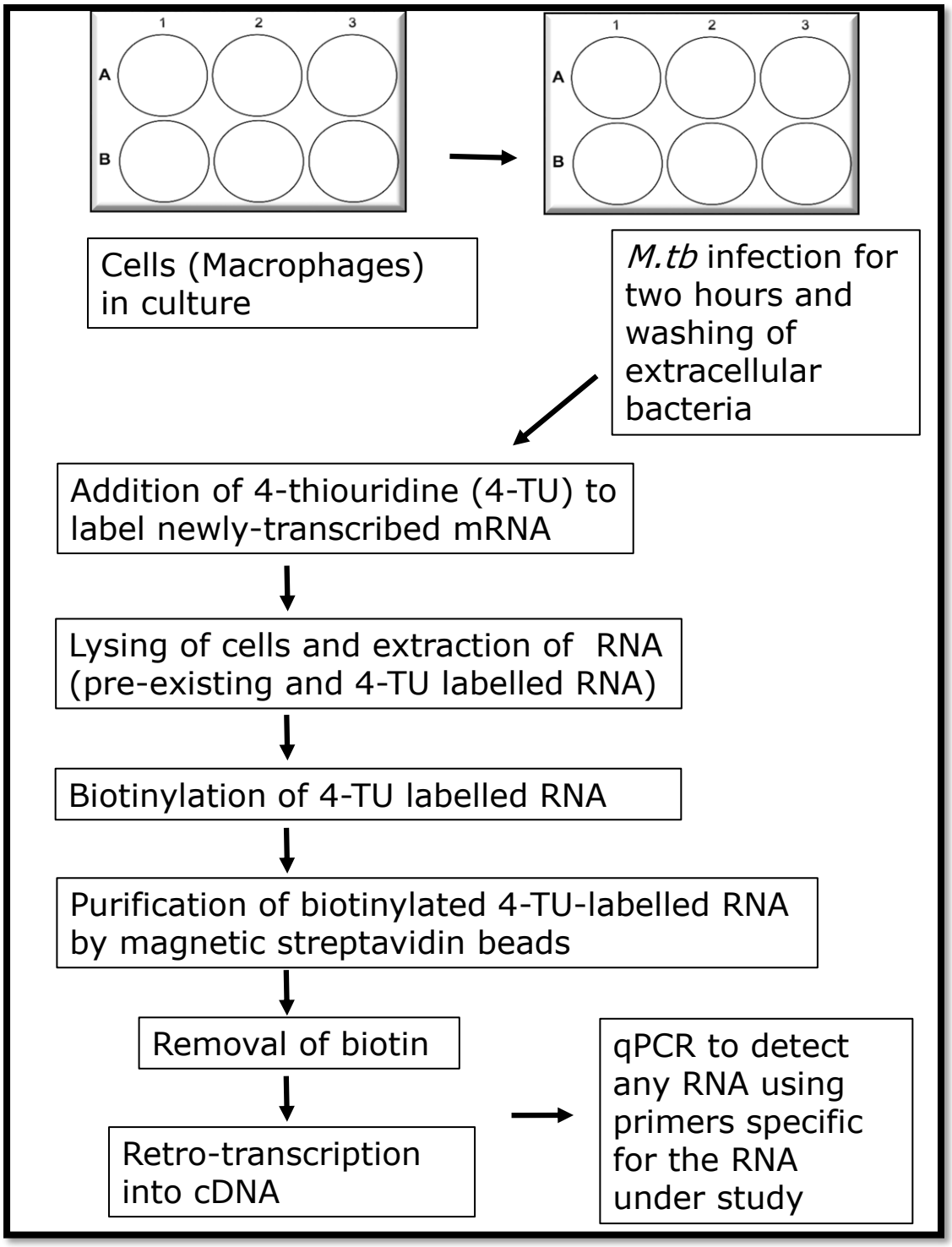


Table 9: Simplified schematic of 4-TU labelling. **This explains the steps involved in 4-TU tagging for isolation of newly transcribed RNA.**

### 2.17.2 Precipitation of biotinylated 4-TU-labelled RNA

Isopropanol (volume equal to the final reaction volume) and 5M NaCl (A 10th of the final reaction volume) were added to the biotinylated 4-TU labelled RNA. The mixture was vortexed and incubated at room temperature for 5 minutes before being centrifuged in a bench top microcentrifuge at maximum speed (13000rpm) for 20mins. The RNA pellet was washed in 250µl of 75% Ethanol by 10 minutes centrifugation, again at top speed for 10 minutes. The pellet was allowed to air-dry until semi-transparent, and RNA was re-suspended in 20-50µl of RNase free water. The re-suspended RNA was purified immediately or stored at -80°C for future pull down experiment.

### 2.17.3 Purification of biotinylated 4-TU labelled RNA (Pull down)

To isolate and purify the 4-TU labelled RNA, Magnetic Porous Glass (MPG) streptavidin beads (Pure Biotech LLC, # MSTR0502) were used to bind and pull down the biotinylated 4-TU labelled RNA. The beads were incubated with tRNA (1µg per 5µl of beads) and rotated at room temperature for 20 minutes. Tubes were placed in magnetic stand beads allowed to collect on the side of the tube for 1minute. This was followed by three washes in 300µl of MPG buffer (1M NaCl, 10mM EDTA, 100mM Tris-HCL at pH 7.4 in RNase free water). Beads were re-suspended in MPG buffer equal to the original volume of beads. The volume of RNA and beads were adjusted to be equal, to allow 1:1 combination ratio. The biotinylated 4-TU RNA was added to the beads and incubated at room temperature with rotation for 1 hour. Beads were collected in magnetic stand for over 1 minute. The supernatant was collected and kept as unbound, non-4TU RNA. Beads were washed two times in 250µl of room temperature MPG buffer, one wash in 65°C MPG buffer, and a final wash in 50µl MPG buffer. The supernatant from the last wash was kept as 'wash RNA' to check for flow through RNA.

### 2.17.4 Elution and precipitation of bound, 4-TU labelled RNA

To elute the bead-bound, 4-TU labelled RNA, freshly prepared 5% β-mecaptoethanol was added at volume equal to original bead volume and incubated at room temperature with rotation for 20 minutes, flipping the tubes to mix well every 5 minutes. The tubes were centrifuged quickly to collect all drops, and beads collected in magnetic stand for over 1 minute. The supernatant was kept as bound, 4-TU RNA. RNA was precipitated as described above by adding 5M NaCl at 1/10$^{th}$ the RNA volume, isopropanol at the same volume as the RNA, and 1µg glycogen. The mixture was incubated at room temperature for 5minutes and centrifuged at maximum speed for at least 20minutes. The RNA pellet was washed in 250µl of 75% Ethanol by 10 minutes centrifugation, at top speed for 5 minutes. The pellet was allowed to air-dry until semi-transparent, and RNA was re-suspended in 20-50µl of RNase free water.

The re-suspended RNA was placed in the magnetic stand for the final time (over 1minute) to collect any residual beads. The supernatant was collected in newly labelled nuclease free tubes as purified, newly synthesised RNA samples.

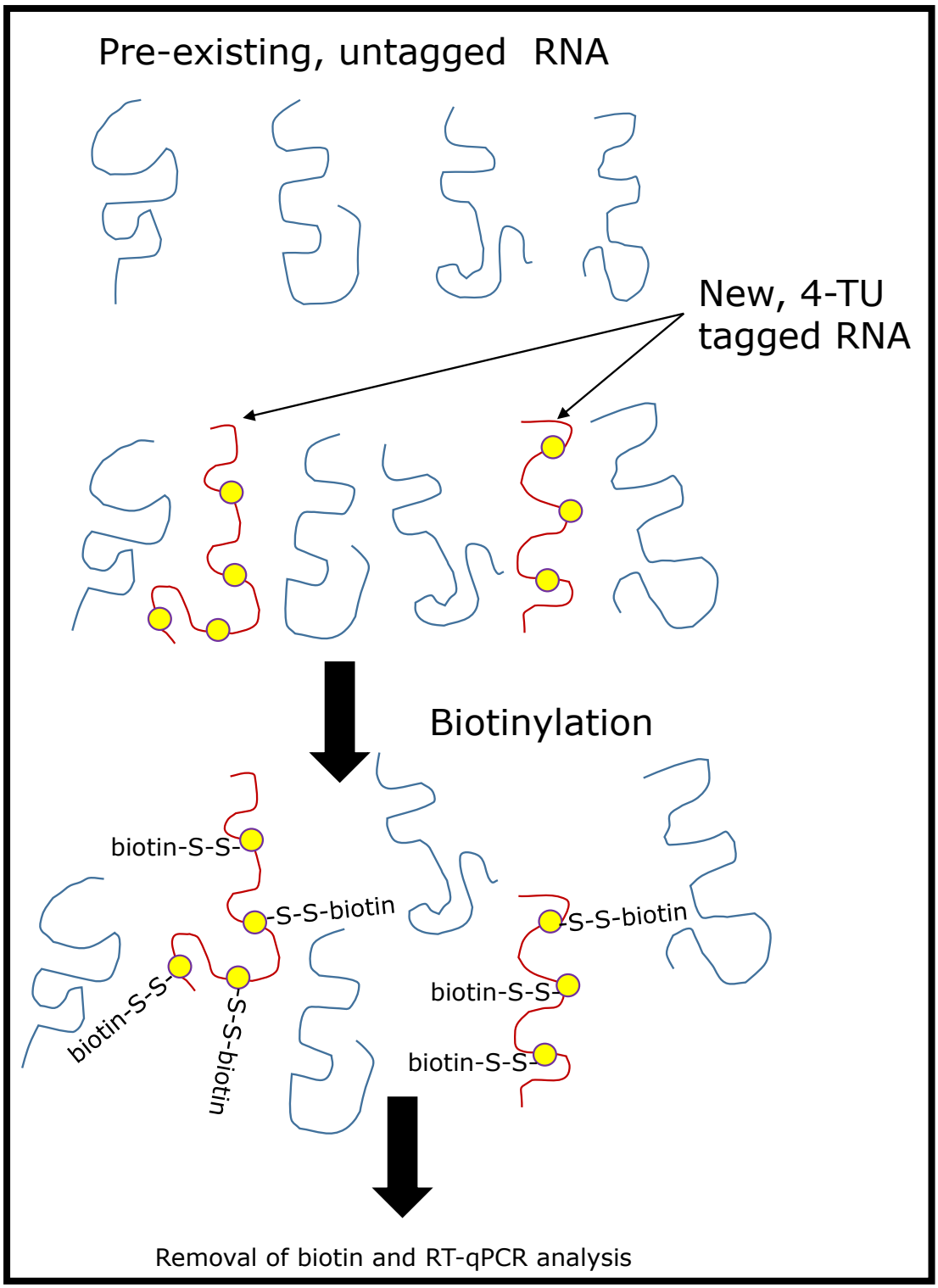


**Table 10: Simplified schematic of 4-TU labelling and RNA pull down.** This explains the steps involved in 4-TU tagging and pull down for isolation of newly transcribed RNA.

### 2.17.5 Superscript III Reverse Transcription

Purified 4TU-labelled RNA was treated with rDNase (DNA-free™ Kit, ambion by life technologies, # AM1906) to remove potential genomic DNA contamination. SuperScript™ III Reverse Transcriptase (Invitrogen, # 18080-044), Oligo (dt)12-18 primer (Invitrogen # 18418-012) and random hexamer (Component of high capacity cDNA kit, Life Technologies Ltd, # 4374966) were used to retro transcribe 5µg of the pulled down RNA to cDNA in a 20µl reaction volume according to the manufacturer's protocol. RNA was added to master mix prepared by adding 1µl each of Oligo (dt) 12-18, random hexamer and dNTP (Component of high capacity cDNA kit, Life Technologies Ltd, #4374966) and nuclease-free water in RNase-free microcentrifuge tubes. The mixture was heated at 65°C for 5mins, after which tubes were incubated on ice for a further 1minute. 4µl, 1µl and 2µl of 5X first strand buffer, 0.1MDTT, SuperScript™ III Reverse Transcriptase respectively (all from Invitrogen, # 18080-044) and 1µl of RNaseOUT (Invitrogen # 10777-019) were added and mixed by pipetting up and down. Reverse transcription was performed by incubating tubes at 25°C for 5 minutes, 55°C for 40 minutes and at 70°C for 15 minutes. The cDNA was stored in -20°C to be used in future as template for qPCR amplification as previously described

## 2.18 Immunohistochemistry

Paraffin-embedded human normal or *M.tb* infected lung tissues were mounted as 4µm sections onto APS coated glass slides and allowed to dry for at least 48 hours in 40°C incubator. Sections were dewaxed stepwise for 5 minutes each time in two different vessels of clearene and then rehydrated through graded alcohol to 70%. Freshly made 0.5% 30% hydrogen peroxide in methanol was used to block endogenous peroxidase for 10 minutes. Sections were washed 3 X 2 minutes in TBS buffer, pH 7.2-7.6. (10X concentrate TBS prepared by mixing 80g Nacl and 6.053g Tris base in 1L of distilled water). Heat induced-epitope retrieval methods were employed by boiling the slides

in 1mM EDTA (pH 8.0) in distilled water for 25 minutes in microwave at 50% power.

Slides were incubated in Avidin solution for 20 minutes, followed by 3 X 2 minutes washes. This was followed by incubation in biotin solution for 20 minutes followed by another wash step. Exposed epitopes that the secondary antibody might non-specifically interact with was blocked using 'culture medium' consisting of Dulbecco's Modified Eagle Medium (DMEM) (supplemented with 10% FCS and 2% human serum) was used to block for 20 minutes. Slides were incubated at 4°C overnight in appropriately diluted primary antibody; 1:1000 dilution of anti-PIK3CD (LifeSpan BioScience, Inc #LS-C338531/63835).

Sections were washed 3 X 5 minutes in TBS and incubated in 1:400 of biotinylated rabbit anti mouse (Dako, #E0413) secondary antibody for 30 minutes. After a second 3 X 5 minutes TBS wash steps, sections were incubated for 30 minutes in streptavidin biotin-peroxidase complexes (Elite vectastain ABC kit, Vector laboratories # PK-6100) was prepared 30 minutes in advance by combining 1:1:75 parts of reagent A, reagent B and TBS respectively. This allows time for streptavidin to form complexes with biotin peroxidase for amplification of signal. Sections were washed and incubated in freshly prepared DAB (2-component DAB pack, BioGenex # HK542-XAK) substrate for 5 minutes followed by a quick rinse in TBS and 5 minutes wash under running tap water. For approximately 1ml of DAB, 32µl of DAB chromogen and 50µl of 15% sodium azide were added to 1ml of stable DAB substrate buffer. Counter staining was performed in Mayer's haematoxylin for 20 seconds after which sections were allowed to blue under running tap water for 5 minutes. Dehydration of slides was performed at 1 minute in each graded alcohols to clearene, followed by mounting in pertex. Sections were allowed to dry and images observed using a standard light microscope. Images were captured on Olympus BX51, CC12 (dotSlide), and Nikon Coolpix 950 microscopes.

Sections from each lung tissue was used for staining for CD68 by IHC using protocols and equipment located within the Southampton General hospital diagnostic IHC laboratory by an automated system. Briefly, 4um FFPE sections were mounted on Superfrost Plus adhesive slides before drying at 60 º C for 30 mins to assist with tissue annealing and removal of excess wax. Deparaffinization, hydration and antigen demasking was completed by heat induced epitope retrieval (HIER) using High pH Target retrieval solution (Dako, K8004) and a standardized protocol on PT Link (Dako, Denmark).

IHC staining was completed using EnvisionFLEX+ (Dako, K8002) detection system and automated Dako Link 48 equipment (Dako). Endogenous Peroxidases were blocked using Peroxidase Blocking Solution. For detection of CD68 the ready-to-use monoclonal mouse antibody, clone PG-M1 (Dako, IR613), was incubated for 20 minutes at room temperature. The primary antibody was detected using a secondary HRP conjugate (EnvisionFLEX+ HRP) for 20minutes. Final visualization used 2x 5minute incubations of DAB to produce a brown chromogenic pigment indicating positivity. Sections were counterstained with Hematoxylin (Dako, K8008) to identify nuclei, dehydrated, cleared and mounted.

## 2.19 Statistical analysis

All data were analysed using GraphPad Prism version 6. Parametric unpaired t-test was used to ascertain significance of results obtained. P values $\leq 0.05$ were considered significant results, otherwise insignificant. In experiments where secreted proteins were analysed, triplicate samples were used and the experiments were performed in three different donors. RT-qPCR experiments were analysed in duplicate and in at least two different donors. All bar charts are a representation of the ± SD of the mean.

# 3. CHAPTER 3: RESULTS PART I

## Characterisation of Cells and their response to pharmacological treatment and *M.tb* infection

### 3.1 Overview

The aim of this project was to identify host regulatory pathways that suppress TB immunopathology. This was investigated by studying the effects of PI3K inhibition on MMP-1 production by macrophages, and by dissecting signalling cascades downstream of the PI3K pathway that modulate pathogenic MMP-1 production in TB.

### 3.2 Methods

Firstly, this project sought to confirm *M.tb* -driven up-regulation of MMP-1 in THP-1 cells and in human primary macrophages. THP-1 cells and human monocytes were differentiated into macrophages and infected with either UV killed or live H37RV strain of *M.tb* . Supernatant samples were harvested at 72 hours post *M.tb* infection, and levels of secreted MMP-1 were determined by ELISA or Luminex assays. In other experiments, PI3Kδ and other downstream effector proteins of the PI3K pathway were pharmacologically inhibited before infecting cells with *M.tb* . Again, secreted MMP-1 was measured in samples harvested at 72 hours post-infection by ELISA. The luminex array system was employed to decipher the global effect of PI3K pathway inhibition on multiple MMPs and on a variety of cytokines and chemokines.

### 3.3 Chapter Hypothesis

Destruction of lung matrix and subsequent cavitation are characteristic hallmarks of Pulmonary TB, the most infectious form of TB (Behr et al., 1999). Crucial roles of MMP-1in various pathogenic conditions have been identified, where their up-

regulation often correlate with disease severity (Zeng et al., 2006). Recent developments have highlighted negative regulatory role of intracellular signalling including the PI3K/AKT/mTOR pathway in disease (Fukao and Koyasu, 2003, Fukao et al., 2002), but this has not been studied in TB. I therefore proposed that signalling downstream of the PI3K pathway negative regulates MMP-1 in macrophages to limit disease progression. This led to the hypothesis that chemical blockade of this pathway and its downstream mediators would accentuate MMP-1 production in macrophages.

## 3.4 Aims

The primary aim of this chapter was to investigate the modulation of *M.tb* -driven MMP-1 by macrophages upon inhibition of the PI3K pathway. The initial experiments sought to carry out various optimisation protocols in order to establish the appropriate cell culture conditions required for this study. Next, the regulatory pathways under study were pharmacologically inhibited to define the effects of such chemicals on MMP production by macrophages. This chapter will highlight the following:

- Characterisation of THP-1 cells and primary macrophages.
- Confirmation of phagocytic ability of MDMs.
- Optimisation of seeding density and kinetics of MMP-1 secretion.
- The effect of pharmacological inhibition of PI3K pathway on MMP-1 secretion by macrophages.
- Dissection of the role of intracellular signalling in regulating protease secretion.

## 3.5 M-CSF-induced Monocyte Derived Macrophages (MDMs)

Monocytes that were isolated from PBMCs by adherence purification were stimulated with 100ng/ml M-CSF as described above. Following adherence purification, monocytes remain attached to tissue culture plates, with a

circular morphology (Figure 16A). Upon incubation with M-CSF, monocytes differentiated to macrophages with the typical 'fried egg' looking morphology (Figure 16B).

### 3.5.1 MDMs express known macrophage markers

Although the observed fried-egg-like morphology of generated MDMs give an indication that the cells are indeed macrophages, it was important to use other approaches to confirm this. Flow cytometry was used to determine whether or not the macrophages expressed cell surface receptors and markers known to be typically expressed by macrophages. This was particularly necessary since adhesion purification was used in isolating MDMs in this project. This method is known to potentially result in contamination of the required cell population by non-adherent cells including lymphocytes. It was therefore important to ensure that the cells that were isolated and used for this study were a true representation of the type of polarised macrophages that are predominant in TB infection. Peripheral and tissue macrophages are known to express cell surface receptors including CD (Cluster of Differentiation) 14, CD80 and CD163. I confirmed that the generated MDMs expressed CD11c, CD14, CD36, CD80 and CD163 (Figure 20).

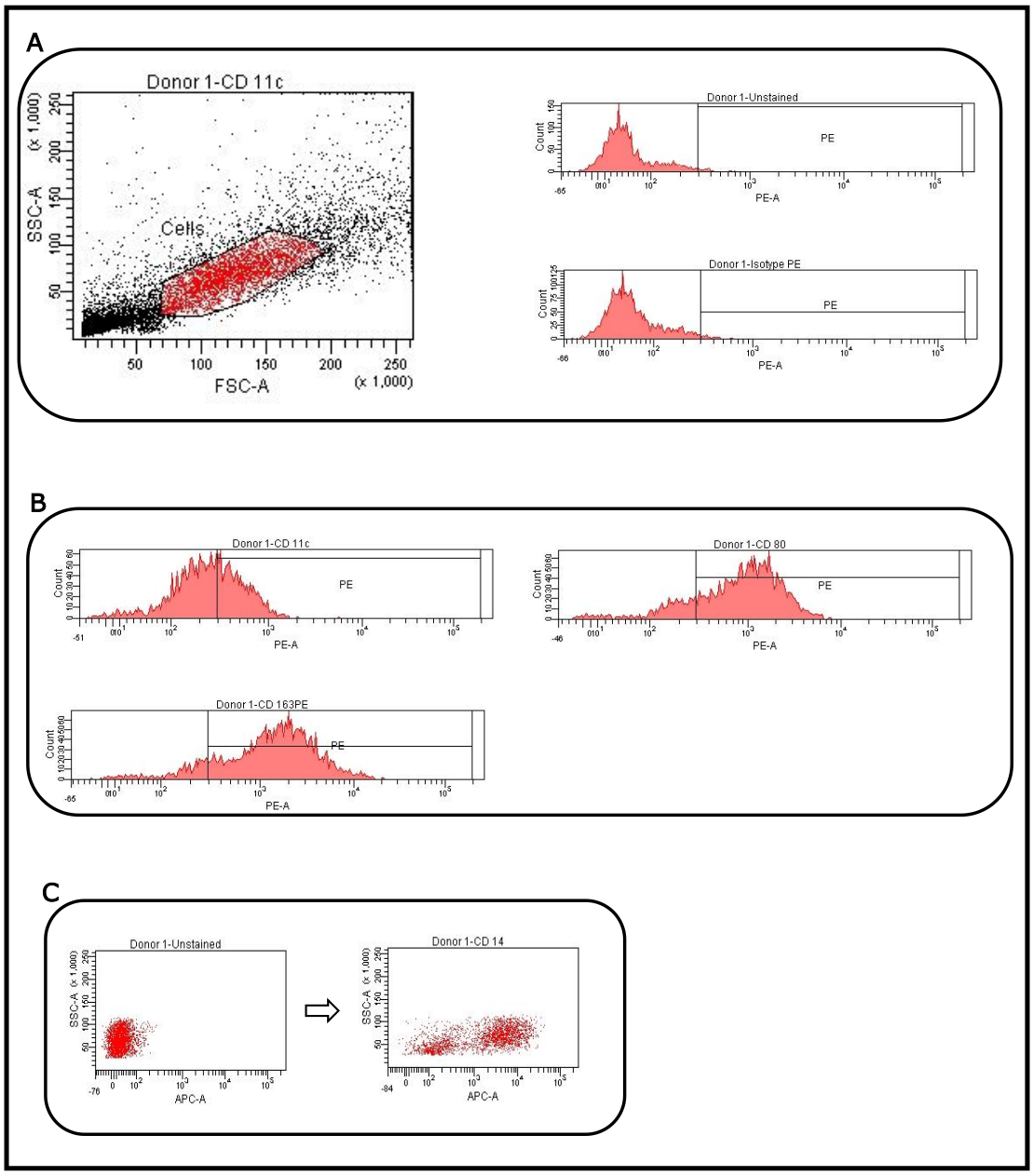
A
Donor 1-CD 11c
SSC-A (x 1,000)
Cells
FSC-A (x 1,000)
Donor 1-Unstained
Donor 1-Isotype PE
PE
PE-A
Count
B
Donor 1-CD 11c
Donor 1-CD 80
Donor 1-CD 163PE
C
Donor 1-Unstained
Donor 1-CD 14
APC-A

**Figure 19: In vitro Monocyte-derived macrophages express receptors that are found on macrophages in vivo.** MDMs were analysed by Flow Cytometry for the expression of known macrophage cell surface receptors. A: Forward and side scatter (Left) indicates the presence of macrophages in the population of cells used. Both the population of cells that were not antibody-stained and those stained with IgG (PE-isotype control) shows no PE signal. B: PE-conjugated antibodies show a shift (to the right) of cell populations that express CD11c, CD80 and CD163. C: APC-conjugated antibodies also show a shift to the right, indicating expression of CD14 by the MDMs.

### 3.5.2 Kinetics of the ability of MDMs to phagocytose *M.tb*

Macrophages play crucial roles in the immune response to TB (Guirado, 2013). The initial host response upon inhalation of *M.tb* is the capture of the bacilli by alveolar macrophages (AM) (Guirado, 2013, Ehlers and Schaible, 2013). Peripheral monocytes are continuesly recruited to developing granulomas at the site of *M.tb* infection, where they engulf bacteria released from dying macrophages and further differentiate to various forms of polarised macrophages in order to attempt to contain the infection (Ehlers and Schaible, 2013). It was therefore important for our system to replicate this phagocytosis ability of macrophages.

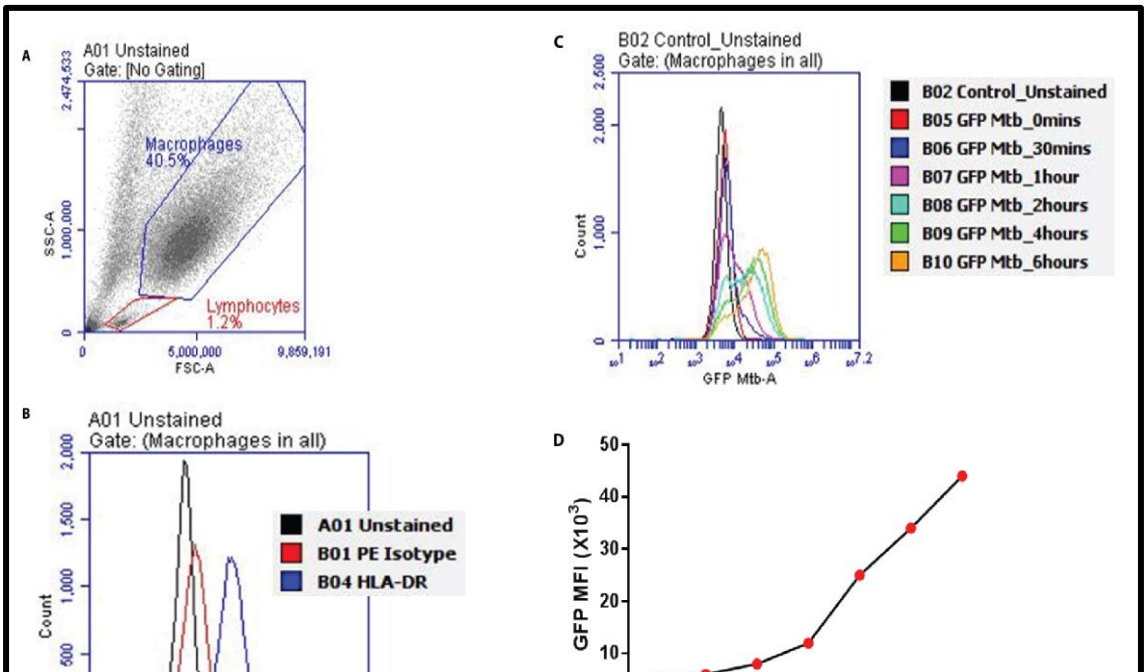

Figure 20: Kinetics of MDMs ability to phagocytose *M.tb* . Cells were infected with GFP-*M.tb* and stained with HLA-DR. A: Adherence purification generates good population of macrophages with a low (1.2%) lymphocyte contamination. B: Specificity of anti-HLA-DR antibody. C & D: Mean fluorescence intensity (MFI) indicating GFP-expressing cells were measured at increasing levels as a function of time. Macrophage ability to capture *M.tb* was determined by Flow Cytometry.

MDMs were infected with GFP-tagged *M.tb* and cells lysed at different time points to ascertain the kinetics of *M.tb* engulfment by macrophages (Figure 21). Antibodies against the macrophage surface marker HLA-DR was used to stain the cells. Macrophage-ingested *M.tb* was measured at different time points for the first 6 hours of infection with increasing levels of *M.tb* engulfed over longer period of time.

## 3.6 Optimisation Experiments

In an *in vitro* study of this nature, most of the investigation was carried out using macrophages and/or macrophage-like cell lines in other to replicate the *in vivo* phenotype. It was therefore necessary to establish the optimal time point to study and appropriate number of cells needed in order to achieve adequate levels of secreted MMP-1 that can be detected by ELISA assay.

### 3.6.1 Kinetics of MMP-1 secretion by MDMs

MDMs were incubated for up to 72 hours post *M.tb* infection in order to ascertain the appropriate incubation time required for ELISA-detectable level of MMP-1. The cells secreted MMP-1 into the supernatant samples, and this

was easily detected by ELISA at 72 hours post *M.tb* infection of MDMs (Figure 22).

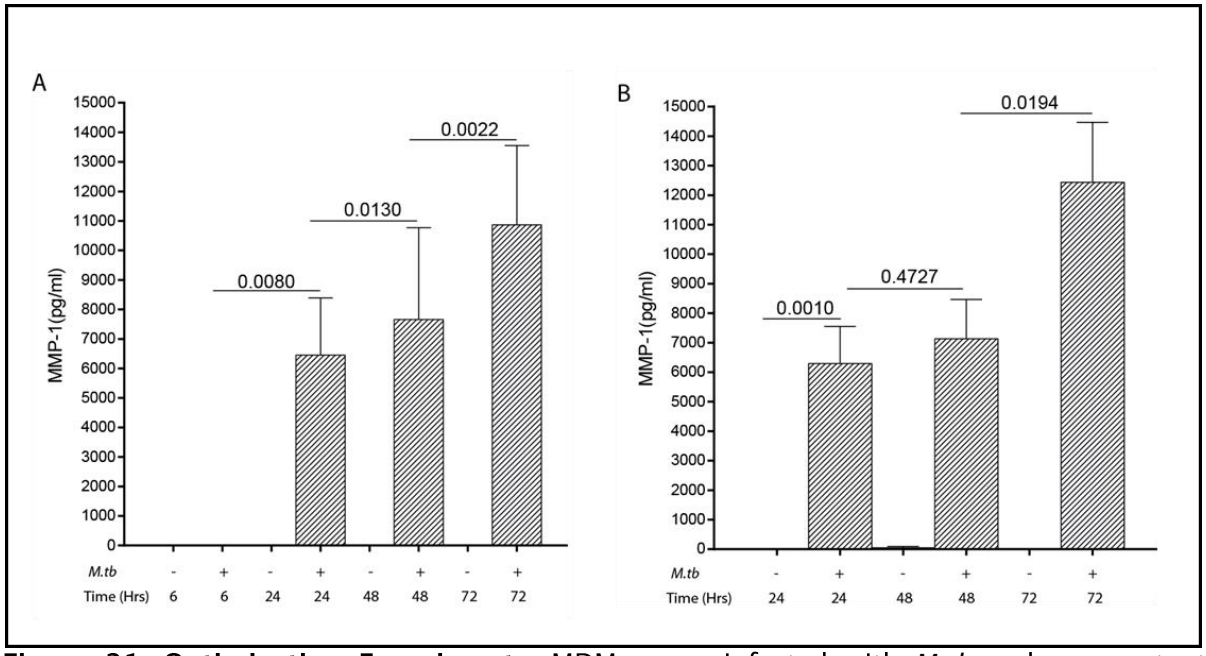


**Figure 21: Optimisation Experiments.** MDMs were infected with *M.tb* and supernatant samples harvested at different time points for MMP-1 analysis by ELISA. **A:** Samples were harvested at 6 hrs, 24 hrs, 48 hrs and 72 hrs post *M.tb* infection. **B:** Samples were harvested at 24 hrs, 48 hrs and 72 hrs post *M.tb* infection. The highest secretion of *M.tb* -driven MMP-1 was measured at 72 hours post infection. A and B are two experiments performed on two different occasions in triplicate conditions. P values are Student's t-test, with P value < 0.05 considered significantly different.

### 3.6.2 MMP-1 secretion profile in THP-1 cell

THP-1 cells were seeded at $2.5x10^5$, $5x10^5$, $1x10^6$ and $1.5x10^6$, in triplicate wells in 48 multi-well tissue culture plates. The highest level of secreted MMP-

1 was detected from supernatant samples that were harvested from wells containing $1.5x10^6$ THP-1 cells (Figure 23). THP-1 cells were therefore seeded at $2.5x10^5$ cells per $cm^2$. However, the surface area of 48 well plate ($.75cm^2$) permits a maximum of $5x10^5$ cells per well, which is inadequate for obtaining ELISA-detectable level of MMP-1 secretion by macrophages. For this reason, subsequent experiments using THP-1 cells were carried out using 24 well plate ($2.00cm^2$) at $1x10^6$ whenever possible.

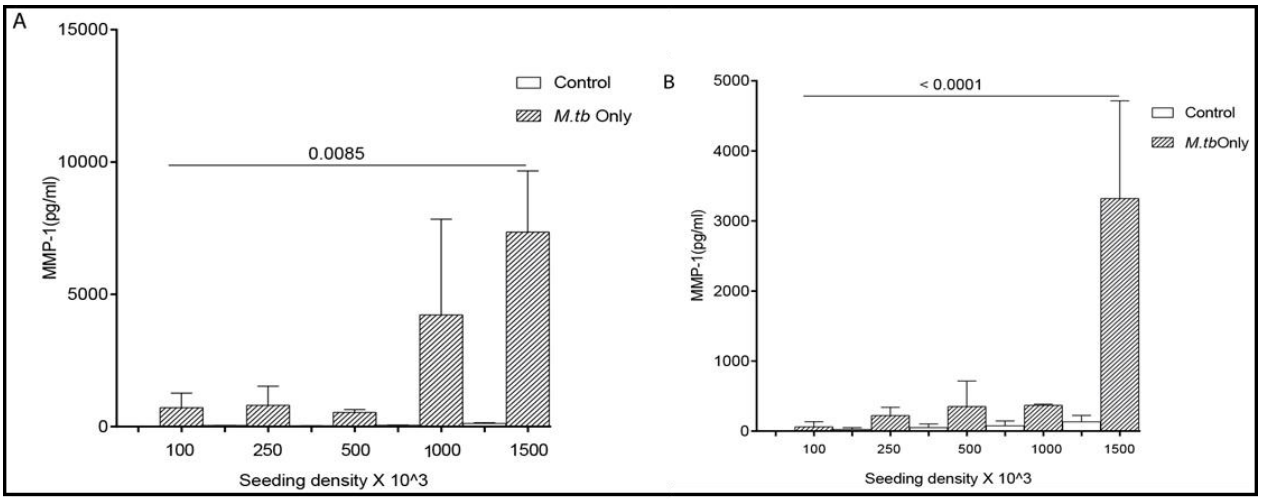


**Figure 22: Optimisation Experiments.** THP-1 cells infected with UV killed *M.tb* secreted MMP-1 at 72 hours post infection in an increasing order of seeding density. A and B are two experiments performed on two different occasions in triplicate conditions. P values are Student's t-test, with P value < 0.05 considered significantly different. Ordinary One-Way ANOVA has been performed to confirm the significance of differences among means.

## 3.7 PI3K signalling negatively regulates MMP-1 in TB

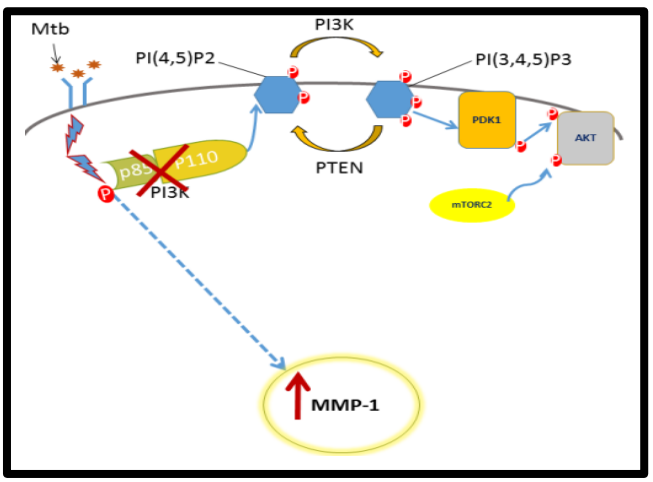

**Figure 23: Simplified schematic of the PI3K pathway (upstream signalling events).** The important effectors of PI3Ks are highlighted. PTEN, PDK1, AKT and mTORC-1 were all targeted by chemical inhibition in this study, and their effect on MMP-1 production ascertained.

### 3.7.1 PI3K inhibitors augment *M.tb* -driven MMP-1 in MDMs

*M.tb* infection significantly upregulated MMP-1 secretion. The pan-PI3K inhibitor, LY294002 surprisingly further enhanced this *M.tb*-driven MMP-1 both at the secretion (Figure 25A) and gene expression (Figure 25B) levels. LY294002 globally inhibits PI3K activity. It was therefore necessary to confirm this result in the context of other inhibitors of PI3K pathway. For this reason, a different compound that also targets the PI3K pathway by blocking PI3Ks and PDK1 (NVP-BAG956) was used to treat the cells prior to *M.tb* infection. Again, *M.tb* -driven MMP-1 produced by macrophages was significantly elevated by NVP-BAG956 (Figure 26).

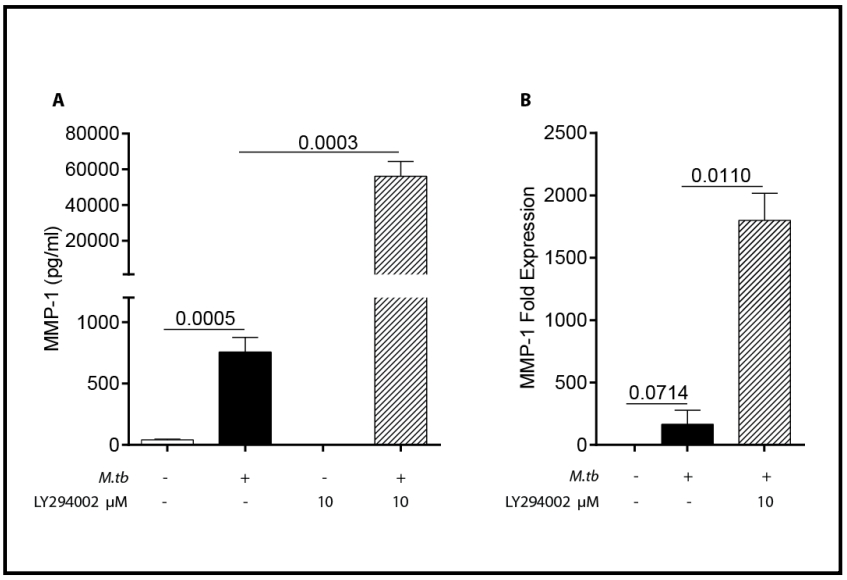


**Figure 24: PI3K inhibitors augment *M.tb* -driven MMP-1.** MDMs were pre-treated with 10µM of LY294002 for two hours prior to *M.tb* infection. A: Supernatant samples were harvested after 72 hours post infection for MMP-1 detection by ELISA. *M.tb* drove secretion

of MMP-1 in macrophages. Global inhibition of PI3K pathway by LY294002 further enhanced this production of MMP-1 by macrophages. B: LY294002 similarly elevated *M.tb* -driven MMP-1 gene expression in macrophages at 48 hours post infection. Data show mean and standard deviation of experiments performed in triplicates and is representative of experiments performed on a minimum of three donors at separate occasions. P values are Student's t-test, with $P < 0.05$ considered significantly different.

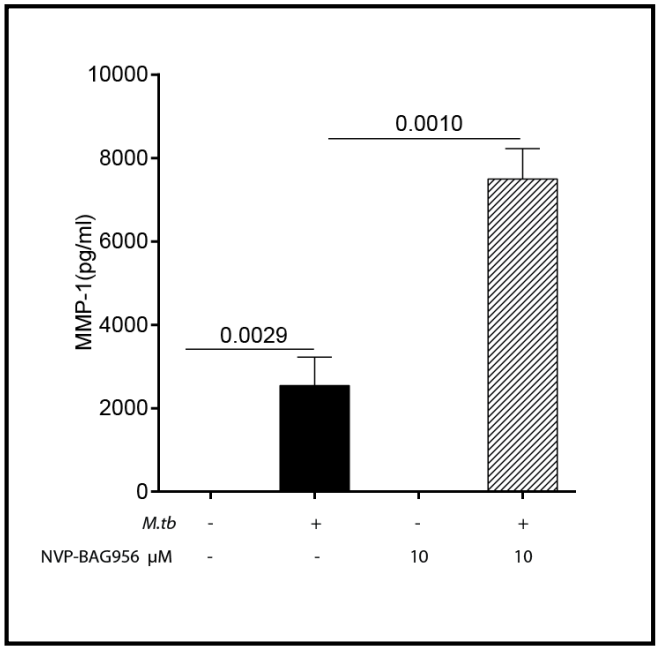


**Figure 25: NVP-BAG956 also augments *M.tb* -driven MMP-1.** MDMs were pre-treated with 10µM of PI3K/PDK1 inhibitor (NVP-BAG956) for two hours prior to *M.tb* infection. Supernatant samples were harvested after 72 hours post infection for MMP-1 detection by ELISA assay. *M.tb* induced MMP-1 secretion in macrophages and this was further enhanced by NVP-BAG956 treatment. Data show mean and standard deviation of experiments performed in triplicates and is representative of experiments performed on a minimum of three donors at separate occasions. P values are Student's t-test, with $P < 0.05$ considered significantly different.

## 3.8 LY294002 represses AKT phosphorylation

Active PI3K consequently leads to AKT phosphorylation. To further confirm that LY294002 directly targets PI3Ks in this system, phosphorylation of AKT at Thr 308 was analysed by western blot. *M.tb* –induced AKT phosphorylation (Figure 27, lane 2) was suppressed by LY294002 (Figure 27, lane 3). PTEN is a phosphatase that antagonises the catalytic action of PI3Ks. Inhibition of PTEN had no effect on *M.tb* –driven AKT phosphorylation (Figure 27, lane 4).

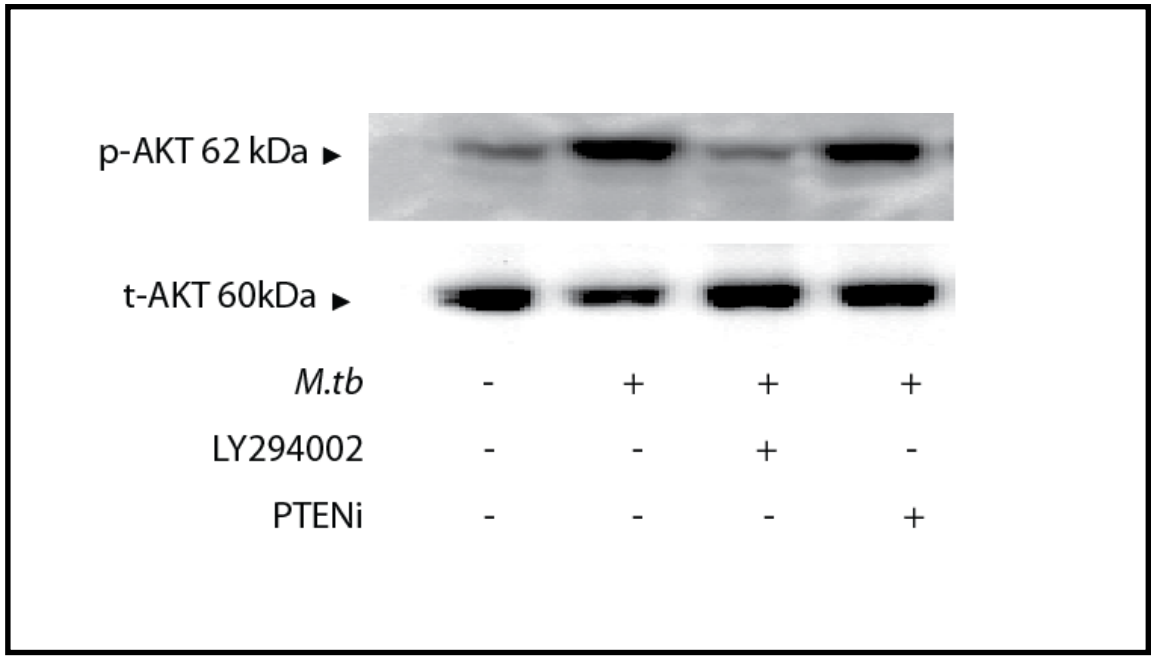


**Figure 26: Modulation of AKT phosphorylation by LY294002 and PTEN inhibitor.** MDMs were pre-treated with 10μM of LY294002 or 10μM PTEN inhibitor (bpv(Phen)) for two hours prior to *M.tb* infection. Western blot analysis shows that LY294002 suppressed, whilst PTEN inhibition exerted no change, on *M.tb* –driven AKT phosphorylation 2 hours post *M.tb* infection. Experiment was performed in on three different occasions.

## 3.9 The delta isoform of PI3K mediates MMP-1 regulation in MDMs

There are eight known PI3K isoforms classified under three main classes. To decipher the exact PI3K isoform that mediates the signalling that culminates in negative regulation of MMP-1 in TB, the isoforms of class IA (α, β and δ); and the class IB (γ) PI3K proteins were targeted by chemical inhibition. Although PI3Kα inhibitor augmented *M.tb* -driven MMP-1 (Figure 28A), the response was not as marked as that driven by PI3Kδ inhibition (Figure 28D). The effect of inhibition of PI3Kβ on MMP-1 began with slightly elevated *M.tb* -driven MMP-1 at a low concentration of 0.015nM, which was repressed when the concentration was increased by 10 and 100 fold respectively (Figure 28B). PI3Kγ inhibitors showed a suppression effect on MMP-1 secretion (Figure 28C).

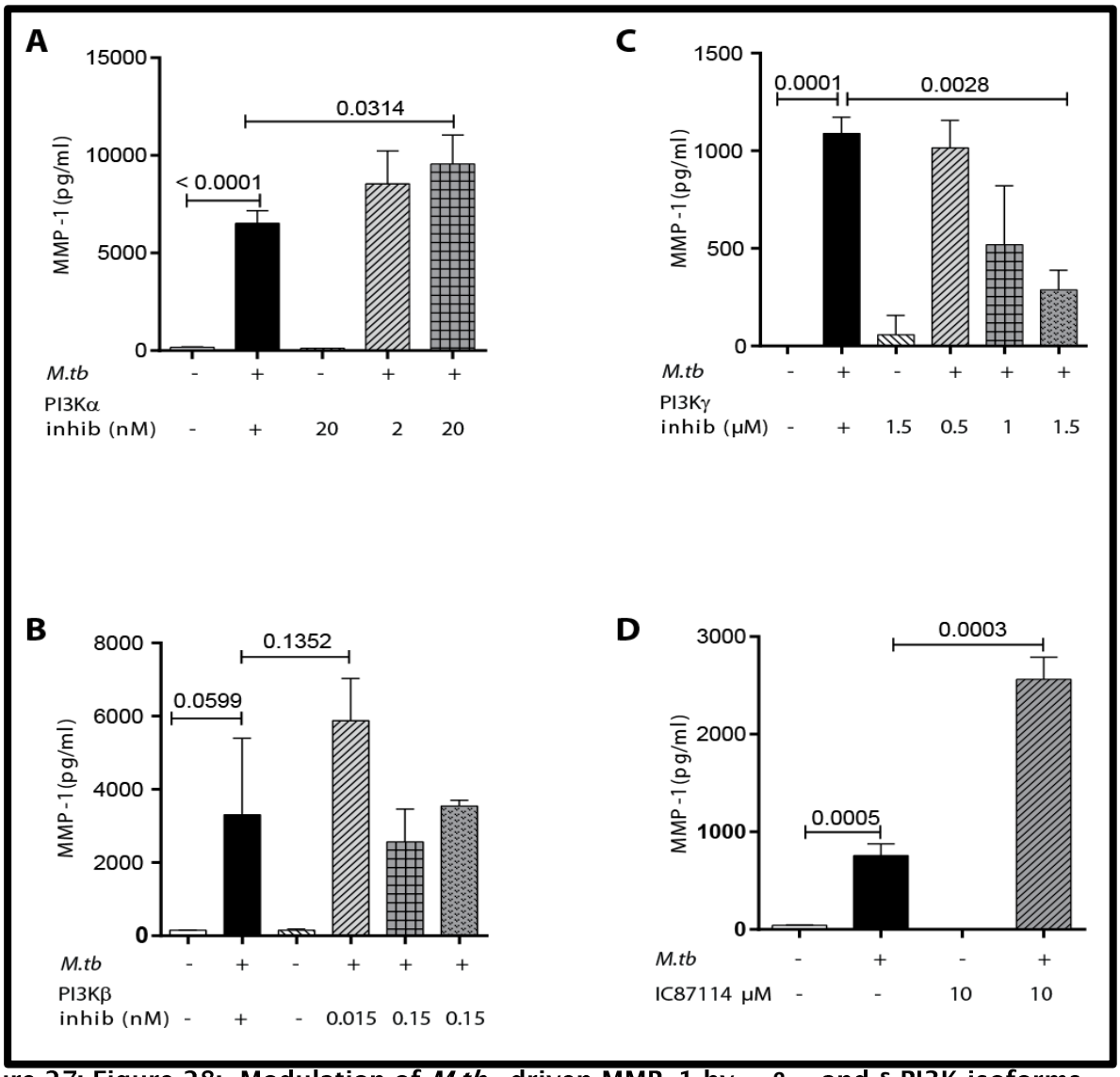


**Figure 27: Figure 28: Modulation of *M.tb* -driven MMP-1 by α, β, γ and δ PI3K isoforms.** MDMs were pre-treated with class I PI3K isoform inhibitors at different concentration for two hours prior to *M.tb* - infection. Supernatant samples were harvested after 72 hours post infection for MMP-1 detection by ELISA assay. **A:** PI3Kα inhibition augments MMP-1 secretion. **B:** Low dose of PI3Kβ inhibitor also elevates MMP-1, with higher concentrations causing a reduction in MMP-1 secretion **C:** PI3K gamma inhibition suppressed MMP-1 in a dose dependent manner. **D:** PI3Kδ inhibition by IC87114 consistently augments MMP-1 secretion in macrophages. Data show mean and standard deviation of experiments performed in triplicates and is representative of experiments performed on three donors at separate occasions. P values are Student's t-test, with $P < 0.05$ considered significantly different.

## 3.10 Targeting PI3K in THP-1 cells suppresses MMP-1

Generation of adequate amount of primary MDMs to undertake an investigation of this nature can be highly costly. For this reason, alternative macrophage-like cell types were explored to determine the most time and cost effective system to use for this study. *M.tb* up-regulates MMP-1 in THP-1 cells and primary macrophages, and PI3K inhibitors further elevating the mRNA and secreted MMP-1 in MDMs. PI3K inhibition was performed using THP-1 cells to establish phenotype reproducibility in surrogate macrophages. THP-1 cells were treated with vitamin D for 4 hours to differentiate to macrophages. Cells were next treated with LY294002 and IC87114 (a selective PI3Kδ inhibitor) for two hours prior to UV-killed *M.tb* infection. Contrary to the results observed in primary macrophages, both the pan PI3K inhibitor, LY294002 and the PI3Kδ specific inhibitor, IC87114, induced repression of *M.tb* -driven MMP-1, (Figure 29) and this was not expected. Following this result, all subsequent experiments were carried out using primary MDMs.

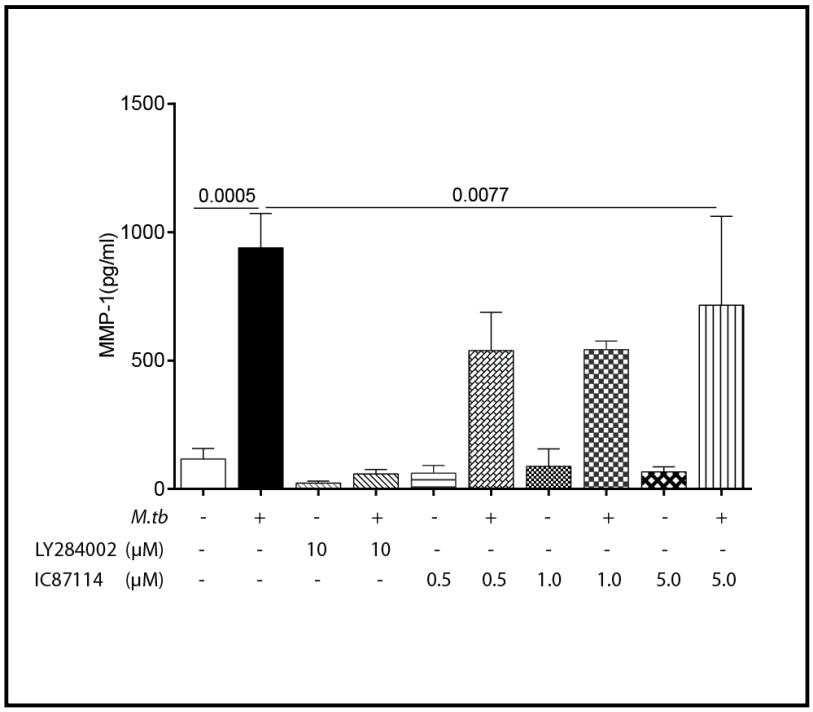


**Figure 28: PI3K inhibition profile in THP-1 cells.** Vitamin D-differentiated THP-1 cells were pre-treated with 10μM of the PI3K inhibitor LY294002, and 0.5 μM, 1.0 μM and 5.0 μM of IC87114 for two hours prior to *M.tb* - infection. Supernatant samples were harvested after 72 hours post infection for MMP-1 detection by ELISA assay. PI3K inhibitors modulate MMP-1 secretion in an unexpected manner, with both LY294002 and IC87114 eliciting suppression of *M.tb* -driven secretion of MMP-1 in THP-1. Data show mean and standard deviation of experiments performed in triplicates and is representative of experiments performed on three occasions. P values are Student's t-test, with $P < 0.05$ considered significantly different.

## 3.11 MMP-1 regulation by PI3K inhibitors is AKT-dependent

AKT is a very important effector of the PI3K pathway (Cantley, 2002). AKT phosphorylates to activate or suppress numerous proteins which are all involved in regulation of cell growth, proliferation and survival (Cantley, 2002, Vanhaesebroeck et al., 2001, Vanhaesebroeck et al., 2012). Inhibition of AKT also significantly augmented *M.tb* -driven MMP-1 in macrophages (Figure 30).

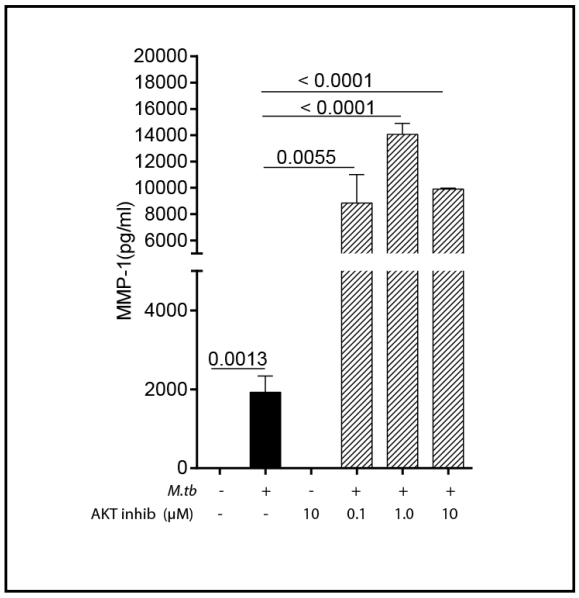


**Figure 29: AKT inhibition drives elevated MMP-1 secretion in *M.tb* -infected macrophages**. MDMs were pre-treated with AKT inhibitor for two hours prior to *M.tb* -infection. Supernatant samples were harvested after 72 hours post infection for MMP-1 detection by ELISA assay. Inhibition of AKT at 0.1μM, 1μM and 10μM by MK-2206 dihydrochloride significantly increased MMP-1 secretion compared to levels driven by *M.tb* alone and control samples. Data show mean and standard deviation of experiments performed in triplicates and is representative of experiments performed on three occasions. P values are Student's t-test, with $P < 0.05$ considered significantly different.

## 3.12 mTOR signalling similarly negatively regulates MMP-1 in macrophages.

PI3K signalling merges with the mTOR pathway, which regulates ribosomal biogenesis and protein synthesis to control cellular response (Di Paolo and De Camilli, 2006, Laplante and Sabatini, 2012). With AKT inhibition resulting in increased MMP-1 secretion, mTOR signalling was investigated next. MDMs were treated with Rapamycin, the classic mTORC-1 inhibitor, to block its activity prior to *M.tb* infection. Rapamycin augmented *M.tb* -driven MMP-1 both at the secretion and gene expression levels (Figure 31 A and B respectively).

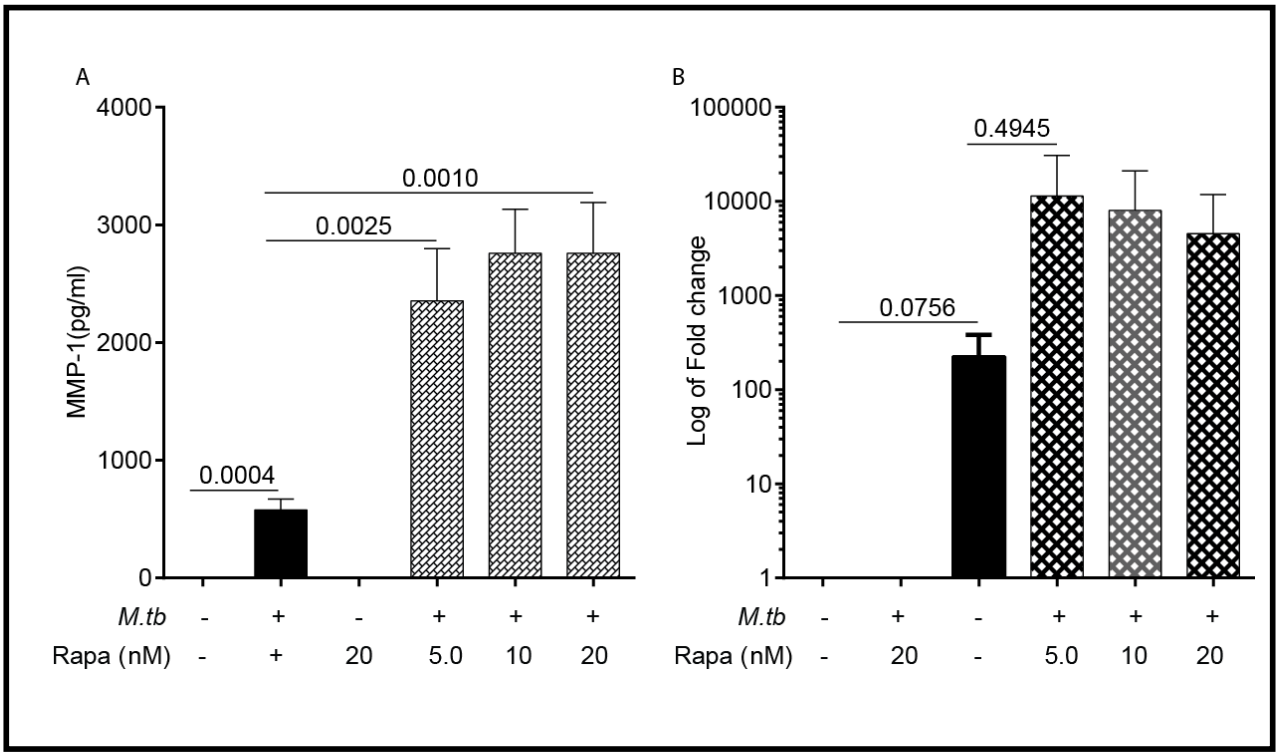


**Figure 30: Rapamycin augments *M.tb* -driven MMP-1.** MDMs were pre-treated with mTORC-1 inhibitor for two hours prior to *M.tb infection*. Supernatant samples were harvested after 72 hours post infection for MMP-1 detection by ELISA assay. In gene expression experiments, cells were treated with Tri Reagent at 48 hours post *M.tb* infection for RNA isolation. **A:** Suppressing mTORC-1 activity with 5nM, 10nM and 20nM of rapamycin caused an increased secretion and **B:** mRNA expression of MMP-1 by *M.tb* infected macrophages. Data show mean and standard deviation of experiments performed in triplicates and are representative of experiments performed on a minimum of three occasions. P values are Student's t-test, with $P < 0.05$ considered significantly different.

## 3.13 Modulation of MMP-1 by PTEN inhibitors

With AKT inhibitors showing such a marked MMP-1 up-regulation, it was reasonable to believe that the main product of PI3K activity within the plasma membrane, $PIP_3$ must be critical in this study. $PIP_3$ is an intracellular second messenger signalling molecule which promotes AKT phosphorylation. $PIP_3$ does so by firstly phosphorylating to fully activate PDK1. As discussed above, mTORC2 and PDK1 then phosphorylate to activate AKT on Ser 473 and Thr

308 respectively (Di Paolo and De Camilli, 2006, Thomas et al., 2005, Vanhaesebroeck et al., 2012).

With this in mind, the next logical experiment was to find out whether increased accumulation of membrane $PIP_3$ caused prolonged AKT activation to suppress MMP-1 secretion. I therefore pre-treated macrophages with various concentrations of the PTEN inhibitor, bpv(phen) (Santa Cruz Biotechnology, Inc # sc-221378), followed by *M.tb* infection. Again, supernatant samples were harvested at 72 hours after *M.tb* infection and used for ELISA analysis of MMP-1. The different concentrations of bpv(phen) used in this study exerted different effects on MMP-1 production by the macrophages (Figure 32).

PTEN inhibition at 0.5μM, 1μM and 10μM bpv(phen) showed slight increasing of MMP-1 effect in a dose-dependent manner. 250nM of bpv(phen) increased MMP-1, whereas suppression effect was observed at 100nM and 500nM. Although different concentrations of the inhibitor appear to have caused increasing trend of MMP-1, this was neither reproducible nor significantly higher than that driven by *M.tb* only infected macrophages. At the gene expression level however, PTEN inhibition showed no change on the accumulation of cellular MMP-1 mRNA compared to levels driven by *M.tb* (Figure 32C)

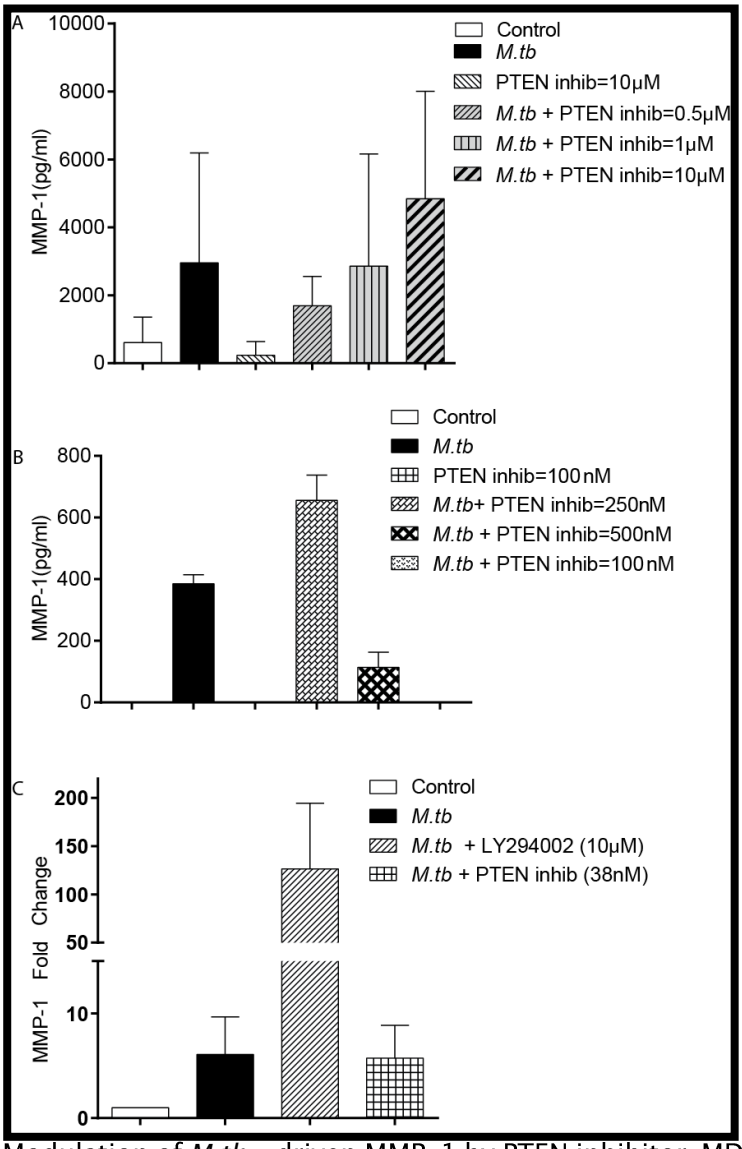


Figure 31: Modulation of *M.tb* -driven MMP-1 by PTEN inhibitor. MDMs were pre-treated with PTEN inhibitor for two hours prior to *M.tb* - infection. Supernatant samples were harvested after 72 hours post infection for MMP-1 detection by ELISA assay. **A:** Although a trend of increasing MMP-1 secretion was observed at 0.5μM, 1μM and 10μM of the PTEN inhibitor, bpv(phen), this was not much higher than levels of MMP-1 driven by *M.tb* only. **B:** 100nM and 500nM of bpv(phen) suppressed *M.tb* -driven MMP-1, whilst 250nM bpv(phen) increased MMP-1. **C:** At the gene expression level, 38nM bpv(phen) exerted no change in MMP-1 expression in the *M.tb* -infected macrophages at 48 hours post infection, whereas 10μM of LY294002 enhanced *M.tb* -driven MMP-1 as expected. Data show each experiment performed on different occasions with error bars representing technical replicates within three samples.

## 3.14 Chemical inhibitors were non-toxic to macrophages

Various pharmacological compounds have been used in this study to suppress activation of target proteins of interest. Lactose dehydrogenase (LDH) is released by dying cells into their supernatant culture media. LDH cytotoxicity assay was performed on supernatant samples to evaluate the effect of the compounds on cell viability. Inhibitors of the various isoforms of PI3K proteins were used at concentrations ranging between 0.5μM and 10μM. AKT and PTEN inhibitors were used at concentrations between 0.5μM and 10μM. Rapamycin on the other hand was used at a much lower concentration range of 5nM to 20nM. At 50nM, rapamycin induced high macrophages death (Figure not shown). However, none of the concentrations of inhibitors used in this study exerted a toxic effect on macrophages (Figure 33). All inhibitors were used at concentrations that were non-toxic to the macrophages.

## 3.15 PI3K and mTORC-1 inhibitors globally modulate multiple MMPs in MDMs

Following the effect of LY294002 and Rapamycin on MMP-1 in macrophages, how these compounds modulate multiple MMPs was investigated next. The MMPs of interest were analysed by Luminex multiplex assay using the same samples that were used to generate the data for figures 25 and 31. Whereas levels of MMP-2,-7, -9 and -12 remained unchanged in all samples, levels of MMP-1, MMP-3 and MMP-10 were elevated in both LY294002 (Figure 34) and Rapamycin (Figure 35) treated macrophages compared to that driven by *M.tb* only and in uninfected samples.

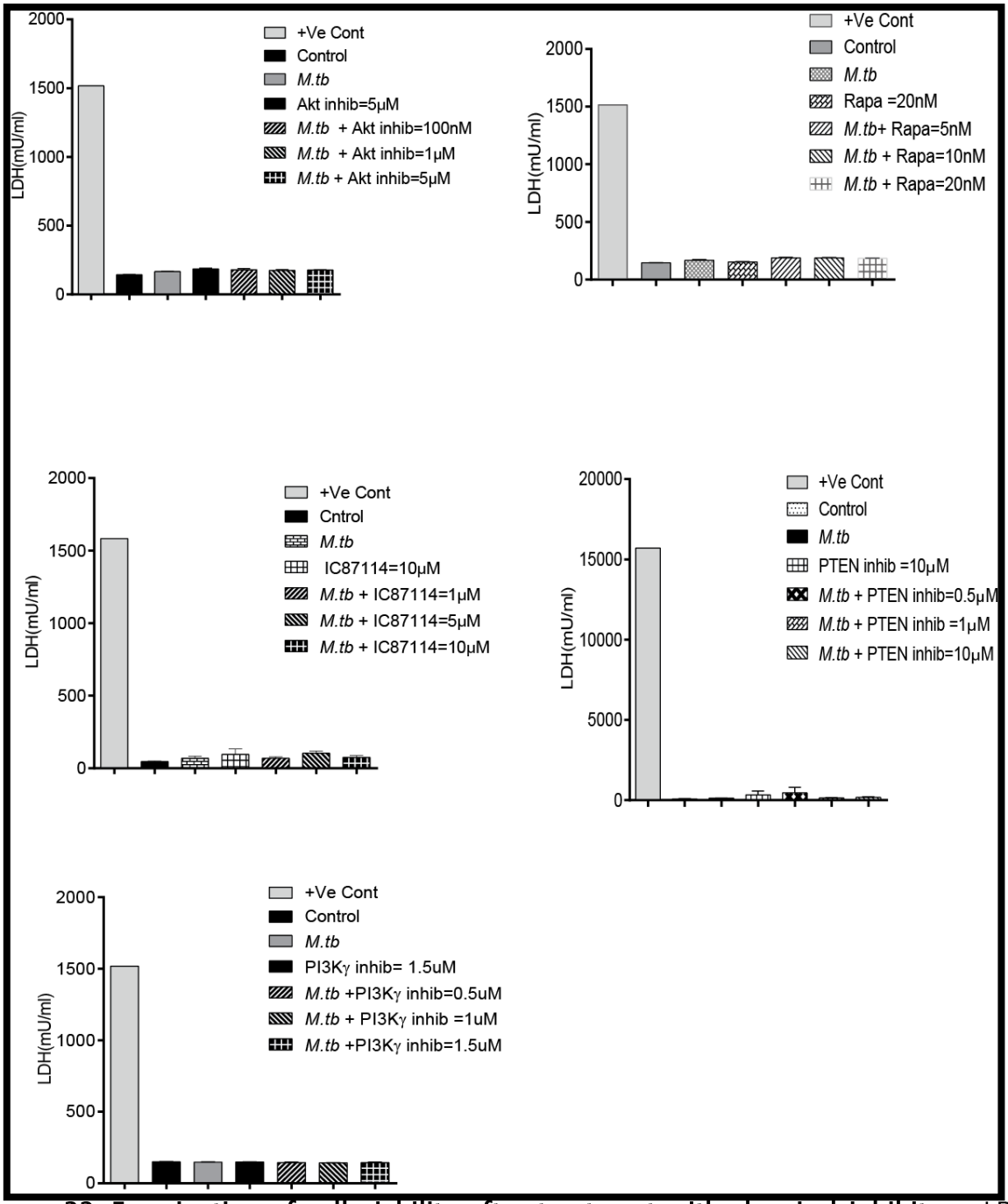


**Figure 32: Examination of cell viability after treatment with chemical inhibitors**. LDH concentration in the supernatant samples used in this study was determined. Inhibitors of the various isoforms of PI3K, AKT and PTEN were used at concentration range of 0.5μM to 10μM. Rapamycin was used at 5nM-20nM. Data show each experiment performed on different occasion with error bars representing technical replicates within three samples. . Experiments were reproducible in all samples used during this project.

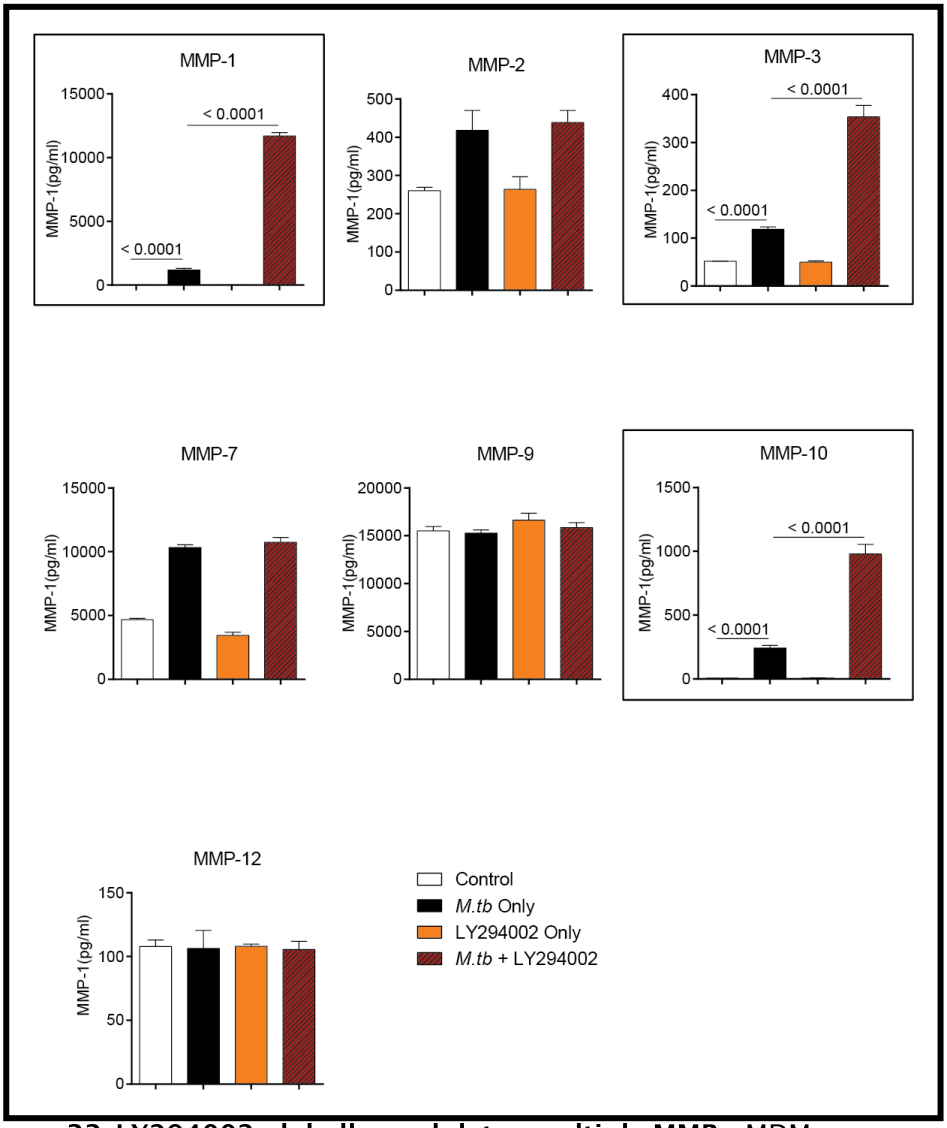


**Figure 33: LY294002 globally modulates multiple MMPs.** MDMs were pre-treated with PI3K inhibitor for two hours prior to *M.tb* – infection. Supernatant samples were harvested after 72 hours post infection for MMP-1 detection by ELISA assay. Luminex profiling of MMPs demonstrate that *M.tb* similarly upregulated several MMPs. LY294002 further augmented MMP-3 and MMP-10 in the same pattern as seen in MMP-1 , but exerted no change in macrophage-secreted MMPs -2, -7, -9 and -12. Luminex experiments were performed on two different occasions in two donors each time. Data show mean and standard deviation of experiments performed in triplicates and is representative of experiments performed on two donors at separate occasions. P values are Student's t-test, with $P < 0.05$ considered significantly different. The error bars represent mean ± SEM analysed using unpaired student t test, with P value < 0.05 considered significantly different.

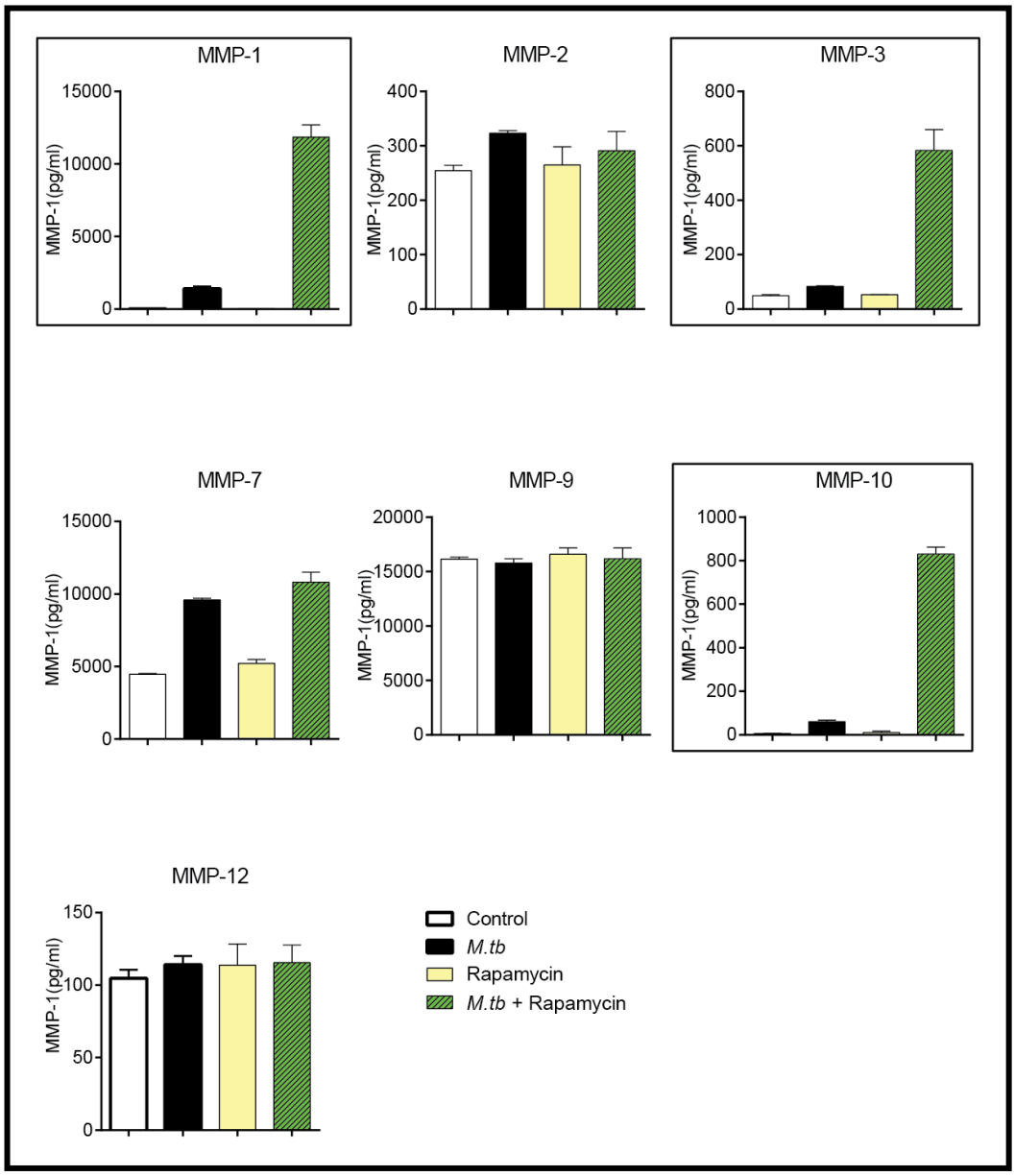


**Figure 34: Rapamycin similarly modulates multiple MMPs globally.** MDMs were pre-treated with mTORC-1 inhibitor for two hours prior to *M.tb* – infection. Supernatant samples were harvested after 72 hours post infection for MMP-1 detection by ELISA assay. Luminex profiling of MMPs demonstrate that *M.tb* similarly upregulated a wide range of MMPs. Rapamycin further augmented MMP-3 and MMP-10 in the same pattern as seen in MMP-1, but exerted no change in macrophage-secreted MMPs -2, -7, -9 and -12. Luminex experiments were performed on two different occasions in two donors each time. Data show mean and standard deviation of experiments performed in triplicates and is representative of experiments performed on two donors at separate occasions. P values are Student's t-test, with $P < 0.05$ considered significantly different.

## 3.16 Pathway inhibition differentially modulates *M.tb* -driven cytokine levels in macrophages

The global effect of intracellular pathway inhibition on pro-inflammatory cytokine responses was then investigated in the samples that were used for the multiple MMPs analysis, to determine whether the effect was limited to MMPs or more global inflammatory immune responses. A 30-plex cytokine assay was performed to examine the effect of the various inhibitors that had been used, on the dynamics of Th1/Th2-type and other cytokines, as well as a selection of chemokines and growth factors (Figures 36-45).

## 3.17 PI3K and mTORC-1 inhibition augments pro-inflammatory cytokine production in *M.tb* infected macrophages

*M.tb* drove the production of pro-inflammatory mediators in macrophages. LY294002 (Figure 36) and Rapamycin (Figure 37) further elevated Th1-type cytokines including IL-1β, IL-6, IL-12 and TNFα.

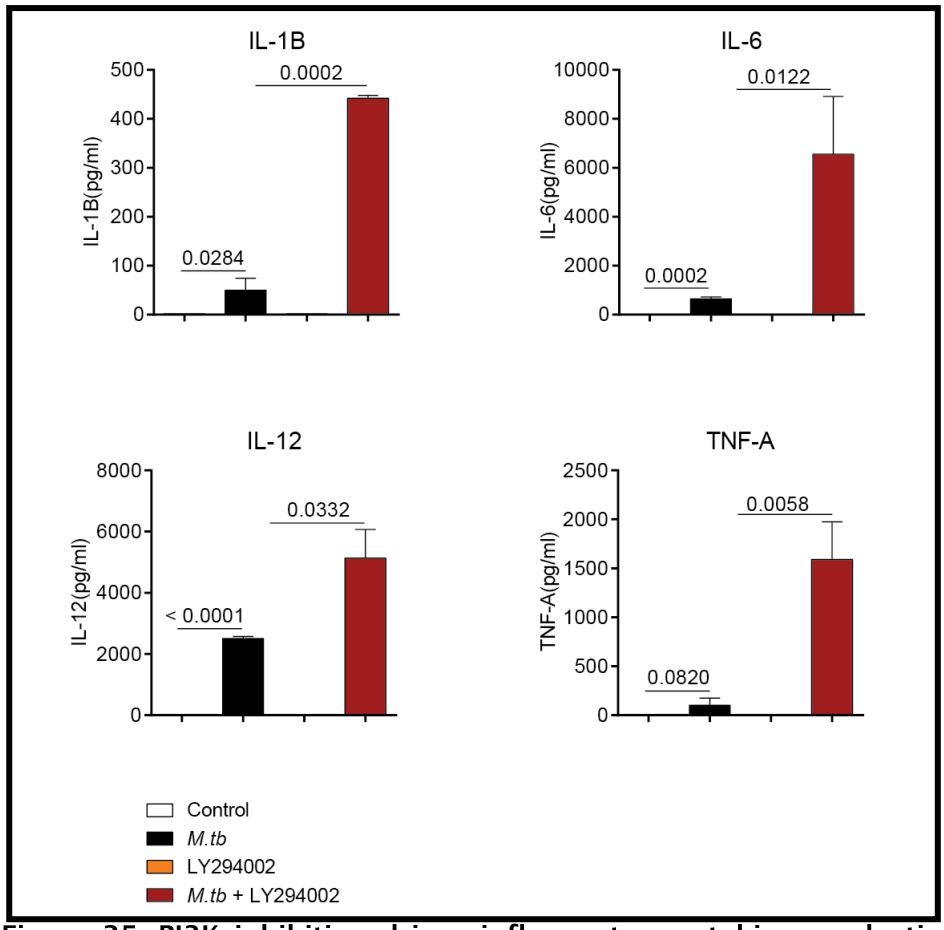


**Figure 35: PI3K inhibition drives inflammatory cytokine production in macrophages.** MDMs were pre-treated with PI3K inhibitor for two hours prior to *M.tb* infection. Supernatant samples were harvested after 72 hours post infection for multiplex analysis. Luminex profiling of macrophages show that *M.tb* infection upregulates pro-inflammatory mediators. These were further elevated when PI3K was blocked by 10μM of LY294002. Luminex experiments were performed on two different occasions in two donors each time. Data show mean and standard deviation of experiments performed in triplicates and is representative of experiments performed on two donors at separate occasions. P values are Student's t-test, with $P < 0.05$ considered significantly different.

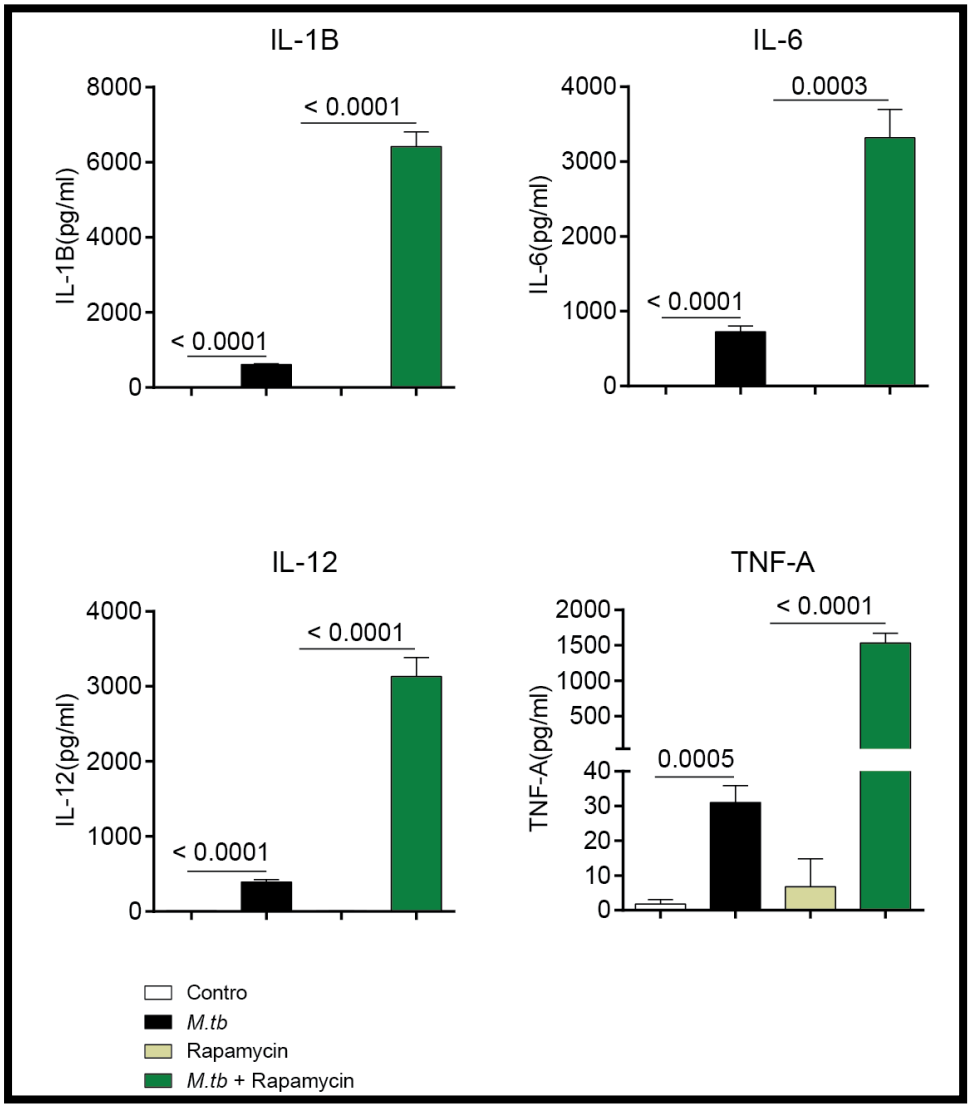


**Figure 36: mTORC-1 inhibition similarly drives inflammatory cytokine production in macrophages.** MDMs were pre-treated with mTORC-1 inhibitor for two hours prior to *M.tb* infection. Supernatant samples were harvested after 72 hours post infection for MMP-1 detection by ELISA assay. Luminex profiling of macrophages show that *M.tb* infection upregulates pro-inflammatory mediators. These were further elevated when mTORC-1 was blocked by 10nM of Rapamycin. Luminex experiments were performed on two different occasions in two donors each time. Data show mean and standard deviation of experiments performed in triplicates and is representative of experiments performed on two donors at separate occasions. P values are Student's t-test, with $P < 0.05$ considered significantly different.

### 3.17.1 PI3K and mTORC-1 inhibition augments Th2-type cytokine production in *M.tb* infected macrophages

*M.tb* drove the production of anti-inflammatory mediators in macrophages. Surprisingly, LY294002 (Figure 38) and Rapamycin (Figure 39) further elevated Th2-type cytokines such as IL-4, IL-10 and IL-13.

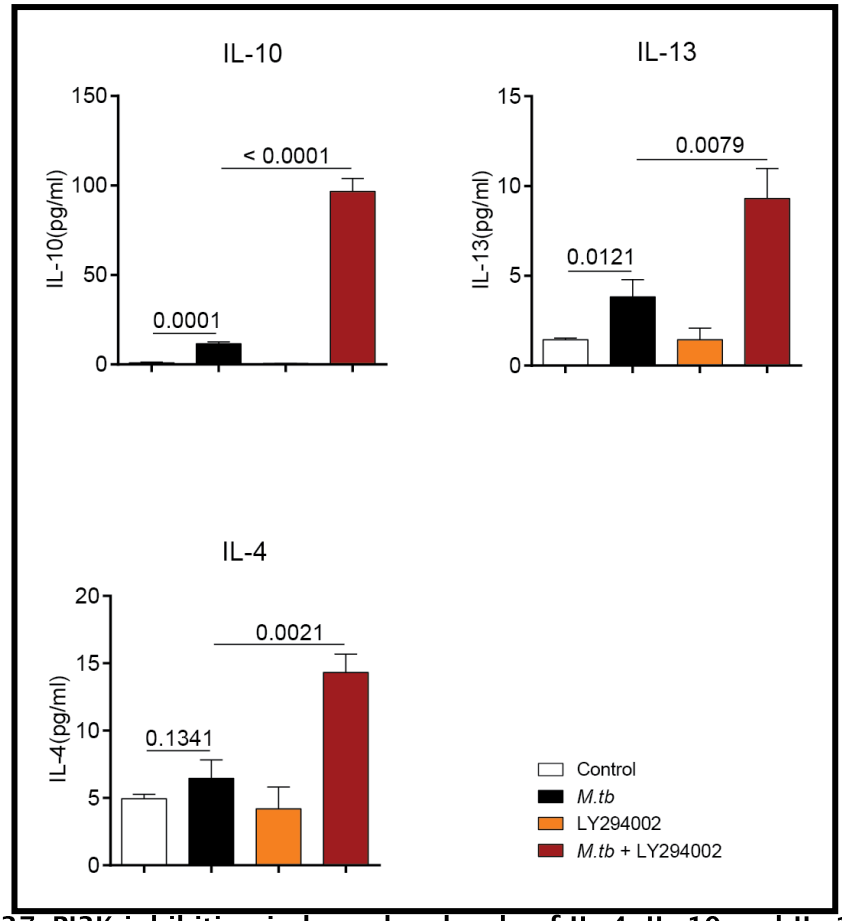


**Figure 37: PI3K inhibition induces low levels of IL-4, IL-10 and IL-13 in macrophages.** MDMs were pre-treated with PI3K inhibitor for two hours prior to *M.tb* infection. Supernatant samples were harvested after 72 hours post infection for multiplex analysis. Luminex profiling of macrophages show that *M.tb* infection induced low levels of anti-inflammatory mediators. These were slightly elevated when PI3K was blocked by 10μM of LY294002. Luminex experiments were performed on two different occasions in two donors each time. Data show mean and standard deviation of experiments performed in triplicates and is representative of experiments performed on two donors at separate occasions. P values are Student's t-test, with $P < 0.05$ considered significantly different.

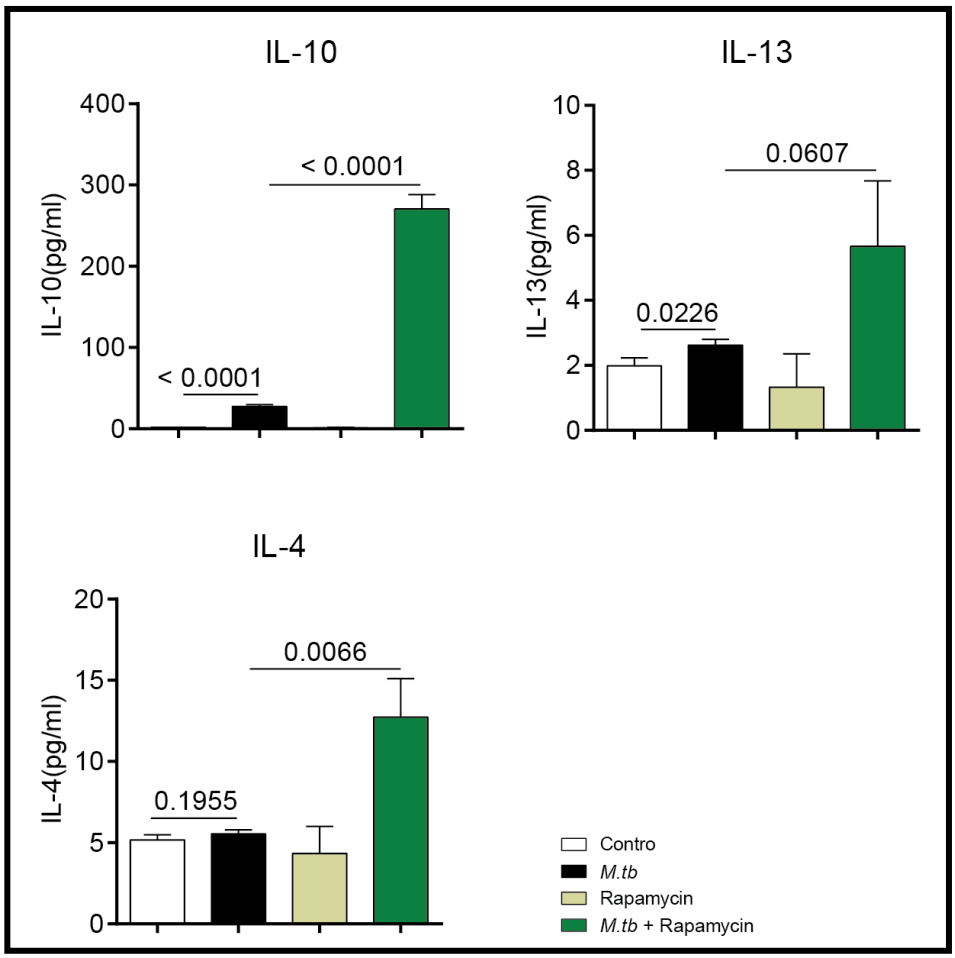


Figure 38: **mTORC-1 inhibition induce low levels of IL-4, IL-10 and IL-13 in macrophages.** MDMs were pre-treated with mTORC-1 inhibitor for two hours prior to *M.tb* infection. Supernatant samples were harvested after 72 hours post infection for multiplex analysis. Luminex profiling of macrophages show that *M.tb* infection induced low levels anti-inflammatory mediators. These were slightly elevated when mTORC-1 was blocked by 10nM of Rapamycin. Luminex experiments were performed on two different occasions in two donors each time. Data show mean and standard deviation of experiments performed in triplicates and is representative of experiments performed on two donors at separate occasions. P values are Student's t-test, with $P < 0.05$ considered significantly different.

### 3.17.2 PI3K and mTORC-1 inhibition differentially modulate chemokine production in *M.tb* infected macrophages

*M.tb* drove the production of a wide range of chemokines in macrophages. Although separate inhibition of PI3K using LY294002 and mTORC-1 by Rapamycin exerted similar effects on a variety of chemokines, there were some differences in the pattern of effect between the two compounds. Whereas both LY294002 (Figure 40) and Rapamycin (Figure 41) further augmented *M.tb* -driven RANTES, MIP-1α and MIP-1β, both compounds exerted no change on the levels of IP-10 and IL-8, but suppressed MCP-1 produced by *M.tb* -infected macrophages. LY294002 exerted no change on *M.tb* -driven MIG, whereas Rapamycin further elevated *M.tb* -driven MIG.

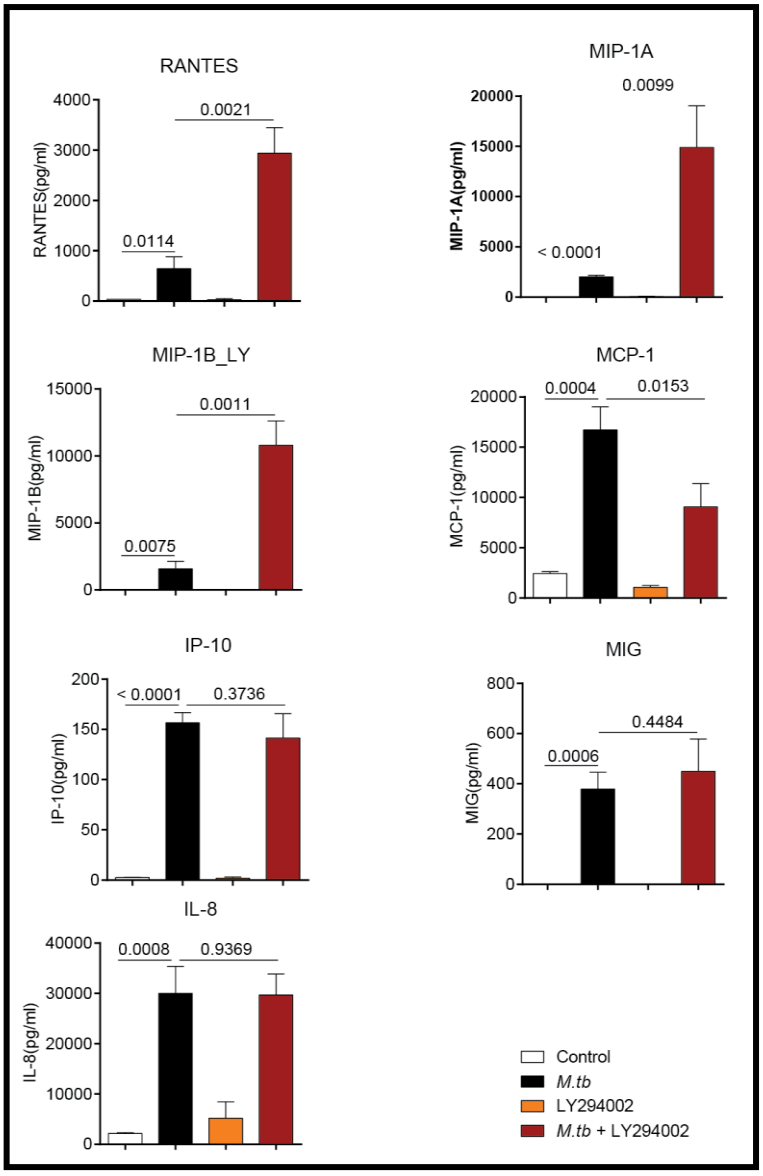


Figure 39: **LY294002 differentially modulates a wide range of chemokines**. MDMs were pre-treated with PI3K inhibitor for two hours prior to *M.tb* infection. Supernatant samples were harvested after 72 hours post infection for multiplex analysis. Luminex profiling of macrophages demonstrate that *M.tb* infection upregulates a wide range of chemokines. Whereas there was no change in levels of IP-10, IL-8 and MIG, and a repressive effect on MCP-1, other chemokines including RANTES, MIP-1α and MIP-1β were all further elevated upon PI3K blockade by 10μM of LY294002. Luminex experiments were performed on two different occasions in two donors each time. Data show mean and standard deviation of experiments performed in triplicates and is representative of experiments performed on two donors at separate occasions. P values are Student's t-test, with $P < 0.05$ considered significantly different.

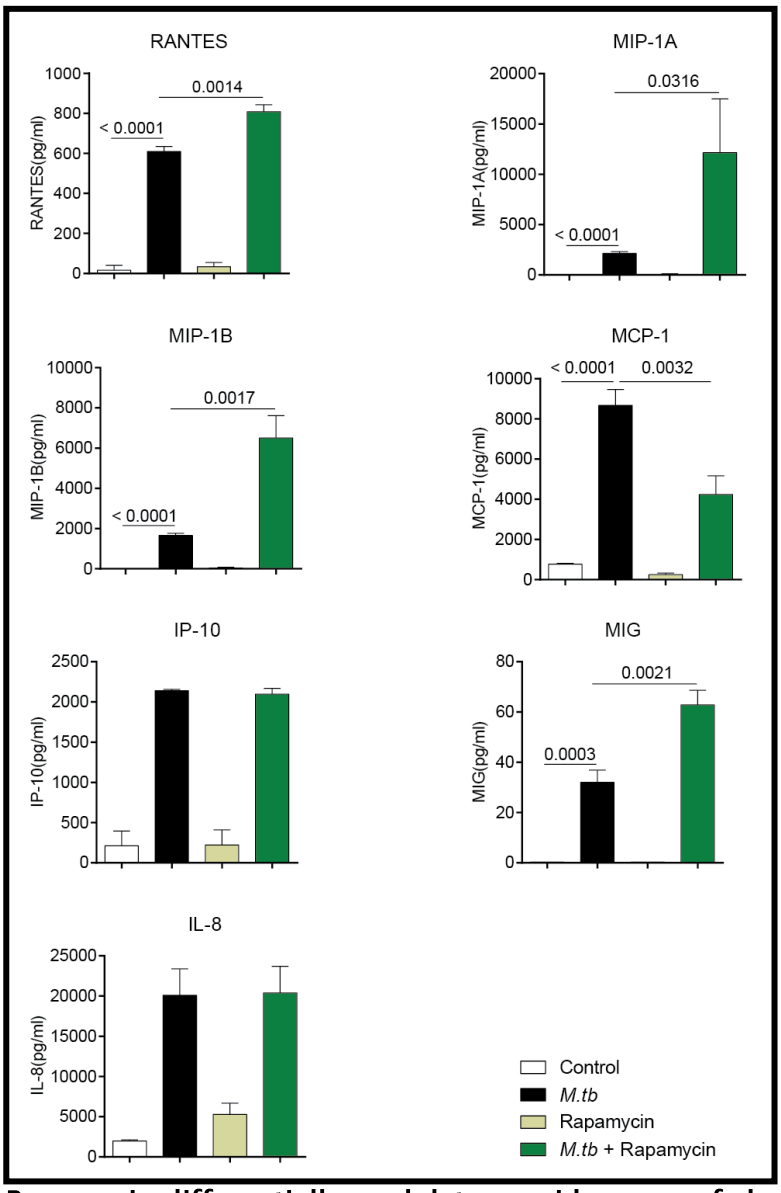


**Figure 40: Rapamycin differentially modulates a wide range of chemokines.** MDMs were pre-treated with mTORC-1 inhibitor for two hours prior to *M.tb* infection. Supernatant samples were harvested after 72 hours post infection for multiplex analysis. Luminex profiling of macrophages demonstrates that *M.tb* infection upregulates a wide range of chemokines. Whereas there was no change in levels of IP-10 and IL-8, and a repressive effect on MCP-1, other chemokines including RANTES, MIP-1α, MIP-1β and MIG were all further elevated upon mTORC blockade by 10nM of Rapamycin. Luminex experiments were performed on two different occasions in two donors each time. Data show mean and standard deviation of experiments performed in triplicates and is representative of experiments performed on two donors at separate occasions. P values are Student's t-test, with $P < 0.05$ considered significantly different.

### 3.17.3 PI3K and mTORC-1 inhibition augment production of growth factors in *M.tb* infected macrophages.

*M.tb* drove the production of a wide range of growth factors in macrophages. Separate inhibition of PI3K using LY294002 and mTORC-1 by Rapamycin exerted marked production of VEGF, G-CSF, and FGF-BASIC with the exception of a slight suppression of EGF by Rapamycin (Figure 43) as opposed to elevation by LY294002 (Figure 42).

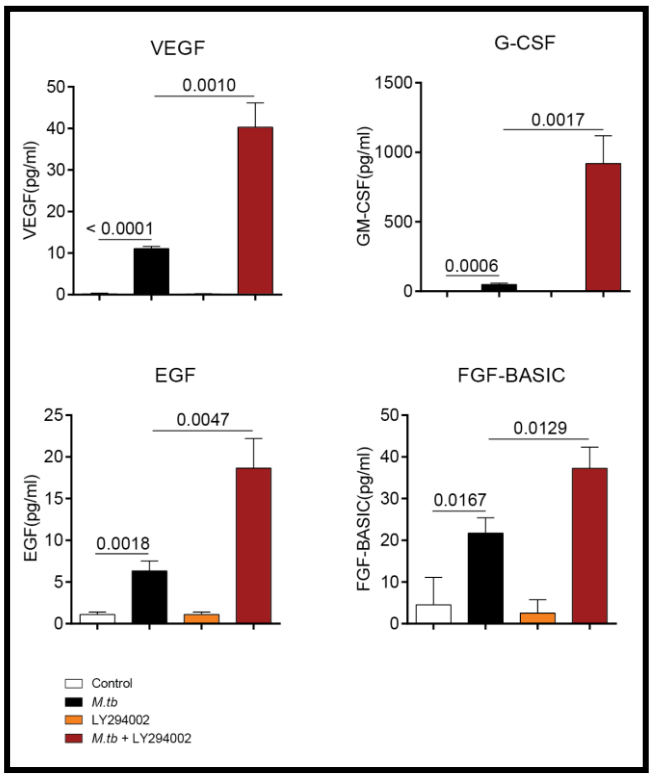


**Figure 41: LY294002 augments a wide range of growth factors in *M.tb* -infected macrophages.** MDMs were pre-treated with PI3K inhibitor for two hours prior to *M.tb* infection. Supernatant samples were harvested after 72 hours post infection for multiplex analysis. Luminex profiling of macrophages demonstrate that *M.tb* infection upregulates a wide range of growth factors. These were further elevated when PI3K was blocked by 10μM of LY294002. Luminex experiments were performed on two different occasions in two donors each time. Data show mean and standard deviation of experiments performed in triplicates and is representative of experiments performed on two donors at separate occasions. P values are Student's t-test, with $P < 0.05$ considered significantly different.

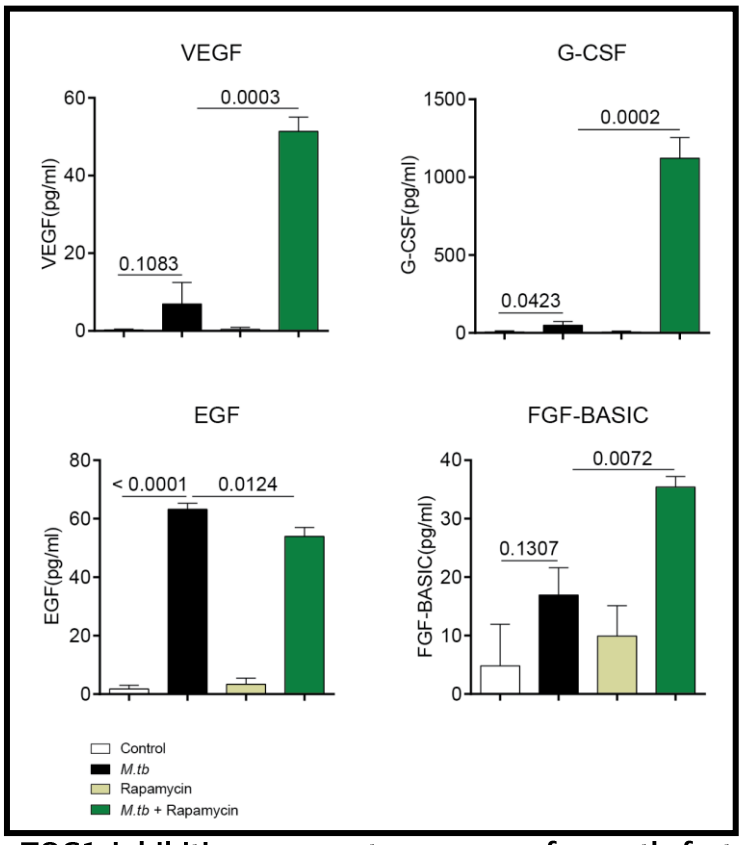


**Figure 42: mTOC1 inhibition augments a range of growth factors in *M.tb* -infected macrophages.** MDMs were pre-treated with mTORC-1 inhibitor for two hours prior to *M.tb* infection. Supernatant samples were harvested after 72 hours post infection for multiplex analysis. Luminex profiling of macrophages demonstrate that *M.tb* infection upregulates a wide range of growth factors. Apart from suppression of EGF, most of the growth factors were further elevated when mTOC1 was blocked by 10nM of Rapamycin. Luminex experiments were performed on two different occasions in two donors each time. Data show mean and standard deviation of experiments performed in triplicates and is representative of experiments performed on two donors at separate occasions. P values are Student's t-test, with $P < 0.05$ considered significantly different.

### 3.17.4 PI3K and mTORC-1 inhibition augment a wide range of cytokines in *M.tb* infected macrophages

*M.tb* drove the production of a variety of other cytokines in macrophages. Separate inhibition of PI3K using LY294002 (Figure 44) and mTORC-1 by Rapamycin (Figure 45) enhanced production of IFN-1, IL-7, and IL-15 with the exception of a slight suppression of IL-RA by LY294002.

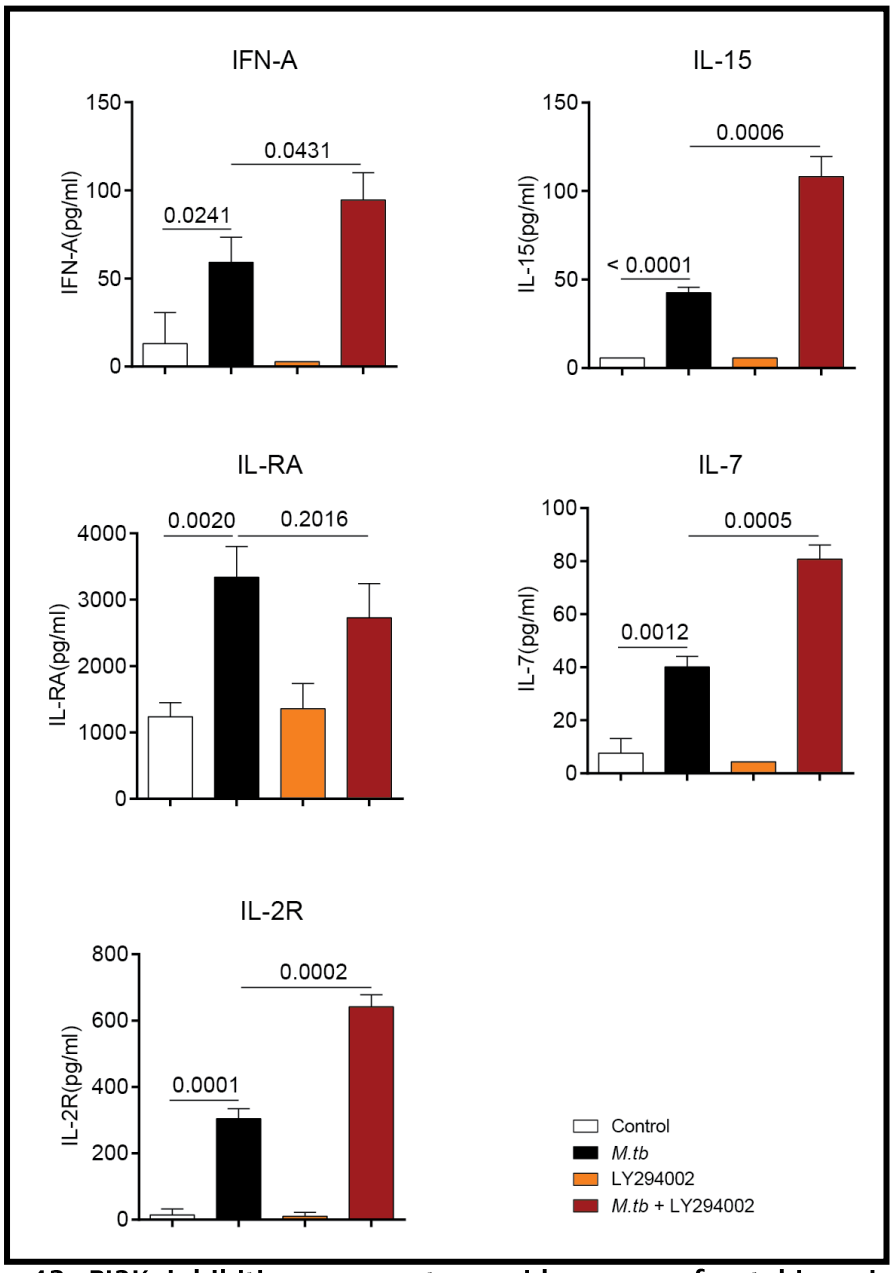


**Figure 43: PI3K inhibition augments a wide range of cytokines in *M.tb* -infected macrophages.** MDMs were pre-treated with PI3K inhibitor for two hours prior to *M.tb* infection. Supernatant samples were harvested after 72 hours post infection for multiplex analysis. Luminex profiling of macrophages demonstrate that *M.tb* infection upregulates a wide range of cytokines. These were further elevated when PI3K was blocked by 10μM of LY294002. Luminex experiments were performed on two different occasions in two donors each time. Data show mean and standard deviation of experiments performed in triplicates and is representative of experiments performed on two donors at separate occasions. P values are Student's t-test, with $P < 0.05$ considered significantly different.

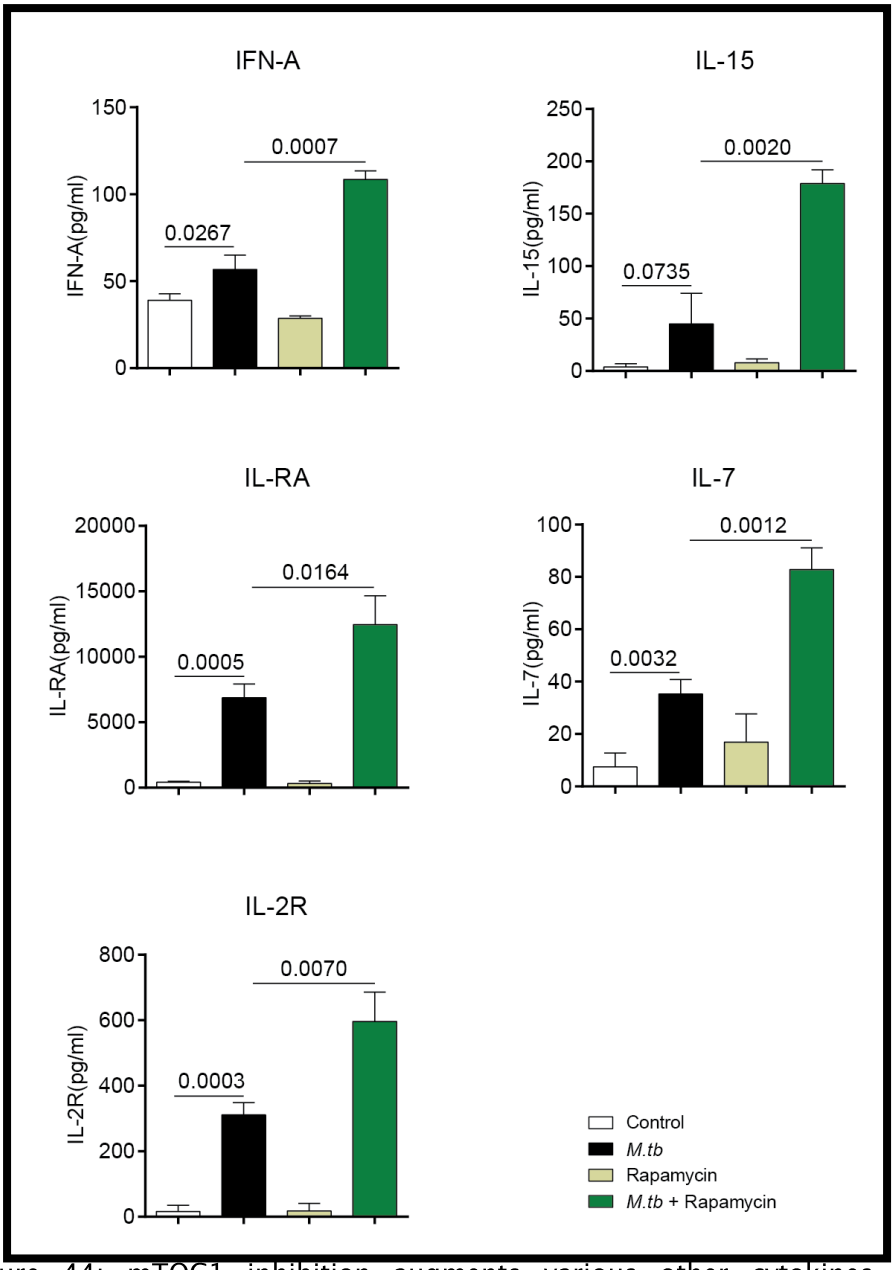


Figure 44: mTOC1 inhibition augments various other cytokines in *M.tb* -infected macrophages. MDMs were pre-treated with mTORC-1 inhibitor for two hours prior to *M.tb* infection. Supernatant samples were harvested after 72 hours post infection for multiplex analysis. Luminex profiling of macrophages demonstrate that *M.tb* infection upregulates a wide range of cytokines. These were further elevated when mTOC1 was blocked by 10nM of Rapamycin. Luminex experiments were performed on two different occasions in two donors each time. Data show mean and standard deviation of experiments performed in triplicates and is representative of experiments performed on two donors at separate occasions. P values are Student's t-test, with $P < 0.05$ considered significantly different

### 3.17.5 Summary of how PI3K and mTORC-1 inhibition has global effects on MMPs, cytokines and chemokines secreted by macrophages.

In order to determine whether the effect on MMP-1 is specific or widespread, Luminex array profiling was performed for multiple MMPs, cytokines, chemokines and growth factors (Figures 34 and 45). The MMPs upregulated including MMP-1, MMP-3 and MMP-10 are frequently synergistically regulated, but the very widespread upregulation of cytokines and chemokines was unexpected. Figures 46 and 47 show a summary of the global effect of PI3K and mTORC-1 inhibition on a wide range of MMPs, cytokines, chemokines and growth factors.

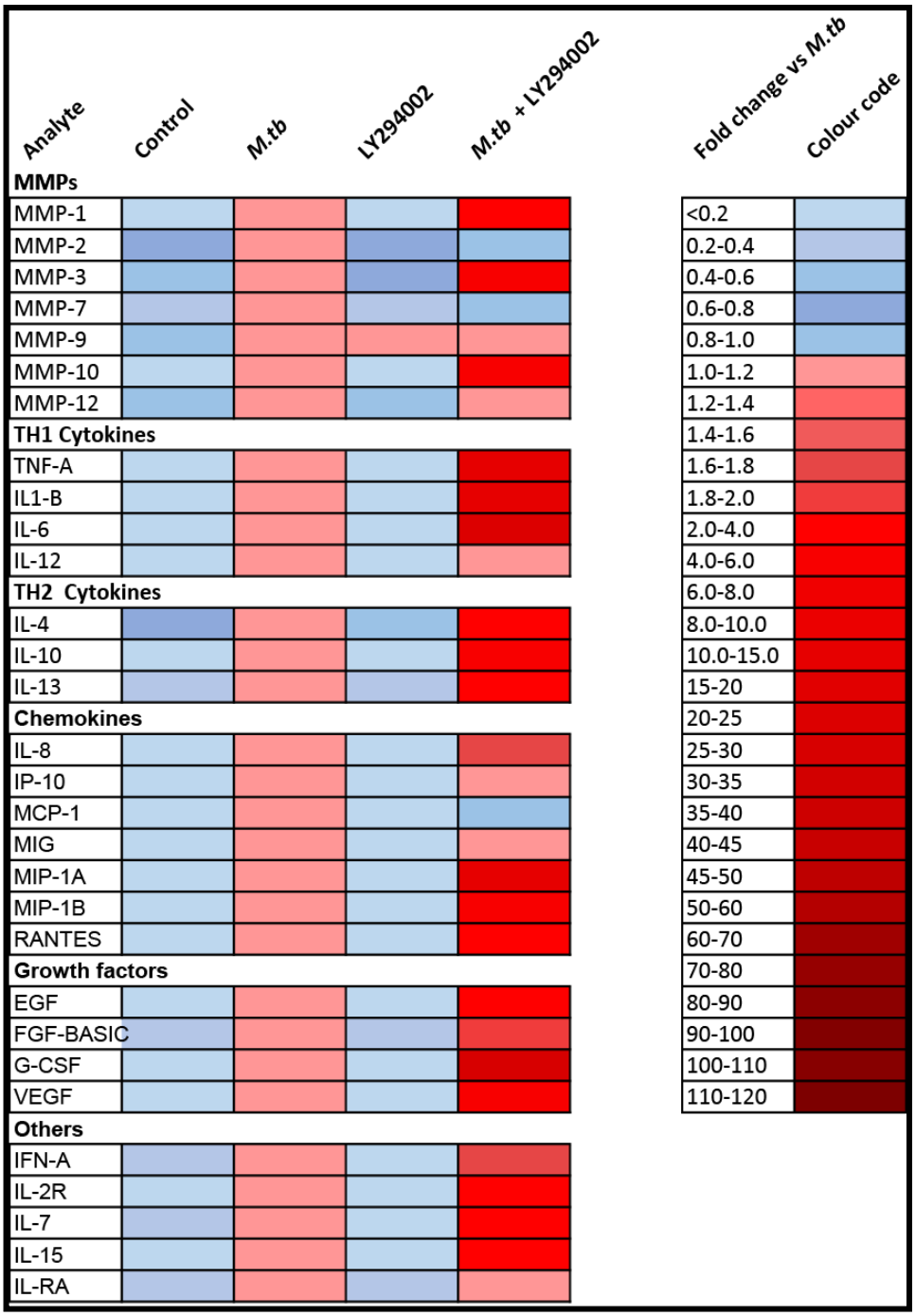


**Figure 45: PI3K inhibition globally modulates a wide range of pro-inflammatory signalling molecule secretion**. MDMs were pre-treated with PI3K inhibitor for two hours prior to *M.tb* infection. Supernatant samples were harvested after 72 hours post infection for multiplex analysis. Luminex profiling of macrophages demonstrate that *M.tb* infection upregulates a wide range of MMPs, cytokines, chemokines and growth factors. Luminex experiments were performed on two different occasions in two donors each time.

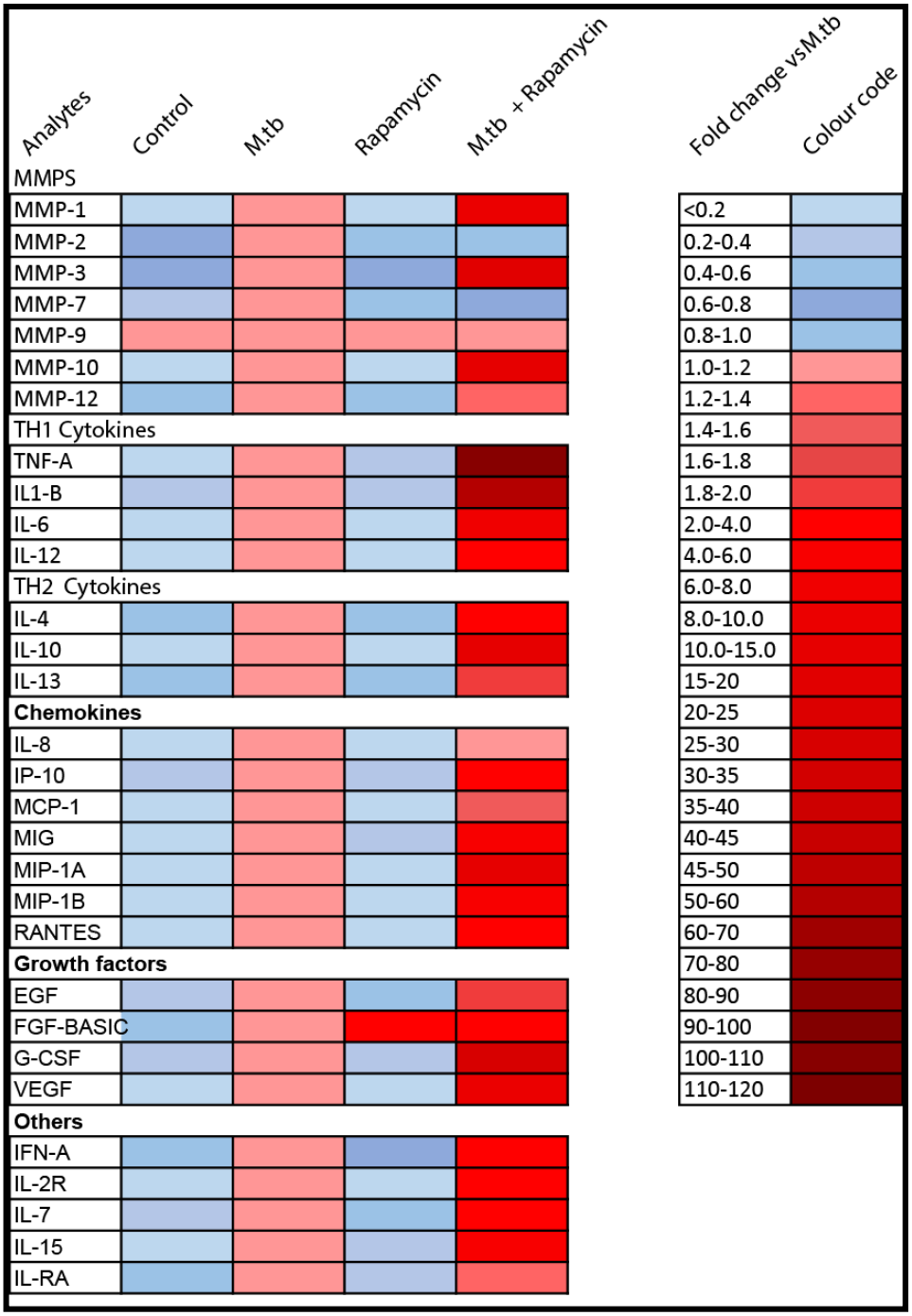


**Figure 46: mTORC-1 inhibition globally modulates a wide range of pro-inflammatory signalling molecule secretion.** MDMs were pre-treated with mTORC-1 inhibitor for two hours prior to *M.tb* infection. Supernatant samples were harvested after 72 hours post infection for multiplex analysis. Luminex profiling of macrophages demonstrate that *M.tb* infection upregulates a wide range of MMPs, cytokines, chemokines and growth factors. These were further elevated when mTORC-1 was blocked by 10nM of Rapamycin. Luminex experiments were performed on two different occasions in two donors each time.

## 3.18 Discussion of results chapter I

This study has confirmed that *M.tb* drives up-regulation of MMP-1 in macrophages. Monocyte-derived macrophages (MDMs) were generated by stimulation of isolated monocytes with M-CSF for five to seven days. The morphology of the cells that were generated (Figure 16) suggests they were macrophages. CD14 (cluster of differentiation 14) is a macrophage-expressed glycosylphosphatidylinositol-linked plasma-membrane glycoprotein which interacts with bacterial lipopolysaccharide (LPS) to induce inflammation, but also mediates recognition and removal of apoptotic cells (Andrew Devitt, 1998). Intracellular pathogens trigger induction of CD80 expression on monocytes, and these interact with T cells and mediate their ability to produce IFN-γ response (Carlos S. Subauste, 1998 ). The cell-surface glycoprotein receptor CD163 belongs to the scavenger receptor cysteine-rich (SRCR) family class B, and is highly expressed on resident tissue macrophages *in vivo* (Fabriek et al., 2005, Fabriek et al., 2009). The expression of CD11c, CD14, CD80 and CD163 by the differentiated monocytes (Figure 20) further suggests that the MDMs generated had the ability to function in a similar manner to macrophages *in vivo* (Khazen, 2005, Martinez-Pomares, 1996, Taylor, 2005).

A major role of macrophages, which is of paramount importance to the development of successful host immunity in infection, is their ability to recognise and phagocytose pathogens (Mohamed A. Elhelu, 1983). Human Leukocyte Antigen – antigen D Related (HLA-DR) is an MHC class II cell surface receptor highly expressed on antigen presenting cells (APCs) including macrophages (Bright and Munro, 1981). The high expression of HLA-DR by the MDMs confirmed that greater population of the cells were macrophages, with the histogram chart indicating specificity of antibody interaction with HLA-DR compared to the PE IgG isotype control (Figure 21). Since GFP-expressing *M.tb* was used to infect MDMs, the high population of cells expressing both HLA-DR and GFP were a strong indication of macrophages that had phagocytosed *M.tb* (Figure 21).

This study hypothesised that intracellular signalling pathways negatively regulate MMP-1 in TB. In this chapter, I demonstrate that indeed *M.tb* consistently drives MMP-1 in THP-1 and in primary macrophages, and that the pan-PI3K inhibitor, LY294002 augments this response in primary macrophages, but not in THP-1 cells. THP-1 cells were first isolated from the blood of a 1 year old with acute monocytic leukaemia (Tsuchiya et al., 1980). These cells are pro-monocytic with a unique ability to differentiate to macrophages upon treatment with 1,25-dihydroxyvitamin D3 (VD3) or 12-myristate 13-acetate (PMA) (Daigneault et al., 2010) (Park et al., 2007). Due to their potential to be physiologically macrophage-like, THP-1 cells are extensively used in the laboratory as substitute for primary macrophages in cell culture models (Schildberger et al., 2013).

In THP-1 cells, PI3K inhibition by LY294002 surprisingly caused suppression of MMP-1 (Figure 29). This was contrary to the effect of LY294002 on MMP-1 secretion in macrophages (Figure 25). Although THP-1 cells share numerous common features with primary macrophages, they exhibit limitations in the ability to replicate all the responses seen with macrophages derived from peripheral blood mononuclear cells (PBMCs) that are freshly isolated from human blood (Schildberger et al., 2013). Moreover, given they are cancerous cells, continues culture of THP-1 cells could induce mutations that renders the PI3K/AKT/mTOR and the Ras to MAPK pathways constitutively active. If any such modifications affect the cell's ability to produce pro-inflammatory mediators, then it is likely that in THP-1 cells, LY294002 potentially alters downstream mediators that positively regulate MMP-1, thereby exerting the MMP-1 suppression observed.

Intracellular signalling is highly complex, with the PI3K/AKT/mTORC-1 axis of the PI3K pathway mediating critical signalling cascades that culminates in downstream cellular responses (Guha and Mackman, 2002, Vanhaesebroeck et al., 2012). Given the crucial role of this pathway in cell growth, proliferation and survival, mutations that lead to constitutive activation of the PI3K pathway has been identified in a variety of cancers (Vara et al., 2004). It is however

becoming increasingly apparent that this pathway also mediates negative regulatory roles in immune disorders and pathological conditions (Fukao and Koyasu, 2003, Aksoy et al., 2012).

As shown in figure 28, although inhibition of PI3Kα and PI3Kβ in *M.tb* infected primary macrophages drives increased MMP-1 secretion, PI3Kδ inhibition results in even marked upregulation of *M.tb* -driven MMP-1. This result suggests that PI3Kα and β isoforms are contributors, rather than the main isoforms involved in the regulatory role proposed. PI3K α, β and δ all belong to the class 1A PI3K proteins. However, whereas PI3Kα and PI3Kβ isoforms are ubiquitously expressed in mammalian tissues, PI3Kδ is selectively highly enriched in leukocytes such as macrophages (Chantry et al., 1997). It is therefore likely that PI3Kδ is the core mediator of the PI3K negative regulatory function in TB. Findings from this study are in concert with previous reports that the delta isoform of PI3Ks mediates negative regulatory role in pathogenic conditions. In LPS-stimulated monocytes, PI3Kδ was shown to suppress the production of TNF, IL-1 and IL-6 which are all potent pro-inflammatory cytokines (Molnarfi et al., 2008). These cytokines have also been linked to necrosis and tissue destruction in TB (Molnarfi et al., 2008). PI3Kδ has been reported to be the specific isoform that drives cellular survival signals in acute and chronic leukaemia (Herman et al., 2010, Sujobert et al., 2005). PI3Kδ has also been demonstrated to mediate a balance between pro- and anti-inflammatory immunity in response to numerous pathogenic insults (Aksoy et al., 2012, Molnarfi et al., 2008).

Suppression of MMP-1 by PI3Kγ was not expected. PI3Kγ belongs to the class 1B PI3Ks and are also selectively enriched in leukocytes (Williams et al., 2009). They are however activated by GPCRs, which may be essential for MMP-1 production, but has not been reported to mediate macrophage responses to *M.tb* infection. A full investigation of the Class II and III PI3K proteins lie beyond the scope of this study and have therefore not been discussed here.

In order to decipher the important mediators in the effect of intracellular pathway inhibition on MMP-1 secretion, components that are downstream of the PI3K pathway such as AKT (Figure 30) and mTORC-1 (Figure 31) were studied. As previously discussed, both AKT and mTORC-1 inhibition also resulted in elevated secretion of MMP-1 in *M.tb* infected macrophages. Crosstalk of PI3K, AKT and mTOR signalling pathways are well documented (Cantley, 2002, Vanhaesebroeck et al., 2012). It was therefore not surprising when inhibition of PI3K, AKT and mTORC-1 all elicited similar MMP-1 up-regulation effect. Active PI3K protein mediates AKT phosphorylation via $PI(3,4,5)P_3$. AKT in turn activates mTORC-1 signalling. Downregulation of MMP-1 and MMP-13 was shown to occur via PI3K-dependent phosphorylation of AKT in human chondrocytes (Litherland et al., 2008). This is consistent with the negative regulatory role of intracellular signalling that was hypothesised by this study. Given the consistent enhancing effect of PI3K/AKT/mTOR pathway inhibition on MMP-1 production in *M.tb* -infected macrophages, this research has shed new insight into negative regulatory functions of this signalling in TB immunopathology.

Following the results discussed so far, this study sought to investigate whether prolonged active PI3K/AKT/mTORC-1 signalling directly represses MMP-1. Membrane $PI(3,4,5)P_3$ localisation was prolonged by inhibiting PTEN, the PI3K antagonist which catalyses the conversion of membrane $PI(3,4,5)P_3$ back to $PI(4,5)P_2$ . Interestingly, the result was inconclusive (Figure 22), with suppression seen but not in a consistent dose-dependent manner.

Enhanced accumulation of $PI(3,4,5)P_3$ did not show direct MMP-1 suppression effect as expected by PI3K signalling. This is likely to be due to the involvement of other PI3K-derived intracellular signalling molecules in MMP-1 regulation. As described above, dephosphorylation of $PI(3,4,5)P_3$ at the 5'-position by SH2 domain-containing inositol 5'-phosphatase(SHIP) and/or inositol polyphosphate 5'-phosphatase (INPP5) leads to the production of PI(3,4)P2, which is also a signalling molecule that mediates various downstream intracellular events (Vanhaesebroeck et al., 2001). It is possible

that PI(3,4)P2 signalling contributes towards the PI3K negative regulation of MMP-1. Although not clear at this stage, one thing can be concluded; be it up-stream or downstream effect, other unknown input(s) contribute towards the negative regulatory role played by the PI3K/AKT/mTORC-1 signalling in TB.

In recent years, a considerable number of studies have documented the tissue destructive role of MMP-1 in various pathogenic conditions such as emphysema (D'Armiento et al., 1992a, Foronjy et al., 2003, Selman et al., 1996), COPD (Finlay G. A., 1997, Rozynska et al., 2005) and TB (Elkington et al., 2011a, Salgame, 2011, Greenlee et al., 2007, D'Armiento et al., 1992b). These studies have heightened the need for deeper understanding of the role that similar pathogenic MMPs play in disease.

Although most MMPs have non-specific substrates and together they have unique ability to degrade all the components of ECM (Parks et al., 2004, David, 1970), a growing body of literature is recognising crucial balances between different MMPs that have similar affinities for common substrates (Green et al., 2011, Friedland et al., 2002). This is likely to underpin why variations in the kinetics of different MMP production in the context of specific cell types may confer critical mechanisms for regulation of tissue remodelling. As shown above, *M.tb* up-regulates MMP-1 in macrophages, and this is further elevated by PI3K inhibitors (Figures 25, 26 and 28).

The interstitial collagenase, MMP-1 is one of the most characterised MMPs in pulmonary TB. Type I fibrillar collagen is abundant in the lung tissue and is relatively resistant against enzymatic cleavage (Crystal, 1997.). Together, the collagenases (MMPs -1, -8 and -13) cleave all types of helical interstitial collagens, with MMP-1 in particular mediating cleavage of types I, II and III fibrillar collagen at neutral pH (Page-McCaw et al., 2007, Parks et al., 2004, Elkington et al., 2011c).

Given that *M.tb* must cause lung tissue destruction to drive pathology, it was not surprising that the bacilli upregulated MMP-1 in macrophages. Analysis of

sputum and bronchoalveolar lavage fluid (BALF) from pulmonary TB patients revealed that *M.tb* infection increases MMP-1, and this was in concert with other data demonstrating that in human primary monocytes, *M.tb* selectively drives MMP-1 secretion and gene expression (Elkington et al., 2011a). The simultaneous *M.tb* -driven up-regulation of MMPs-2, -3, -7 and MMP-10 (Figure 34) was however not expected.

Although human Stromelysins (Stromelysin-1 or MMP-3, Stromelysin-2 or MMP-10 and Stromelysin-3 or MMP-11) do not directly degrade types I and II fibrillary collagen, they nevertheless contribute towards connective tissue remodelling both directly and indirectly. MMP-3 degrades collagen IV, V, IX, X, and laminin (Woessner, 1991), whilst MMP-10 cleaves collagen III, IV, V and elastin (Justilien et al., 2012, Barksby et al., 2006). Both MMP-3 and MMP-10 degrade gelatin, proteoglycans and fibronectin (Barksby et al., 2006, Vincenti and Brinckerhoff, 2007). Interestingly, these Stromelysins are believed to indirectly mediate ECM tissue destruction due to their ability to mediate activation of other pathogenic MMPs. Within the ECM, MMP-3 cleaves to activate MMP-13 (collagenase-3) whilst MMP-10 activates MMP-7 (Matrilysin) (Barksby et al., 2006). Most importantly, both MMP-3 and MMP-10 mediate cleavage of the inactive pro-forms of the collagenases (MMP-1 and MMP-8) and Gelatinase B (MMP-9), resulting in their full activation and subsequent collagenase activity in the ECM (Barksby et al., 2006).

As mentioned above, the upregulation of MMP-2 and MMP-7 by *M.tb* (Figure 34) was also unexpected. Whereas data on the direct and indirect tissue destructive roles of MMP-1, MMP-3 and MMP-10 continue to grow, the role of MMP-2 and MMP-7 in TB remain relatively unclear. MMP-2 (Gelatinase A) is constitutively expressed at elevated levels by a variety of cells, with substrates including gelatin, types IV collagen, proteoglycans, fibronectin, α2-macroglobulin, laminin and elastin (Green et al., 2011). The basement membrane derives its structural support from the presence of type IV collagen. As a type IV collagenase, MMP-2 degrades the basement membrane and has been linked to regulation of vascularization and endometrial menstrual

breakdown (Green et al., 2011). To date, there has been no reliable evidence of tissue destructive role of MMP-2 in pulmonary TB. However, few studies have investigated the role of MMP-2 in TB meningitis (TBM), where the enzyme is believed to mediate neuronal apoptosis (Green et al., 2011).

MMP-7 (Matrilysin) cleaves casein, type I, II, IV, and V gelatins, fibronectin and proteoglycan (Yokoyama et al., 2008). Functions of MMP-7 have not been extensively investigated in TB. Although *M.tb* drove upregulation of MMP-1 and MMP-7 in human primary macrophages, demonstrable evidence led to the conclusion that MMP-7 production in macrophages is not *M.tb* specific (Elkington et al., 2005). However, since MMP-10 (also up-regulated by *M.tb* in the same samples) cleaves to activate MMP-7, it is likely that MMP-7 also contributes towards tissue destruction in TB. MMP-7 has been speculated to be involved in extracellular matrix macromolecule degradation during pathological conditions *in vivo* (Imai et al., 1995).

In this study, uninfected macrophages secreted high levels of basal MMP-9 and *M.tb* infection did not increase this any higher than that secreted by uninfected macrophages (Figure 34). Gelatinase B (MMP-9) is a type IV and V collagenase, with other substrates including proteoglycans, fibronectin and elastin (Van den Steen et al., 2002). Physiological MMP-9 concentrations is essential for tissue remodelling-mediated cellular processes such as wound healing (Buisson et al., 1996), angiogenesis (Vu et al., 1998) and migration of polymorphonuclear neutrophil across basement membrane, possibly following activation of the zymogen form of MMP-9 by elastase (Delclaux et al., 1996).

Although monocytes have been reported to produce greater amount of MMP-9 compared to other MMPs, secretion of the pro-form MMP-9 is tightly regulated transcriptionally in monocytes (Price et al., 2003). Due to this high level of transcriptional control, human primary macrophages have not been commonly used for MMP-9 research in TB. Instead, primary human bronchial epithelial cells (NHBE) are typically used for a number of MMP-9 studies. NHBE are known to produce MMP-9 in the context of combined host- and pathogen-

derived soluble mediators (Elkington et al., 2007), and in response to LPS stimulation (Pardo et al., 1997, Hetzel et al., 2003). Although MMP-9 was highly expressed within granulomas *in vivo*, direct *M.tb* infection of NHBEs *in vitro* did not enhance basal level MMP-9 production (Elkington et al., 2007, Singh et al., 2014). Macrophages have a pivotal role in host immunity to *M.tb* , and MMP-9 may mediate tissue remodelling during granuloma formation by promoting recruitment of monocytes to ensure stability of the developing granuloma (Price et al., 2003).

The inability of *M.tb* to further elevate basal level of macrophage-secreted MMP-9 re-enforces their tight transcriptional regulation. This also suggests that in order to drive TB pathology, the bacteria has evolved to specifically up-regulate MMPs that have potent tissue destructive activities such as the collagenases (rather than gelatinases) in macrophages. In fact during the early development of granuloma, it is believed that epithelial cells secrete MMP-9 which is essential for monocyte recruitment to the site of infection. However, at the advanced stages of TB, macrophages then secrete high levels of MMP-1 which play crucial role in lung ECM destruction (Salgame, 2011).

Similar to the dynamics of MMP-9 production, the un-infected macrophages used in this study secreted high levels of basal MMP-12, and *M.tb* infection did not increase this any higher than that secreted by un-infected macrophages (Figure 34). Just like any other MMP, the macrophage metalloelastase (MME) MMP-12, also possess unique abilities to degrade the ECM in normal physiological conditions, but unrestricted activity causes detrimental tissue injury in disease processes. MMP-12 is responsible for the elastase activity of macrophages (Shapiro et al., 1993b). Existing research recognises the crucial functions of macrophages-produced MMP-12 in mice, but this role continues to be unclear in humans (Demedts et al., 2006). Emerging reports suggest that MMP-12 plays a critical role in the pathogenesis of cigarette smoke-induced COPD. This is because elevated levels of the enzyme was determined in induced sputum recovered from COPD patients compared to those from healthy donors (Demedts et al., 2006,

Shapiro et al., 1993b). MMP-12 has not been extensively investigated in TB. It is therefore likely that physiological concentrations of macrophage-produced MMP-9 and MMP-12 are important for balance, whereas uncontrolled MMP-9 (produced by either macrophages or NHBEs) and MMP-12 activity promotes tissue destruction in TB.

Both PI3K and mTORC-1 inhibition by LY294002 and rapamycin respectively further enhanced the production of MMP-1, -3 and -10 without altering *M.tb* -driven MMP-2 and MMP-7 (Figures 34 and 35). These results suggest that whereas the bacteria deliberately drives production of pathogenic MMPs, the PI3K pathway functions to supress such pathogenic MMPs that have potent collagenase and/or direct tissue destructive activity. This way, the intracellular signalling pathway is able to negatively regulate MMP-mediated tissue destruction in TB.

Using Luminex array profiling for a range of cytokines, chemokines and growth factors, this study has demonstrated that inhibition of the PI3 kinase and mTOR pathways have a widespread effect, with mostly enhanced secretion of Th1/Th2-type cytokines and differential modulation of a number of chemokines and growth factors (Figures 36 to 45). This observation was of major interest because appropriate levels of Th1-type cytokines mediate a protective antimicrobial immunity during infection, which in TB is essential for depriving *M.tb* of its intracellular niche. Uncontrolled production of Th1-type molecules can however be deleterious and may accentuate disease progression.

IL-1β has been demonstrated to induce up-regulation of a range of antimicrobial effectors to directly kill and limit intracellular *M.tb* replication in murine models and in human MDMs (Jayaraman et al., 2013). The critical role of IL-1β in host resistance to *M.tb* infection had been reported by other groups previously (Mayer-Barber et al., 2010, Juffermans et al., 2000). This notwithstanding, over-exuberant production of IL-1β in TB can drive disease progression by inflicting chronic tissue damage (Zhang et al., 2014). As a

result of its potential to cause excessive inflammation and tissue damage, the biological activity of IL-1β is tightly controlled (Dinarello, 2009).

In the same way as IL-1β, physiological production of IL-6, IL-12 and TNF-α in *M.tb* infection is also essential for host defence against pathogenic challenge (Martinez et al., 2013, Cooper et al., 1997, Stenger, 2005). In fact, IL-1β must promote recruitment of IL-6 and TNF in order to mediate the host protection against *M.tb* survival and growth in macrophages (Jayaraman et al., 2013). However, unregulated over-expression of these Th1-type molecules has previously been implicated in disease exacerbation by mediating tissue destruction (Law et al., 1996, Mootoo et al., 2009, Zhang et al., 2012).

Inhibition of both PI3K (Figure 36) and mTORC-1 (Figure 37) signalling resulted in even marked secretion of IL1-β, IL-6, IL-12 and TNF-α by *M.tb* -infected macrophages (Figure 38). Fukao *et al* described a similar phenotype, implicating the PI3K pathway as a negative regulator of IL-12p70 production in TLR signalling by disrupting the p85α regulatory subunit of class 1A PI3Ks in mice. In this study, the group demonstrated elevated IL-12 production in splenic DCs and BMDCs isolated from mutant compared to wild type mice. In line with this observation, the PI3K inhibitor, wortmannin also elicited pronounced IL-12p70 secretion (Fukao, 2002). Interestingly, IL-12p70 overproduction correlated with loss of anti-parasitic immunity due to sensitivity to intestinal parasite, strongyloides venezuelensisthis, and this was restored with TH-2 conditioned BMMCs but not with standard BMMCs. Data from this study indicates that the PI3K pathway negatively regulates IL-12 production in mice, and this ensures appropriate balance of Th1/Th2-type response to infection (Fukao et al., 2002).

Taken together, this study suggests that important intracellular signalling pathways play crucial negative regulatory role to restrict tissue damage in TB by controlling overproduction of TH1-type cytokines. The pathway inhibitors similarly augmented a wide range of Th2-type cytokines, chemokines and growth factors, which was not expected (Figures 38-45). A high level of fine

tuning of inflammatory effector molecules is required to ensure appropriate balance between antimicrobial immunity and the chronic tissue damage that is associated with pulmonary TB. It is therefore likely that the negative regulatory role of intracellular signalling observed is not restricted to known pro-inflammatory molecules, but also Th2-type cytokines, chemokines and growth factors alike.

# 4. CHAPTER 4: RESULTS PART II

## MNK1 signalling modulates MMP-1 in TB:

### 4.1 Overview

This study sought to investigate the regulatory role of important intracellular signalling pathways in TB pathogenesis. MMPs mediate lung tissue destruction that propagates cavitation in TB (Elkington et al., 2011c). This study has demonstrated how inhibition of PI3Ks (PI3Kδ in particular), AKT and mTORC-1 signalling all resulted in even more marked *M.tb* -driven MMP-1, the dominant collagenase. mTOR is an important downstream target of active AKT. Following activation by AKT, mTORC-1 drives ribosomal biogenesis and protein synthesis by activating S6K and phosphorylating 4E-BP at multiple sites to cause its dissociation from eIF4E. Given that rapamycin exerts a high MMP-1 up-regulation effect both at the mRNA transcription and translation levels, it was necessary to investigate other proteins that regulate mRNA translation by modulating protein synthesis in a similar manner to mTORC-1.

### 4.2 Methods

Macrophages were pre-treated with Mnk inhibitors for two hours before being infected with *M.tb* . supernatant sample would be harvested at 72 hours post infection for MMP-1 ELISA and/or multiplex luminex analysis. For the purposes of gene expression studies, MDMs were infected for up to 24 hours before cellular RNA was isolated for RT-QPCR analysis as described in chapter 2.

### 4.3 Chapter Hypothesis

Previous studies have identified 4E-BP (and not S6K1) as the main mTORC-1 substrate that predominantly mediates cell growth, thereby

driving tumorigenesis (Dowling et al., 2010). The ultimate aim of hyper-phosphorylation of 4E-BP by mTORC-1 is to cause the dissociation of eIF4E from the 4E-BP-eIF4E complex, thereby releasing eIF4E to begin the process of eukaryotic initiation complex (eIF4F) formation. This suggests that eIF4E activation plays a key role in mTORC-1 signalling and in cell proliferation as well as tumour formation. Apart from mTORC-1, the activity of eIF4E is further regulated post-translationally by MAP kinase-interacting kinases (Mnks), Mnk1/2. These protein kinases are themselves substrates of ERK and p38 MAP kinase proteins, important downstream components of MAP kinase signalling (reviewed by (Scheper and Proud, 2002a). Given the crucial role of Mnk1 in eIF4E-dependent formation and stabilisation of eukaryotic initiation complex, I hypothesised that pharmacological inhibition of Mnk1 would lead to reduced translation and subsequent repression of MMP-1 synthesis.

## 4.4 Aims

This chapter aimed to dissect signalling downstream of the MAP kinase pathway that feeds into mTORC-1 signalling, and to investigate their effect on MMP-1 production in *M.tb* -infected macrophages. Initial experiments sought to utilise chemical inhibition to determine the effect of Mnk1 signalling on MMP-1 secretion. This chapter would highlight the following:

- Utilisation of different Mnk inhibitors to ascertain the effect of Mnk signalling on MMP-1 in macrophages.
- Establish the specificity of the compound of interest on their predicted target protein mediators by Western blot.
- Dissect the role of Mnk1 signalling in regulating MMP-1 secretion in macrophages.

## 4.5 Mnk1 inhibitors drive elevated MMP-1 in *M.tb* infected macrophages

In order to dissect pathways that also negatively regulate MMP-1 by feeding into mTORC-1 signalling, the Mnk pathway was investigated using pharmacological inhibition (Mnk1 specific inhibitors were kindly provided by Prof C.G Proud). This study reports for the first time that signalling via the Mnk1 pathway also negatively regulates MMP-1 production in TB.

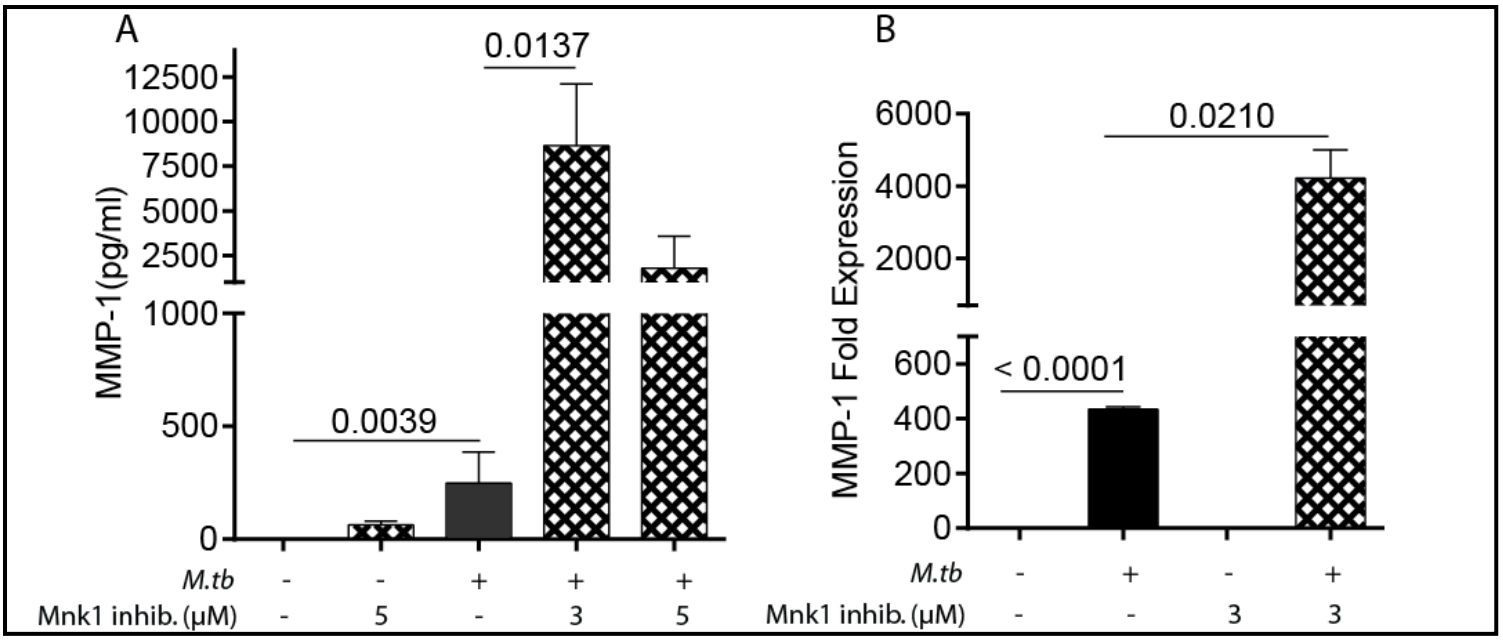


**Figure 47: Mnk1 inhibitor enhances *M.tb* -driven MMP-1**. MDMs were pre-treated with Mnk1 inhibitor for two hours prior to *M.tb* infection. Supernatant samples were harvested after 72 hours post infection for MMP-1 detection by ELISA assay. *M.tb* drives MMP-1 production in macrophages. Specific blockade of Mnk1 significantly further increased this response both at the secretion **(A)** and gene expression **(B)** levels. Data represent experiments performed in triplicate on a minimum of three occasions. Mean and standard deviations are shown and p values are student t-test.

Given the key role of the Mnk substrate, eIF4E, in formation and stabilisation of the eukaryotic initiation complex, eIF4F, it was hypothesised that Mnk1 inhibition would directly block protein translation

and therefore suppress MMP-1 production. Surprisingly, inhibition of Mnk1 resulted in a significant elevation of *M.tb* -driven secreted MMP-1 (Figure 48A).The increased secretion was secondary to increased MMP-1 gene expression (Figure 48B). This suggests that precluding mRNA translation by repressing the activity of eIF4E (that is by interfering with the formation of eIF4F), results in even marked MMP-1 protein synthesis.

## 4.6 The modulation of MMP-1 by Mnk1 inhibitors is not via the eIF4F complex

Mnks phosphorylates to activate eIF4E to promote 5'-cap-dependent mRNA synthesis (Hou et al., 2012). Interaction between eIF4E and the scaffolding protein eIF4G is necessary for eIF4E activity and subsequent formation of the eukaryotic initiation complex eIF4F (Pyronnet et al., 1999). I therefore next determined whether formation of the eIF4F complex, via direct activation of eIF4E by Mnk1 was critical in the MMP-1 production observed.

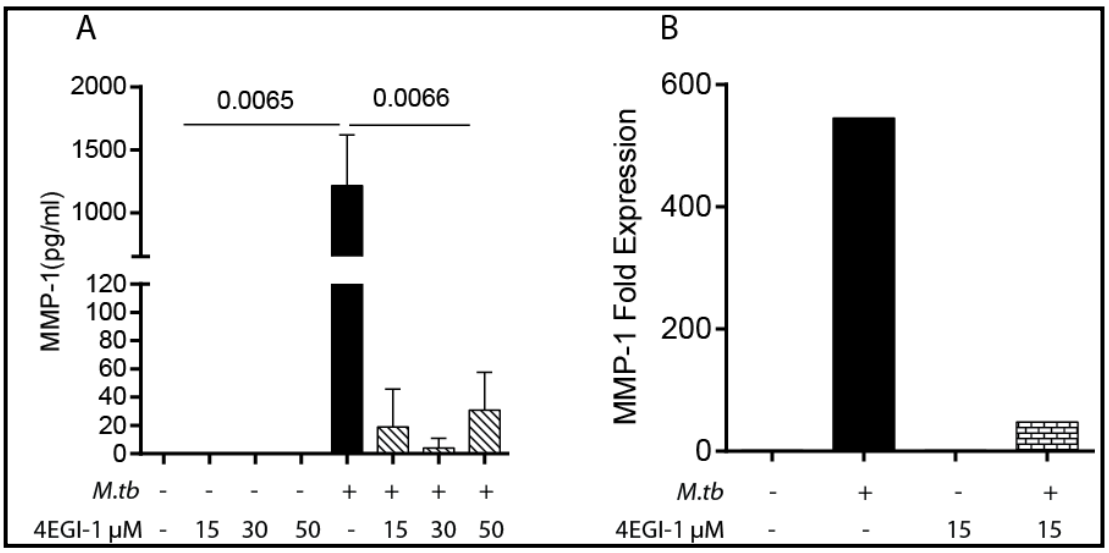


**Figure 48: Interfering with the interaction between eIF4E and eIF4G suppresses MMP-1.** MDMs were pre-treated with 4EGI-1(a compound that prevents eIF4E/eIF4G complex formation) for two hours prior to *M.tb* infection. Supernatant samples were harvested after 72 hours post infection for MMP-1 detection by ELISA assay. Different concentrations of 4EGI-1 cause repression of MMP-1 both at the secretion **(A)** and mRNA **(B)** levels in *M.tb* infected macrophages. Data represent experiments performed in triplicate on a minimum of three occasions. Mean and standard deviations are shown and p values are student t-test.

Macrophages were pre-treated with 4EGI-1, a compound that potently disrupts interaction between eIF4E and eIF4G. 4EGI-1 has been used to interfere with eukaryotic translation initiation in a number of studies. Interestingly, 4EGI-1 significantly suppressed *M.tb* -driven MMP-1 both

at the mRNA and protein translation levels (Figure 49). This suggests that indeed the formation and stability of eukaryotic initiation complex eIF4F is necessary for *M.tb* -driven MMP-1 synthesis by macrophages.

To address the issue of a potential by-stander effect, macrophages were pre-treated with different Mnk (MRT80, Compound E and CGP57380) inhibitors to ascertain their effect on MMP-1 secretion compared to the Mnk1-specific inhibitor used. Interestingly, all three compounds exerted significant suppression of *M.tb* -driven MMP-1 (Figure 50A, B and C), and this was not expected.

One of the compounds known to have a drastic effect on blocking eIF4E phosphorylation is CGP57380 (Li et al., 2010). In order to investigate the specificity of the compounds that have been used in this study on the suppression of Mnk1 activity, the macrophages were treated with the Mnk1 inhibitor of study, and with CGP57380, followed by total and phosphorylated eIF4E Western blotting. *M.tb* infection drove eIF4E phosphorylation, with the Mnk1 specific inhibitor and CGP57380 repressing this phosphorylation effect (Figure 51). This result confirmed that indeed the compounds do target Mnk signalling.

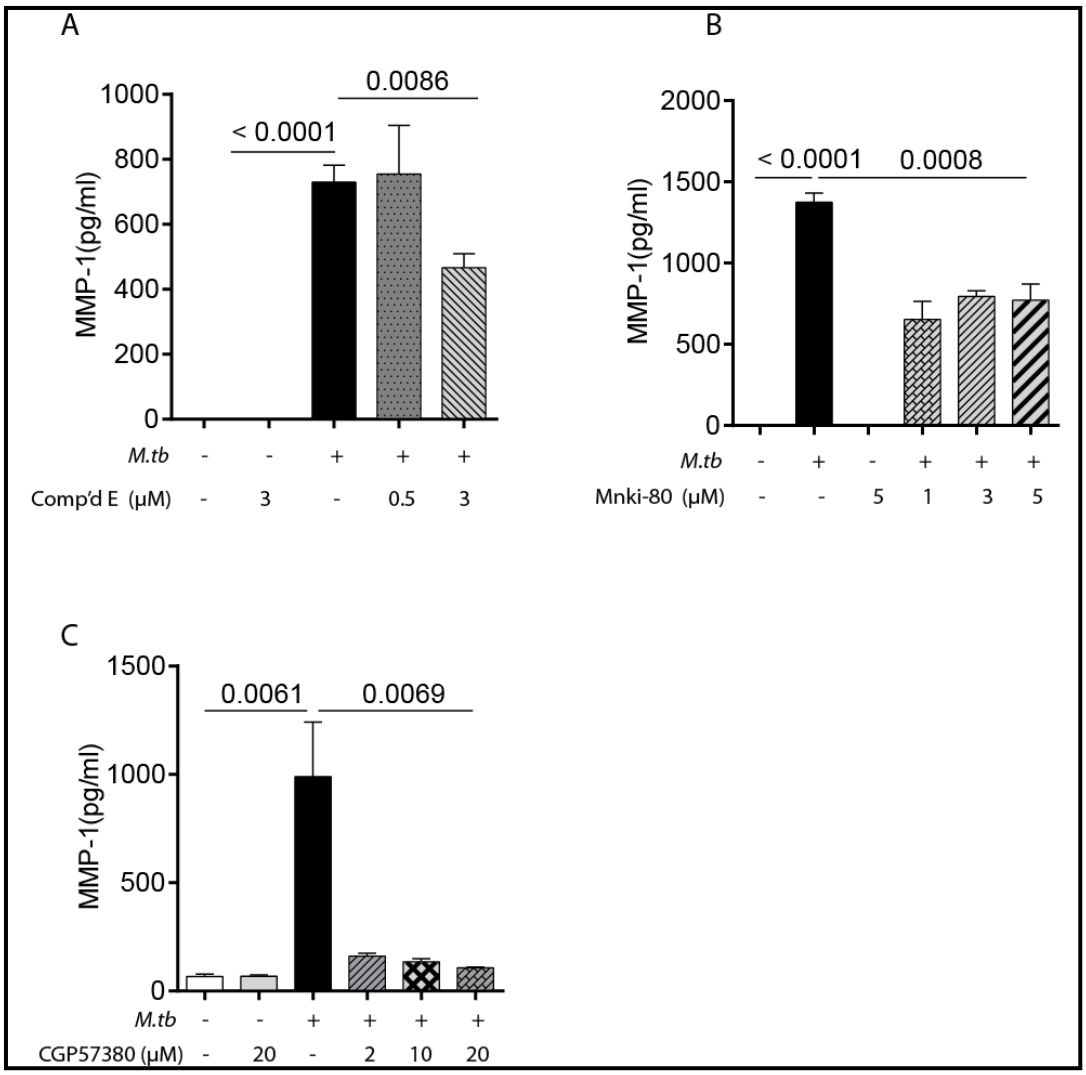


**Figure 49: Various Mnk1 inhibitors suppress *M.tb* -driven MMP-1 in macrophages.** MDMs were pre-treated with different types of Mnk1 inhibitors for two hours prior to *M.tb* infection. Supernatant samples were harvested after 72 hours post infection for MMP-1 detection by ELISA assay. **A:** Compound E; **B: Mnki-80**; **C:** CGP57380**.** The Mnk inhibitors Mnki-80 and CGP57380 both suppressed eIF4E phosphorylation at 72 hours post *M.tb* infection. Compound E exerted no change on *M.tb* -driven MMP-1 at 0.5μM, but suppressed it at 3 μM. Data represent experiments performed in triplicate on a minimum of three occasions. Mean and standard deviations are shown and p values are student t-test.

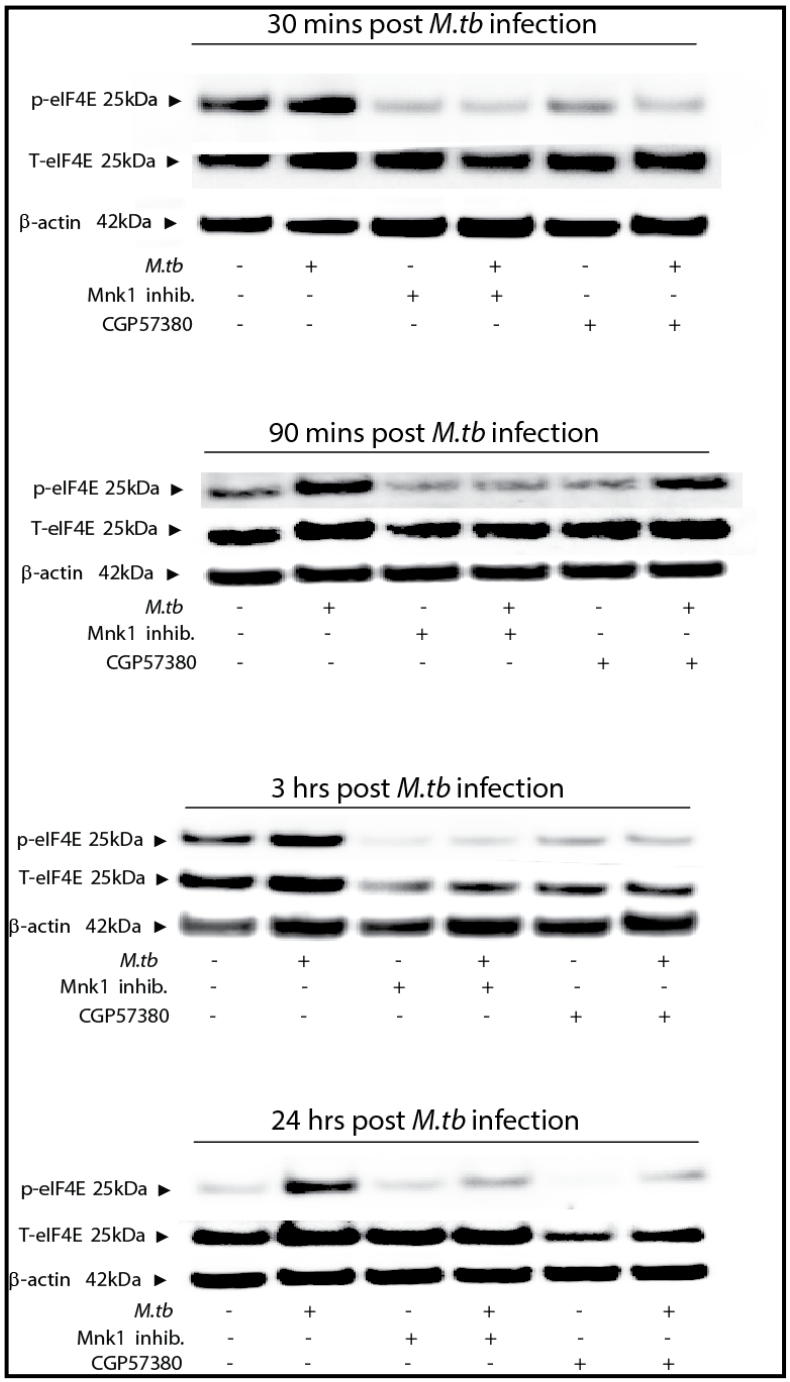


Figure 50: Mnk inhibitors suppress eIF4E phosphorylation. Modulation of eIF4E phosphorylation by Mnk1specific and pan-Mnk inhibitor (CGP57380) was investigated to ascertain targeting effect. Both inhibitors suppressed eIF4E phosphorylation after

30mins and up to 24hours post *M.tb* infection. CGP57380 appear to lose inhibition at 90mins in the contest of *M.tb* infection. Experiment was performed on three different occasions.

## 4.7 The negative regulatory to MMP-1 is via Mnk but not p90RSK signalling

Given that Mnk is downstream of Erk and p38 MAPK pathway, it was necessary to determine whether other molecules downstream of this pathway similarly modulated MMP-1. Other known downstream kinases of Erk1/Erk2 are the RSK family of proteins. It was hypothesised that inhibition of the ribosomal S6 kinase, p90RSK which is also downstream of Erk pathway and phosphorylates eIF4B would augment MMP-1 production in *M.tb* infected macrophages. BI-D1870 was identified to be a potent inhibitor of the RSK isoforms (Sapkota et al., 2007). Interestingly, BI-D1870 exerted no significant change on MMP-1 secretion (Figure 52), demonstrating that the crosstalk was not via this pathway.

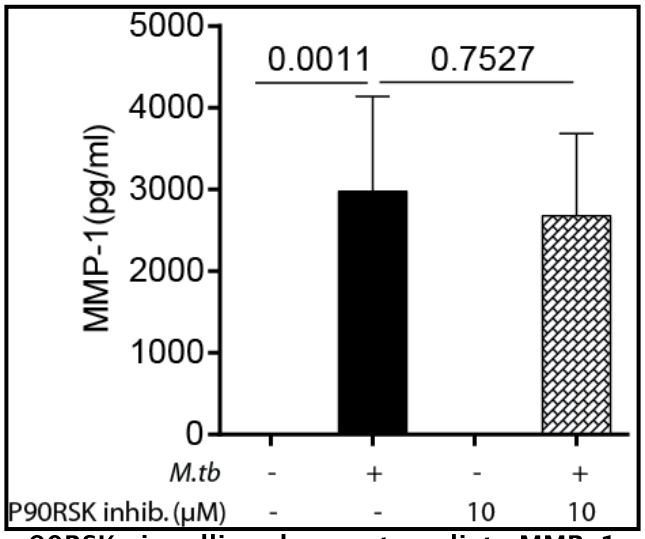


**Figure 51: p90RSK signalling does not mediate MMP-1 regulation.** MDMs were pre-treated with with 10μM of **p90RSK** inhibitor (BI-D1870) for two hours prior to *M.tb* infection. Supernatant samples were harvested after 72 hours post infection for MMP-1 detection by ELISA assay. Inhibition of p90RSK signalling in *M.tb* -infected macrophages did not inflict any significant change in MMP-1 secretion. Data represent experiments

performed in triplicate on three occasions. Mean and standard deviations are shown and p values are student t-test

## 4.8 PI3K and Mnk pathways crosstalk in the negative regulatory to MMP-1

The pan-PI3K inhibitor, LY294002 had been reported to suppress eIF4E phosphorylation. To determine whether there was a pathway convergence between the PI3K and Mnk signalling, Western blotting was performed for eIF4E in the context of stimulating the PI3K pathway with insulin and chemically blocking both the PI3K and Mnk pathways (Figure 53). Interestingly, insulin which activates the PI3K pathway drove high levels of eIF4E phosphorylation (Figure 53 lane 1), and this was suppressed by both LY284002 (Figure 53 lane 2), and Mnk inhibitor (Figure 53 lane 4). The PI3K/PDK1 inhibitor did not induce any change in eIF4E phosphorylation (Figure 53 lane 5), compared to basal levels phosphorylation (Figure 53 lane 3). *M.tb* -driven eIF4E phosphorylation (Figure 53 lane 6) was suppressed by both Mnk and PI3K/PDK1 inhibition (Figure 53 lanes 7 and 8 respectively). This result shows evidence of crosstalk between PI3K and Mnk signalling at this level.

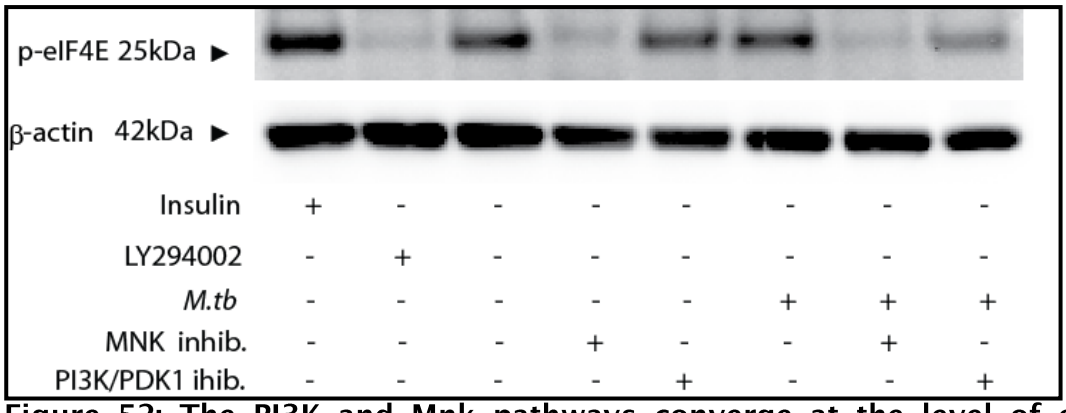


**Figure 52: The PI3K and Mnk pathways converge at the level of eIF4E phosphorylation.** Macrophages were pre-treated with 10nM insulin, 10μM LY294002, 10μM Mnk1 inhibitor or 10μM PI3K/PDK1 inhibitor before being infected with M.tb for a further 6 hours. Insulin which drives PI3K signalling, also drives eIF4E phosphorylation

whilst PI3K inhibition suppresses it. Details of this result have been explained in text above. Western blot experiments were performed at least two times.

## 4.9 Mnk regulation of MMPs is relatively specific

This study has shown that although levels of MMP-2,-7,-9 and -12 remained unchanged in all samples, levels of MMP-1, MMP-3 and MMP-10 were elevated in both LY294002 (Figure 34) and Rapamycin (Figure 35) treated macrophages compared to that driven by *M.tb* alone and by uninfected macrophages. Using the same luminex profiling analysis, the effect of Mnk1 inhibition on multiple MMPs, Th1/Th2-type cytokines, chemokines, growth factors and a number of cytokines were investigated. I hypothesised that Mnk1 inhibition would exert similar effect on multiple MMPs as that mediated by PI3K and mTORC-1 inhibition. Similar to the effect of LY294002 and rapamycin, global analysis of MMPs demonstrated that Mnk inhibition also significantly augments *M.tb* -driven MMP-1, -3 and MMP-10 but not MMP-2, -7, -9 and MMP-12 (Figure 54). Conversely, Mnk1 inhibition suppressed *M.tb* -driven Th1/Th2-type cytokines, as well as a wide range of chemokines and growth factors, demonstrating that the negative regulatory effect of Mnk1 is relatively MMP-specific.

## 4.10 Mnk1 inhibition suppresses *M.tb* -driven cytokine levels in macrophages

The global effect of Mnk1 pathway inhibition on pro-inflammatory cytokine response was also investigated in the samples that were used for the multiple MMPs analysis. A 30-plex cytokine assay was performed to examine the effect of Mnk1 inhibitor on the dynamics of Th1/Th2-type and other cytokines, as well as a selection of chemokines and growth factors (Figures 54-59).

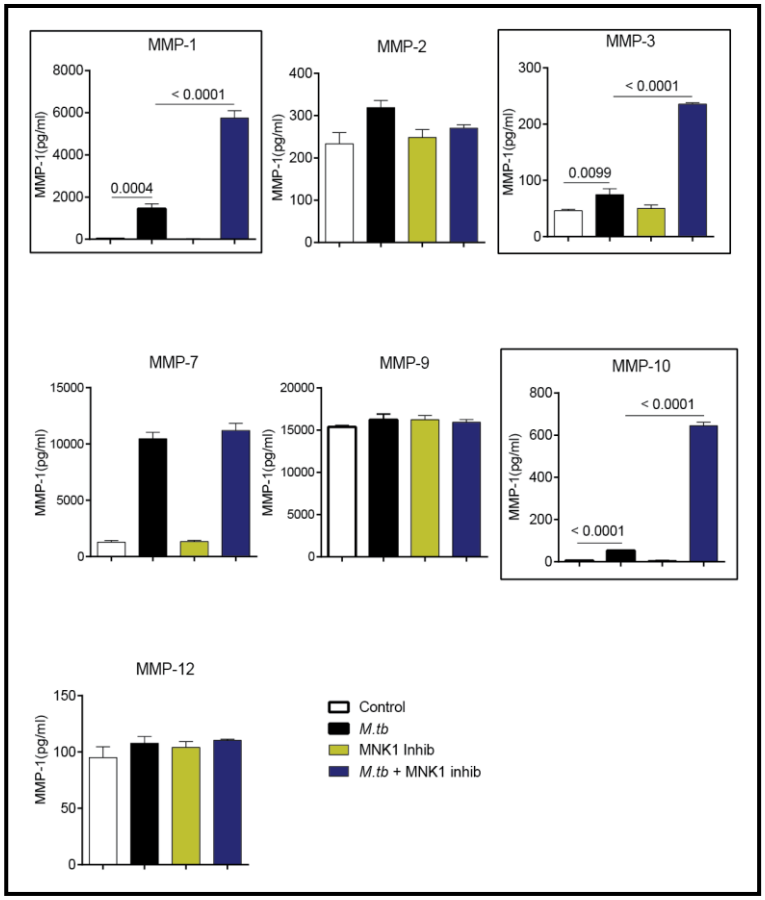


**Figure 53: Mnk1 inhibition globally modulates multiple MMPs in MDMs.** MDMs were pre-treated with Mnk1 inhibitor for two hours prior to *M.tb* infection. Supernatant samples were harvested after 72 hours post infection for MMP multiplex analysis. Luminex profiling of MMPs demonstrate that *M.tb* upregulated a wide range of MMPs. Inhibition of Mnk1 further augmented MMP-3 and MMP-10 in the same pattern as seen in MMP-1 , but exerted no change in macrophage-secreted MMPs -2, -7, -9 and -12. Luminex experiments were performed on two different occasions in two donors each time. Data show mean and standard deviation of experiments performed in triplicates and is representative of experiments performed on two donors at separate occasions. P values are Student's t-test, with $P < 0.05$ considered significantly different.

## *4.11* Mnk1 inhibition suppresses pro-inflammatory cytokine production in *M.tb* infected macrophages

*M.tb* drove the production of pro-inflammatory mediators in macrophages. In contrast to PI3K inhibition, Mnk inhibition significantly suppressed Th1-type cytokines including IL-1β, IL-6, IL-12 and TNF-α (Figure 55).

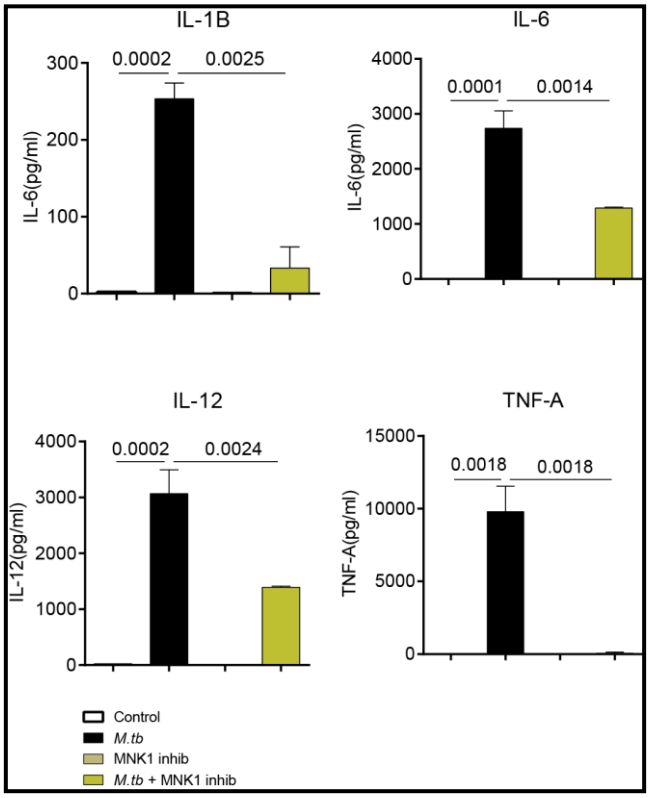


**Figure 54: Mnk1 inhibition suppresses cytokine production in macrophages.** MDMs were pre-treated with Mnk1 inhibitor for two hours prior to *M.tb* infection. Supernatant samples were harvested after 72 hours post infection for cytokine multiplex analysis. Luminex profiling of macrophages demonstrates that *M.tb infection* upregulates pro-inflammatory mediators. These were suppressed when Mnk1 was chemically blocked. Luminex experiments were performed on two different occasions in two donors each time. Data show mean and standard deviation of experiments performed in triplicates and is representative of experiments performed on two donors at separate occasions. P values are Student's t-test, with $P < 0.05$ considered significantly different.

## 4.9 Mnk inhibition suppresses Th2-type cytokine production in *M.tb* -infected macrophages.

*M.tb* drove the production of anti-inflammatory mediators in macrophages. Inhibition of Mnk1 suppressed Th2-type cytokines such as IL-4, IL-10 and IL-13. (Figure 56).

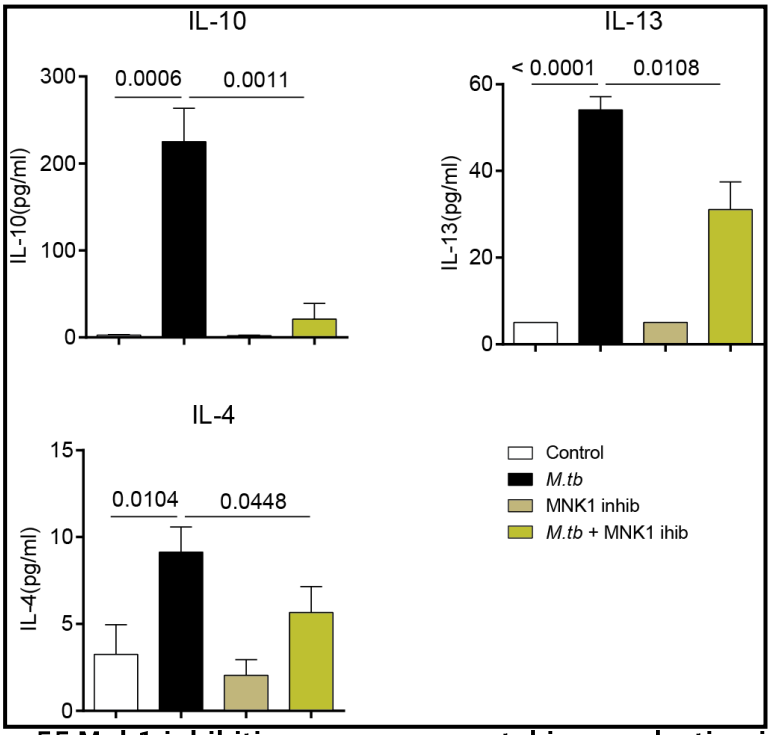


**Figure 55:Mnk1 inhibition suppresses cytokine production in macrophages.** MDMs were pre-treated with Mnk1 inhibitor for two hours prior to *M.tb* infection. Supernatant samples were harvested after 72 hours post infection for cytokine multiplex analysis. Luminex profiling of macrophages show *M.tb* infection induce low production of anti-inflammatory mediators. These were slightly suppressed when Mnk1 was chemically blocked. Luminex experiments were performed on two different occasions in two donors each time. Data show mean and standard deviation of experiments performed in triplicates and is representative of experiments performed on two donors at separate occasions. P values are Student's t-test, with $P < 0.05$ considered significantly different.

## 4.12 Mnk1 inhibition differentially modulate chemokine production in *M.tb* -infected macrophages

*M.tb* drove the production of a wide range of chemokines in macrophages. Mnk1 inhibition either suppressed or exerted no change on the chemokines under study. Mnk1 inhibition supressed *M.tb* -driven RANTTES, MIP-1α and MIP-1β, but exerted no change on the levels of MCP-1, IP-10, MIG and IL-8 produced by *M.tb* -infected macrophages (Figure 57).

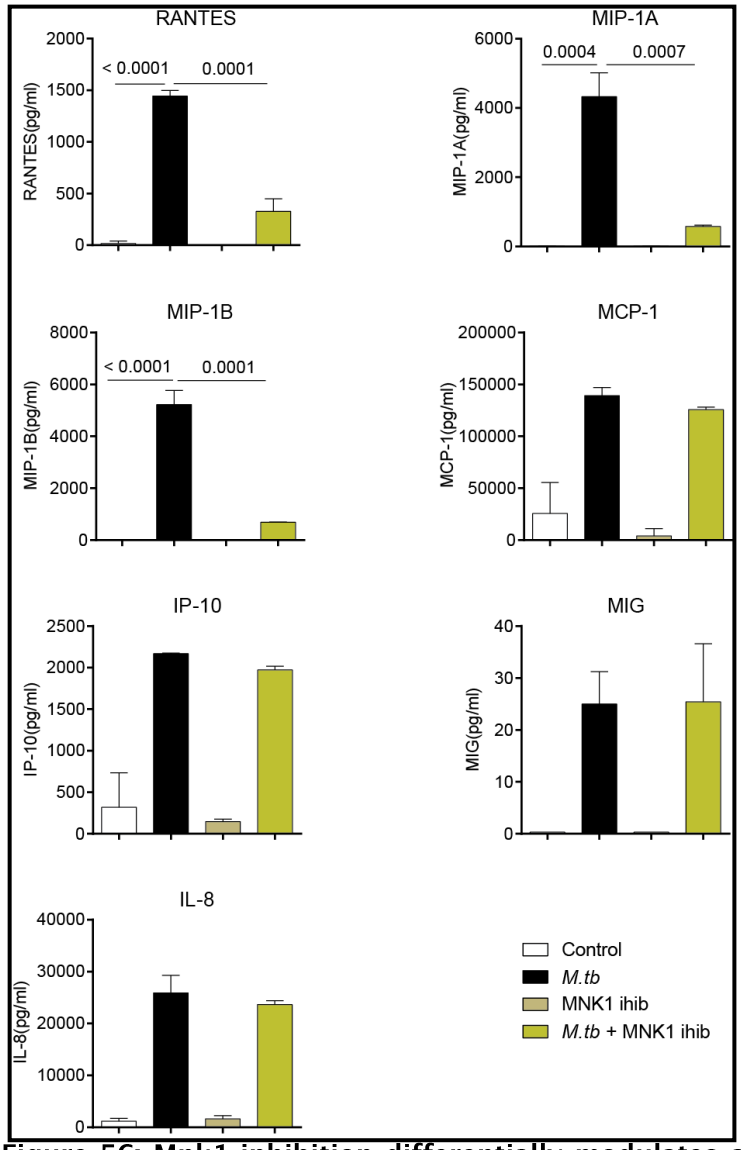


**Figure 56: Mnk1 inhibition differentially modulates a wide range of chemokines.** MDMs were pre-treated with Mnk1 inhibitor for two hours prior to *M.tb* infection. Supernatant samples were harvested after 72 hours post infection for multiplex analysis. Luminex profiling of macrophages demonstrate that *M.tb* infection upregulates a wide range of chemokines. Details have been explained in text above. Luminex experiments were performed on two different occasions in two donors each time. Data show mean and standard deviation of experiments performed in triplicates and is representative of experiments performed on two donors at separate occasions. P values are Student's t-test, with $P < 0.05$ considered significantly different.

## 4.13 Mnk1 inhibition suppresses production of growth factors in *M.tb* -infected macrophages

*M.tb* drove the production of a wide range of growth factors in macrophages. Mnk1 inhibition suppressed *M.tb* -driven VEGF, G-CSF, EGF and FGF-BASIC (Figure 58).

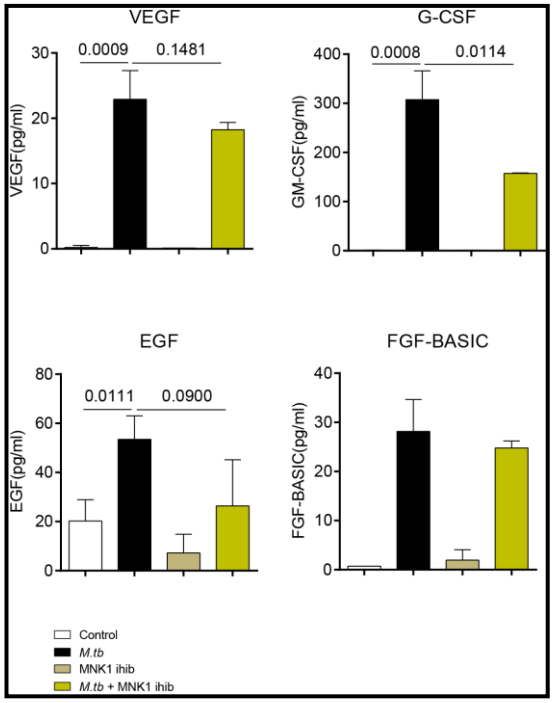


**Figure 57: Mnk1 inhibition suppressed growth factor secretion by *M.tb* -infected macrophages.** MDMs were pre-treated with Mnk1 inhibitor for two hours prior to *M.tb* infection. Supernatant samples were harvested after 72 hours post infection for cytokine multiplex analysis. Luminex profiling of macrophages demonstrate that *M.tb* infection upregulates a wide range of growth factors. These were either slightly suppressed upon Mnk1 blockade. Luminex experiments were performed on two different occasions in two donors each time. Data show mean and standard deviation of experiments performed in triplicates and is representative of experiments performed on two donors at separate occasions. P values are Student's t-test, with $P < 0.05$ considered significantly different.

## 4.14 Mnk1 inhibition exerted no significant change in a wide range of cytokines in *M.tb* -infected macrophages.

*M.tb* drove the production of a variety of a number of cytokines in macrophages (Figure 59).

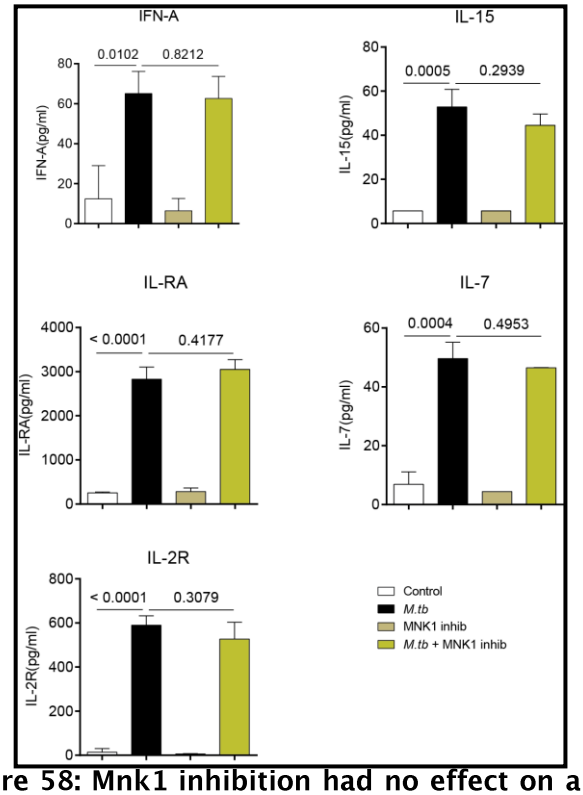


**Figure 58: Mnk1 inhibition had no effect on a wide range of cytokines in *M.tb* -infected macrophages.** MDMs were pre-treated with Mnk1 inhibitor for two hours prior to *M.tb* infection. Supernatant samples were harvested after 72 hours post infection for cytokine multiplex analysis. Luminex profiling of macrophages demonstrate that *M.tb* infection upregulates a wide range of cytokines. There was no significant difference in levels of cytokines produced when Mnk1 was chemically blocked. Luminex experiments were performed on two different occasions in two donors each time. Data show mean and standard deviation of experiments performed in triplicates and is representative of experiments performed on two donors at separate occasions. P values are Student's t-test, with $P < 0.05$ considered significantly different.

## 4.15 Summary of the effect of Mnk1 inhibition on multiple MMPs, cytokines and chemokines.

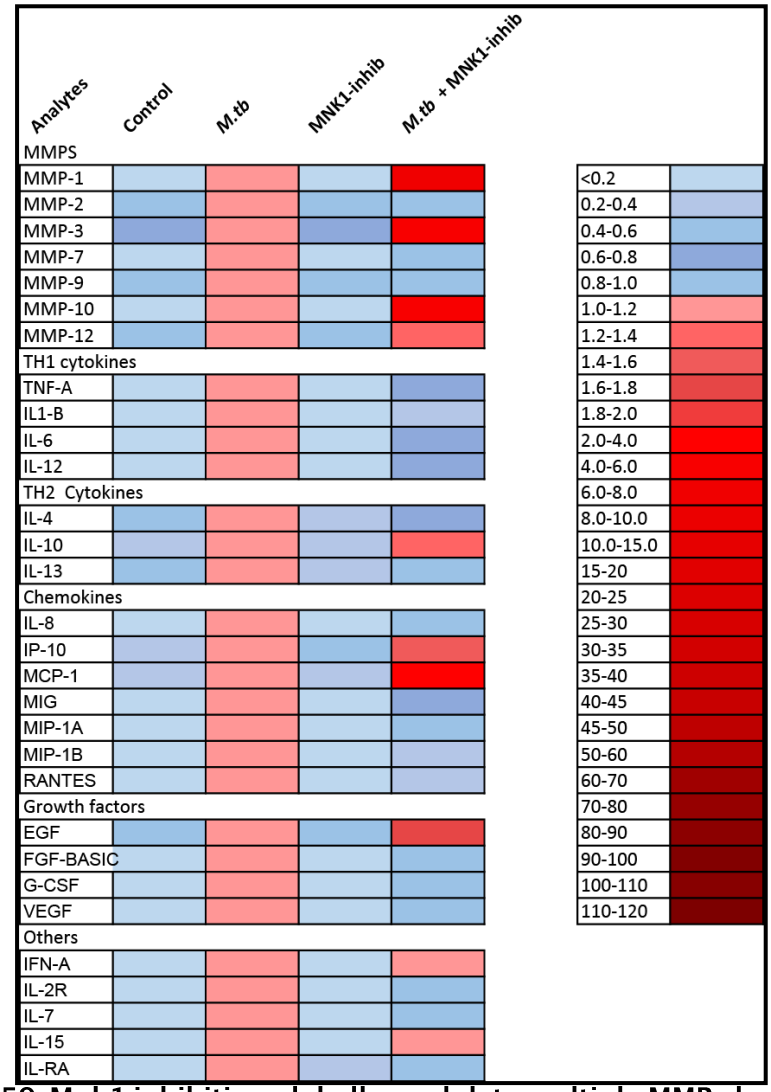


**Figure 59: Mnk1 inhibition globally modulate multiple MMPs but suppresses a wide range of pro-inflammatory signalling molecule secretion.** MDMs were pre-treated with Mnk1 inhibitor for two hours prior to *M.tb* infection. Supernatant samples were harvested after 72 hours post infection for cytokine multiplex analysis. Luminex profiling of macrophages demonstrate that *M.tb* infection upregulates a wide range of MMPs, cytokines, chemokines and growth factors. These were either suppressed or unchanged when Mnk1 was blocked chemically. Luminex experiments were performed on two different occasions in two donors each time.

## 4.16 Discussion of results chapter II

Activation of intracellular signalling such as the MAPK pathway culminate in the activation of Mnk1 (Waskiewicz et al., 1997, Wang et al., 1998, Joshi et al., 2011, Joshi et al., 2009). Activation of Mnk2 on the other hand is independent of phosphorylation input from up-stream kinases (Waskiewicz et al., 1997, Parra et al., 2005). The 5'-cap-binding protein, eIF4E, is the most well studied and main substrate of the Mnk family of protein kinases. Active Mnk1 phosphorylate to activate eIF4E on Ser 209 (Waskiewicz et al., 1997, Flynn and Proud, 1995) and active eIF4E in turn promotes cap-dependent translation. For this reason, this study predicted that specific inhibition of Mnk1 would limit translation of mRNA into protein. The data from this study surprisingly contradicted this proposal, and I found that Mnk1 inhibition resulted in enhanced *M.tb* -driven MMP-1 secretion by macrophages.

The biological functions of phosphorylated-eIF4E in protein translation remain controversial. Previous reports demonstrated that translation initiation complex, eIF4F, is better stabilised upon the binding of phosphorylated eIF4E (Bu et al., 1993), and that the binding affinity of eIF4E to the 5' cap of mRNA is strengthened following eIF4E phosphorylation (Minich et al., 1994). Several lines of evidence have since supported the notion that active eIF4E is important for the initiation of mRNA 5' cap-binding protein synthesis (Furic et al., 2010, Pyronnet et al., 1999).

Contrary to these reports, recent emerging biochemical research have also revealed that Mnk1 also regulates cap-independent translation in an eIF4E-independent manner (Knauf et al., 2001). These studies have revealed that eIF4E phosphorylation on Ser 209 is not a necessity for cap-dependent translation per se, but rather this phosphorylation weakens the binding affinity of eIF4E for the 5'-cap structure of mRNA (Knauf et al., 2001, Scheper and Proud, 2002a, Scheper et al., 2002). In fact

phosphorylation of eIF4E was shown to be essential for cell proliferation in cancer but not in normal cells (Hay, 2010, Ueda et al., 2004), neither was it indispensable for normal cell growth (Ueda et al., 2004). Mnk 1/2 knock-out mice did not exhibit developmental or physiological impairments (Ueda et al., 2004). It is therefore likely that in the case of translational modulation of MMP-1 mRNA, Mnk1 functions to limit uncontrolled protein synthesis in a cap-independent translation mechanism that is independent of eIF4E activity.

Although eIF4E is the most characterised Mnk substrate (Waskiewicz et al., 1997), various other Mnk1/2 targets are known, including ones that are specific for particular members of the Mnk group of kinases (Buxade et al., 2008). Heterogeneous nuclear ribonucleoprotein A1 (hnRNPA1), binds to AU-rich elements (ARE) on the 3'-UTR of various cytokine transcripts including TNF-α mRNA to regulate their translation. Mnks phosphorylate hnRNPA1 on Ser 192, 310, 311 and Ser 312 to release it from binding to the TNF- α message, thereby enabling translation of TNF-α mRNA (Buxade et al., 2008). To propose that Mnk1 regulate MMP-1 secretion via hnRNPA1 activation, it must first be determined that MMP-1 mRNA contain ARE sequence at the 3'-UTR, and that hnRNPA1 stably bind to this sequence in resting cells. Furthermore, to attribute these findings to Mnk1 mediated phosphorylation of hnRNPA1, active hnRNPA1 must bind to MMP-1 'ARE' to suppress its mRNA translation in un-stimulated cell.

It is possible that different downstream Mnk substrate molecule(s) mediate the surprisingly high MMP-1 secretion effect of Mnk inhibition. It is however difficult to reconcile Mnk1 phosphorylated hnRNPA1 activity with the findings of this study. This is because this study has also demonstrated that chemical inhibition of the PI3K/AKT/mTORC-1 pathway augments MMP-1 in *M.tb* infected macrophages. Mnk-phosphorylated-hnRNPA1 mediated repression of RTKs signalling pathway, and this would consequently inhibit the PI3K/AKT/mTORC-1

signalling. Mnk1 inhibition should therefore block the hnRNPA1 suppressive effect on RTK, to drive activation of PI3K pathway, which should negatively regulate MMP-1. Instead, MMP-1 was elevated in the context of Mnk1 inhibition.

Mnks phosphorylates PSF (polypyrimidine tract-binding (PTB) protein associated splicing factor) on Ser 8 and Ser 283 (Buxade et al., 2008). Similar to hnRNPA1, PSF and its binding partner p54 (nrb) interact with 'ARE' sequences on 3'-UTR of mRNAs. However, whereas Mnk phosphorylation of hnRNPA1 causes its dissociation from the TNF-α mRNA, phosphorylation of PSF.p54 (nrb) enhances its interaction with the mRNA transcript. The functional consequences of SPF.p54 (nrb) binding on mRNA translation is unclear. Based on the findings from this study, it can be proposed that during *M.tb* infection, Mnk proteins phosphorylate to activate and enhance the binding of SPF.p54nrb to 3'-UTR portion of MMP-1 mRNA in order to repress its translation. It is likely that inhibition of Mnk1 in *M.tb* infection result in dissociation of SPF.p54nrb from the MMP-1 mRNA, liberating it to be available for translation.

Another downstream effector of the Mnks is Sprouty2 (Spry2). Once phosphorylated, Spry2 exerts an inhibitory feedback on the Ras/Erk/MAPK signalling to negatively regulate RTK signalling (Cabrita and Christofori, 2008). Although they may not be functionally important in this system, various other Mnk targets exist and ongoing biochemical research continues to discover more. Cytosolic phospholipase A2 (cPLA2) becomes activated in response to elevated calcium levels in the cytoplasm, to mediate the production of arachidonic acids which play important regulatory role in inflammation. Mnk1 phosphorylates cPLA2 on Ser 727 to reinforce its activation and function, thereby modulating eicosanoid signalling. Mnk2b (described below) has been reported to bind the oestrogen receptor β (ERβ), but the functional implications of the interaction between Mnk2b and ERβ is still unresolved (Slentz-Kesler et al., 2000).

Plectin is a universally expressed protein that modulates cytoskeletal integrity. Mnk2 phosphorylation of plectin on Ser 4642 has been shown to abrogate the interactions between plectin and intermediate filament. More relevant to our work, Mnk2 was shown to directly interact with mTORC-1 resulting in inactivation of phospho-p70S6K in muscle atrophy (Hu et al., 2012). This does not involve phosphorylation, which is indicative of the ability of Mnks to negatively regulate pathways that lead to ribosomal biogenesis and translation in specific cellular context.

To determine the interpretation of the data, the effect of Mnk1 inhibition on MMP-1 message accumulation was investigated. It was expected that Mnk1 inhibition must drive MMP-1 mRNA accumulation within the first 24 hours post *M.tb* infection to have caused such high levels of secreted (translated mRNA) MMP-1. In fact Mnk inhibition consistently drove significant MMP-1 cellular message accumulation after 72 hours (Figure 48B), but not within the first 24 hours of *M.tb* infection (Figures not shown).

Both Mnk1/2 and eIF4E are present in the nucleus. At their transcriptional level, Mnk1 and Mnk2 undergo alternative splicing to generate different isoform variants (Mnk1a, Mnk1b, Mnk2a and Mnk2b) (O'Loghlen et al., 2004, Slentz-Kesler et al., 2000). Nuclear export sequences on the 'a' isoforms allow the nuclear transport and cytoplasmic localisation of Mnk1a and Mnk2a. On the other hand, the 'b' isoforms possess nuclear localisation but not export sequence, and are therefore retained in the nucleus. A fraction of cytoplasmic eIF4E is transported to the nucleus by the aid of the shuttling protein, 4E-T that binds eIF4E (Dostie et al., 2000). Nuclear Mnks phosphorylate to activate nuclear eIF4E to engage in cellular functionalities that are completely different from active cytoplasmic eIF4E. Active nuclear eIF4E is thought to mediate export of mRNA into the cytoplasm in specific cellular states. For example, nuclear eIF4E is believed to mediate the transport of cyclin D1 message to the cytoplasm, where it promotes cell cycle entry (Rousseau et al., 1996).

In tumour cells, active nuclear eIF4E has been reported to affect particular mRNAs. These include matrix metalloproteinases MMP-1 and MMP-9 mRNAs, which are known to promote tumour invasiveness (Hay, 2010, Furic et al., 2010) (other roles of nuclear eIF4E have not been discussed in this study). The effect of the Mnk1 inhibitor on inhibition of nuclear Mnk1/2 activity and nuclear eIF4E phosphorylation has not been examined in this study. However, the possibility that the activity of nuclear phosphorylated eIF4E may play a role in the discrepancies observed at the message level within the first 24 hours of *M.tb* infection have not been ruled out. Future research would examine whether the observed effect of Mnk1 inhibition on MMP-1 is transcriptional, post-transcriptional or post-translational. This can throw more light on understanding the importance of Mnk and eIF4E activity in MMP-1 mRNA and protein synthesis.

The implication of our data that eukaryotic initiation complex, eIF4F, is not important for MMP-1 translation was however puzzling. Compared to all the other components of eIF4F, it is believed that eIF4E is the least abundant initiation factor (Hiremath et al., 1985). On the other hand, the scaffolding protein eIF4G, is abundant in the cell, and in association with eIF4E, play a critical role in the formation and stability of eIF4F (Pyronnet et al., 1999). 4EGI-1 potently disrupts the eIF4E-eIF4G complex, which is essential for initiation, progression and stability of eIF4F complex (Pyronnet et al., 1999). Interestingly, disrupting the interaction between eIF4E and eIF4G using 4EGI-1 resulted in abrogation of *M.tb* -driven MMP-1 both at the secretion and gene expression levels (Figure 49). This implies that indeed eIF4F plays a key role in MMP-1 protein translation. Whereas this data confirmed that eIF4F formation and stability was necessary for MMP-1 synthesis, I could not explain the suppression of MMP-1 gene expression by 4EGI-1 because I did not expect 4EGI-1 to exert an effect at the transcriptional level.

Apart from the Mnk1-specific inhibitor of choice, which augmented *M.tb* -driven MMP-1, different Mnk inhibitors exerted a general suppression effect on MMP-1 secretion, and this was not expected (Figure 50). I have not investigated the reason behind the differential modulation of MMP-1 by the different Mnk inhibitors. The specificity of MNKi-80 and Compound E on Mnk1 blockade is not fully characterised. However, CGP57380 is a known Mnk1/Mnk2 inhibitor, and has been extensively used in the study of Mnk signalling for many years (Hou et al., 2012, Knauf et al., 2001). Although CGP57380 blocks eIF4E phosphorylation (Buxade et al., 2005), it is also known to exert by-stander effect on a range of other proteins kinases including MKK1, Aurora B, CK1, DYRK, Lck and SGK (Hou et al., 2012) (Bain et al., 2007). The off-target effect of CGP57380 was evident in other studies where the compound repressed the anti-apoptotic protein Mcl-1 and blocked the upregulation of the oncoprotein c-Myc (Hou et al., 2012). Since CGP57380 has the potential to target a number of proteins non-specifically, it is therefore possible that this effect may contribute to the MMP-1 suppression effect of CGP57380. Experiments performed in the laboratory after the completion of my thesis using MNK-knock-out cells confirmed that the up-regulation of pro-inflammatory mediators following disruption of the MNK pathway was specific to MMPs.

In fact, CGP57380 was reported to reduce eIF4G in initiation complex, eIF4F (Chrestensen et al., 2007, Hou et al., 2012). This finding is important to us because as discussed above, eIF4G activity is essential for eIF4F formation and stability. Apart from its interaction with eIF4E, eIF4G provides a docking site for Mnk1 binding which allows Mnk1 to be in close proximity with eIF4E, allowing its phosphorylation by Mnk1 (Pyronnet et al., 1999). eIF4G also serves as a scaffolding protein for the assembly of other initiation factors including the mRNA helicase, eIF4A (Pyronnet et al., 1999). As discussed above, disruption of eIF4G activity destabilises eIF4F complex and blocks MMP-1 translation. Given that CGP57380

reduces eIF4G within the eIF4F complex, it is likely that CGP57380 is exerting MMP-1 suppression effect that is similar to that exerted by the eIF4E/eIF4F inhibitor, 4EGI-1.

Both Mnk1 specific inhibitor and CGP57380 greatly suppressed phosphorylation of eIF4E in *M.tb* infected macrophages (Figure 51). This I expected because it confirms the specificity of the compounds used in this study. The inability of the p90RSK inhibitor BI-D18070, to modulate *M.tb*-driven MMP-1 (Figure 52) suggests that the effect of Mnk inhibition observed is not via this pathway. With insulin driving eIF4E phosphorylation and LY294002 suppressing this, I were able to show evidence of crosstalk between the PI3K and Mnk pathways (Figure 53). In order to determine whether the effect on of Mnk inhibition on MMP-1 is specific or widespread, Luminex array profiling was performed for multiple MMPs, cytokines, chemokines and growth factors (Figures 54-59). The MMPs upregulated including MMP-1, MMP-3 and MMP-10 are frequently synergistically regulated, however the very widespread suppression of cytokines and chemokines was unexpected. This suggests that the effect of Mnk1 inhibition observed was specific to pathogenic MMPs. This also implies a specific negative regulatory role of the Mnk pathway in dampening down tissue destructive TB immunopathology.

# 5. CHAPTER 5: RESULTS PART III

## *M.tb* subverts intracellular signalling pathways that negatively regulate MMP-1

### 5.1 Overview

*M.tb* drives secretion of MMPs in MDMs, and recent developments have indicated key roles played by MMPs in lung tissue destruction, which is critical for TB transmission (Elkington et al., 2011c). I have so far demonstrated that pharmacological blockade of the PI3K/AKT/mTORC-1 pathway and Mnk signalling augments MMP-1 secretion in *M.tb* infected macrophages. This suggests that these signalling pathways negatively regulate lung tissue destruction in TB by limiting MMP-1. A number of research groups have dissected and reported mechanisms by which *M.tb* successfully overcomes host immunity to survive in macrophages. *M.tb* has evolved to evade host immunity by modulating several cellular events in host macrophages (Poirier and Av-Gay, 2012). However, data on how the pathogen evades critical host immune responses to successfully mediate lung tissue destruction and subsequent cavitation is limited.

### 5.2 Methods

Primary human macrophages were cultured and infected with *M.tb* as previously described. Modulation of MMP-1 and PI3Kδ mRNA and protein levels by *M.tb* was studied using RT-qPCR and Western blotting analysis respectively. 4-Thio Uridine (4-TU) incorporation into RNA and subsequent pull down analyses was performed by firstly stimulating *M.tb* infected macrophages with 100μM of 4-TU for between 24 hours and 72 hours. Following extraction of total cellular RNA by TRI-Reagent® Solution (Sigma-Aldrich), a second step of RNA purification by Magnetic Porous Glass (MPG) streptavidin beads (Pure Biotech LLC) to isolate and purify the

newly transcribed RNA that has 4-TU incorporated within the transcript. This RNA was then purified and used for RT-qPCR analysis of the gene of interest. Immunohistochemistry was performed to investigate PI3K expression *in vivo* using paraffin-embedded human lung lesions from patients confirmed to have pulmonary TB.

## 5.3 Chapter hypothesis

*M.tb* secretes Protein-tyrosine phosphatase A (PtpA) into culture media, and this interferes with host signalling pathways in order to establish successful survival and disease progression (Yoder, 2004). *M.tb* is able to completely evade host phagolysosome killing by removing all PI3P protein from the phagolysosome membrane (Malik et al). It is therefore likely that *M.tb* may have evolved ways of subverting important host signalling pathways that may otherwise play regulatory roles to limit the production of tissue-destructive MMPs. Despite the activity of the signalling pathways under study, TB is currently the most lethal infectious disease, having recently been surpassed HIV-AIDs.

To further dissect how *M.tb* is able to successfully drive disease progression amidst the complex regulatory signalling pathways, I investigated how *M.tb* subverts the PI3K pathway in MDMs to promote disease pathogenesis. Given the tissue destructive role of MMPs in TB, I hypothesised that *M.tb* must target important components of the PI3K/AKT/mTORC-1 (and Mnk1 signalling) axis of intracellular signalling pathways in order to successfully drive MMP-mediated tissue destruction.

## 5.4 Aim

In order to investigate pathway targeting, this chapter sought to investigate how *M.tb* modulates the gene and protein expression of important mediators

of the pathway under study. This chapter would seek to investigate the following:

- The effect of *M.tb* on the expression of PIK3CD, MKNK1, and MLST8 genes.
- In vivo studies to investigate PI3Kδ expression in caseating granulomas
- Dissection of the role of *M.tb* in subverting regulatory intracellular pathways that limit protease secretion in TB.

## 5.5 *M.tb* suppresses PI3Kδ mRNA in infected macrophages

In order to investigate how *M.tb* modulates the regulatory pathways under study, I initially examined the effect of *M.tb* infection on PI3Kδ gene expression. Whereas MMP-1 mRNA was highly up-regulated by *M.tb* (Figure 61, A), *M.tb* repressed PI3Kδ mRNA in the same cells (Figure 61, B). In the presence of *M.tb* , suppression of PI3Kδ gene occurred when cells were also treated with the PI3K inhibitors LY294002 and IC87114. (Figure 61, C). This indicates that the *M.tb* -driven increase in MMP-1 is accompanied by *M.tb* -induced suppression of PI3Kδ in infected macrophages.

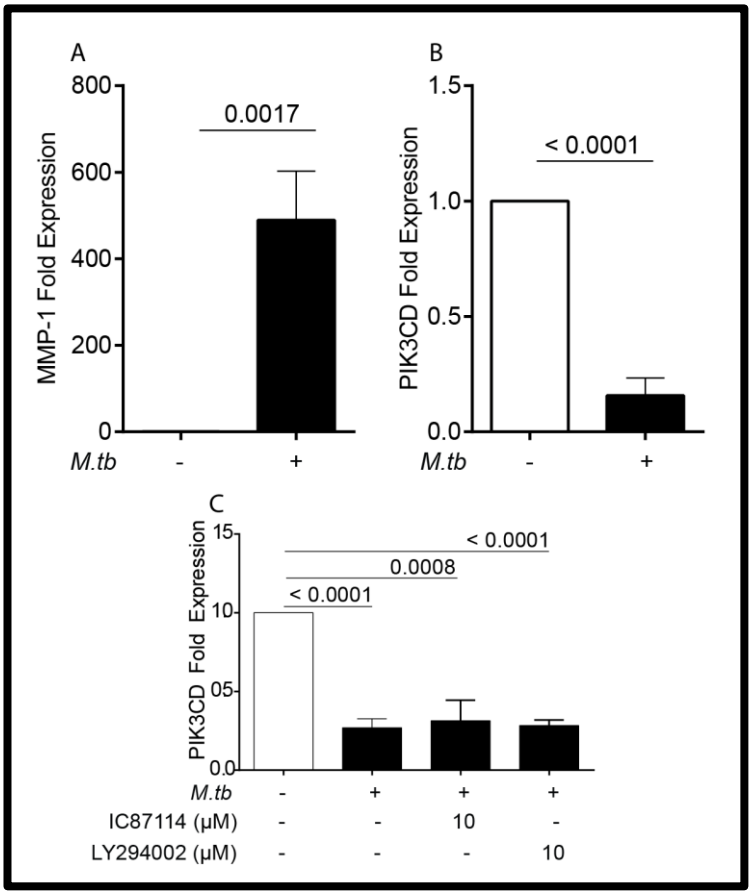


**Figure 60: *M.tb* suppresses PI3Kδ mRNA.** RT-qPCR was performed to ascertain the degree of PI3Kδ gene expression following *M.tb* infection for 24 hours. *M.tb* significantly drove MMP-1 gene expression **(A)** but reduced PI3Kδ message accumulation **(B)** in the same macrophages. **C:** There was no change between the degree at which PI3K inhibitors and *M.tb* suppressed PI3Kδ mRNA accumulation. Experiments were performed in triplicate and are representative of at least three donors. P values are t-test comparisons between groups.

## 5.6 *M.tb* represses PI3Kδ protein in infected macrophages

In order to determine the effect of *M.tb* modulation of PI3Kδ protein expression, I performed Western blot analysis on total protein isolated from *M.tb* infected and un-infected macrophages over a period of 30mins to 72hours post *M.tb* infection. PI3Kδ protein was slightly up-regulated in *M.tb* infected MDMs at 30mins, 60mins and 6hours (Figure 62, lanes 1-2, 3-4 and 5-6)., but no obvious change at 48 hours post-infection compared to control cells (Figure 62, lanes 7-8). After 72 hours post infection however, there was a reduction in the amount of PI3Kδ protein in infected cells compared to control samples (Figure 62, lanes 9-10). This suggests that *M.tb* induces downregulation of PI3Kδ protein in MDMs at later time points.

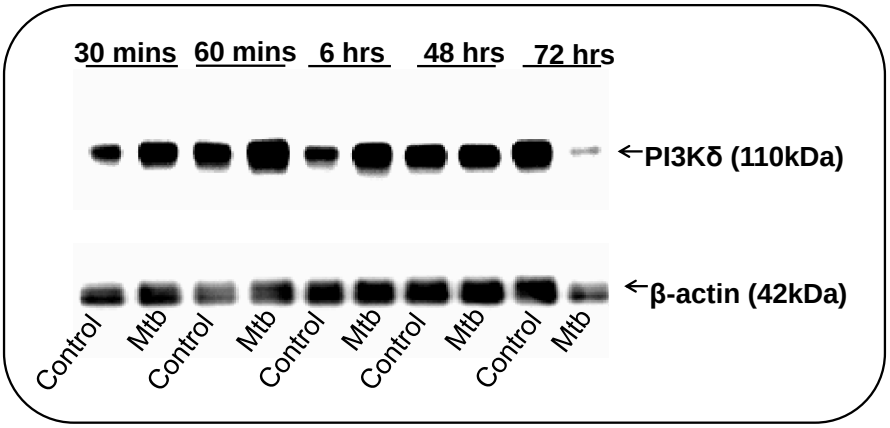


**Figure 61: *M.tb* -induced suppression of PI3Kδ protein.** *M.tb* drives a slight increase in total PI3Kδ protein level in macrophages within the first 6 hours of infection. This increasing trend in PI3Kδ protein production appears to halt by 48 hours post infection, with contrasting suppression of PI3Kδ protein by 72 hours post *M.tb* infection. PI3Kδ protein levels were determined by Western blotting at different time points post *M.tb* infection. Data show experiment performed in one donor. The M.tb -induced suppression of PI3Kδ protein at 72 hours post infection was not consistently reproducible in subsequent experiments.

## 5.7 *M.tb* represses PI3Kδ expression in TB lung tissues

Next I sought to investigate PI3Kδ expression profile in lung granulomas of patients with TB. I analysed PI3Kδ expression in human lung tissues recovered from patients confirmed to have pulmonary TB, using normal lung tissues from healthy individuals as control sections. Initially, I determined the specificity of the antibodies employed in this study. Following the recommendations of the suppliers of PI3Kδ antibody (LifeSpan BioScience,Inc), I used human kidney tissue to test for positive PI3Kδ immune reactivity (Figure 63). Capturing images at low power objective lens set of x4 (Figure 63A), medium objective lens set of x10 (Figure 63B) and high power objective lens set of x20 (Figure 63C), I demonstrated that this anti-PI3Kδ antibody strongly reacts with PI3Kδ epitopes in kidney tissue. Figure 63D shows a negative control images with no PI3Kδ immune reactivity, suggesting specificity of antibody binding. Here the kidney tissue was incubated with secondary but not primary anti- PI3Kδ antibody.

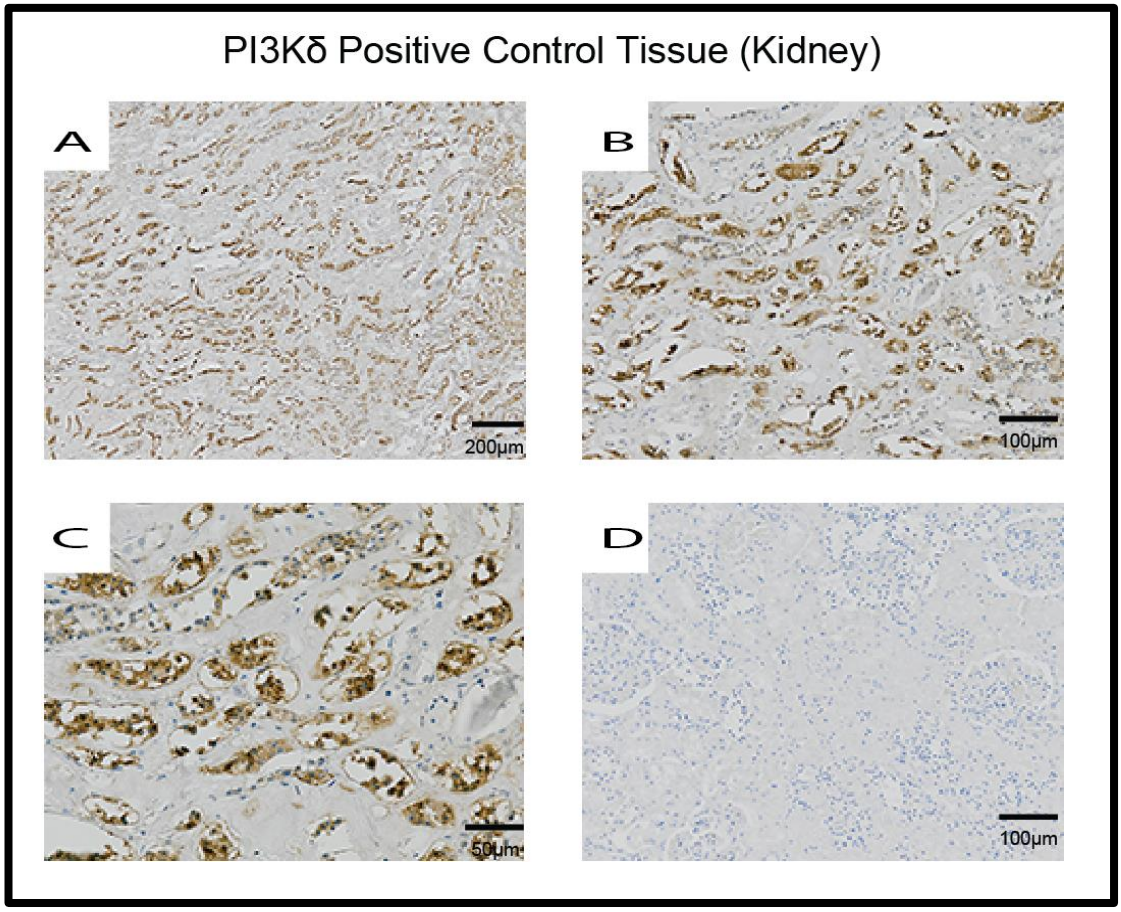


**Figure 62: Anti-PI3Kδ antibodies show immune reactivity on positive control tissue.** Using immunohistochemistry, kidney tissue was used to ascertain the specificity of binding of the anti-PI3Kδ antibody employed for this study. D: Negative control where the tissue was incubated with secondary but not primary antibodies shows no immune reactivity. This confirms that besides its target PI3Kδ antigens, the antibody does not react non-specifically with any other epitopes on the tissue. Experiment was performed in tissues from three different donors (data not shown). Images were captured using different objective lenses at x4 (low)-A, x10(Medium)-B and x20(high) using Nikon Elipse 80i.

I utilised anti-CD68 antibodies to confirm the presence of alveolar macrophages in the lung tissues that were used for this study. Similar to using kidney as PI3Kδ positive control tissue, tonsil tissue was employed as a positive control tissue for CD68 immunoreactivity. Figure 64 shows that the antibody reacts specifically with CD68 antigens (expressed on macrophages) in tonsils.

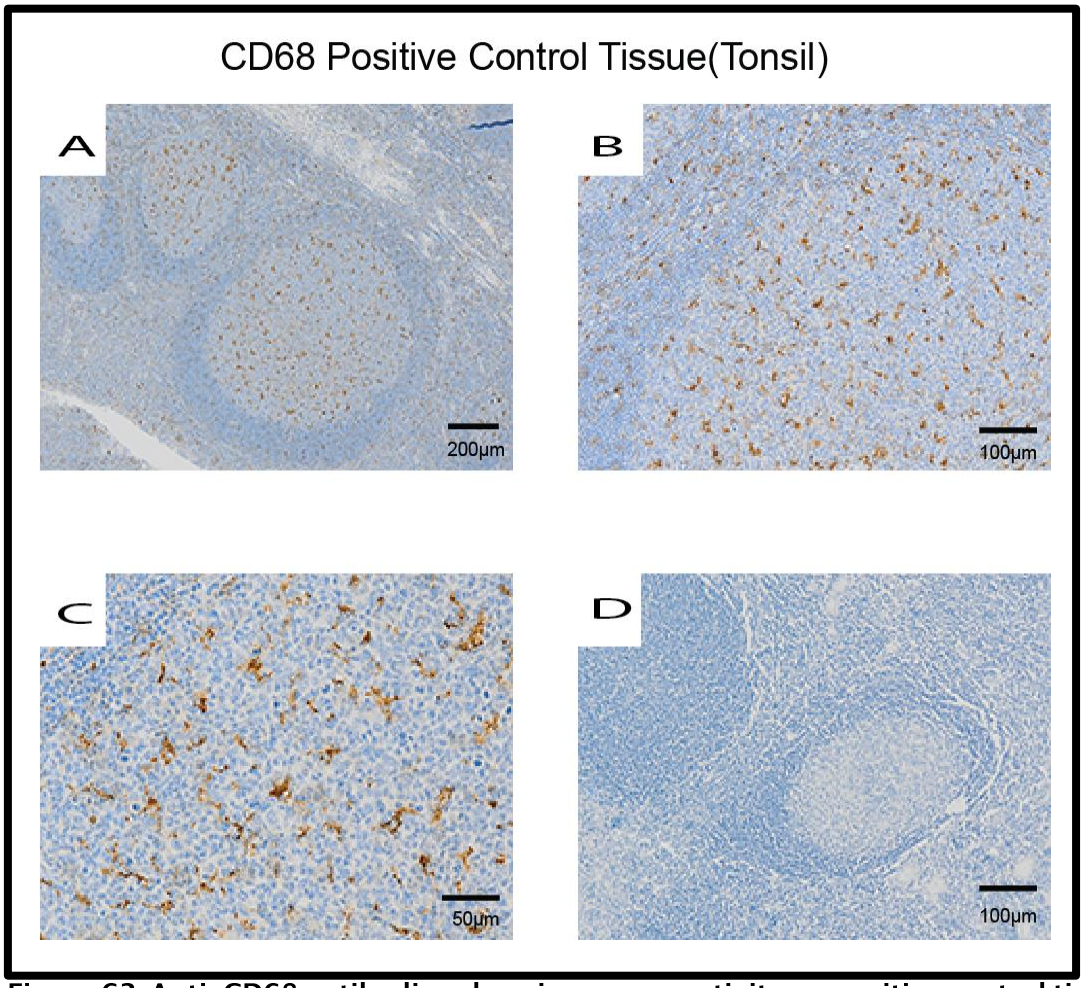


**Figure 63: Anti-CD68 antibodies show immune reactivity on positive control tissue.** Paraffin-embedded tonsil tissue was used to ascertain the specificity of binding of the anti-CD68 antibody employed for this study, using Immunohistochemistry. D: Negative control where the tissue was incubated with secondary but not primary antibodies shows no immune reactivity. This confirms that but for CD68 antigens, the antibody does not react non-specifically with any other epitopes on the tissue. Experiment was performed in tissues from three different donors (data not shown). Images were captured using different objective lenses set at x4 (low power)-A, x10(medium power)-B and D and x20(high power) using Nikon Elipse 80i.

Given the high specificity of binding between the antibodies of study and the epitopes of interest, I next performed immunohistochemistry for anti-CD68 and anti- PI3Kδ (both of which are expressed in alveolar macrophages) using normal, non-TB infected lung tissue. I demonstrate a wide spread expression of alveolar macrophages in normal lung tissue

(Figure 65). PI3Kδ was expressed in macrophages at levels comparable to CD68 (Figure 65, comparing A, C and E to B, D and F). This confirms that alveolar macrophages are indeed present within the normal lung tissues used in this study, and that these cells also expressed PI3Kδ.

Next I investigated PI3Kδ expression profile in *M.tb*-infected lung tissues. The initial formation of granulomas comprise of very high population of macrophages (Lugo-Villarino et al., 2012). For this reason, I predicted that although PI3Kδ may continue to be present within the core of granulomas, *M.tb* may supress PI3Kδ expression within infected cells surrounding the granulomas including the monocyte-derived macrophages which are recruited during the progression of granulomas formation, and multinucleated giant cells as well as foamy macrophages that develop at the site of infection.

Whereas alveolar macrophages globally expressed CD68 in TB lungs (Figure 66 A, C and E), PI3Kδ was completely absent, with no PI3Kδ immune reactivity even within caseating granulomas (Figure 66 B, D and F). The global absence of PI3Kδ in TB lungs was consistent across different granuloma lesions (Figures 67-68), with PI3Kδ expression also completely absent within giant cells and foamy macrophages (Figure 67B and 67D). This was not expected as I predicted moderate PI3Kδ expression within the central part of granulomas, with very little or no PI3Kδ expressed at the periphery of the granulomas. However, this observation strongly supports our hypothesis that *M.tb* does repress PI3Kδ expression within the lungs in order to drive tissue destructive disease progression, and that it is likely that this repression of PI3Kδ expression begins at the earlier stages and continues throughout the process of granuloma formation.

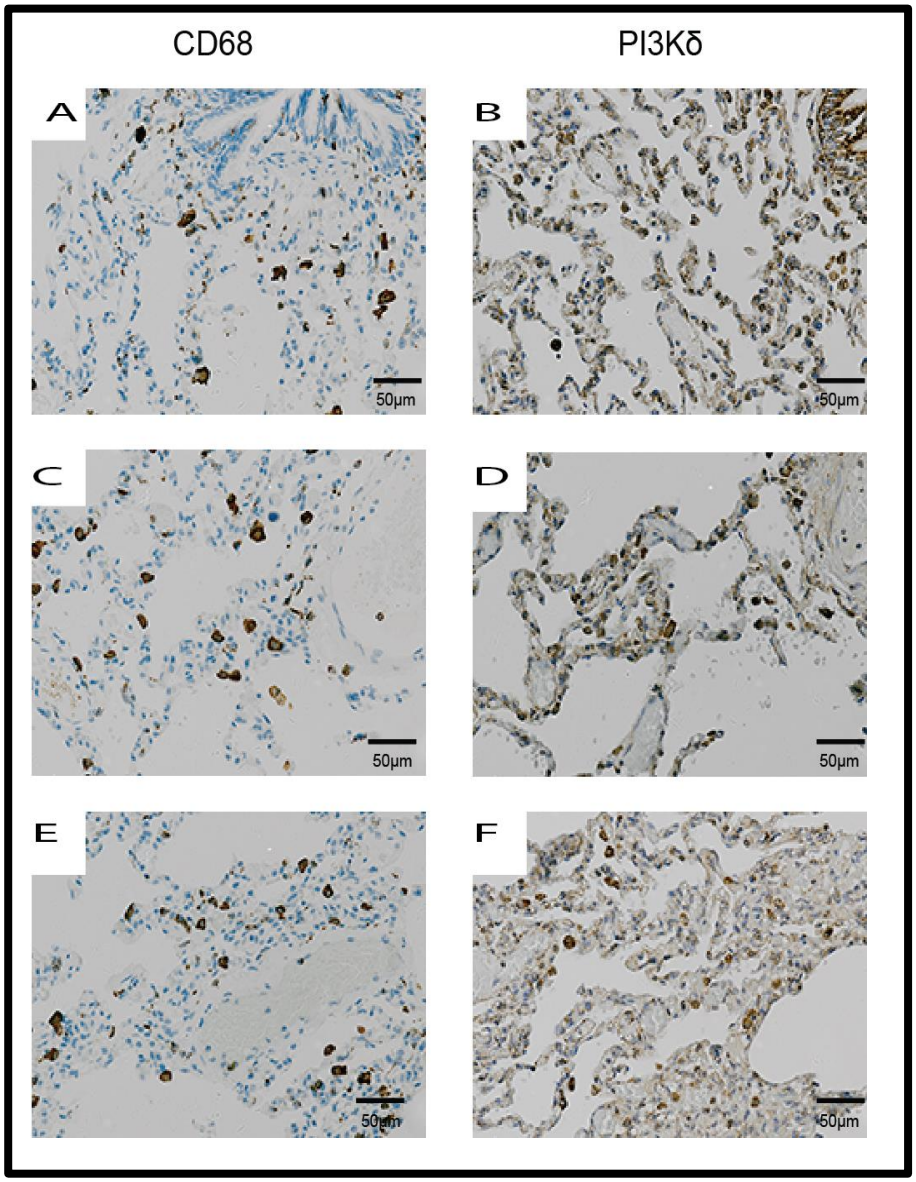


**Figure 64: Alveolar macrophages express both CD68 and PI3Kδ in normal lungs.** CD68 immune reactivity (A, C and E) suggests the presence of alveolar macrophages in the tissue. PI3Kδ was also expressed within the same region of lung tissue where alveolar macrophages were present (B, D and F). Data show images of stained tissues from 3 different donors. Immunohistochemistry was performed on paraffin-embedded normal lung tissues from total of 6 donors, and images of the same region of normal lung were captured using Nikon Elipse 80i.

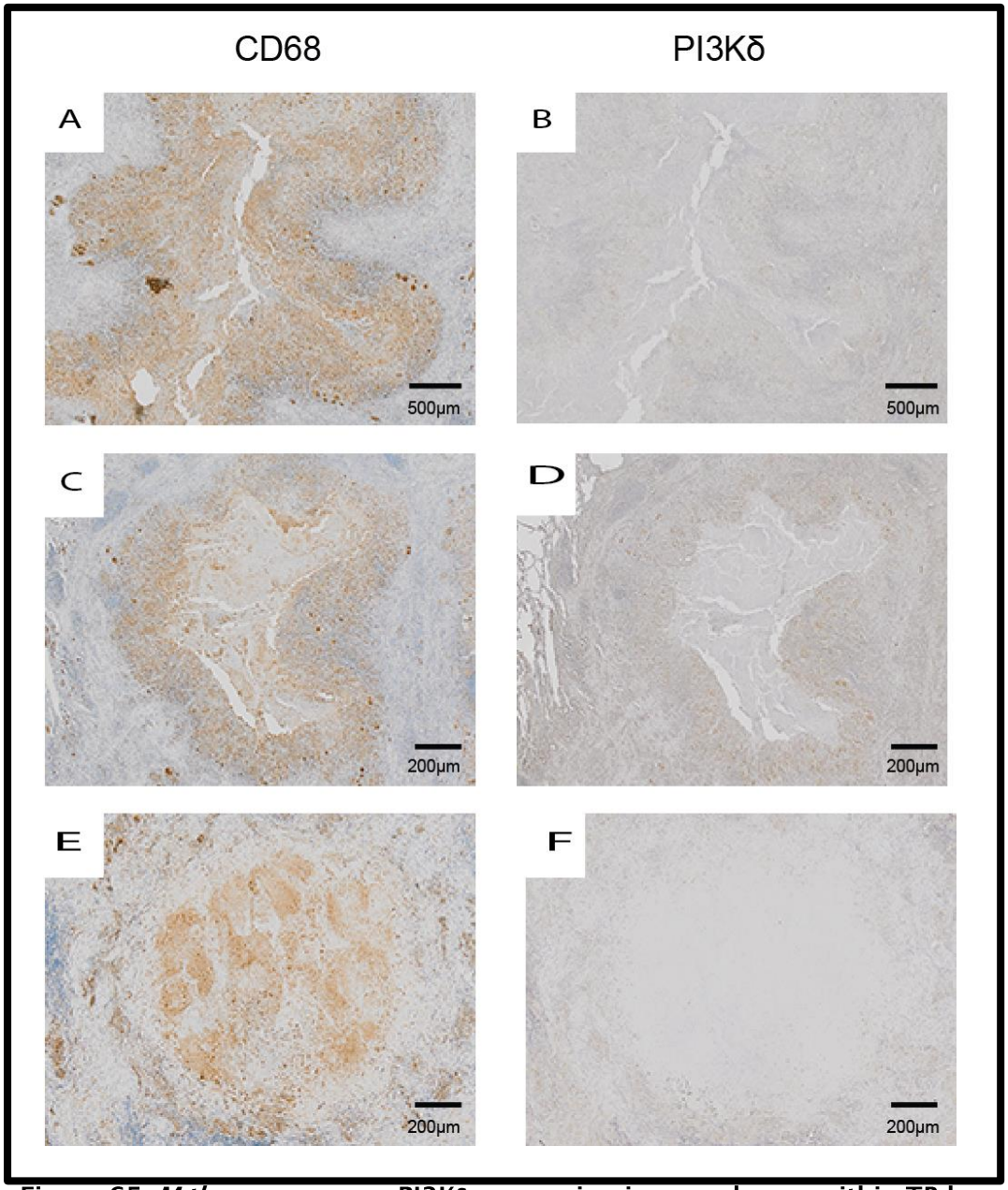


**Figure 65: *M.tb* suppresses PI3Kδ expression in granulomas within TB lungs. A, C** and **E**: CD68 is globally expressed in TB lungs and within caseating granulomas, demonstrating the presence of macrophages. B, D and F: PI3Kδ expression is however completely absent within the same TB granulomas. Data show images of stained tissues from 3 different donors. Immunohistochemistry was performed on paraffin-embedded normal lung tissues from total of 6 donors. Images of the same region of TB lung were captured using Olympus BX51-CC12 (DotSlide).

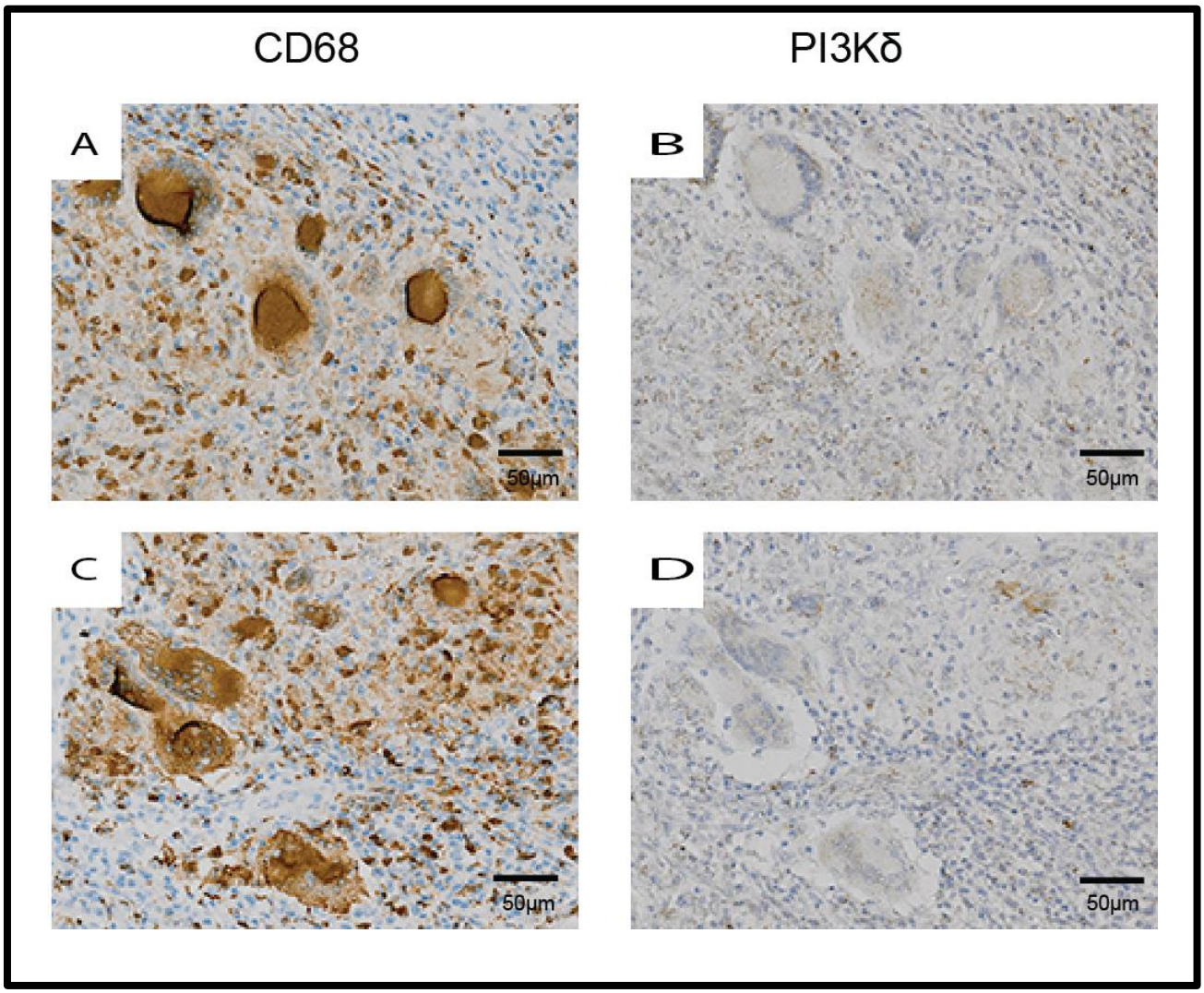


**Figure 66: *M.tb* suppresses PI3Kδ expression in giant cells.** A and C: CD68 is highly expressed within multinucleate giant cells. B and D: PI3Kδ expression is however completely absent within the same giant cells. Data show images of stained tissues from two different donors. Immunohistochemistry was performed on paraffin-embedded normal lung tissues from total of 6 donors, and images of the same region of TB lungs were captured using Olympus BX51-CC12 (DotSlide).

In all the TB lung tissues used for this study, PI3Kδ was significantly reduced or completely absent within CD68-expressing macrophages. In fact, this observation was marked enough to be captured by a dot slide showing the whole tissue sections. Figure 68 presents a dotslide plot

images showing CD68 (A, C, E, G, and I) and PI3Kδ (B, D, F, H, and J) expression profiles in different TB lung tissues that were used for this investigation. Figure 69 shows negative control images of A: Normal lung, B:Dotslide plot of a large caseating granuloma in TB lung (B= same TB lung as shown in Figure 68D), C: Caseating granuloma from a different donor (C= same TB lung as figures 66E and 66F), D:High objective power image of C. Whereas CD68 expression was consistently highly expressed across all lung tissues, PI3Kδ expression was comparable to that of our negative control data (figure 63D), where sections were incubated with secondary but not primary antibodies. This confirms that indeed *M.tb* suppresses PI3Kδ expression in TB, indicating that in order to drive tissue destruction, *M.tb* has evolved to target important components of regulatory signalling such as the PI3K/AKT/mTORC-1 pathway that function to limit MMPs.

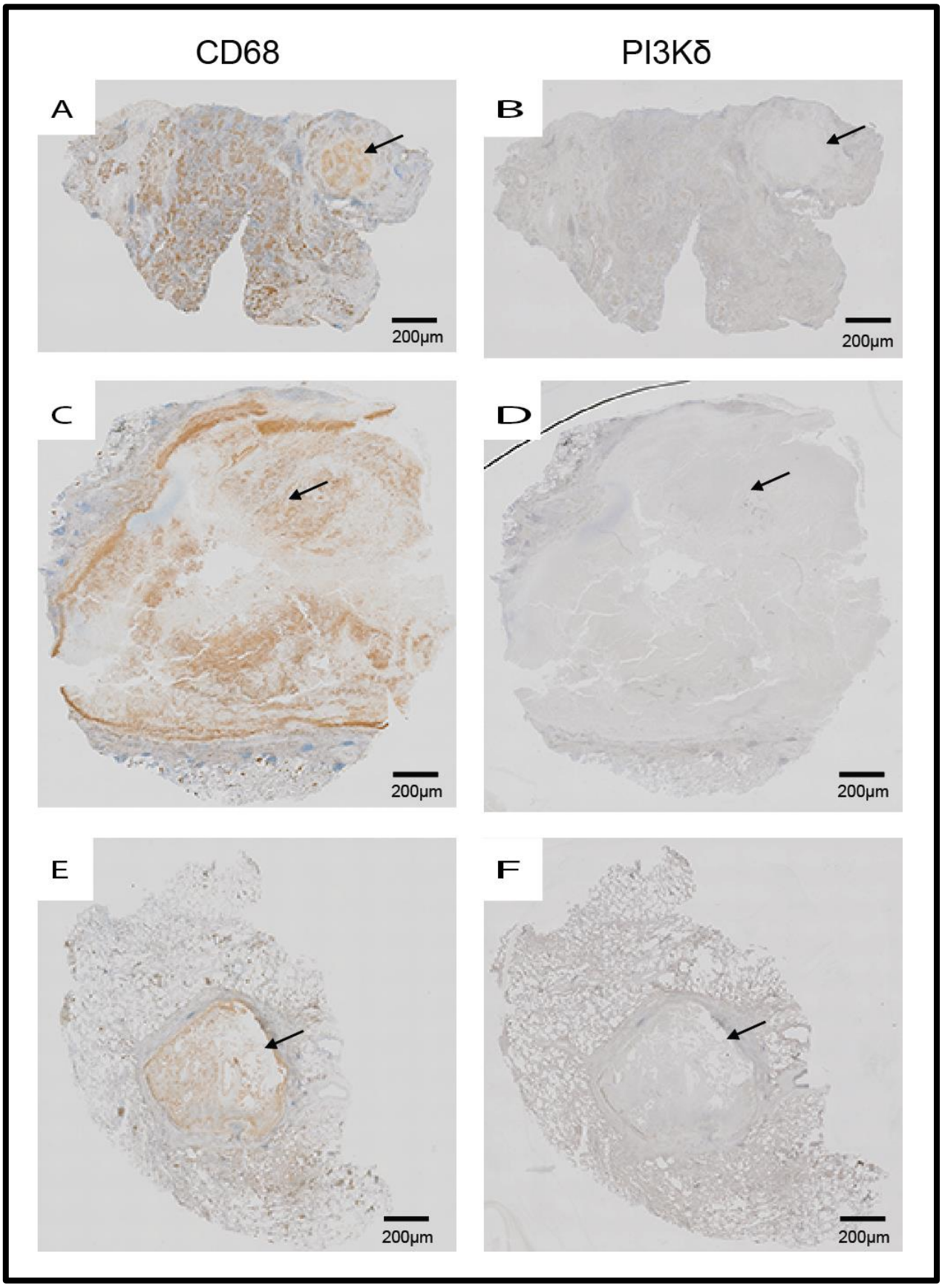
CD68
PI3Kδ
A
B
C
D
E
F
200μm
200μm
200μm
200μm
200μm
200μm

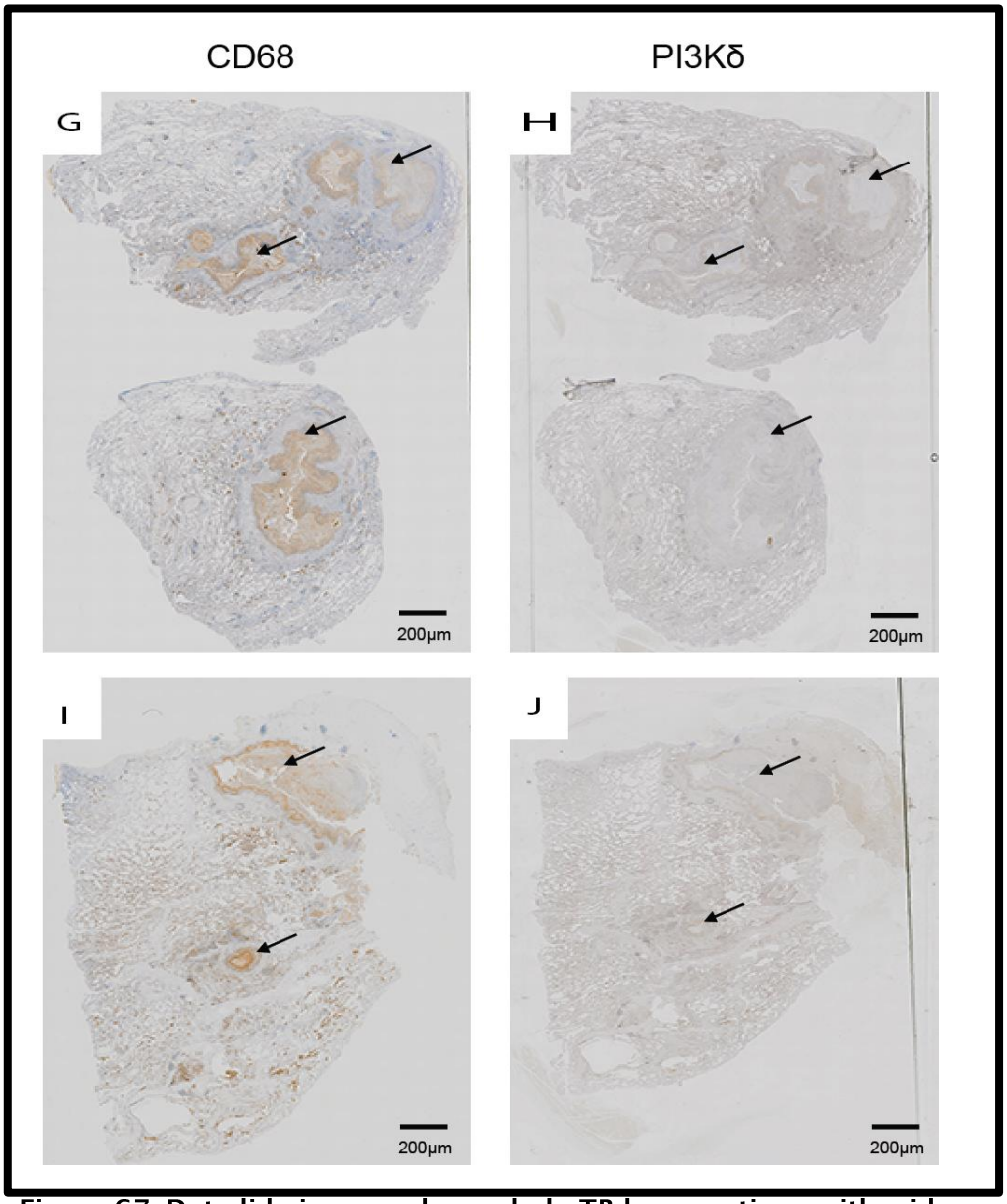


**Figure 67: Dot slide images show whole TB lung sections with wide spread CD68, but little or no PI3Kδ expression. A, C, E, G** and **I**: Alveolar macrophages are globally expressed across the tissue, and highly localised around and within granulomas. **B, D, F, H** and **J**: PI3Kδ expression is greatly reduced or absent within the same lung tissue and granuloma lesions. The arrows point to a number of granuloma lesions within the tissues. Data show images of stained tissues from five different donors. Immunohistochemistry was performed on paraffin-embedded normal lung tissues. Images of TB lungs from six different donors were captured using Olympus BX51-CC12 (DotSlide).

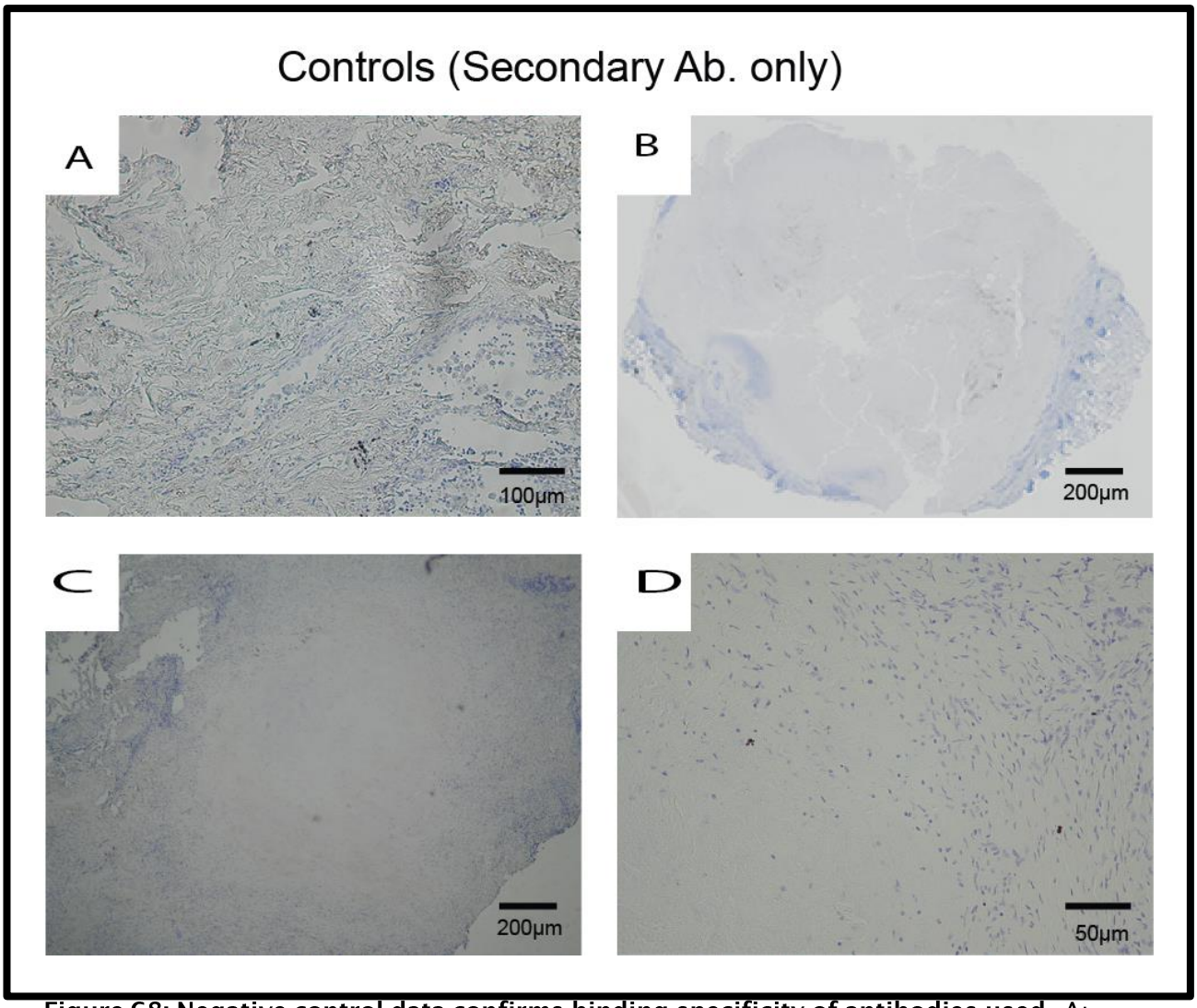


**Figure 68: Negative control data confirms binding specificity of antibodies used.** A: Normal lung, B: Dotslide plot of a large caseating granuloma in TB lung (B= same TB lung as shown in Figure 71D), C: Caseating granuloma from a different donor (C= same TB lung as figures 69E and 69F), D: High objective power image of C. Data show images of stained tissues from four different donors. Immunohistochemistry was performed on paraffin-embedded normal lung tissues from a total of six different donors, and Images were captured using Nikon Elipse 80i for A, C and D, and Olympus BX51-CC12 (DotSlide) for B.

## 5.8 *M.tb* post transcriptionally represses PI3Kδ via micro RNAs

Next, I sought to determine the point at which the observed regulatory event on PI3Kδ expression occurs within the cellular processes. Firstly, I aimed to investigate whether the PI3Kδ suppression effect exerted by *M.tb* was via transcriptional or translational modulation. After infecting macrophages with *M.tb*, I incubated the macrophages with 4-thio uridine (4-TU). This way any mRNA transcribed after 4-TU addition would incorporate 4-TU into the transcript in place of Uradine. This would allow isolation of newly transcribed PI3Kδ mRNA following *M.tb* infection and analysis of that in comparison with accumulated PI3Kδ mRNA which do not contain 4-TU within its transcript. Whereas the gene expression of PI3Kδ, MNK1 and MLST8 were up-regulated within 24 hours following *M.tb* infection, the accumulated mRNA was down-regulated by 72 hours (Figure 70). This suggests that although the genes of study are transcribed following *M.tb* infection, the mRNAs have reduced stability, implicating a post-transcriptional regulation of these genes.

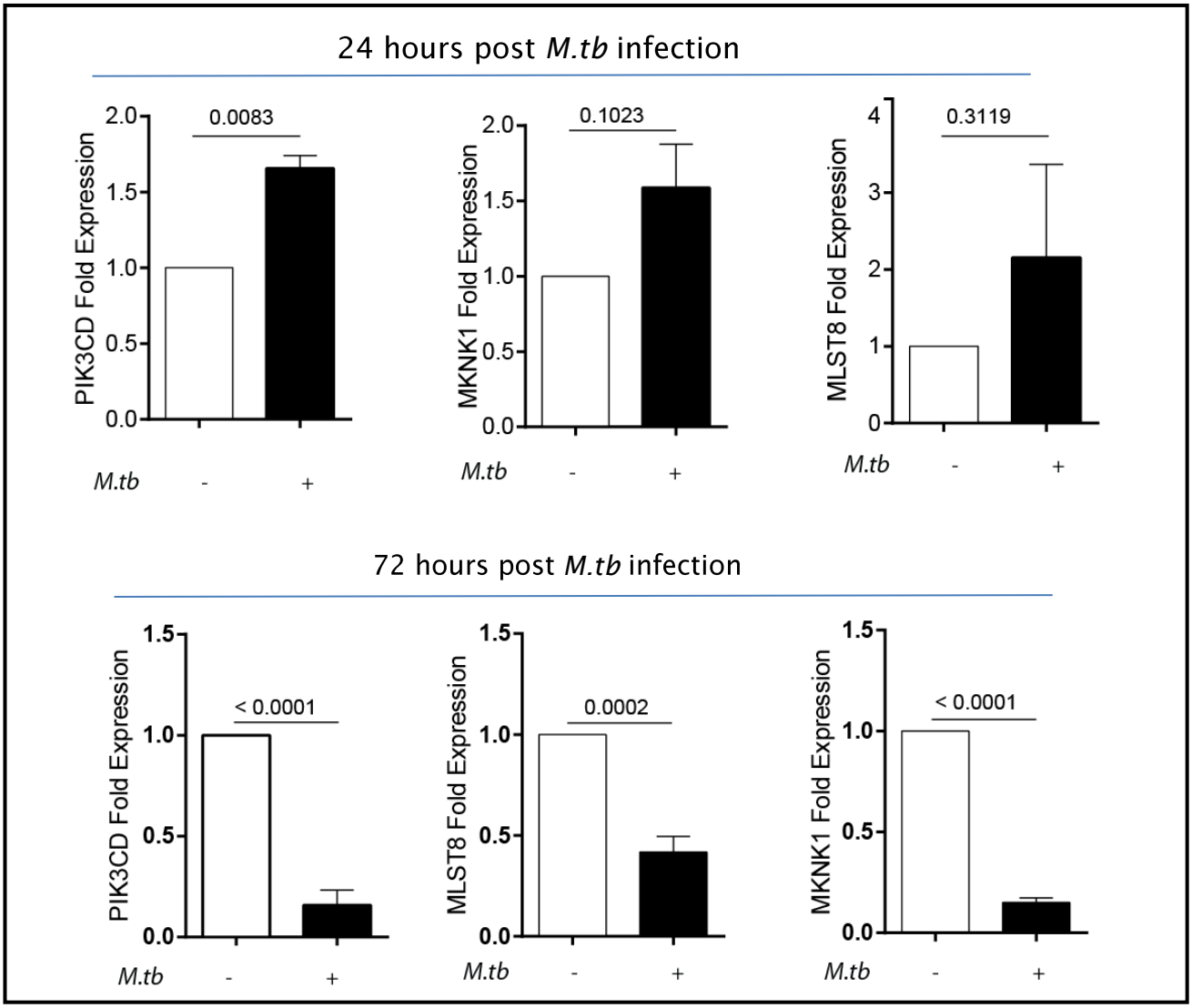


**Figure 69: M.tb reduces mRNA stability of PIK3CD, MKNK1 and MLST8 genes.** M.tb infection of macrophages increases PIK3CD, MKNK1 and MLST8 mRNA synthesis by 24 hours (Top panel). The newly synthesised mRNA reduces over time, with total accumulation of PIK3CD, MKNK1 and MLST8 mRNA suppressed by 72 hours (Lower panel). Data show mean and standard deviation of experiments performed in triplicates and is representative of experiments performed on two donors at separate occasions. P values are Student's t-test, with $P < 0.05$ considered significantly different.

Following observations that *M.tb* supresses pathways that regulate tissue destruction in TB, it was predicted that one of the mechanisms by which *M.tb* targets the PI3K, mTORC-1 and MNK signalling may be by inducing up-regulation of micro RNAs that target the mRNA transcripts of PI3Kδ, MNK1 and MLST8. To investigate this, a bio-informatics search using 'TargetScanHuman 6.2'' was carried out to identify existing micro RNAs predicted to target PI3Kδ, MNK1 and MLST8 mRNA for degradation or translational repression. This search resulted in the identification of multiple micro RNAs that are predicted to either separately or cooperatively target PIK3CD, MKNK1 and the MLST8 genes at the 3'-UTR (Tables 11a, b and c). Out of these, 8 micro RNAs including miR-7, -22, -27a, -30a, -221, -125b, -199 and miR-135a were investigated. Figure 71 is a schematic representation mapping of the micro RNAs under study and their corresponding target mRNA.

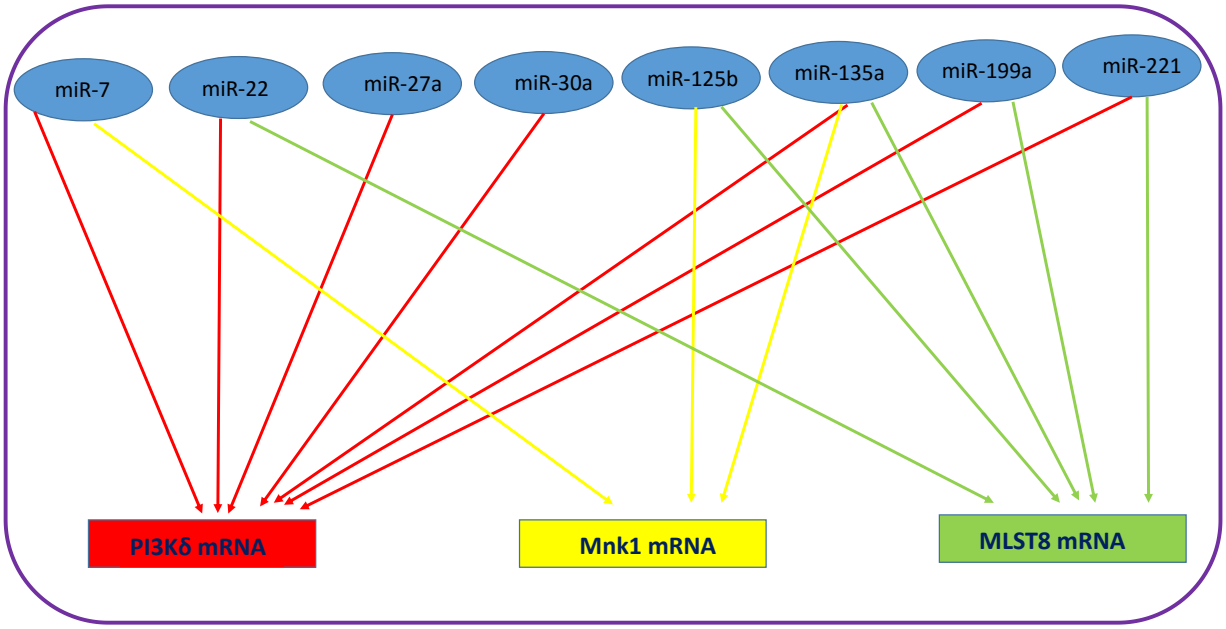


**Figure 70: A Schematic diagram of the micro RNAs studied and their mRNA targets.** Multiple micro RNAs target the same mRNA transcript.

| hsa-miR ID | Binding position on PIK3CD 3' UTR | hsa-miR and target mRNA alignment sequence |
|---|---|---|
| hsa-miR-27a (7mer-1A) | 1828-1834 | 5' ...GUUGAGACCAGCACUCUGUGAAA... 3'<br>\|\|\|\|\|\|<br>3' CGCCUUGAAUCGGUGACACUU 5' |
| hsa-miR-30a (8mer) | 127-133 | 5' ...GACAUGGCUGCCUUUUGUUUACA... 3'<br>\|\|\|\|\|\|\|<br>3' GAAGGUCAGCUCCUACAAAUGU 5' |
| hsa-miR-135a (7mer-1A) | 178-184 | 5' ...UUUAAGGAGCUAAACAGCCAUAA... 3'<br>\|\|\|\| \|\|\|\|\|\|<br>3' AGUGUAUCCUUAUUUU-UCGGUAU 5' |
| hsa-miR-7 (7mer-m8) | 782-788 | 5' ...UUUUUUUGAGAUGGGGUCUUCCU... 3'<br>\|\|\|\|\|\|\|<br>3' UGUUGUUUUAGUGAUCAGAAGGU 5' |
| hsa-miR-7 (7mer-1A) | 1118-1124 | 5' ...GGAUGAGGCCAGAACUCUUCCAG... 3'<br>\|\|\|\|\|\|<br>3' UGUUGUUUUAGUGAUCAGAAGGU 5' |

| | | |
|---|---|---|
| hsa-miR-199a-5p | 132-138 | 5' ...GGCUGCCUUUUGUUUACACUGGU... 3'<br>\|\|\|\|\|\|\|<br>3' CUUGUCCAUCAGACUUGUGACCC 5' |
| hsa-miR-199b-5p<br>(7mer-m8) | 132-138 | 5' ...GGCUGCCUUUUGUUUACACUGGU. 3'<br>\|\|\|\|\|\|\|<br>3' CUUGUCUAUCAGAUUUGUGACCC 5' |
| hsa-miR-22 (7mer-m8) | 451-457 | 5' ...CCUAGACUGAGUUCUGGCAGCUC 3'<br>\|\|\|\|\|\|\|<br>3' UGUCAAGAAGUUGACCGUCGAA 5' |
| hsa-miR-221<br>(7mer-m8) | 689-695 | 5' ...AGAGAUCUGGGCCUCAUGUAGCU 3'<br>\|\|\|\|\|\|\|<br>3' CUUUGGGUCGUCUGUUACAUCGA 5' |

**Table 11a:** Alignment and sequence information about the micro RNAs of interest and their corresponding target mRNA binding sites (PIK3CD).

| hsa-miR ID | Binding position on MKNK1 3' UTR | hsa-miR and target mRNA alignme sequence |
|---|---|---|
| hsa-miR-7<br>(7mer-m8) | 558-564 | 5' ...CAGGAAAUCAAAUCAGUCUUCCG...<br>\|\|\|\|\|\| \|\|\|\|\|\|<br>3' UGUUGUUUUAGUGAU--CAGAAGGU 5 |
| hsa-miR-125b<br>(7mer-1A) | 514-520 | 5' ...AGCCAUCCCCUCAAUUCAGGGAA...<br>\|\|\|\|\|\|<br>3' AGUGUUCAAUCCCAGAGUCCCU 5' |
| hsa-miR-135a<br>(7mer-m8) | 498-504 | 5' ...UCCCUUGGCUGAGCAAAGCCAUC...<br>\|\|\|\|\|\|\|<br>3' AGUGUAUCCUUAUUUUUCGGUAU 5' |

**Table 11b:** Alignment and sequence information about the micro RNAs of interest and their corresponding target mRNA bindings sites (MKNK1).

| hsa-miR ID | Binding position on MLST8 3' UTR | hsa-miR and target mRNA alignment sequence |
|---|---|---|
| hsa-miR-22-3p<br><br>(7mer-m8) | 295-301 | 5' ...CCUGGUGCAGGUGGUG<br>GCAGCUG 3'<br>\|\|\|\|\|\|\|<br>3' UGUCAAGAAGUUGACC<br>GUCGAA 5' |
| hsa-miR-199a-5p | 703-709 | 5' ...GUGGCCUGGCCAGCC<br>CACUGGAU 3'<br>\|\|\|\|\|\|<br>3' CUUGUCCAUCAGACUU<br>GUGACCC 5' |
| hsa-miR-199b-5p | 703-709 | 5' ...GUGGCCUGGCCAGCC<br>CACUGGAU...<br>\|\|\|\|\|\|<br>3' CUUGUCUAUCAGAUU<br>UGUGACCC |

**Table 11c:** Alignment and sequence information about the micro RNAs of interest and their corresponding target mRNA bindings sites (MLST8).

## 5.9 *M.tb* induces upregulation of micro RNAs predicted to target regulatory pathways

Micro RT-qPCR was performed next to examine *M.tb* induced modulation of our micro RNAs of interest. The micro RNAs of interest were up-regulated in the same RNA samples where *M.tb* suppressed the gene expressions of PI3Kδ, MNK1 and MLST8 (Figure 72). This suggests that *M.tb* induces upregulation of micro RNAs predicted to target important components of the pathways under study, in order to suppress their negative regulatory function.

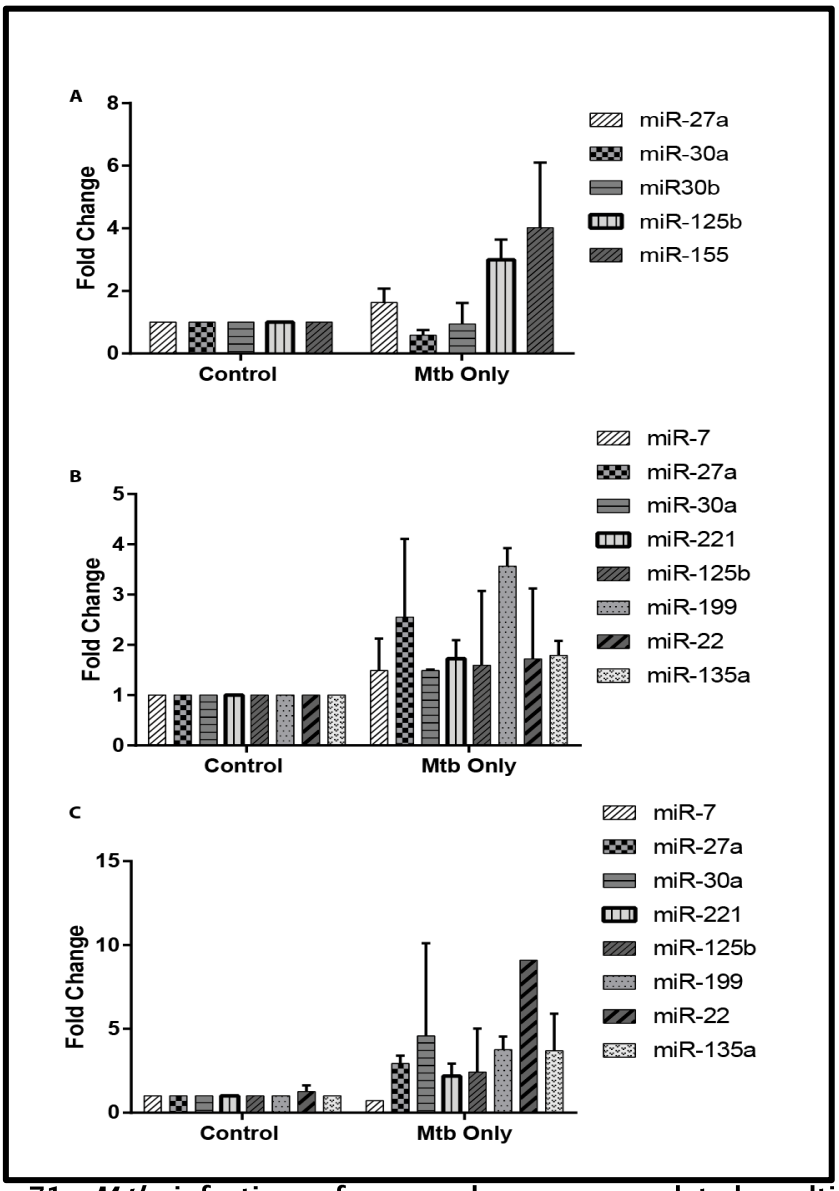


**Figure 71: *M.tb* infection of macrophages upregulated multiple microRNAs predicted to target negative regulatory pathways.** MDMs were infected with *M.tb* for 24 hours, after which RNA samples were analysed for miR profiling. RNA samples where *M.tb* induced suppression of PI3Kδ, MNK1 and MLST8 were used to perform micro-RT-qPCR. MicroRNAs that are predicted to target PI3Kδ, MNK1 and MLST8 gene expression are up-regulated in cells where the mRNA of the same intracellular signalling components was significantly suppressed by *M.tb*. Data show all three experiments performed in different occasions.

The micro RNAs chosen have been predicted, but have not been experimentally proven to suppress the expression of their predicted

target genes. I predicted that stimulating macrophages with anti-micro RNAs (anti-miRs) would reverse the micro RNA-induced repression of PI3Kδ, MNK1 and MLST8 gene expression. I proposed that if specific micro RNAs are responsible for the down-regulation of either of our genes of interest (i.e. PI3Kδ, MNK1 and MLST8 genes), then their corresponding anti-miRs would block the activity of such micro RNAs, thereby allowing their respective mRNAs to be stably accumulated in order to be detected by RT-qPCR.

Data from initial experiment using anti-miRs 30a and 135a showed up-regulation of PI3Kδ gene (Figure 73A) with accompanying down-regulation of MMP-1 by a combination of anti-miRs 30a and 135a (Figure 73B). Interestingly, although antimiR_30a failed to repress *M.tb* -driven MMP-1, there was no change in *M.tb* -driven MMP-1 gene expression in macrophages treated with antimiR_135a compared to that driven by *M.tb* only. However, data from subsequent repeated experiments were inconclusive (Figure 74).

In all experiments, *M.tb* consistently suppressed PI3Kδ, MNK1 and MLST8 genes as expected, and the anti-miRs reversed this suppression effect when compared to control macrophages. However, given that the negative control anti-miR exerted effect in similar manner to the un-infected control cells (Figure 74), this data was deemed inconclusive as I could not exclude a non-specific effect. Although antimiR_135a (but not antimiR_30a) failed to reverse *M.tb* -driven MMP-1, anti-miRs_27a, 30a and a combination of all three anti-miRs caused no change in *M.tb* -driven MMP-1 expression. *M.tb* -driven MMP-1 was greatly repressed in cells treated with the negative control anti-miR. Given that this 'negative control' anti-miR reverses *M.tb* -driven PIK3CD, MKNK1 and MLST8 genes, with accompanying MMP-1 repression in the same cells, this confirms that rather than acting as negative control, in fact this control anti-miR may target our genes of interest directly or the effect may be non-specific. When an alternative method of analysis where the data was

normalised to the non-specific negative control instead of the uninfected control, the anti-miRs clearly reversed the *M.tb* -induced suppression of PIK3CD, MKNK1 and MLST8 gene expression (Figure 75)

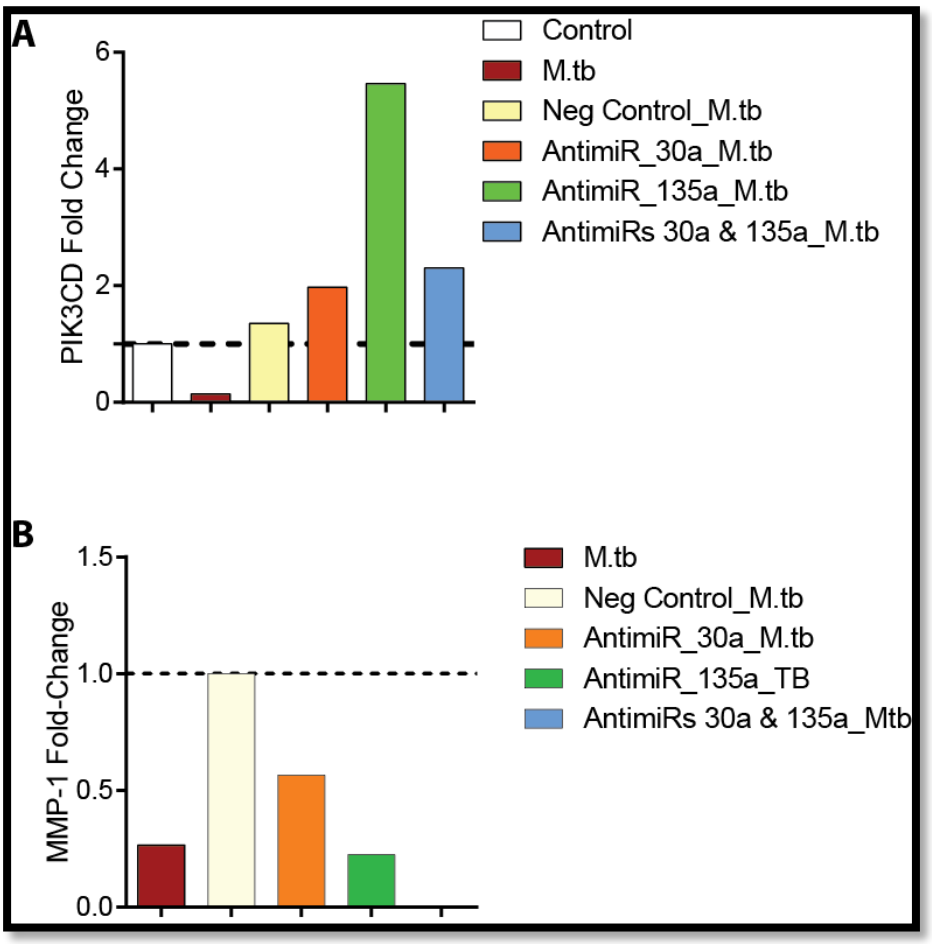


**Figure 72: Anti-miRs reverse *M.tb* effect on PIK3CD and MMP-1genes.** MDMs were transfected with the said anti-mIRs for 24 after which RNA was isolated for gene expression analysis. **A:** Anti-miRs-30a and 135a induced upregulation of PIK3CD in *M.tb* infected macrophages. **B:** Whereas antimiR-30a failed to reverse *M.tb* -driven MMP-1, antimiR-135a exerts no change, with a combination of the two anti-miRs greatly suppressing *M.tb* -driven MMP-1. In both A and B, the negative control anti-miR (Not expected to elicit any effect on *M.tb* activity) exerted up-regulation effect on both PIK3CD and MMP-1 genes. This data shows one of the experiments performed on at least three different donors.

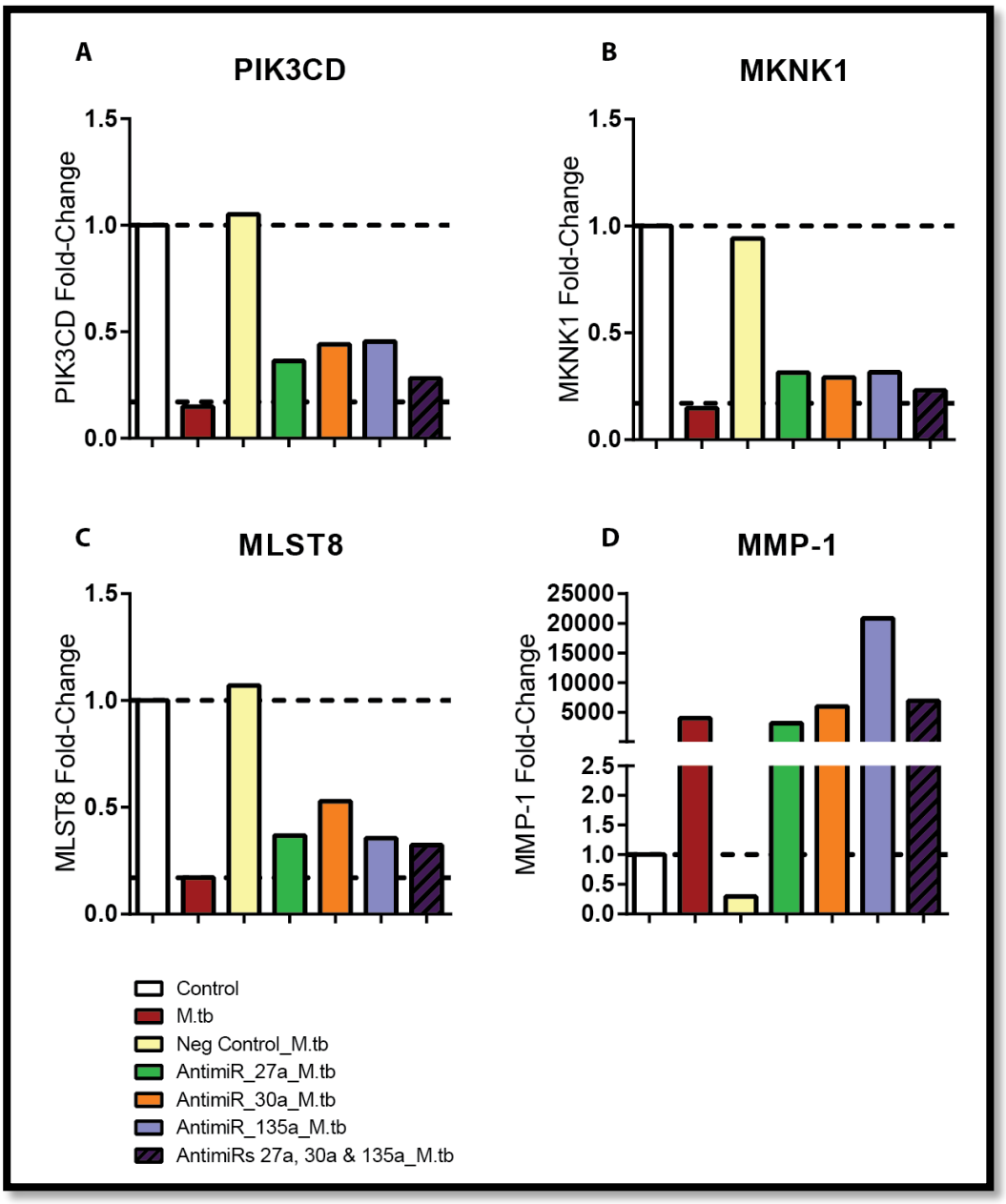


**Figure 73: Anti-miRs modulate PIK3CD, MKNK1, MLST8 MMP-1 genes. A, B,** and **C:** Anti-miRs-27a, -30a and -135a reversed *M.tb* -induced suppression of PIK3CD, MKNK1 and MLST8 genes, with the negative control anti-miR exerting a greater reversal effect on these genes. **D:** Although the negative control anti-miR supressed MMP-1, the anti-miRs of study failed to suppress *M.tb* -driven MMP-1. This data shows one of the experiments performed on at least three different donors.

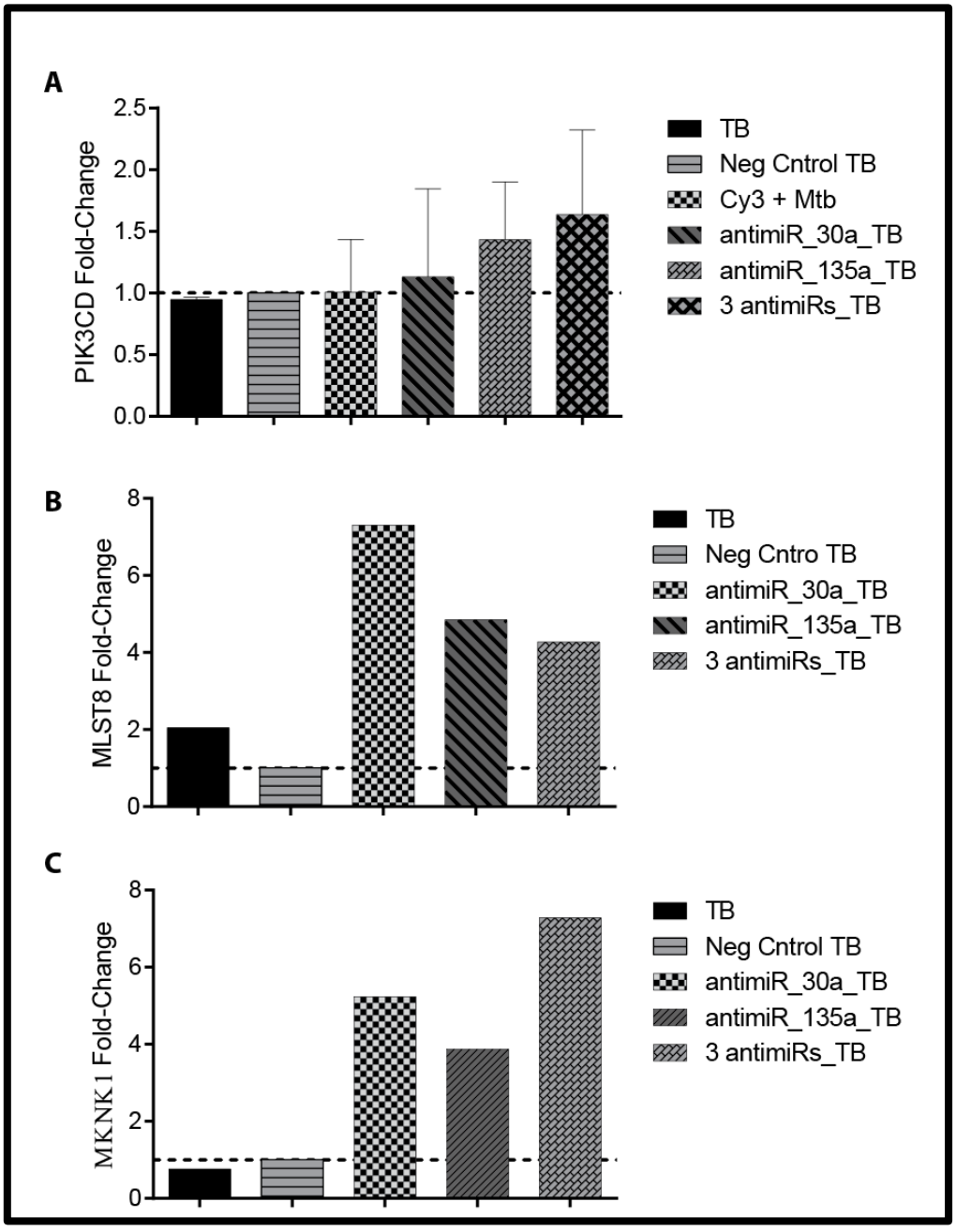


**Figure 74: Anti-miRs drive upregulation of PIK3CD, MKNK1 and MLST8 genes in *M.tb* infected macrophages. A, B** and **C:** The non-specific negative control anti-miR was for standardisation as an alternative method of analysis. In this analysis, the data support the hypothesis that miRs cause suppression of negative regulatory pathways. This data shows one of the experiments performed on at least three different donors.

## 5.10 Discussion of results chapter III

This study has demonstrated that *M.tb* drives MMP-1 production in TB, and MMPs have been linked to lung tissue destruction which is crucial for cavitation (Elkington et al., 2011c, Ong et al., 2014). It has also demonstrated that the inhibition of PI3K/AKT/mTORC-1 and Mnk signalling pathways results in elevated MMP-1 production by *M.tb* infected macrophages. This suggests that the pathways exert a suppression effect on MMP-1 production in TB, and this is indicative of negative regulation of tissue destruction. Given the global success of TB, It was hypothesised that the bacilli must be targeting important components of the regulatory pathways to drive disease progression.

In order to evade host defence and enhance their survival, *M.tb* is known to have devised a number of mechanisms to interfere with and attenuate macrophage-triggered anti-mycobacterial immunity (Hestvik et al., 2005). Data from this study has revealed that *M.tb* significantly drives MMP-1 (Figure 61A), whilst suppressing PI3Kδ gene expressions in the same cells (Figure 61B and 61C). Given my hypothesis that signalling via the PI3K pathway negatively regulates MMP-1, this data was supportive of my prediction that *M.tb* has evolved to target intracellular signalling that negatively regulate tissue destruction in TB.

At the gene level, *M.tb* significantly repressed gene expression of PI3Kδ (PIK3CD), and Mnk1 (MKNK1) and a subunit of the mTOR complex-1, MLST8 after 72 hours of infection (Figure 70). The repressed mRNA did not translate to reduced protein expression in *M.tb* -infected macrophages at early time points. I have shown in one dataset that *M.tb* down-regulates PI3Kδ protein in infected macrophages by 72 hours (Figure 62). However, our attempt to reproduce this data was not always successful. Thus, the changes I observed at the gene expression level did

not always reflect the same trend at the protein level. This is not uncommon, since mRNA production and protein levels do not always correlate (Vogel and Marcotte, 2012). It is likely that the biochemical diversity of proteins is partly responsible for the differences in individual correlation levels with the associated mRNA. With an average half-life of 2.6-7 hours for mRNA compared to 46 hour for protein, mRNA are known to be generally less stable than proteins in mammalian cells (Vogel and Marcotte, 2012, Schwanhausser et al., 2011). Furthermore, the rate of mRNA transcription in mammalian cells is much slower compared to protein synthesis. Only about two copies of a given mRNA is produced per hour in mammalian cells, compared to multiples of tens of protein copies translated per mRNA per hour (Vogel and Marcotte, 2012). These factors are therefore likely to account for the discrepancies in our gene versus protein expression data, and it may be necessary to do later time points to investigate whether PI3K protein levels fall after *M.tb* infection.

Next I investigated PI3Kδ protein expression profile in lung tissues biopsied from patients confirmed to have pulmonary TB. PI3Kδ expression was globally suppressed in TB lung tissues (Figures 66-68). In fact the high expression of CD68 by giant cells in TB lungs, with the accompanying lack of PI3Kδ expression supports our data where *M.tb* repressed PI3Kδ gene expression in infected macrophages (Figure 61).

This study next attempted to dissect the underlying mechanisms that underpin the ability of *M.tb* to block important effectors of regulatory pathways including PI3Kδ, Mnk1 and MLST8. It was identified that although early stages of *M.tb* infection in macrophages results in upregulated PI3Kδ, Mnk1 and MLST8 gene expression, the resulting mRNA transcripts are not stable (Figure 70). It was predicted that *M.tb* intervention of host defence is posttranscriptional, involving microRNAs. Micro RNAs target mRNAs for their degradation or translational repression (Singh et al., 2013).

Micro RNA-155 (miR-155) which was upregulated in system (Figure 72 A) is a well characterised micro RNA known to be frequently up-regulated in inflammation and in a variety of pathological conditions. In *M.tb* infection, autophagy induced death of macrophages has been reported to enhance *M.tb* killing (Bao et al., 2013). miR-155 was shown to be up-regulated in *M.tb* infection, where it interacts with Rheb to prevent it from repressing autophagy, thereby promoting mycobacterial killing via increased macrophage autophagy. Thus, although miR-155 up-regulated in TB can be interpreted as a mechanism to increase *M.tb* killing in macrophages, suppression of Rheb by miR-155 could also result in repression of mTORC-1 activity, which I have demonstrated to negatively regulate MMP-1. Thus, the up-regulation of miR-155 could be a host immune response to eradicate *M.tb* , or a mechanism devised by *M.tb* to subvert mTORC-1 signalling in order to successfully drive *M.tb* pathogenesis.

It was propose that one of the ways by which *M.tb* suppresses the PI3/AKT/mTORC-1 and Mnk1 signalling is by inducing up-regulation of micro RNAs that target PI3Kδ, Mnk1 and MLST8. This study has demonstrated that indeed, *M.tb* induces up-regulation of microRNAs that are predicted to target PI3Kδ, Mnk1 and MLST8 in this model (Figure 72).

Micro RNA-7 (miR-7) has been demonstrated to target the PIK3CD gene, and the overexpression of miR-7 in alternative systems resulted in repression of mTORC-1 and p70S6K activity, whereas levels of 4E-BP1 were elevated. This resulted in inhibition of cell growth in hepatocellular carcinoma (HCC), thereby decreasing tumour progression in HCC (Fang et al., 2012). This work has shown that signalling via mTORC-1 also negatively regulates MMP-1 in TB (Figure 31). It is therefore likely that in order for *M.tb* to drive disease progression, the bacilli induce the up-regulation of miR-7 (as well as the other identified miRs under study) to target both PIK3CD, MLST8 and MKNK1 genes in order to remove the regulatory effects exerted by these signalling pathways.

Despite the growing knowledge of the involvement of micro RNAs in TB, the above miRs have not been extensively investigated in the context of tissue destruction in TB. In order to confirm the target specificity of the identified micro RNAs under study, I transfected *M.tb* infected macrophages with a selection of anti-miRs. I expected that this would counteract the suppression effect of their corresponding miRs on PI3Kδ, Mnk1 and MLST8 gene expression. It was expected that the anti-mIRs would block the activities of the identified miRs, and prevent the miRs from degrading the mRNAs under study. This would cause a reverse of the observed *M.tb*-induced suppression effect and thereby increase the gene expression of PI3Kδ, Mnk1 and MLST8.

The data from the anti-miR study was inconclusive and difficult to interpret. Compared to un-infected, control cells, *M.tb* consistently suppressed PI3Kδ, Mnk 1 and MLST8 genes as expected, and the anti-miRs increased the expression of these genes to levels higher than that of *M.tb* infected cells which were not treated with anti-miRs. However, apart from figure 73A, where the anti-miRs drove higher PI3Kδ expression compared to that driven by *M.tb* alone, all subsequent data did not reproduce this phenomenon.

In figure 73B, it was predicted that blocking the miRs under study from targeting PI3Kδ, Mnk1 and MLST8 would enable a direct negative regulatory role of the signalling pathways on MMP-1 production. For this reason, it was expected that the anti-miRs would exert a suppression effect on MMP-1 gene expression. However, data from this study did not support this prediction. In fact although MMP-1 was driven by *M.tb* infection, the non-specific negative control anti-miR exerted marked MMP-1 upregulation in *M.tb* infected macrophages, and this was not expected. Although anti-miRs -30a and -135a suppressed the effect of the negative control on MMP-1 production, the extent of suppression was not lower than levels of MMP-1 that was driven by *M.tb* alone.

Interestingly, a combination of the two anti-miRs (anti-miRs -30a and -135a) completely abolished MMP-1 gene expression.

A careful consideration of figure 73A and 73B suggests that but for the unexpected activity of the negative control (non-specific-anti-miR), it can be speculated that indeed the anti-miRs block their respective target miRs, and that this reverses the suppression effect of *M.tb* on PI3Kδ, indirectly leading to PI3Kδ (Mnk1 and MLST8)-induced suppression of MMP-1. However, given that the non-specific negative antimiR control (with *M.tb* infection) increased PI3Kδ gene expression greater than that driven by *M.tb* alone, it is difficult to arrive at such definitive conclusions. In fact for all the anti-miR data, the non-specific anti-miR control exerted some level of activity in infected macrophages, up-regulating PIK3CD, MKNK1 and MLST8 gene expression to levels greater than that driven by *M.tb* alone, and comparable to levels driven by un-infected macrophages.

This study did not investigate the reasons why I did not observe a direct and consistent reverse expression of *M.tb*-induced suppression of PI3Kδ, Mnk1 and MLST8 genes from low to high, when miRs predicted to target their corresponding mRNA transcripts were blocked. A number of factors could account for the discrepancies in this observation. Firstly, I did not expect the negative control, which is a non-specific anti-miR, to exert activity on the infected macrophages. This data however shows that the negative control overcame the *M.tb* suppression effect on our genes of interest, which compromises the reliability of the data. Future studies should investigate the effect of a number of non-specific anti-miR negative controls on gene expression, in the context of *M.tb* infection in macrophages. Secondly, micro RNAs function to silence gene expression via mRNA degradation or translational downregulation (Singh et al., 2013)

Multiple micro RNAs are known to combine in order to cooperatively target particular mRNAs, and this results in a synergistic down regulation of gene expression (Rupani et al., 2013). It is therefore likely that other

micro RNAs that have not investigated in this study may combine with any or all of the micro RNAs under study to repress PIK3CD, MKNK1 and MLST8 gene expression. Future studies should investigate the expression profile of a broader spectrum of micro RNAs that have been predicted to target PIK3CD, MKNK1 and MLST8 gene expression in *M.tb* infected macrophages. Once the relevant micro RNAs are identified, multiple anti-miRs that are specific for the identified micro RNAs can then be included in the investigation in order to reach a decisive conclusion.

Taken together, this work has demonstrated that in order to drive disease progression, *M.tb* induces upregulation of micro RNAs that are predicted to target important effectors of signalling pathways that negatively regulate tissue destruction in TB. Future studies should dissect the exact micro RNAs involved and determine their specificity with their predicted target genes.

# 6. CHAPTER 6: GENERAL DISCUSSION AND FUTURE WORK

Pulmonary TB patients develop cavities within their lungs and are thought to be the global drivers of the TB pandemic (Yoder, 2004). MMP-1 secreted by *M.tb* infected macrophages have been shown to mediate

destruction of lung extracellular matrix (ECM), ultimately resulting in cavitation (Elkington et al., 2011a). This work has demonstrated that intracellular signalling pathways negatively regulate MMP-1 production in TB, and that the PI3Kδ isoform of the class IA PI3Ks plays a pivotal role in suppressing MMP-1. Thus this *in vitro* study has confirmed the emerging notion that the PI3K/AKT/mTORC-1 (and Mnk1) signalling play negative regulatory roles in disease pathogenesis.

I have examined *M.tb* modulation of MMP-1 production in infected macrophages, and explored how this response is affected by chemical compounds that block the intracellular signalling pathways under study. The PI3K/AKT/mTORC-1 pathway plays a crucial role in immune response to pathogens by balancing pro- and anti-inflammation, hence its critical function in health and disease. However, as a result of the signalling cascade's ability to trigger diseases that emanate from uncontrolled cell growth, various compounds that inhibit distinct components of this pathway have been designed as novel therapies for cancer.

In human prostate cancer, PI3K (together with FAK and PKCδ) signalling has been reported to mediate MMP-1 dependent invasion (Zeng et al., 2006). It is however becoming increasingly clear that this pathway also play vital regulatory role in inflammation to limit diseases pathogenesis (Thomas et al., 2005, Fukao et al., 2002, Aksoy et al., 2012, Tsukamoto et al., 2008, Xia et al., 2004). I have shown here that *M.tb* drives MMP-1 secretion in macrophages and that PI3K, AKT, mTORC-1 (and Mnk1) inhibitors further augment MMP-1 production in *M.tb* infected macrophages, suggesting a negative regulatory role played by the PI3K/AKT/mTORC-1 pathway in TB. The premise that lipid kinases and their intracellular signalling cascade components play a negative regulatory role has been supported by numerous studies (Molnarfi et al., 2008, Guha and Mackman, 2002, Tengku-Muhammad et al., 1999, Weinstein et al., 2000). In Lipopolysaccharides (LPS) stimulated dendritic cells (DCs), although IL-12 secretion is essential to initiate a Th1-type,

cell-mediated response to the invading pathogens, excessive production of IL-12 is detrimental to the host. Enhanced IL-12 suppressed anti-inflammatory Th2-type immunity, rendering the host susceptible to parasitic infections (Fukao et al., 2002, Finkelman et al., 1997), and causing endotoxin shock (Gately et al., 1998, Ulevitch and Tobias, 1995). PI3K has been shown to limit excessive IL-12 production by LPS stimulated dendritic cells (DCs), mediating a balance between Th1/Th2-type response, thereby limiting LPS induced endotoxin shock (Fukao et al., 2002).

In line with this finding, PI3K inhibition also blocked IL-10 (an anti-inflammatory cytokine) secretion whilst enhancing that of IL-12 in *Porphyromonas gingivalis* lipopolysaccharide infected monocytes (Molnarfi et al., 2008, Martin et al., 2003). Consistent with findings from this work, the negative regulation of IL-12 secretion by PI3K pathway was confirmed in a study where primary macrophages were infected with H37Rv strain of *M.tb* (Yang et al., 2006b). Following activation by cytokines, LY294002 and Wortmannin treated T cells isolated from rheumatoid arthritis patients caused human monocytes to secrete the pro-inflammatory cytokine TNF, at levels much higher than non-treated cells (Brennan and Foey, 2002) with the opposite effect on IL-10 secretion by macrophages (Foey et al., 2002).

PI3Kδ has been reported to be the specific isoform that mediate a balance between pro- and anti-inflammatory immunity in response to numerous pathogenic insults (Aksoy et al., 2012, Molnarfi et al., 2008). In LPS-infected monocytes, PI3Kδ was shown to suppress the production of TNF, IL-1 and IL-6 which are all potent pro-inflammatory cytokines (Molnarfi et al., 2008) which have also been linked to necrosis and tissue destruction in TB (Fenhalls et al., 2002). Although inhibition of PI3Kα and PI3Kβ in *M.tb* infected primary macrophages up-regulates MMP-1 secretion (Figure 28), PI3Kδ inhibition results in even marked upregulation of *M.tb*-driven MMP-1. This result suggests that PI3Kα and

β isoforms are contributors, rather than the main isoforms involved in the regulatory role proposed, and that the PI3Kδ isoform predominantly mediates the negative regulatory role of PI3K observed in this model.

The current paradigm of the formation of TB-associated lung cavitation implicates TNF-α and IL-1β as the key cytokines that mediate necrosis and have been suggested to promote tissue destruction. Lipoarabinomannan (LAM), a component of mycobacterial cell wall triggers TNF-α and IL-1β production in macrophages (Fenhalls et al., 2002), and PI3Kδ has been reported to suppress LPS-induced secretion of these cytokines (TNF-α, IL-6 and IL-1β) in macrophages (Molnarfi et al., 2008). TNF-α and IL-1β are reported to play crucial role in putative tissue damage in TB. Even though exaggerated production of these pro-inflammatory cytokines may play a role in necrosis-associated cell death that has been implicated in early phase pathogenesis of cavitation, as they have no proteolytic activities, it is unlikely that the cytokines solely cause the extensive ECM degradation observed in later stages of cavity formation. The notion that PI3Kδ negatively regulates the secretion of cytokines that have been linked to tissue damage is consistent with findings from this work.

A key downstream substrate of the PI3K/AKT pathway is mTORC-1. mTORC-1 signals in a very similar fashion to PI3Ks in that its activation results in up-regulation of cell proliferation, growth, differentiation, cell migration and many other cell survival processes, as well as initiation of protein synthesis (Laplante and Sabatini, 2012). mTORC-1 has been shown to negatively regulate IL-12 production in LPS-stimulation DCs as seen in PI3K activity, however mTORC-1 requires local production of IL-10 (Ohtani et al., 2008). Consistent with this observation, enhanced MMP-1 production was observed in MDMs which were pre-treated with the classic mTORC-1 inhibitor, rapamycin (Figure 31).

Both PI3K and mTORC-1 inhibition by LY294002 and rapamycin respectively further enhanced the production of MMPs-1, -3 and -10 without altering *M.tb* -driven MMP-2 and MMP-7 (Figures 34 and 35). These results suggest that whereas the bacteria deliberately drives production of pathogenic MMPs, the PI3K pathway functions to supress such pathogenic MMPs that have potent collagenase and/or direct tissue destructive activity. By so doing, the intracellular signalling pathway is able to negatively regulate MMP-mediated tissue destruction in TB.

This study has demonstrated that inhibition of the PI3 kinase and mTOR pathways have a widespread effect, with mostly enhanced secretion of Th1/Th2-type cytokines and differential modulation of a number of chemokines and growth factors (Figures 36 to 45). This observation was of major interest because appropriate levels of Th1-type cytokines are likely to mediate a protective antimicrobial immunity during infection, which in TB is essential for depriving *M.tb* of its intracellular niche. In contrast, uncontrolled production of Th1-type molecules can be deleterious and may accentuate disease progression.

Although physiological production of IL-6, IL-12 and TNF-α in *M.tb* infection is essential for host defence against pathogenic challenge (Martinez et al., 2013, Cooper et al., 1997, Stenger, 2005), unregulated over-expression of these Th1-type molecules has previously been implicated in disease exacerbation by mediating tissue destruction (Law et al., 1996, Mootoo et al., 2009, Zhang et al., 2012). Inhibition of both PI3K and mTORC-1 signalling resulted in even marked secretion of IL1-β, IL-6, IL-12 and TNF-α by *M.tb* -infected macrophages (Figure 36 and 37). This suggests that important intracellular signalling pathways play crucial negative regulatory role to restrict tissue damage in TB by controlling overproduction of Th1-type pro-inflammatory cytokines. The pathway inhibitors similarly augmented a wide range of Th2-type cytokines, chemokines and growth factors (although the levels were relatively low), which was not expected (Figures 38-45). A high level of

fine tuning of inflammatory effector molecules is required to ensure appropriate balance between antimicrobial immunity and the chronic tissue damage that is associated with pulmonary TB. It is therefore likely that the negative regulatory role of intracellular signalling observed is not restricted to known pro-inflammatory molecules, but also Th2-type cytokines, chemokines and growth factors alike.

Further down the signalling cascade, Mnk1 signalling is widely known to drive cap-dependent translation via eIF4E activation (Knauf et al., 2001). Mnk1 inhibition also enhanced *M.tb*-driven MMP-1 secretion by macrophages (Figure 48). Mnk1 signalling has long been known to regulate protein translation via eIF4E phosphorylation. It was therefore surprising to observe an enhanced MMP-1 synthesis by *M.tb* infected macrophages when translation was supposed to have been interfered with through chemical inhibition of Mnk1. However, it has previously been reported that eIF4E phosphorylation on Ser 209 weakens the binding affinity of eIF4E for the 5'-cap structure of mRNA (Scheper and Proud, 2002a, Scheper et al., 2002, Knauf et al., 2001), and that phosphorylation of eIF4E is not indispensable for normal cell growth (Ueda et al., 2004). It is therefore likely that in the case of translational modulation of MMP-1 mRNA, Mnk1 functions to limit uncontrolled protein synthesis in a cap-independent translation mechanism that is independent of eIF4E activity. Although eIF4E is the most characterised Mnk substrate (Waskiewicz et al., 1997), various other Mnk1/2 targets are known, including ones that are specific for particular members of the Mnk group of kinases (Buxade et al., 2008). It therefore cannot be excluded that the effect of Mnk1 inhibition on MMP-1 is via mechanisms of other downstream substrates of Mnk1.

Mnk1 inhibition upregulated MMP-1, MMP-3 and MMP-10, (which are frequently synergistically regulated) with a widespread suppression of cytokines and chemokines (Figures 54-59), and this was not expected. This suggests that the effect of Mnk1 inhibition observed was specific to

pathogenic MMPs, implying a specific negative regulatory role of the Mnk pathway in dampening down tissue destructive TB immunopathology.

*M.tb* is known to employ several mechanisms, including interfering with essential signalling pathways, to evade host immune response in order to successfully survive in host cells and to drive the progression of disease (Hestvik et al., 2005). However, mechanisms by which *M.tb* is able to avoid host regulatory processes to drive the extensive tissue destruction seen in chest radiographs of patients with cavitary TB is much less well understood. *M.tb* induces a PIP-free environment in the phagosomal membrane to achieve oppression of phagosome maturation (Poirier and Av-Gay, 2012). This study has demonstrated that in macrophages, *M.tb* significantly suppresses PI3Kδ gene expression levels by 24 hours post infection (Figure 61). This study has also reported for the first time that PI3Kδ expression is absent in TB lungs with granuloma lesions (Figures 66-68). This data has revealed that *M.tb* significantly drives MMP-1 (Figure 61A), whilst suppressing PI3Kδ gene expressions in the same cells (Figure 61B). Given my hypothesis that signalling via the PI3K pathway negatively regulates MMP-1, these data were in concert with the second hypothesis that *M.tb* has evolved to target intracellular signalling that negatively regulate tissue destruction in TB.

Attempts to dissect the underlying mechanisms that underpin the ability of *M.tb* to block important effectors of regulatory pathways including PI3Kδ, Mnk1 and MLST8 led to the conclusion that although early stages of *M.tb* infection in macrophages results in upregulated PI3Kδ, Mnk1 and MLST8 gene expression, the resulting mRNA transcripts are not stable (Figure 70), implicating a posttranscriptional mechanism, potentially involving microRNAs.

Micro RNAs target mRNAs for their degradation or translational repression (Singh et al., 2013). This work has demonstrated that indeed, *M.tb* induces up-regulation of microRNAs that are predicted to target

PI3Kδ, Mnk1 and MLST8 in the same cells where *M.tb* suppresses PI3Kδ (Figure 72), but drives MMP-1 gene expression. Recent years has seen growing interest in the role of micro RNAs in TB pathogenesis, with miR-155, miR -125b, miR-99b, miR-7 and miR29 implicated in host immunity (Singh et al., 2013, Sharbati et al., 2011), and several micro RNAs have been linked to mechanisms by which *M.tb* evades host immunity to promote its survival (Singh et al., 2013). This data suggests that by inducing up-regulation of micro RNAs that target negative regulatory pathways, *M.tb* exerts an effect of skewing the transcriptional response to a matrix-degrading phenotype.

Taken together, This work has demonstrated that signalling downstream of the PI3K/AKT/mTORC-1 axis and Mnk1 pathway play a negative regulatory role in TB, and that *M.tb* induces suppression of important components of these signalling pathways. I have identified a novel strategy employed by *M.tb* to drive immunopathology by subverting negative regulatory pathways, both in primary macrophages and in TB patients. I demonstrate for the first time, a role of Mnk1 signalling as a negative regulator of MMPs in *M.tb* infected macrophages. Figure 76 is a schematic representation of proposed model based on summary of findings from this study. Here I propose that the PI3K/AKT/mTORC-1 signalling negatively regulates MMP-1 in tuberculosis. Whereas *M.tb*-induced signalling downstream of p38 and Erk drives MMP-1 via activation of COXII and $PGE_2$, the opposite can be said of Mnk1 signalling, which is also downstream of p38 and Erk MAP kinases. In fact the negative

regulation of pro-inflammatory mediators by Mnk1 signalling is pathogenic MMP specific.

**Figure 75: Proposed model**. *M.tb* infection triggers intracellular signalling which culminates in the modulation of MMP-1 production in infected macrophages. In order

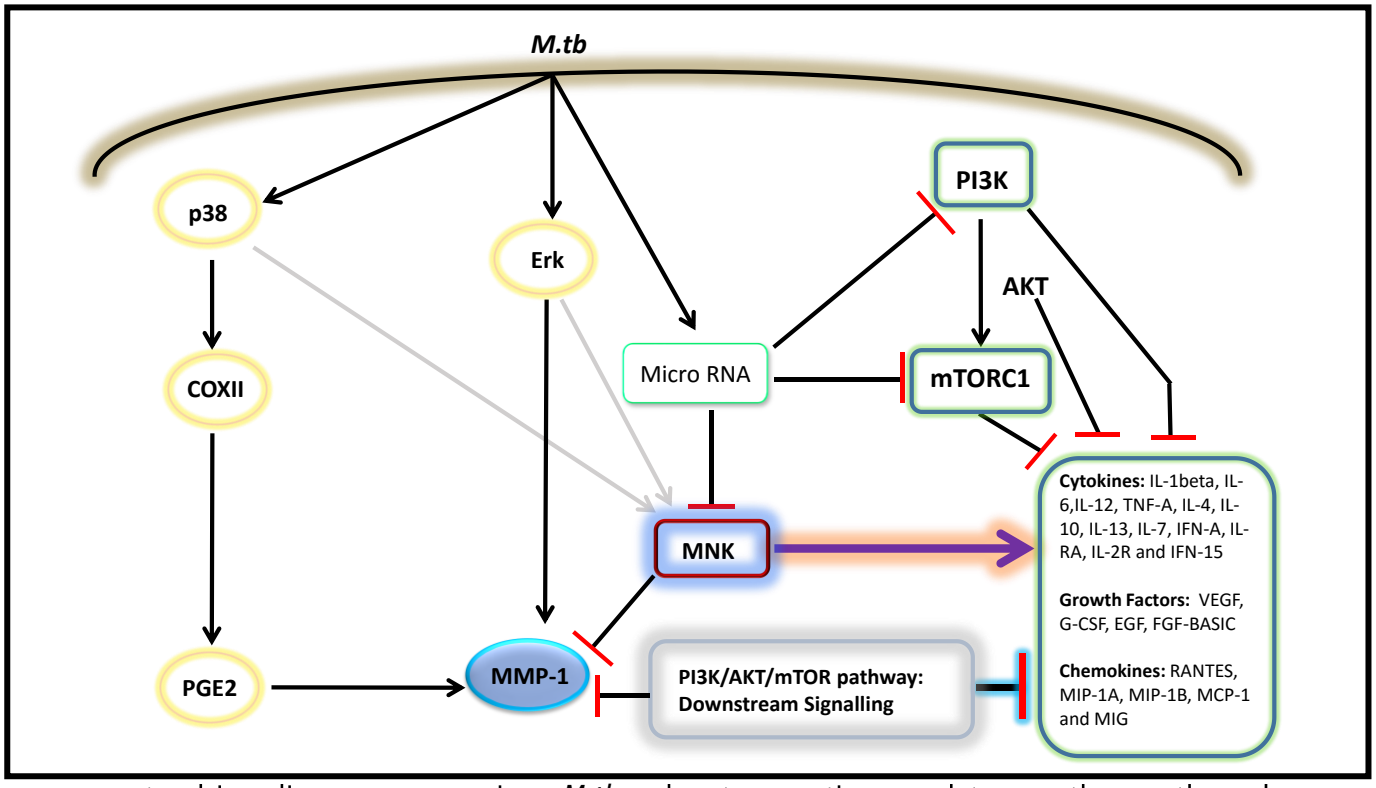


to drive disease progression, *M.tb* subverts negative regulatory pathways through upregulation of micro RNAs. I have shown that the PI3K/AKT/mTORC-1 axis and Mnk1 signalling function to limit *M.tb* -driven MMP-1, with Mnk1 regulation being specific to pathogenic MMP-1. Interestingly, *M.tb* -induced signalling downstream of p38, COXII, $PGE_2$ and Erk have all been previously shown to drive MMP-1.

## 6.1 CONCLUDING REMARKS

Taken together, this study has confirmed that *M.tb* induces MMP-1 secretion in primary macrophages, and that signalling downstream of PI3K/AKT/mTORC-1 and Mnk1 pathways function to limit the excessive production of such tissue damaging proteases. Consequently, this work

has demonstrated that *M.tb* suppresses the transcription of PI3Kδ mRNA in macrophages and PI3Kδ protein levels in TB patients, through up-regulation of micro RNAs that target the pathways under study. Interestingly, attempts to determine intracellular components that play negative regulatory role in TB have identified signalling pathways which are frequently switched on in cancer. This suggests that these signalling pathways may potentially possess evolutionary homeostatic role in TB and in other infectious diseases. PI3K inhibitors are currently in clinical trials for cancer and diabetes therapies, and I propose that they may also dampen down important host protective responses in TB, thereby accentuating the disease.

## 6.2 FUTURE WORK

Ideally, I would like to further dissect the negative regulatory pathways to build on my findings. Time and the technical challenges have meant that I have followed the pathways as far as I could, but inevitably there are further avenues to explore to build the overall macrophage signalosome. For example, another key downstream target of PI3K pathway is GSK3α/β signalling. In a study where mTORC-1 was shown to negatively regulate IL-12 production in LPS-stimulation DCs via local production of IL-10, GSK3 was also shown to drive IL-12 secretion in acute LPS infection, but did not require IL-10 (Ohtani et al., 2008). The function of GSK3 reported there supports the findings of a different group's work which demonstrated that in acute/infectious inflammatory conditions such as LPS-stimulation, GSK3 drives the secretion of pro-inflammatory cytokines (Martin et al., 2005). However, during chronic/sterile inflammatory condition as occurs in rheumatoid arthritis, GSK3 functions to suppress production of pro-inflammatory cytokines (Bommhardt et al., 2004, Hirsch et al., 2000, Williams et al., 2004). Since GSK3 is involved in the regulation of numerous transcription factors, it would be interesting to

decipher the effect of the PI3K/AKT/GSK3 axis of the PI3K pathway on MMP production in *M.tb* infected macrophages.

This study has utilised a number of pharmacological inhibitors to dissect the negative regulatory role of intracellular signalling in TB. Such compounds are known to exert non-specific by-stander effect on other effectors that may be critical for the phenotype described. Going forward, alternative methods such as direct targeting of the pathways in macrophages via si-RNA should be employed to further validate the findings of from this study, or via CRISP-R gene editing.

This study did not investigate the mechanism via which Mnk1 inhibition drives pathogenic MMPs, but not other pro-inflammatory cytokines. Although eIF4E is the most characterised Mnk substrate (Waskiewicz et al., 1997), various other Mnk1/2 targets are known, including ones that are specific for particular members of the Mnk group of kinases (Buxade et al., 2008). It is likely that different downstream Mnk substrate molecule(s) mediate the surprisingly high MMP-1 secretion effect of Mnk1 inhibition. It is therefore worth investigating the role of other Mnk1 targets in MMP production in the context of *M.tb* infection, and this finding is likely to be of broad interest to the Mnk signalling field.

It was proposed that one of the ways by which *M.tb* suppresses the PI3/AKT/mTORC-1 and Mnk1 signalling is by inducing up-regulation of micro RNAs that target PI3Kδ, Mnk1 and MLST8. This work further demonstrated that indeed, *M.tb* induces up-regulation of microRNAs that are predicted to target PI3Kδ, Mnk1 and MLST8 in this model. However, attempts to confirm specificity of the identified micro RNAs with their corresponding predicted target was inconclusive. Further studies would be required to confirm direct targeting of the micro RNAs of study to their predicted mRNA transcripts. This can be carried out by utilising a number of different non-specific anti-miRs as negative controls. The specificity of micro RNAs on targets can also be ascertained by cloning the 3' UTR

of PIK3CD, MKNK1 and MLST8 genes for luciferase assay analysis. This represents a significant body of work but would provide mechanistic evidence that the micro RNAs are exerting the hypothesised effect. Moreover, the micro RNAs under study were only a fraction of dozens predicted to target the pathways of study. Future work should include a broader range of micro RNAs to confirm further validate the findings.

# 7. APPENDICES

Appendix 1: Materials and buffer recipes

Appendix 2: Culture of *M.tb* (H37RV)

Appendix 3: Manufacturer's protocols used

Appendix 4: Software used

## 7.1 Appendix 1: Materials and buffer recipes

- **Complete media**

RPMI-1640 (Sigma-Aldrich, #R7509-6X500ML) supplemented with 5% L. Glutamine (Sigma-Aldrich Company Ltd., #G7513-100ML), 5% ampicillin (Sigma-Aldrich Company Ltd., #A0166-5G) and 10% foetal bovine serum(Life Technologies Ltd #FB-1001/500).

Middlebrook 7H9 medium (BD Bioscience)

10% ADC enrichment medium (BD Bioscience), 0.2% glycogen (Life Technologies Ltd) and 0.02% Tween 80 (Fisher Scientific UK Ltd #BPE338-500)

Preparation of Ampicillin stock solution

Weigh 500mg of Ampicillin powder (Ampicillin sodium salt, sigma A0166) in falcon tube. Re-suspend in 5ml of endotoxin free water and vortex. Top up to 50ml by adding 45ml of endotoxin free water. Filter sterilise into 5ml aliquots. Label and store in -20°C.

Materials and buffer recipes for ELISA

- **PBS (10X)**

0.9 Litres $H_2O$, 137mM NaCl (80g), 2.7mM KCl (2g), 8.1mM $Na_2HPO_4$ (11.1g), 1.5mM $KH_2PO_4$ (2g), Adjust to pH 7.2-7.4 (0.2 µm filter before use); Make up to 1L.

- **Capture (primary) antibody 2.0 µg/ml**

Stock 360µg/ml stored at -80° in 60µl aliquots; 10mls 1X PBS 55.6µl stock.

- **Wash buffer**

1 litre 1x PBS (pH 7.2 – 7.4), 0.5ml Tween 20 (0.05%)

- **Reagent diluent**

1 X PBS, 1% BSA.

- **Detection antibody (biotinylated) 50ng/ml**

Stock 72µg/ml stored at -80°C, 10mls Reagent diluent, 55.6µl Stock = 4 µg

- **Streptavidin-HRP (dilute 1 in 200)**

10mls Reagent diluent, 50µl streptavidin

- **Stop solution 2M H2SO4 (for 5ml)**

4.5mls dd$H_20$, 540µl concentration $H_2SO_4$

Buffer recipes for gel casting

- **Separating gel buffer (1 M Tris-HCl, pH 8.8)**

Add 30.3 g Tris to about 150 mL water; adjust to pH 8.8 with HCl

Bring to 250 mL with water

- **50% Sucrose**

50.0 g Sucrose. Bring to 100 mL with distilled water

- **10% SDS**

10.0 g SDS. Bring to 100 mL with distilled water

- **50% Acrylamide/BIS (29:1)**

48.3 g Acrylamide, 1.7 g BIS. Bring to 100 mL with water

- **Stacking gel buffer (0.375 M Tris HCl, pH 6.8)**

Add 11.4 g Tris to about 150 mL water; adjust to pH 6.8 with HCl. Bring to 250 mL with distilled water.

- **Catalyst (made fresh on the day of use)**

100 mg Ammonium persulfate in 2 mL of distilled water

Western blotting materials and buffers

- **Preparation of 1X NuPAGE® MOPS SDS running buffer Using NuPAGE® SDS Running Buffer (20X) as follows:**

| | |
|---|---|
| NuPAGE® SDS Running Buffer (20X, MES or MOPS) | 50 ml |
| Deionized Water | 950 ml |
| Total Volume | 1000 ml |

- **Preparation of 1L transfer buffer (20X)**

| | |
|---|---|
| NuPAGE® Transfer Buffer (20X) | 50 mL |
| Methanol | 100 mL |
| Deionized Water | 850 mL |

- **Concentrated TBS (10x)**

24.23g of Trizma/HCL

80.06g of NaCL

Mix in 800mL ultra-pure water and bring to pH 7.6 by adding HCL and top up to 1L

- **TBS tween (TBST)**

For 1 L: 100 ml of TBS X10 + 900 ml Ultra-pure water + 1ml Tween20

(OR 1X PBS, 0.1% Tween was used as Washing Buffer)

- **Blocking reagent**

To prepare a 5% milk or BSA solution,

5g per 100 ml of Tris Buffer Saline Tween20 (TBST) buffer

Mix well and filter (Failure to filter can lead to “spotting” where tiny dark grains will contaminate the blot during development)

(Or 4% BSA in 1 X PBS was used as blocking buffer)

## 7.2 Appendix 2: Culture of *M.tb* (H37RV)

The handling of pure cultures of Mycobacterium tuberculosis is the most hazardous procedure performed in the TB laboratory and therefore must only be performed by an experienced operator who is taking time and care over the procedure. Subculture must be done at the rear of the class II MSC and the MSC must be clutter-free at all times.

Subculture of *M.tb*

*M.tb* is cultured in 2mls Middlebrook 7H9 media in sealed 8ml falcons, held in racks in a secondary Bio jar. Bio jars are kept closed with zinc tape to ensure that they do not progressively loosen while shaking. Bio jars must never be opened outside the MSCs. *M.tb* will be sub-cultured weekly. 200, 300, 400, 600 and 800µl of *M.tb* suspension is transferred to fresh falcon tubes containing 2mls sterile 7H9 medium so that *M.tb* at the appropriate OD is available the following week for experiments.

*M.tb* Colony counts

Middle brook 7H11 agar plates will be used. Each plate is divided into 8, clearly labelled and infected with sequential dilutions of TB culture in the MSC. Plates are left to air dry for half an hour prior to stacking upside-down After placing in two secondary Petri dish sleeves and taping closed, they will be transferred to the incubator for culture. Plates must be regularly checked for contamination and discarded if contaminated. Plates will be autoclaved after 6 weeks.

Freezing *M.tb* stocks

Aliquot *M.tb* mixed with 30% glycerol into cryovials for freezing. Wipe the exterior of vials twice with gauze soaked in 70% ethanol. Place in secondary container (plastic Eppendorf box) and close carefully. Mark box with "*M.tb* stocks – danger of infection". Wipe exterior of secondary container with 70% ethanol. Place in -80°C freezer.

Killing of *M.tb* with ultraviolet light

This protocol is used to kill M. tuberculosis by exposure to high intensity UV light for 90 minutes, in order to use whole killed bacilli with intact extracellular proteins for experiments outside the CL3 suite. The following protocol has been optimised through 3 test runs in the CL3 suite at Imperial College Hammersmith and has been demonstrated to be efficacious.

Grow up multiple aliquots of 2mls *M.tb* in the shaking incubator.

When the optical density reaches 0.60 measured on the WPA cell density meter in the class II MSC, perform UV killing as described below. (OD =0.6 corresponds to 1 x $10^8$ CFU /ml)

Pipette 1ml *M.tb* broth into a 60mm sterile petri dish and seal carefully around the edge with parafilm. Ensure that the parafilm does not obscure the base of the Petri dish at any point. Slowly rotate the dish so that the *M.tb* forms a thin monolayer across the entire surface. Perform the same process for up to 8 petri dishes.

Keep a 100ul aliquot of *M.tb* as positive control for the culture confirmation of killing.

Carefully slide each Petri dish into a zip lock plastic bag. Each dish must be kept horizontal as it is placed in the zip lock bag. Carefully seal the zip lock bag along its entire length. This ensures the samples are double contained.

Dispose the outer gloves within the cabinet and put on new ones outside. Wipe the surface of the zip lock bag with 70% ethanol before removing them from the MSC and placing on the UV illuminator in class I or III microbiological safety cabinet (MSC).

Close the cover of the illuminator, turn to full power and switch on. Irradiate the *M.tb* for 90 minutes.

Place the zip lock bag back in the class II MSC.

Pipette all the UV killed *M.tb* into a single 15ml falcon, close the lid and invert to ensure that bacteria are fully mixed. All Petri dishes must be tested for sterility simultaneously, in case one UV bulb is underperforming.

Plate 100ul UV killed *M.tb* onto 3 separate 7H11 agar plates and spread with a sterile loop. Plate 100ul control untreated TB onto a fourth 7H11 agar plate.

Allow to air dry for 30 mins, double bag and place in the incubator at 37 degrees with plates inverted.

Aliquot the rest of the UV killed *M.tb* into screw-top Eppendorf's, label and place in a box. Label box with date and "UV-killed TB, awaiting culture confirmation of sterilization". Place the box at -80°C in containment laboratory. The samples must not be removed from the TB lab until sterility confirmed by culture.

Plates must be read at 6 weeks to confirm sterility. The positive control must show excellent *M.tb* growth and the UV treated plates must be completely devoid of any colonies. If either case is not fulfilled, samples must be discarded as efficacy of killing has not been proven.

If plates are sterile and *M.tb* has grown on positive control plate, then the aliquots frozen at -80°C are proven to be sterile and can be removed from the TB lab after external decontamination with 70% ethanol.

Each and every batch of UV-killed TB must be tested as above prior to release from the CL3 as the performance of UV bulbs may decline over time.

Although the UV illuminator has a protective lid and gaps will be covered, the UV killing should be during a time when the TB lab is not being used by others. Therefore, liaise with other users in advance of performing the

UV killing to identify a convenient time, perform during a 90 minute period when the lab will not be in use, and place the “BIOHAZARD NO ENTRY” sign on the door while the irradiation is underway.

## 7.3 Appendix 3: Manufacturer's protocols used

- High capacity cDNA Reverse Transcription Kit (Applied Biosystems™, #4374967)
- Taqman® Gene expression Assays (Applied Biosystems™)
- Protein assay kit, BCA Thermo Scientific Pierce (Life Technologies Ltd., # 10741395)
- Human cytokine 30-plex assay (Invitrogen)
- MMP multiplex assay (R&D Systems)
- MMP-1 and IL-8 DuoSet ELISA developing System (R and D systems)
- Cytotoxicity Detection Kit PLUS (LDH) (Roche, #04744926001)

## 7.4 Appendix 4: Software used

- SDS version 2.3 sequence detection systems (Applied Biosystems™).
- Graph Pad Prism version 5 (Graph Pad Software, San Diego California USA)
- qbase PLUS (Biogazelle)

# 8. LIST OF REFERENCES

ADAMS, D. O. 1975. Structure of Mononuclear Phagocytes Differentiating Invivo .2. Effect of Mycobacterium-Tuberculosis. *American Journal of Pathology,* 80**,** 101-116.

AKSOY, E., TABOUBI, S., TORRES, D., DELBAUVE, S., HACHANI, A., WHITEHEAD, M. A., PEARCE, W. P., BERENJENO-MARTIN, I., NOCK, G., FILLOUX, A., BEYAERT, R., FLAMAND, V. & VANHAESEBROECK, B. 2012. The p110delta isoform of the kinase PI(3)K controls the subcellular compartmentalization of TLR4 signaling and protects from endotoxic shock. *Nat Immunol,* 13**,** 1045-54.

ALQURASHI, N., HASHIMI, S. M. & WEI, M. Q. 2013. Chemical Inhibitors and microRNAs (miRNA) Targeting the Mammalian Target of Rapamycin (mTOR) Pathway: Potential for Novel Anticancer Therapeutics. *International Journal of Molecular Sciences,* 14**,** 3874-3900.

ANDREW DEVITT, O. D. M., CHANDRA RAYKUNDALIA, J. DONALD CAPRA, DAVID L. SIMMONS§ & CHRISTOPHER D. GREGORY 1998. Human CD14 mediates recognition and phagocytosis of apoptotic cells. *Nature,* 392**,** 505-509.

ANNE-CLAUDE GINGRAS, BRIAN RAUGHT, A. & SONENBERG, N. 1999. eIF4 Initiation Factors: Effectors of mRNA Recruitment to Ribosomes and Regulators of Translation. *Annual Review of Biochemistry,* 68**,** 913-963.

ARBIBE, L., MIRA, J. P., TEUSCH, N., KLINE, L., GUHA, M., MACKMAN, N., GODOWSKI, P. J., ULEVITCH, R. J. & KNAUS, U. G. 2000. Toll-like receptor 2-mediated NF-kappa B activation requires a Racl-dependent pathway. *Nature Immunology,* 1**,** 533-540.

ARTHUR W. CLARKA, C. A. K., SHAO-SUN BOUA, KEVIN R. CHAPMANA, DYLAN R. EDWARDSB 1997. Increased gelatinase A (MMP-2) and gelatinase B (MMP-9)

activities in human brain after focal ischemia. *Neuroscience Letters* 238**,** 53-56.

BAIN, J., PLATER, L., ELLIOTT, M., SHPIRO, N., HASTIE, C J., MCLAUCHLAN, H., KLEVERNIC, I., ARTHUR, J SIMON C., ALESSI, DARIO R. & COHEN, P. 2007. The selectivity of protein kinase inhibitors: a further update. *The Biochemical Journal,* 408**,** 297-315.

BAO, Y., LIN, C., REN, J. & LIU, J. 2013. MicroRNA-384-5p regulates ischemia-induced cardioprotection by targeting phosphatidylinositol-4,5-bisphosphate 3-kinase, catalytic subunit delta (PI3K p110δ). *Apoptosis,* 18**,** 260-270.

BARKSBY, H. E., MILNER, J. M., PATTERSON, A. M., PEAKE, N. J., HUI, W., ROBSON, T., LAKEY, R., MIDDLETON, J., CAWSTON, T. E., RICHARDS, C. D. & ROWAN, A. D. 2006. Matrix metalloproteinase 10 promotion of collagenolysis via procollagenase activation: implications for cartilage degradation in arthritis. *Arthritis Rheum,* 54**,** 3244-53.

BARMINA, O. Y., WALLING, H. W., FIACCO, G. J., FREIJE, J. M., LOPEZ-OTIN, C., JEFFREY, J. J. & PARTRIDGE, N. C. 1999. Collagenase-3 binds to a specific receptor and requires the low density lipoprotein receptor-related protein for internalization. *J Biol Chem,* 274**,** 30087-93.

BARTEL , D. P. 2004. MicroRNAs: Genomics, Biogenesis, Mechanism, and Function *cell,* 116**,** 281-297.

BARTEL, D. P. 2004. MicroRNAs: genomics, biogenesis, mechanism, and function. *Cell,* 116**,** 281-97.

BEHR, M. A. 1999. Transmission of Mycobacterium tuberculosis from patients smear-negative for acid-fast bacilli (vol 353, pg 444, 1999). *Lancet,* 353**,** 1714-1714.

BEHR, M. A., WARREN, S. A., SALAMON, H., HOPEWELL, P. C., DE LEON, A. P., DALEY, C. L. & SMALL, P. M. 1999. Transmission of Mycobacterium tuberculosis from patients smear-negative for acid-fast bacilli. *Lancet,* 353**,** 444-449.

BENATOR, D., BHATTACHARYA, M., BOZEMAN, L., BURMAN, W., CANTAZARO, A., CHAISSON, R., GORDIN, F., HORSBURGH, C. R., HORTON, J., KHAN, A., LAHART, C., METCHOCK, B., PACHUCKI, C., STANTON, L., VERNON, A., VILLARINO, M. E., WANG, Y. C., WEINER, M. & WEIS, S. 2002. Rifapentine and isoniazid once a week versus rifampicin and isoniazid twice a week for treatment of drug-susceptible pulmonary tuberculosis in HIV-negative patients: a randomised clinical trial. *Lancet,* 360**,** 528-34.

BENTWICH, I. B., Z. ET AL 2005. Identification of hundreds of conserved and nonconserved human microRNAs. *Nat Genet,* 37**,** 766-70.

BHASKAR, P. T. & HAY, N. 2007. The two TORCs and Akt. *Dev Cell,* 12**,** 487-502.

BODE, W., GOMIS-RUTH, F. X. & STOCKLER, W. 1993. Astacins, serralysins, snake venom and matrix metalloproteinases exhibit identical zinc-

binding environments (HEXXHXXGXXH and Met-turn) and topologies and should be grouped into a common family, the 'metzincins'. . *FEBS Lett. ,* 331**,** 34-140

BOMMHARDT, U., CHANG, K. C., SWANSON, P. E., WAGNER, T. H., TINSLEY, K. W., KARL, I. E. & HOTCHKISS, R. S. 2004. Akt decreases lymphocyte apoptosis and improves survival in sepsis. *J Immunol,* 172**,** 7583-91.

BRACE, P. T., TEZERA, L. B., BIELECKA, M. K., MELLOWS, T., GARAY, D., TIAN, S., RAND, L., GREEN, J., JOGAI, S., STEELE, A. J., MILLAR, T. M., SANCHEZ-ELSNER, T., FRIEDLAND, J. S., PROUD, C. G. & ELKINGTON, P. T. 2017. Mycobacterium tuberculosis subverts negative regulatory pathways in human macrophages to drive immunopathology. *PLoS Pathog,* 13**,** e1006367.

BRENNAN, F. & FOEY, A. 2002. Cytokine regulation in RA synovial tissue: role of T cell/macrophage contact-dependent interactions. *Arthritis Res,* 4 Suppl 3**,** S177-82.

BRIGHT, S. & MUNRO, A. J. 1981. Studies on the role of HLA-DR in macrophage-T cell interactions. *Tissue Antigens,* 18**,** 217-231.

BRINCKERHOFF, C. E. & MATRISIAN, L. M. 2002. Matrix metalloproteinases: a tail of a frog that became a prince. *Nat Rev Mol Cell Biol,* 3**,** 207-14.

BROWN, J., WANG, H., SUTTLES, J., GRAVES, D. T. & MARTIN, M. 2011. Mammalian target of rapamycin complex 2 (mTORC2) negatively regulates Toll-like receptor 4-mediated inflammatory response via FoxO1. *J Biol Chem,* 286**,** 44295-305.

BU, X., HAAS, D. W. & HAGEDORN, C. H. 1993. Novel phosphorylation sites of eukaryotic initiation factor-4F and evidence that phosphorylation stabilizes interactions of the p25 and p220 subunits. *J Biol Chem,* 268**,** 4975-8.

BUISSON, A.-C., ZAHM, J.-M., POLETTE, M., PIERROT, D., BELLON, G., PUCHELLE, E., BIREMBAUT, P. & TOURNIER, J.-M. 1996. Gelatinase B is involved in the in vitro wound repair of human respiratory epithelium. *Journal of Cellular Physiology,* 166**,** 413-426.

BUXADE, M., MORRICE, N., KREBS, D. L. & PROUD, C. G. 2008. The PSF.p54nrb complex is a novel Mnk substrate that binds the mRNA for tumor necrosis factor alpha. *J Biol Chem,* 283**,** 57-65.

BUXADE, M., PARRA, J. L., ROUSSEAU, S., SHPIRO, N., MARQUEZ, R., MORRICE, N., BAIN, J., ESPEL, E. & PROUD, C. G. 2005. The Mnks are

novel components in the control of TNF alpha biosynthesis and phosphorylate and regulate hnRNP A1. *Immunity,* 23**,** 177-89.

CABRITA, M. A. & CHRISTOFORI, G. 2008. Sprouty proteins, masterminds of receptor tyrosine kinase signaling. *Angiogenesis,* 11**,** 53-62.

CANTLEY, L. C. 2002. The phosphoinositide 3-kinase pathway. *Science,* 296**,** 1655-7.

CARLOS S. SUBAUSTE, R. D. W. M. A. F. F. 1998 Role of CD80 (B7.1) and CD86 (B7.2) in the Immune Response to an Intracellular Pathogen. *J Immunol ;,* 160**,** 1831-1840;

CHANG, J. C., WYSOCKI, A., TCHOU-WONG, K. M., MOSKOWITZ, N., ZHANG, Y. & ROM, W. N. 1996. Effect of Mycobacterium tuberculosis and its components on macrophages and the release of matrix metalloproteinases. *Thorax,* 51**,** 306-11.

CHANTRY, D., VOJTEK, A., KASHISHIAN, A., HOLTZMAN, D. A., WOOD, C., GRAY, P. W., COOPER, J. A. & HOEKSTRA, M. F. 1997. p110δ, a Novel Phosphatidylinositol 3-Kinase Catalytic Subunit That Associates with p85 and Is Expressed Predominantly in Leukocytes. *Journal of Biological Chemistry,* 272**,** 19236-19241.

CHOI, J., CHEN, J., SCHREIBER, S. L. & CLARDY, J. 1996. Structure of the FKBP12-Rapamycin Complex Interacting with Binding Domain of Human FRAP. *Science,* 273**,** 239-242.

CHRESTENSEN, C. A., ESCHENROEDER, A., ROSS, W. G., UEDA, T., WATANABE-FUKUNAGA, R., FUKUNAGA, R. & STURGILL, T. W. 2007. Loss of MNK function sensitizes fibroblasts to serum-withdrawal induced apoptosis. *Genes Cells,* 12**,** 1133-40.

COOPER, A. M., MAGRAM, J., FERRANTE, J. & ORME, I. M. 1997. Interleukin 12 (IL-12) is crucial to the development of protective immunity in mice intravenously infected with mycobacterium tuberculosis. *J Exp Med,* 186**,** 39-45.

COOPER, A. M., PEARL, J. E., BROOKS, J. V., EHLERS, S. & ORME, I. M. 2000. Expression of the nitric oxide synthase 2 gene is not essential for early control of Mycobacterium tuberculosis in the murine lung. *Infect Immun,* 68**,** 6879-82.

CORBETT, E. L., WATT, C. J., WALKER, N., MAHER, D., WILLIAMS, B. G., RAVIGLIONE, M. C. & DYE, C. 2003. The growing burden of tuberculosis: global trends and interactions with the HIV epidemic. *Arch Intern Med,* 163**,** 1009-21.

CRAWFORD, H. C. & MATRISIAN, L. M. 1996. Mechanisms controlling the transcription of matrix metalloproteinase genes in normal and neoplastic cells. *Enzyme Protein,* 49**,** 20-37.

CRYSTAL, R. G., J. B. WEST. 1997. The Lung: Scientific Foundations 1997 Lippincott, Philadelphia.

D'ARMIENTO, J., DALAL, S. S., OKADA, Y., BERG, R. A. & CHADA, K. 1992a. Collagenase expression in the lungs of transgenic mice causes pulmonary emphysema. *Cell,* 71**,** 955-961.

D'ARMIENTO, J., DALAL, S. S., OKADA, Y., BERG, R. A. & CHADA, K. 1992b. Collagenase expression in the lungs of transgenic mice causes pulmonary emphysema. *Cell,* 71**,** 955-61.

DAIGNEAULT, M., PRESTON, J. A., MARRIOTT, H. M., WHYTE, M. K. B. & DOCKRELL, D. H. 2010. The Identification of Markers of Macrophage Differentiation in PMA-Stimulated THP-1 Cells and Monocyte-Derived Macrophages. *PLoS ONE,* 5**,** e8668.

DANNENBERG, A. M., JR. 2009. Liquefaction and cavity formation in pulmonary TB: a simple method in rabbit skin to test inhibitors. *Tuberculosis (Edinb),* 89**,** 243-7.

DANNENBERG, A. M., JR. & SUGIMOTO, M. 1976. Liquefaction of caseous foci in tuberculosis. *Am Rev Respir Dis,* 113**,** 257-9.

DAVID, H. L. 1970. Probability distribution of drug-resistant mutants in unselected populations of Mycobacterium tuberculosis. *Appl Microbiol,* 20**,** 810-4.

DAVIDSON, J. M. 1990. Biochemistry and turnover of lung interstitium *Eur Respir J* 3**,** 1048-1068.

DELCLAUX, C., DELACOURT, C., D'ORTHO, M. P., BOYER, V., LAFUMA, C. & HARF, A. 1996. Role of gelatinase B and elastase in human polymorphonuclear neutrophil migration across basement membrane. *American Journal of Respiratory Cell and Molecular Biology,* 14**,** 288-295.

DEMEDTS, I. K., MOREL-MONTERO, A., LEBECQUE, S., PACHECO, Y., CATALDO, D., JOOS, G. F., PAUWELS, R. A. & BRUSSELLE, G. G. 2006. Elevated MMP-12 protein levels in induced sputum from patients with COPD. *Thorax,* 61**,** 196-201.

DI PAOLO, G. & DE CAMILLI, P. 2006. Phosphoinositides in cell regulation and membrane dynamics. *Nature,* 443**,** 651-7.

DINARELLO, C. A. 2009. Immunological and inflammatory functions of the interleukin-1 family. *Annu Rev Immunol,* 27**,** 519-50.

DOSTIE, J., FERRAIUOLO, M., PAUSE, A., ADAM, S. A. & SONENBERG, N. 2000. A novel shuttling protein, 4E-T, mediates the nuclear import of the mRNA 5' cap-binding protein, eIF4E. *EMBO J,* 19**,** 3142-56.

DOWLING, R. J., TOPISIROVIC, I., ALAIN, T., BIDINOSTI, M., FONSECA, B. D., PETROULAKIS, E., WANG, X., LARSSON, O., SELVARAJ, A., LIU, Y., KOZMA, S. C., THOMAS, G. & SONENBERG, N. 2010. mTORC1-mediated cell proliferation, but not cell growth, controlled by the 4E-BPs. *Science,* 328**,** 1172-6.

DYE, C. W., B. G. 2010. The population dynamics and control of tuberculosis. *Science,* 328**,** 856-61.

EHLERS, S. & SCHAIBLE, U. E. 2013. The granuloma in tuberculosis: Dynamics of a host-pathogen collusion. *Frontiers in Immunology,* 3.

ELKINGTON, P., SHIOMI, T., BREEN, R., NUTTALL, R. K., UGARTE-GIL, C. A., WALKER, N. F., SARAIVA, L., PEDERSEN, B., MAURI, F., LIPMAN, M., EDWARDS, D. R., ROBERTSON, B. D., D'ARMIENTO, J. & FRIEDLAND, J. S. 2011a. MMP-1 drives immunopathology in human tuberculosis and transgenic mice. *J Clin Invest,* 121**,** 1827-33.

ELKINGTON, P. T., D'ARMIENTO, J. M. & FRIEDLAND, J. S. 2011b. Tuberculosis immunopathology: the neglected role of extracellular matrix destruction. *Sci Transl Med,* 3**,** 71ps6.

ELKINGTON, P. T., GREEN, J. A., EMERSON, J. E., LOPEZ-PASCUA, L. D., BOYLE, J. J., O'KANE, C. M. & FRIEDLAND, J. S. 2007. Synergistic Up-Regulation of Epithelial Cell Matrix Metalloproteinase-9 Secretion in Tuberculosis. *American Journal of Respiratory Cell and Molecular Biology,* 37**,** 431-437.

ELKINGTON, P. T., GREEN, J. A. & FRIEDLAND, J. S. 2009. Analysis of matrix metalloproteinase secretion by macrophages. *Methods Mol Biol,* 531**,** 253-65.

ELKINGTON, P. T., UGARTE-GIL, C. A. & FRIEDLAND, J. S. 2011c. Matrix metalloproteinases in tuberculosis. *Eur Respir J,* 38**,** 456-64.

ELKINGTON, P. T. G. & FRIEDLAND, J. S. 2006. Matrix metalloproteinases in destructive pulmonary pathology. *Thorax,* 61**,** 259-266.

ELKINGTON, P. T. G., NUTTALL, R. K., BOYLE, J. J., O'KANE, C. M., HORNCASTLE, D. E., EDWARDS, D. R. & FRIEDLAND, J. S. 2005. Mycobacterium tuberculosis, but Not Vaccine BCG, Specifically Upregulates Matrix Metalloproteinase-1. *American Journal of Respiratory and Critical Care Medicine,* 172**,** 1596-1604.

FABRIEK, B. O., DIJKSTRA, C. D. & VAN DEN BERG, T. K. 2005. The macrophage scavenger receptor CD163. *Immunobiology,* 210**,** 153-60.

FABRIEK, B. O., VAN BRUGGEN, R., DENG, D. M., LIGTENBERG, A. J., NAZMI, K., SCHORNAGEL, K., VLOET, R. P., DIJKSTRA, C. D. & VAN DEN BERG, T. K. 2009. The macrophage scavenger receptor CD163 functions as an innate immune sensor for bacteria. *Blood,* 113**,** 887-92.

FANG, Y., XUE, J.-L., SHEN, Q., CHEN, J. & TIAN, L. 2012. MicroRNA-7 inhibits tumor growth and metastasis by targeting the phosphoinositide 3-kinase/Akt pathway in hepatocellular carcinoma. *Hepatology,* 55**,** 1852-1862.

FENG, G. J., GOODRIDGE, H. S., HARNETT, M. M., WEI, X. Q., NIKOLAEV, A. V., HIGSON, A. P. & LIEW, F. Y. 1999. Extracellular signal-related kinase (ERK) and p38 mitogen-activated protein (MAP) kinases differentially regulate the lipopolysaccharide-mediated induction of inducible nitric oxide synthase and IL-12 in macrophages: Leishmania phosphoglycans subvert macrophage IL-12 production by targeting ERK MAP kinase. *Journal of Immunology,* 163**,** 6403-6412.

FENHALLS, G., STEVENS, L., MOSES, L., BEZUIDENHOUT, J., BETTS, J. C., HELDEN PV, P., LUKEY, P. T. & DUNCAN, K. 2002. In situ detection of Mycobacterium tuberculosis transcripts in human lung granulomas reveals differential gene expression in necrotic lesions. *Infect Immun,* 70**,** 6330-8.

FINKELMAN, F. D., SHEA-DONOHUE, T., GOLDHILL, J., SULLIVAN, C. A., MORRIS, S. C., MADDEN, K. B., GAUSE, W. C. & URBAN, J. F., JR. 1997. Cytokine regulation of host defense against parasitic gastrointestinal nematodes: lessons from studies with rodent models. *Annu Rev Immunol,* 15**,** 505-33.

FINLAY G. A., KENNETH J RUSSELL, KEVIN J MCMAHON, ELIZABETH M D'ARCY, JAMES B MASTERSON, MUIRIS X FITZGERALD, CLARE M O'CONNOR 1997. Elevated levels of matrix metalloproteinases inbronchoalveolar lavage fluid of emphysematous patients *Thorax,* 52**,** 502-506.

FINLAY, G. A., RUSSELL, K. J., MCMAHON, K. J., D'ARCY E, M., MASTERSON, J. B., FITZGERALD, M. X. & O'CONNOR, C. M. 1997. Elevated levels of matrix metalloproteinases in bronchoalveolar lavage fluid of emphysematous patients. *Thorax,* 52**,** 502-6.

FLETCHER, C. & PETO, R. 1977. The natural history of chronic airflow obstruction. *Br Med J,* 1**,** 1645-8.

FLYNN, A. & PROUD, C. G. 1995. Serine 209, not serine 53, is the major site of phosphorylation in initiation factor eIF-4E in serum-treated Chinese hamster ovary cells. *J Biol Chem,* 270**,** 21684-8.

FOEY, A., GREEN, P., FOXWELL, B., FELDMANN, M. & BRENNAN, F. 2002. Cytokine-stimulated T cells induce macrophage IL-10 production dependent on phosphatidylinositol 3-kinase and p70S6K: implications for rheumatoid arthritis. *Arthritis Res,* 4**,** 64-70.

FORONJY, R. F., OKADA, Y., COLE, R. & D'ARMIENTO, J. 2003. Progressive adult-onset emphysema in transgenic mice expressing human MMP-1 in the lung. *American Journal of Physiology - Lung Cellular and Molecular Physiology,* 284**,** L727-L737.

FRIEDLAND, J. S., SHAW, T. C., PRICE, N. M. & DAYER, J. M. 2002. Differential regulation of MMP-1/9 and TIMP-1 secretion in human monocytic cells in response to Mycobacterium tuberculosis. *Matrix Biology,* 21**,** 103-110.

FUKAO, T. & KOYASU, S. 2003. PI3K and negative regulation of TLR signaling. *Trends in Immunology,* 24**,** 358-363.

FUKAO, T., TANABE, M., TERAUCHI, Y., OTA, T., MATSUDA, S., ASANO, T., KADOWAKI, T., TAKEUCHI, T. & KOYASU, S. 2002. PI3K-mediated negative feedback regulation of IL-12 production in DCs. *Nat Immunol,* 3**,** 875-81.

FURIC, L., RONG, L., LARSSON, O., KOUMAKPAYI, I. H., YOSHIDA, K., BRUESCHKE, A., PETROULAKIS, E., ROBICHAUD, N., POLLAK, M., GABOURY, L. A., PANDOLFI, P. P., SAAD, F. & SONENBERG, N. 2010. eIF4E phosphorylation promotes tumorigenesis and is associated with prostate cancer progression. *Proc Natl Acad Sci U S A,* 107**,** 14134-9.

GASCHE, Y., COPIN, J. C., SUGAWARA, T., FUJIMURA, M. & CHAN, P. H. 2001. Matrix metalloproteinase inhibition prevents oxidative stress-associated blood-brain barrier disruption after transient focal cerebral ischemia. *J Cereb Blood Flow Metab,* 21**,** 1393-400.

GATELY, M. K., RENZETTI, L. M., MAGRAM, J., STERN, A. S., ADORINI, L., GUBLER, U. & PRESKY, D. H. 1998. The interleukin-12/interleukin-12-receptor system: role in normal and pathologic immune responses. *Annu Rev Immunol,* 16**,** 495-521.

GREEN, J. A., DHOLAKIA, S., JANCZAR, K., ONG, C. W. M., MOORES, R., FRY, J., ELKINGTON, P. T., RONCAROLI, F. & FRIEDLAND, J. S. 2011. Mycobacterium tuberculosis-infected human monocytes down-regulate microglial MMP-2 secretion in CNS tuberculosis via TNFα, NFκB, p38 and caspase 8 dependent pathways. *Journal of Neuroinflammation,* 8**,** 46-46.

GREENLEE, K. J., WERB, Z. & KHERADMAND, F. 2007. Matrix metalloproteinases in lung: multiple, multifarious, and multifaceted. *Physiol Rev,* 87**,** 69-98.

GREGORY, I. R. S., R. ET AL 2005. Human RISC Couples MicroRNA Biogenesisand Posttranscriptional Gene Silencing *Cell* 123**,** 631 – 640.

GREGORY, R. I., CHENDRIMADA, T. P., COOCH, N. & SHIEKHATTAR, R. 2005. Human RISC couples microRNA biogenesis and posttranscriptional gene silencing. *Cell,* 123**,** 631-40.

GRIFFITHS-JONES, S., ET AL 2008. Micro RNA Research, fundamentals, Reviews and perspective. (Exiqon Collection Booklet_V5). 1-20.

GROSS, J. L., C. M. 1962. Collagenolytic activity in amphibian tissues: a tissue culture assay. . *Proc. Natl Acad. Sci. USA* 47**,** 1014-1022.

GUERTIN, D. A. & SABATINI, D. M. 2007. Defining the role of mTOR in cancer. *Cancer Cell,* 12**,** 9-22.

GUHA, M. & MACKMAN, N. 2002. The phosphatidylinositol 3-kinase-Akt pathway limits lipopolysaccharide activation of signaling pathways and expression of inflammatory mediators in human monocytic cells. *J Biol Chem,* 277**,** 32124-32.

GUIRADO, E., SCHLESINGER, L. S. & KAPLAN, G. 2013. Macrophages in tuberculosis: friend or foe. *Semin Immunopathol,* 35**,** 563-83.

GUIRADO, E., SCHLESINGER,LARRY 2013. Modeling the Mycobacterium tuberculosis granuloma – The critical battlefield in host immunity and disease. *Frontiers in Immunology,* 4**,** 1-7.

HAY, N. 2010. Mnk earmarks eIF4E for cancer therapy. *Proc Natl Acad Sci U S A,* 107**,** 13975-6.

HE, L. & HANNON, G. J. 2004. MicroRNAs: small RNAs with a big role in gene regulation. *Nat Rev Genet,* 5**,** 522-31.

HELKE, K. L., MANKOWSKI, J. L. & MANABE, Y. C. 2006. Animal models of cavitation in pulmonary tuberculosis. *Tuberculosis,* 86**,** 337-348.

HELMING, L. & GORDON, S. 2007. The molecular basis of macrophage fusion. *Immunobiology,* 212**,** 785-793.

HERMAN, S. E. M., GORDON, A. L., WAGNER, A. J., HEEREMA, N. A., ZHAO, W., FLYNN, J. M., JONES, J., ANDRITSOS, L., PURI, K. D., LANNUTTI, B. J., GIESE, N. A., ZHANG, X., WEI, L., BYRD, J. C. & JOHNSON, A. J. 2010. Phosphatidylinositol 3-kinase-δ inhibitor CAL-101 shows promising preclinical activity in chronic lymphocytic leukemia by antagonizing intrinsic and extrinsic cellular survival signals. *Blood,* 116**,** 2078-2088.

HESTVIK, A. L., HMAMA, Z. & AV-GAY, Y. 2005. Mycobacterial manipulation of the host cell. *FEMS Microbiol Rev,* 29**,** 1041-50.

HETZEL, M., WALCHER, D., GRUB, M., BACH, H., HOMBACH, V. & MARX, N. 2003. Inhibition of MMP-9 expression by PPARgamma activators in human bronchial epithelial cells. *Thorax,* 58**,** 778-83.

HIREMATH, L. S., WEBB, N. R. & RHOADS, R. E. 1985. Immunological detection of the messenger RNA cap-binding protein. *J Biol Chem,* 260**,** 7843-9.

HIRSCH, E., KATANAEV, V. L., GARLANDA, C., AZZOLINO, O., PIROLA, L., SILENGO, L., SOZZANI, S., MANTOVANI, A., ALTRUDA, F. & WYMANN, M. P. 2000. Central role for G protein-coupled phosphoinositide 3-kinase gamma in inflammation. *Science,* 287**,** 1049-53.

HOU, J., LAM, F., PROUD, C. & WANG, S. 2012. Targeting Mnks for cancer therapy. *Oncotarget,* 3**,** 118-31.

HU, S. I., KATZ, M., CHIN, S., QI, X., CRUZ, J., IBEBUNJO, C., ZHAO, S., CHEN, A. & GLASS, D. J. 2012. MNK2 inhibits eIF4G activation through a pathway involving serine-arginine-rich protein kinase in skeletal muscle. *Sci Signal,* 5**,** ra14.

HUANG, H. & TINDALL, D. J. 2011. Regulation of FOXO protein stability via ubiquitination and proteasome degradation. *Biochimica et Biophysica Acta (BBA) - Molecular Cell Research,* 1813**,** 1961-1964.

HUBER, K., CHRIST, G., WOJTA, J. & GULBA, D. 2001. Plasminogen activator inhibitor type-1 in cardiovascular disease - Status report 2001. *Thrombosis Research,* 103**,** S7-S19.

HWANG, H. W. & MENDELL, J. T. 2006. MicroRNAs in cell proliferation, cell death, and tumorigenesis. *Br J Cancer,* 94**,** 776-80.

HWANG, H. W. A. M., J. T. 2006. MicroRNAs in cell proliferation, cell death, and tumorigenesis. *Br J Cancer,* 94**,** 776-80.

IMAI, K., YOKOHAMA, Y., NAKANISHI, I., OHUCHI, E., FUJII, Y., NAKAI, N. & OKADA, Y. 1995. Matrix Metalloproteinase 7 (Matrilysin) from Human Rectal Carcinoma Cells: ACTIVATION OF THE PRECURSOR, INTERACTION WITH OTHER MATRIX METALLOPROTEINASES AND ENZYMIC PROPERTIES. *Journal of Biological Chemistry,* 270**,** 6691-6697.

JASTI S.RAO, P. S., SANJEEVA MOHANAM,WILLIAMG.STETLER-STEVENSON, LANCEA.LIOTTA, AND & SAWAVA, R. 1993. Elevated LevelsofMr92,000 TypeIV Collagenase in HumanBrainTumors. *CANCER RESEARCH* 53**,** 2208-2211.

JAYARAMAN, P., SADA-OVALLE, I., NISHIMURA, T., ANDERSON, A. C., KUCHROO, V. K., REMOLD, H. G. & BEHAR, S. M. 2013. IL-1beta promotes antimicrobial immunity in macrophages by regulating TNFR signaling and caspase-3 activation. *J Immunol,* 190**,** 4196-204.

JO, E. K., YANG, C. S., CHOI, C. H. & HARDING, C. V. 2007. Intracellular signalling cascades regulating innate immune responses to Mycobacteria: branching out from Toll-like receptors. *Cellular Microbiology,* 9**,** 1087-1098.

JOSHI, S., KAUR, S., REDIG, A. J., GOLDSBOROUGH, K., DAVID, K., UEDA, T., WATANABE-FUKUNAGA, R., BAKER, D. P., FISH, E. N., FUKUNAGA, R. & PLATANIAS, L. C. 2009. Type I interferon (IFN)-dependent activation of Mnk1 and its role in the generation of growth inhibitory responses. *Proc Natl Acad Sci U S A,* 106**,** 12097-102.

JOSHI, S., SHARMA, B., KAUR, S., MAJCHRZAK, B., UEDA, T., FUKUNAGA, R., VERMA, A. K., FISH, E. N. & PLATANIAS, L. C. 2011. Essential role for Mnk kinases in type II interferon (IFNgamma) signaling and its suppressive effects on normal hematopoiesis. *J Biol Chem,* 286**,** 6017-26.

JUFFERMANS, N. P., FLORQUIN, S., CAMOGLIO, L., VERBON, A., KOLK, A. H., SPEELMAN, P., VAN DEVENTER, S. J. & VAN DER POLL, T. 2000.

Interleukin-1 signaling is essential for host defense during murine pulmonary tuberculosis. *J Infect Dis,* 182**,** 902-8.

JUSTILIEN, V., REGALA, R. P., TSENG, I. C., WALSH, M. P., BATRA, J., RADISKY, E. S., MURRAY, N. R. & FIELDS, A. P. 2012. Matrix Metalloproteinase-10 Is Required for Lung Cancer Stem Cell Maintenance, Tumor Initiation and Metastatic Potential. *PLoS ONE,* 7**,** e35040.

KATO-MAEDA, M., RHEE, J. T., GINGERAS, T. R., SALAMON, H., DRENKOW, J., SMITTIPAT, N. & SMALL, P. M. 2001. Comparing genomes within the species Mycobacterium tuberculosis. *Genome Res,* 11**,** 547-54.

KESSENBROCK, K., PLAKS, V. & WERB, Z. 2010. Matrix metalloproteinases: regulators of the tumor microenvironment. *Cell,* 141**,** 52-67.

KHAZEN, W. M. B. J., P. TOMKIEWICZ, C. BENELLI, C. CHANY, C. ACHOUR, A. FOREST, C. 2005. Expression of macrophage-selective markers in human and rodent adipocytes. *FEBS Lett,* 579**,** 5631-4.

KLOPPER, M., WARREN, R. M., HAYES, C., GEY VAN PITTIUS, N. C., STREICHER, E. M., MULLER, B., SIRGEL, F. A., CHABULA-NXIWENI, M., HOOSAIN, E., COETZEE, G., DAVID VAN HELDEN, P., VICTOR, T. C. & TROLLIP, A. P. 2013. Emergence and spread of extensively and totally drug-resistant tuberculosis, South Africa. *Emerg Infect Dis,* 19**,** 449-55.

KNAUF, U., TSCHOPP, C. & GRAM, H. 2001. Negative regulation of protein translation by mitogen-activated protein kinase-interacting kinases 1 and 2. *Mol Cell Biol,* 21**,** 5500-11.

KOHLER, H. P. & GRANT, P. J. 2000. Mechanisms of disease: Plasminogen-activator inhibitor type 1 and coronary artery disease. *New England Journal of Medicine,* 342**,** 1792-1801.

KURIG, B., SHYMANETS, A., BOHNACKER, T., PRAJWAL, BROCK, C., AHMADIAN, M. R., SCHAEFER, M., GOHLA, A., HARTENECK, C., WYMANN, M. P., JEANCLOS, E. & NURNBERG, B. 2009. Ras is an indispensable coregulator of the class IB phosphoinositide 3-kinase p87/p110gamma. *Proc Natl Acad Sci U S A,* 106**,** 20312-7.

LAPLANTE, M. & SABATINI, D. M. 2012. mTOR signaling in growth control and disease. *Cell,* 149**,** 274-93.

LAW, K., WEIDEN, M., HARKIN, T., TCHOU-WONG, K., CHI, C. & ROM, W. N. 1996. Increased release of interleukin-1 beta, interleukin-6, and tumor necrosis factor-alpha by bronchoalveolar cells lavaged from

involved sites in pulmonary tuberculosis. *Am J Respir Crit Care Med,* 153**,** 799-804.

LEE, T. & PELLETIER, J. 2011. Eukaryotic initiation factor 4F: a vulnerability of tumor cells. *Future Medicinal Chemistry,* 4**,** 19-31.

LEPPERT, D., LEIB, S. L., GRYGAR, C., MILLER, K. M., SCHAAD, U. B. & HOLLANDER, G. A. 2000. Matrix metalloproteinase (MMP)-8 and MMP-9 in cerebrospinal fluid during bacterial meningitis: association with blood-brain barrier damage and neurological sequelae. *Clin Infect Dis,* 31**,** 80-4.

LI, Y., YUE, P., DENG, X., UEDA, T., FUKUNAGA, R., KHURI, F. R. & SUN, S. Y. 2010. Protein phosphatase 2A negatively regulates eukaryotic initiation factor 4E phosphorylation and eIF4F assembly through direct dephosphorylation of Mnk and eIF4E. *Neoplasia,* 12**,** 848-55.

LITHERLAND, G. J., DIXON, C., LAKEY, R. L., ROBSON, T., JONES, D., YOUNG, D. A., CAWSTON, T. E. & ROWAN, A. D. 2008. Synergistic collagenase expression and cartilage collagenolysis are phosphatidylinositol 3-kinase/Akt signaling-dependent. *J Biol Chem,* 283**,** 14221-9.

LUGO-VILLARINO, G., HUDRISIER, D., BENARD, A. & NEYROLLES, O. 2012. Emerging trends in the formation and function of tuberculosis granulomas. *Front Immunol,* 3**,** 405.

M.K. MATYSZAK *, V. H. P. 1996. hypersensitivity lesions in the central nervous system are prevented by inhibitors of matrix metalloproteinases. *Journal of Neuroimmunology,* 69**,** 141-149.

MAITI, D., BHATTACHARYYA, A. & BASU, J. 2001. Lipoarabinomannan from Mycobacterium tuberculosis Promotes Macrophage Survival by Phosphorylating Bad through a Phosphatidylinositol 3-Kinase/Akt Pathway. *Journal of Biological Chemistry,* 276**,** 329-333.

MALEMUD, C. J. 2006. Matrix metalloproteinases (MMPs) in health and disease: an overview *Frontiers in Bioscience* 11**,** 11, 1696-1701.

MALIK, Z. A., DENNING, G. M. & KUSNER, D. J. 2000. Inhibition of Ca(2+) signaling by Mycobacterium tuberculosis is associated with reduced phagosome-lysosome fusion and increased survival within human macrophages. *J Exp Med,* 191**,** 287-302.

MANCINI, J. A. D. B. A. 2006. Transcriptional regulation of matrix metalloprotease gene expression in health and disease *Frontiers in Bioscience* 11**,** 423-446

MARTELLI, A. M., EVANGELISTI, C., CHAPPELL, W., ABRAMS, S. L., BASECKE, J., STIVALA, F., DONIA, M., FAGONE, P., NICOLETTI, F., LIBRA, M., RUVOLO, V., RUVOLO, P., KEMPF, C. R., STEELMAN, L. S. & MCCUBREY, J. A. 2011. Targeting the translational apparatus to improve leukemia therapy: roles of the PI3K/PTEN/Akt/mTOR pathway. *Leukemia,* 25**,** 1064-1079.

MARTIN, M., REHANI, K., JOPE, R. S. & MICHALEK, S. M. 2005. Toll-like receptor-mediated cytokine production is differentially regulated by glycogen synthase kinase 3. *Nat Immunol,* 6**,** 777-84.

MARTIN, M., SCHIFFERLE, R. E., CUESTA, N., VOGEL, S. N., KATZ, J. & MICHALEK, S. M. 2003. Role of the phosphatidylinositol 3 kinase-Akt pathway in the regulation of IL-10 and IL-12 by Porphyromonas gingivalis lipopolysaccharide. *J Immunol,* 171**,** 717-25.

MARTINEZ-POMARES, L. P., N. MCKNIGHT, A. J. DA SILVA, R. P.GORDON, S. 1996. Macrophage Membrane Molecules: Markers of Tissue Differentiation and Heterogeneity. *Immunobiology,* 195**,** 407-416.

MARTINEZ, A. N., MEHRA, S. & KAUSHAL, D. 2013. Role of interleukin 6 in innate immunity to Mycobacterium tuberculosis infection. *J Infect Dis,* 207**,** 1253-61.

MAYER-BARBER, K. D., BARBER, D. L., SHENDEROV, K., WHITE, S. D., WILSON, M. S., CHEEVER, A., KUGLER, D., HIENY, S., CASPAR, P., NUNEZ, G., SCHLUETER, D., FLAVELL, R. A., SUTTERWALA, F. S. & SHER, A. 2010. Caspase-1 independent IL-1beta production is critical for host resistance to mycobacterium tuberculosis and does not require TLR signaling in vivo. *J Immunol,* 184**,** 3326-30.

MENDOZA, M. C., ER, E. E. & BLENIS, J. 2011. The Ras-ERK and PI3K-mTOR pathways: cross-talk and compensation. *Trends in Biochemical Sciences,* 36**,** 320-328.

MIGLIORI GB, D. I. G., BESOZZI G, CENTIS R, & DM., C. 2007. First tuberculosis cases in Italy re-sistant to all tested drugs. . *Euro Surveill* 12**,** E070517.1.

MINICH, W. B., BALASTA, M. L., GOSS, D. J. & RHOADS, R. E. 1994. Chromatographic resolution of in vivo phosphorylated and nonphosphorylated eukaryotic translation initiation factor eIF-4E: increased cap affinity of the phosphorylated form. *Proc Natl Acad Sci U S A,* 91**,** 7668-72.

MOHAMED A. ELHELU, W., DC 1983. The role of macrophages in Immunology. *JOURNAL OF THE NATIONAL MEDICAL ASSOCIATION,* 75**,** 314-417.

MOLNARFI, N., BRANDT, K. J., GRUAZ, L., DAYER, J. M. & BURGER, D. 2008. Differential regulation of cytokine production by PI3Kdelta in human monocytes upon acute and chronic inflammatory conditions. *Mol Immunol,* 45**,** 3419-27.

MOOTOO, A., STYLIANOU, E., ARIAS, M. A. & RELJIC, R. 2009. TNF-alpha in tuberculosis: a cytokine with a split personality. *Inflamm Allergy Drug Targets,* 8**,** 53-62.

MUKAI, Y., WANG, C. Y., RIKITAKE, Y. & LIAO, J. K. 2007. Phosphatidylinositol 3-kinase/protein kinase Akt negatively regulates plasminogen activator inhibitor type 1 expression in vascular endothelial cells. *Am J Physiol Heart Circ Physiol,* 292**,** H1937-42.

NORTH, R. J. & JUNG, Y. J. 2004. Immunity to tuberculosis. *Annu Rev Immunol,* 22**,** 599-623.

O'GARRA, A., REDFORD, P. S., MCNAB, F. W., BLOOM, C. I., WILKINSON, R. J. & BERRY, M. P. 2013. The immune response in tuberculosis. *Annu Rev Immunol,* 31**,** 475-527.

O'LOGHLEN, A., GONZALEZ, V. M., PINEIRO, D., PEREZ-MORGADO, M. I., SALINAS, M. & MARTIN, M. E. 2004. Identification and molecular characterization of Mnk1b, a splice variant of human MAP kinase-interacting kinase Mnk1. *Exp Cell Res,* 299**,** 343-55.

OHTANI, M., NAGAI, S., KONDO, S., MIZUNO, S., NAKAMURA, K., TANABE, M., TAKEUCHI, T., MATSUDA, S. & KOYASU, S. 2008. Mammalian target of rapamycin and glycogen synthase kinase 3 differentially regulate lipopolysaccharide-induced interleukin-12 production in dendritic cells. *Blood,* 112**,** 635-43.

ONG, C. W., ELKINGTON, P. T. & FRIEDLAND, J. S. 2014. Tuberculosis, pulmonary cavitation, and matrix metalloproteinases. *Am J Respir Crit Care Med,* 190**,** 9-18.

ONKAR SAHOTA, A. B., KIT MALTHOUSE,MURAD QURESHI AND VALERIE SHAWCROSS (MEMBERS OF LONDON HEALTH COMMITEE) (MEMBERS OF LONDON HEALTH COMMITEE) 2015. Tackling TB in London.

OVERALL, C. 2002. Molecular determinants of metalloproteinase substrate specificity. *Molecular Biotechnology,* 22**,** 51-86.

OVERALL, C. M., WRANA, J. L. & SODEK, J. 1991. Transcriptional and post-transcriptional regulation of 72-kDa gelatinase/type IV collagenase by transforming growth factor-beta 1 in human fibroblasts.

Comparisons with collagenase and tissue inhibitor of matrix metalloproteinase gene expression. *J Biol Chem,* 266**,** 14064-71.

PAGE-MCCAW, A., EWALD, A. J. & WERB, Z. 2007. Matrix metalloproteinases and the regulation of tissue remodelling. *Nat Rev Mol Cell Biol,* 8**,** 221-33.

PARDO, A., RIDGE, K., UHAL, B., SZNAJDER, J. I. & SELMAN, M. 1997. Lung alveolar epithelial cells synthesize interstitial collagenase and gelatinases A and B in vitro. *Int J Biochem Cell Biol,* 29**,** 901-10.

PARK, E. K., JUNG, H. S., YANG, H. I., YOO, M. C., KIM, C. & KIM, K. S. 2007. Optimized THP-1 differentiation is required for the detection of responses to weak stimuli. *Inflammation Research,* 56**,** 45-50.

PARKS, W. C. & SHAPIRO, S. D. 2001. Matrix metalloproteinases in lung biology. *Respir Res,* 2**,** 10-9.

PARKS, W. C., WILSON, C. L. & LOPEZ-BOADO, Y. S. 2004. Matrix metalloproteinases as modulators of inflammation and innate immunity. *Nat Rev Immunol,* 4**,** 617-29.

PARRA, J. L., BUXADE, M. & PROUD, C. G. 2005. Features of the catalytic domains and C termini of the MAPK signal-integrating kinases Mnk1 and Mnk2 determine their differing activities and regulatory properties. *J Biol Chem,* 280**,** 37623-33.

PATHAK, S. K., BHATTACHARYYA, A., PATHAK, S., BASAK, C., MANDAL, D., KUNDU, M. & BASU, J. 2004. Toll-like Receptor 2 and Mitogen- and Stress-activated Kinase 1 Are Effectors of Mycobacterium avium-induced Cyclooxygenase-2 Expression in Macrophages. *Journal of Biological Chemistry,* 279**,** 55127-55136.

PAULSON, T. 2013. Epidemiology: A mortal foe. *Nature,* 502**,** S2-S3.

PETERSON, R. T. & SCHREIBER, S. L. 1998. Translation control: Connecting mitogens and the ribosome. *Current Biology,* 8**,** R248-R250.

POIRIER, V. & AV-GAY, Y. 2012. Mycobacterium tuberculosis modulators of the macrophage's cellular events. *Microbes Infect,* 14**,** 1211-9.

PRICE, N. M., GILMAN, R. H., UDDIN, J., RECAVARREN, S. & FRIEDLAND, J. S. 2003. Unopposed Matrix Metalloproteinase-9 Expression in Human Tuberculous Granuloma and the Role of TNF-α-Dependent Monocyte Networks. *The Journal of Immunology,* 171**,** 5579-5586.

PULLEN, N. & THOMAS, G. 1997. The modular phosphorylation and activation of p70s6k. *FEBS Letters,* 410**,** 78-82.

PYRONNET, S., IMATAKA, H., GINGRAS, A. C., FUKUNAGA, R., HUNTER, T. & SONENBERG, N. 1999. Human eukaryotic translation initiation factor 4G (eIF4G) recruits mnk1 to phosphorylate eIF4E. *EMBO J,* 18**,** 270-9.

RAND, L., GREEN, J. A., SARAIVA, L., FRIEDLAND, J. S. & ELKINGTON, P. T. 2009. Matrix metalloproteinase-1 is regulated in tuberculosis by a p38 MAPK-dependent, p-aminosalicylic acid-sensitive signaling cascade. *J Immunol,* 182**,** 5865-72.

RAUGHT, B. & GINGRAS, A.-C. 1999. eIF4E activity is regulated at multiple levels. *The International Journal of Biochemistry & Cell Biology,* 31**,** 43-57.

ROUSSEAU, D., KASPAR, R., ROSENWALD, I., GEHRKE, L. & SONENBERG, N. 1996. Translation initiation of ornithine decarboxylase and nucleocytoplasmic transport of cyclin D1 mRNA are increased in cells overexpressing eukaryotic initiation factor 4E. *Proc Natl Acad Sci U S A,* 93**,** 1065-70.

ROZYNSKA, R., JAHNZ-ROZYK, K., TARGOWSKI, T., GRABOWSKA, P. & FROM, S. 2005. [The influence of smoking on the metalloproteinase 1 (MMP-1) concentration in serum in the group of patients with chronic obstructive pulmonary disease]. *Przegl Lek,* 62**,** 1047-50.

RUPANI, H., SANCHEZ-ELSNER, T. & HOWARTH, P. 2013. MicroRNAs and respiratory diseases. *Eur Respir J,* 41**,** 695-705.

RUSSELL, D. G. 2007. Who puts the tubercle in tuberculosis? *Nat Rev Microbiol,* 5**,** 39-47.

SAITOH, M., PULLEN, N., BRENNAN, P., CANTRELL, D., DENNIS, P. B. & THOMAS, G. 2002. Regulation of an Activated S6 Kinase 1 Variant Reveals a Novel Mammalian Target of Rapamycin Phosphorylation Site. *Journal of Biological Chemistry,* 277**,** 20104-20112.

SALEH, M. T. & BELISLE, J. T. 2000. Secretion of an acid phosphatase (SapM) by Mycobacterium tuberculosis that is similar to eukaryotic acid phosphatases. *J Bacteriol,* 182**,** 6850-3. SALGAME, P. 2011. MMPs in tuberculosis: granuloma creators and tissue destroyers.

SALMON, R. A., GUO, X. C., TEH, H. S. & SCHRADER, J. W. 2001. The p38 mitogen-activated protein kinases can have opposing roles in the antigen-dependent or endotoxin-stimulated production of IL-12 and IFN-gamma. *European Journal of Immunology,* 31**,** 3218-3227.

SAPKOTA, G. P., CUMMINGS, L., NEWELL, F. S., ARMSTRONG, C., BAIN, J., FRODIN, M., GRAUERT, M., HOFFMANN, M., SCHNAPP, G., STEEGMAIER, M., COHEN, P. & ALESSI, D. R. 2007. BI-D1870 is a specific inhibitor of the p90 RSK (ribosomal S6 kinase) isoforms in vitro and in vivo. *Biochem J,* 401**,** 29-38.

SCHEPER, G. C. & PROUD, C. G. 2002a. Does phosphorylation of the cap-binding protein eIF4E play a role in translation initiation? *Eur J Biochem,* 269**,** 5350-9.

SCHEPER, G. C. & PROUD, C. G. 2002b. Does phosphorylation of the cap-binding protein eIF4E play a role in translation initiation? *European Journal of Biochemistry,* 269**,** 5350-5359.

SCHEPER, G. C., VAN KOLLENBURG, B., HU, J., LUO, Y., GOSS, D. J. & PROUD, C. G. 2002. Phosphorylation of eukaryotic initiation factor 4E markedly reduces its affinity for capped mRNA. *J Biol Chem,* 277**,** 3303-9.

SCHILDBERGER, A., ROSSMANITH, E., EICHHORN, T., STRASSL, K. & WEBER, V. 2013. Monocytes, Peripheral Blood Mononuclear Cells, and THP-1 Cells Exhibit Different Cytokine Expression Patterns following Stimulation with Lipopolysaccharide. *Mediators of Inflammation,* 2013**,** 697972.

SCHNEIDERMAN, J., SAWDEY, M. S., KEETON, M. R., BORDIN, G. M., BERNSTEIN, E. F., DILLEY, R. B. & LOSKUTOFF, D. J. 1992. Increased Type-1 Plasminogen-Activator Inhibitor Gene-Expression in Atherosclerotic Human Arteries. *Proceedings of the National Academy of Sciences of the United States of America,* 89**,** 6998-7002.

SCHWANHAUSSER, B., BUSSE, D., LI, N., DITTMAR, G., SCHUCHHARDT, J., WOLF, J., CHEN, W. & SELBACH, M. 2011. Global quantification of mammalian gene expression control. *Nature,* 473**,** 337-42.

SELMAN, M., MONTANO, M., RAMOS, C., VANDA, B., BECERRIL, C., DELGADO, J., SANSORES, R., BARRIOS, R. & PARDO, A. 1996. Tobacco smoke-induced lung emphysema in guinea pigs is associated with increased interstitial collagenase. *American Journal of Physiology - Lung Cellular and Molecular Physiology,* 271**,** L734-L743.

SHAPIRO, S. D., DOYLE, G. A., LEY, T. J., PARKS, W. C. & WELGUS, H. G. 1993a. Molecular mechanisms regulating the production of collagenase and TIMP in U937 cells: evidence for involvement of

delayed transcriptional activation and enhanced mRNA stability. *Biochemistry,* 32**,** 4286-92.

SHAPIRO, S. D., KOBAYASHI, D. K. & LEY, T. J. 1993b. Cloning and characterization of a unique elastolytic metalloproteinase produced by human alveolar macrophages. *Journal of Biological Chemistry,* 268**,** 23824-23829.

SHARBATI, J., LEWIN, A., KUTZ-LOHROFF, B., KAMAL, E., EINSPANIER, R. & SHARBATI, S. 2011. Integrated microRNA-mRNA-analysis of human monocyte derived macrophages upon Mycobacterium avium subsp. hominissuis infection. *PLoS One,* 6**,** e20258.

SHIOZAWA, J., ITO, M., NAKAYAMA, T., NAKASHIMA, M., KOHNO, S. & SEKINE, I. 2000. Expression of matrix metalloproteinase-1 in human colorectal carcinoma. *Mod Pathol,* 13**,** 925-33.

SINGH, P. K., SINGH, A. V. & CHAUHAN, D. S. 2013. Current understanding on micro RNAs and its regulation in response to Mycobacterial infections. *J Biomed Sci,* 20**,** 14.

SINGH, S., SARAIVA, L., ELKINGTON, P. T. G. & FRIEDLAND, J. S. 2014. Regulation of matrix metalloproteinase-1, -3, and -9 in Mycobacterium tuberculosis-dependent respiratory networks by the rapamycin-sensitive PI3K/p70S6K cascade. *The FASEB Journal,* 28**,** 85-93.

SKOLNIK, E., BATZER, A., LI, N., LEE, C., LOWENSTEIN, E., MOHAMMADI, M., MARGOLIS, B. & SCHLESSINGER, J. 1993. The function of GRB2 in linking the insulin receptor to Ras signaling pathways. *Science,* 260**,** 1953-1955.

SLENTZ-KESLER, K., MOORE, J. T., LOMBARD, M., ZHANG, J., HOLLINGSWORTH, R. & WEINER, M. P. 2000. Identification of the human Mnk2 gene (MKNK2) through protein interaction with estrogen receptor beta. *Genomics,* 69**,** 63-71.

SOBEL, B. E., TAATJES, D. J. & SCHNEIDER, D. J. 2003. Intramural plasminogen activator inhibitor type-1 and coronary atherosclerosis. *Arteriosclerosis Thrombosis and Vascular Biology,* 23**,** 1979-1989.

SONENBERG, N. 2008. eIF4E, the mRNA cap-binding protein: from basic discovery to translational research. *Biochem Cell Biol,* 86**,** 178-83.

STENGER, S. 2005. Immunological control of tuberculosis: role of tumour necrosis factor and more. *Ann Rheum Dis,* 64 Suppl 4**,** iv24-8.

STOCKER, W. E. A. 1995. The metzincins--topological and sequential relations between the astacins, adamalysins, serralysins, and matrixins (collagenases) define a superfamily of zinc-peptidases. . *Protein Science* 4**,** 823-840.

SUJOBERT, P., BARDET, V., CORNILLET-LEFEBVRE, P., HAYFLICK, J. S., PRIE, N., VERDIER, F., VANHAESEBROECK, B., MULLER, O., PESCE, F., IFRAH, N., HUNAULT-BERGER, M., BERTHOU, C., VILLEMAGNE, B., JOURDAN, E., AUDHUY, B., SOLARY, E., WITZ, B., HAROUSSEAU, J. L., HIMBERLIN, C., LAMY, T., LIOURE, B., CAHN, J. Y., DREYFUS, F., MAYEUX, P., LACOMBE, C. & BOUSCARY, D. 2005. Essential role for the p110δ isoform in phosphoinositide 3-kinase activation and cell proliferation in acute myeloid leukemia. *Blood,* 106**,** 1063-1066.

TAYLOR, P. R. M.-P., L. STACEY, M. LIN, H. H. BROWN, G. D. GORDON, S. 2005. Macrophage receptors and immune recognition. *Annu Rev Immunol,* 23**,** 901-44.

TELZAK, E. E., FAZAL, B.A., POLLARD C.L., GLENN S. TURETT, JESSICA E. JUSTMAN, AND STEVE BLUM 1997. Factors Influencing Time to Sputum Conversion Among Patients with

Smear-Positive Pulmonary Tuberculosis. *Clinical Infectious Diseases,* 25**,** 666-670.

TENGKU-MUHAMMAD, T. S., HUGHES, T. R., CRYER, A. & RAMJI, D. P. 1999. Involvement of both the tyrosine kinase and the phosphatidylinositol-3' kinase signal transduction pathways in the regulation of lipoprotein lipase expression in J774.2 macrophages by cytokines and lipopolysaccharide. *Cytokine,* 11**,** 463-8.

THOMAS, M. J., SMITH, A., HEAD, D. H., MILNE, L., NICHOLLS, A., PEARCE, W., VANHAESEBROECK, B., WYMANN, M. P., HIRSCH, E., TRIFILIEFF, A., WALKER, C., FINAN, P. & WESTWICK, J. 2005. Airway inflammation: chemokine-induced neutrophilia and the class I phosphoinositide 3-kinases. *Eur J Immunol,* 35**,** 1283-91.

TSAO, T. C., HONG, J., LI, L. F., HSIEH, M. J., LIAO, S. K. & CHANG, K. S. 2000. Imbalances between tumor necrosis factor-alpha and its soluble receptor forms, and interleukin-1beta and interleukin-1 receptor antagonist in BAL fluid of cavitary pulmonary tuberculosis. *Chest,* 117**,** 103-9.

TSUCHIYA, S., YAMABE, M., YAMAGUCHI, Y., KOBAYASHI, Y., KONNO, T. & TADA, K. 1980. Establishment and characterization of a human acute monocytic leukemia cell line (THP-1). *International Journal of Cancer,* 26**,** 171-176.

TSUKAMOTO, K., HAZEKI, K., HOSHI, M., NIGORIKAWA, K., INOUE, N., SASAKI, T. & HAZEKI, O. 2008. Critical roles of the p110 beta subtype of phosphoinositide 3-kinase in lipopolysaccharide-induced Akt activation and negative regulation of nitrite production in RAW 264.7 cells. *J Immunol,* 180**,** 2054-61.

TZENAKI, N. & PAPAKONSTANTI, E. A. 2013. p110delta PI3 kinase pathway: emerging roles in cancer. *Front Oncol,* 3**,** 40.

UDWADIA ZF, A. R., AJBANI KK, RODRIGUEZ C. 2012. Totally drug - resistant tuberculosis in India. *Clin Infect Dis* 54**,** 579-81. .

UEDA, T., SASAKI, M., ELIA, A. J., CHIO, II, HAMADA, K., FUKUNAGA, R. & MAK, T. W. 2010. Combined deficiency for MAP kinase-interacting kinase 1 and 2 (Mnk1 and Mnk2) delays tumor development. *Proc Natl Acad Sci U S A,* 107**,** 13984-90.

UEDA, T., WATANABE-FUKUNAGA, R., FUKUYAMA, H., NAGATA, S. & FUKUNAGA, R. 2004. Mnk2 and Mnk1 are essential for constitutive and inducible phosphorylation of eukaryotic initiation factor 4E but not for cell growth or development. *Mol Cell Biol,* 24**,** 6539-49.

ULEVITCH, R. J. & TOBIAS, P. S. 1995. Receptor-dependent mechanisms of cell stimulation by bacterial endotoxin. *Annu Rev Immunol,* 13**,** 437-57.

V. WEE YONG, C. P., PETER FORSYTH* AND DYLAN R. EDWARDS 2001. Metalloproteinases in biology and pathology of the nervous system. *Nat Rev Neurosci* 2**,** 502-511.

VAN CREVEL, R., KARYADI, E., PREYERS, F., LEENDERS, M., KULLBERG, B. J., NELWAN, R. H. & VAN DER MEER, J. W. 2000. Increased production of interleukin 4 by CD4+ and CD8+ T cells from patients with tuberculosis is related to the presence of pulmonary cavities. *J Infect Dis,* 181**,** 1194-7.

VAN DEN STEEN, P. E., DUBOIS, B., NELISSEN, I., RUDD, P. M., DWEK, R. A. & OPDENAKKER, G. 2002. Biochemistry and Molecular Biology of Gelatinase B or Matrix Metalloproteinase-9 (MMP-9). *Critical Reviews in Biochemistry and Molecular Biology,* 37**,** 375-536.

VAN WART, H. E. & BIRKEDAL-HANSEN, H. 1990. The cysteine switch: a principle of regulation of metalloproteinase activity with potential applicability to the entire matrix metalloproteinase gene family. *Proc Natl Acad Sci U S A,* 87**,** 5578-82.

VANHAESEBROECK, B., GUILLERMET-GUIBERT, J., GRAUPERA, M. & BILANGES, B. 2010. The emerging mechanisms of isoform-specific PI3K signalling. *Nat Rev Mol Cell Biol,* 11**,** 329-41.

VANHAESEBROECK, B., LEEVERS, S. J., AHMADI, K., TIMMS, J., KATSO, R., DRISCOLL, P. C., WOSCHOLSKI, R., PARKER, P. J. & WATERFIELD, M. D. 2001. Synthesis and function of 3-phosphorylated inositol lipids. *Annu Rev Biochem,* 70**,** 535-602.

VANHAESEBROECK, B., STEPHENS, L. & HAWKINS, P. 2012. PI3K signalling: the path to discovery and understanding. *Nat Rev Mol Cell Biol,* 13**,** 195-203.

VARA, J. Á. F., CASADO, E., DE CASTRO, J., CEJAS, P., BELDA-INIESTA, C. & GONZÁLEZ-BARÓN, M. 2004. PI3K/Akt signalling pathway and cancer. *Cancer Treatment Reviews,* 30**,** 193-204.

VELAYATI, A. A., FARNIA P, MASJEDI M.R. 2013. The totally drug resistant tuberculosis (TDR-TB). *Int J Clin Exp Med* 6**,** 307-309.

VELAYATI, A. A., MASJEDI, M. R, FARNIA, P, TABARSI, P, GHANAVI, J, ZIAZARIFI, A. H, HOFFNER, S. E. 2009. Emergence of new forms of totally drug-resistant tuberculosis bacilli: super extensively drug-resistant tuberculosis or totally drug-resistant strains in iran. *Chest,* 136**,** 420-5.

VERGNE, I., CHUA, J., LEE, H. H., LUCAS, M., BELISLE, J. & DERETIC, V. 2005. Mechanism of phagolysosome biogenesis block by viable Mycobacterium tuberculosis. *Proc Natl Acad Sci U S A,* 102**,** 4033-8.

VINCENTI, M. P. & BRINCKERHOFF, C. E. 2007. Signal transduction and cell-type specific regulation of matrix metalloproteinase gene expression: can MMPs be good for you? *J Cell Physiol,* 213**,** 355-64.

VOGEL, C. & MARCOTTE, E. M. 2012. Insights into the regulation of protein abundance from proteomic and transcriptomic analyses. *Nat Rev Genet,* 13**,** 227-32.

VOS, C. M., GARTNER, S., RANSOHOFF, R. M., MCARTHUR, J. C., WAHL, L., SJULSON, L., HUNTER, E. & CONANT, K. 2000. Matrix metalloprotease-9 release from monocytes increases as a function of differentiation: implications for neuroinflammation and neurodegeneration. *J Neuroimmunol,* 109**,** 221-7.

VU, T. H., SHIPLEY, J. M., BERGERS, G., BERGER, J. E., HELMS, J. A., HANAHAN, D., SHAPIRO, S. D., SENIOR, R. M. & WERB, Z. 1998. MMP-9/Gelatinase B Is a Key Regulator of Growth Plate Angiogenesis and Apoptosis of Hypertrophic Chondrocytes. *Cell,* 93**,** 411-422.

WAGNER, K. R. & BISHAI, W. R. 2001. Issues in the treatment of Mycobacterium tuberculosis in patients with human immunodeficiency virus infection. *AIDS,* 15 Suppl 5**,** S203-12.

WANG, H., ZHANG, Q., WEN, Q., ZHENG, Y., LAZAROVICI, P., JIANG, H., LIN, J. & ZHENG, W. 2012. Proline-rich Akt substrate of 40 kDa (PRAS40): A novel downstream target of PI3k/Akt signaling pathway. *Cellular Signalling,* 24**,** 17-24.

WANG, X., FLYNN, A., WASKIEWICZ, A. J., WEBB, B. L., VRIES, R. G., BAINES, I. A., COOPER, J. A. & PROUD, C. G. 1998. The phosphorylation of eukaryotic initiation factor eIF4E in response to phorbol esters, cell stresses, and cytokines is mediated by distinct MAP kinase pathways. *J Biol Chem,* 273**,** 9373-7.

WASKIEWICZ, A. J., FLYNN, A., PROUD, C. G. & COOPER, J. A. 1997. Mitogen-activated protein kinases activate the serine/threonine kinases Mnk1 and Mnk2. *EMBO J,* 16**,** 1909-20.

WEINSTEIN, S. L., FINN, A. J., DAVE, S. H., MENG, F., LOWELL, C. A., SANGHERA, J. S. & DEFRANCO, A. L. 2000. Phosphatidylinositol 3-kinase and mTOR mediate lipopolysaccharide-stimulated nitric oxide production in macrophages via interferon-beta. *J Leukoc Biol,* 67**,** 405-14.

WEISS, C. & BOYAR-MANSTEIN, M. L. 1951. On the mechanism of liquefaction of tubercles. I. The behavior of endocellular proteinases in tubercles developing in the lungs of rabbits. *Am Rev Tuberc,* 63**,** 694-705.

WEISS, C. & SINGER, F. M. 1953. Mechanism of softening of tubercles. II. Behavior of desoxyribonuclease in tubercles developing in the lungs of rabbits. *AMA Arch Pathol,* 55**,** 516-30.

WEISS, C., TABACHNICK, J. & COHEN, H. P. 1954. Mechanism of softening of tubercles. III. Hydrolysis of protein and nucleic acid during anaerobic autolysis of normal and tuberculous lung tissue in vitro. *AMA Arch Pathol,* 57**,** 179-93.

WILLIAMS, D. L., LI, C., HA, T., OZMENT-SKELTON, T., KALBFLEISCH, J. H., PREISZNER, J., BROOKS, L., BREUEL, K. & SCHWEITZER, J. B. 2004. Modulation of the phosphoinositide 3-kinase pathway alters innate resistance to polymicrobial sepsis. *J Immunol,* 172**,** 449-56.

WILLIAMS, R., BERNDT, A., MILLER, S., HON, W.-C. & ZHANG, X. 2009. Form and flexibility in phosphoinositide 3-kinases. *Biochemical Society Transactions,* 37**,** 615-626.

WOESSNER, J. F. 1991. Matrix metalloproteinases and their inhibitors in connective tissue remodeling. *The FASEB Journal,* 5**,** 2145-54.

XIA, H., NHO, R. S., KAHM, J., KLEIDON, J. & HENKE, C. A. 2004. Focal adhesion kinase is upstream of phosphatidylinositol 3-kinase/Akt in regulating fibroblast survival in response to contraction of type I collagen matrices via a beta 1 integrin viability signaling pathway. *J Biol Chem,* 279**,** 33024-34.

YANG, C.-S., LEE, J.-S., SONG, C.-H., HUR, G. M., LEE, S. J., TANAKA, S., AKIRA, S., PAIK, T.-H. & JO, E.-K. 2007. Protein kinase C zeta plays an essential role for Mycobacterium tuberculosis-induced extracellular signal-regulated kinase 1/2 activation in monocytes/macrophages via Toll-like receptor 2. *Cellular Microbiology,* 9**,** 382-396.

YANG, C.-S., SONG, C.-H., LEE, J.-S., JUNG, S.-B., OH, J.-H., PARK, J., KIM, H.-J., PARK, J.-K., PAIK, T.-H. & JO, E.-K. 2006a. Intracellular network of phosphatidylinositol 3-kinase, mammalian target of the rapamycin/70 kDa ribosomal S6 kinase 1, and mitogen-activated protein kinases pathways for regulating mycobacteria-induced IL-23 expression in human macrophages. *Cellular Microbiology,* 8**,** 1158-1171.

YANG, C. S., LEE, J. S., JUNG, S. B., OH, J. H., SONG, C. H., KIM, H. J., PARK, J. K., PAIK, T. H. & JO, E. K. 2006b. Differential regulation of interleukin-12 and tumour necrosis factor-alpha by phosphatidylinositol 3-kinase and ERK 1/2 pathways during Mycobacterium tuberculosis infection. *Clin Exp Immunol,* 143**,** 150-60.

YANG, Z., STRICKLAND, D. K. & BORNSTEIN, P. 2001. Extracellular matrix metalloproteinase 2 levels are regulated by the low density lipoprotein-related scavenger receptor and thrombospondin 2. *J Biol Chem,* 276**,** 8403-8.

YI, A. K., YOON, J. G., YEO, S. J., HONG, S. C., ENGLISH, B. K. & KRIEG, A. M. 2002. Role of mitogen-activated protein kinases in CpG DNA-mediated IL-10 and IL-12 production: Central role of extracellular signal-regulated kinase in the negative feedback loop of the CpG DNA-mediated Th1 response. *Journal of Immunology,* 168**,** 4711-4720.

YI, R., QIN, Y., MACARA, I. G. & CULLEN, B. R. 2003. Exportin-5 mediates the nuclear export of pre-microRNAs and short hairpin RNAs. *Genes Dev,* 17**,** 3011-6.

YODER, M. A., LAMICHHANE G., AND BISHAI W. R. 2004. Cavitary Pulmonary tuberculosis: The Holy Grail of disease transmission. *Current Science,* 86**,** 74-81.

YOKOYAMA, Y., GRÜNEBACH, F., SCHMIDT, S. M., HEINE, A., HÄNTSCHEL, M., STEVANOVIC, S., RAMMENSEE, H.-G. & BROSSART, P. 2008. Matrilysin (MMP-7) Is a Novel Broadly Expressed Tumor Antigen Recognized by Antigen-Specific T Cells. *American Association for Cancer Research,* 14**,** 5503-5511.

YOUNG, D. 2009. Animal models of tuberculosis. *Eur J Immunol,* 39**,** 2011-4.

ZENG, Z. Z., JIA, Y., HAHN, N. J., MARKWART, S. M., ROCKWOOD, K. F. & LIVANT, D. L. 2006. Role of focal adhesion kinase and phosphatidylinositol 3'-kinase in integrin fibronectin receptor-mediated, matrix metalloproteinase-1-dependent invasion by metastatic prostate cancer cells. *Cancer Res,* 66**,** 8091-9.

ZHANG, G., ZHOU, B., LI, S., YUE, J., YANG, H., WEN, Y., ZHAN, S., WANG, W., LIAO, M., ZHANG, M., ZENG, G., FENG, C. G., SASSETTI, C. M. & CHEN, X. 2014. Allele-specific induction of IL-1beta expression by C/EBPbeta and PU.1 contributes to increased tuberculosis susceptibility. *PLoS Pathog,* 10**,** e1004426.

ZHANG, G., ZHOU, B., WANG, W., ZHANG, M., ZHAO, Y., WANG, Z., YANG, L., ZHAI, J., FENG, C. G., WANG, J. & CHEN, X. 2012. A Functional Single-Nucleotide Polymorphism in the Promoter of the Gene Encoding Interleukin 6 Is Associated With Susceptibility to Tuberculosis. *The Journal of Infectious Diseases,* 205**,** 1697-1704.